Quaternary Studies near Summer Lake, Oregon

Friends of the Pleistocene
Ninth Annual Pacific Northwest Cell Field Trip
September 28-30, 2001

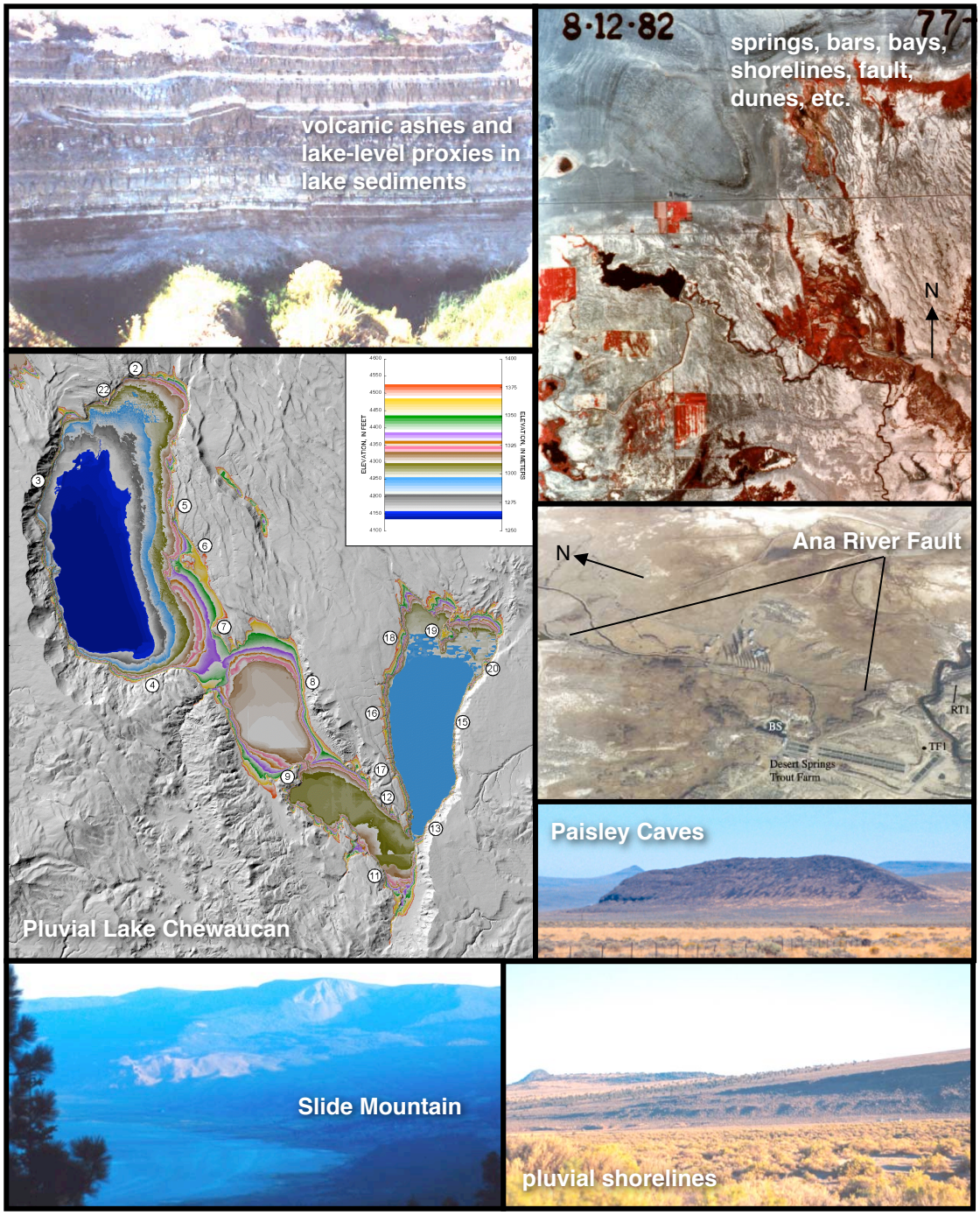

Quaternary Studies near Summer Lake, Oregon

Friends of the Pleistocene
Ninth Annual Pacific Northwest Cell Field Trip
September 28-30, 2001

Rob Negrini, Silvio Pezzopane and Tom Badger, Editors

Trip Leaders
Rob Negrini, California State University, Bakersfield, CA
Silvio Pezzopane, United States Geological Survey, Denver, CO
Rob Langridge, Institute of Geological and Nuclear Sciences, Lower Hutt, New Zealand
Ray Weldon, University of Oregon, Eugene, OR
Marty St. Louis, Oregon Department of Fish and Wildlife, Summer Lake, Oregon
Daniel Erbes, Bureau of Land Management, Carson City, Nevada
Glenn Berger, Desert Research Institute, University of Nevada, Reno, NV
Manuel Palacios-Fest, Terra Nostra Earth Sciences Research, Tucson, Arizona
Peter Wigand, California State University, Bakersfield, CA
Nick Foit, Washington State University, Pullman, WA
Steve Kuehn, Washington State University, Pullman, WA
Andrei Sarna-Wojcicki, United States Geological Survey, Menlo Park, CA
Cynthia Gardner, USGS, Cascades Volcano Observatory, Vancouver, WA
Rick Conrey, Washington State University, Pullman, WA
Duane Champion, United States Geological Survey, Menlo Park, CA
Michael Qulliam, California State University, Bakersfield, CA
Steve Van Denburgh, United States Geological Survey, Carson City, NV
Gary Simpson, SHN Consulting Geologists, Eureka, CA
Mladen Zic, California State University, Bakersfield, CA
Joe Licciardi, Woods Hole Oceanographic Institute, Woods Hole, MA
Blair Jones, United States Geological Survey, Reston, VA
Dolly Friedel, Sonoma State University, Rohnert Park, CA
Mel Aikens, University of Oregon, Eugene, OR
Larry Hills, United States Forest Service, Lakewood, OR
Ken Gobalet, California State University, Bakersfield, CA
Michelle Casterline, California State University, Bakersfield, CA
John Huff, California State University, Bakersfield, CA
Tom Badger, Mackay School of Mines, University of Nevada, Reno, NV

Contents

Introduction

Rob Negrini, CSU Bakersfield

Geography and Origins of Place Names

The 2001 Friends of the Pleistocene (FOP) trip for the Pacific NW Cell is in the subbasins of Pluvial Lake Chewaucan located in south-central Oregon. Most of the area can be accessed from State Highway 31 and Interstate Highway 395 which traverse the two main ~N-S arms of this pluvial system (see Figure R1 in Road Log).

The subasins are, from NW to SE: Summer Lake, the Upper Chewaucan Marsh, the Lower Chewaucan Marsh, and Lake Abert. The Pluvial Lake derives its name from the marshes and the Chewaucan River which enters the basin at the town of Paisley at the northwestern end of the upper marsh. According to MacArthur (1973) the name "Chewaucan" derives its origin from the Klamath Indians' word for wild potato (*tchua*) and a suffix denoting locality (*keni*). Allison (1940) first used this name for the Pleistocene pluvial lake.

Summer Lake and the adjacent Winter Rim were named by J.C. Fremont during the Winter of 1843. Fremont, an army colonel, was leading soldiers eastward through knee-deep snow when they came upon the rim of the impressive Winter Rim escarpment bordering the Summer Lake basin and viewed a lake surrounded by green vegetation thousands of feet below them. Fremont also named Lake Abert for one of his officers. See discussions in Allison (1982) and Grayson (1993) for more detail.

Some confusion will no doubt arise from the published name of paleo- and modern lakes. Allison (1940; 1945; 1982) referred to the pluvial lake occupying all of the subbasins during much of the Pleistocene as Pluvial Lake Chewaucan. He then referred to the two separate lakes which occupied the Summer Lake subbasin and the rest of the subbasins as Winter Lake and ZX Lake, respectively. The latter is named after a ranch originally located in the subbasin of the Upper Chewaucan Marsh.

Some Notes on the History of Quaternary Science in the Chewaucan Basins

As is the case for much of the Great Basin, I.C. Russell (1884) was one of the first geologists to study the area. He visited the Chewaucan basin as part of a reconnaissance study of southern Oregon to investigate both the bedrock geology and the surficial deposits. Based on shoreline evidence he concluded the following:

> "The Quaternary lake that occupied the valleys of Abert Lake, Chewaucan Marsh, and Summer Lake, was 260 feet deep over the Chewaucan Marsh, and 300 feet deep in the valley now occupied by Summer Lake."

In 1982, Ira Allison, a Professor of Geology at Oregon State University, published a revised maximum depth of ~370 feet in Geology of Pluvial Lake Chewaucan, essential reading for anyone interested in the Quaternary prehistory of this region (See Pezzopane in this volume for a comprehensive study of shoreline elevations around the basin). Included in the Preface of Allison's book is a history of early to middle 20th century research in the area. Briefly, research was spurred by the archeological studies of Luther Cressman of the University of Oregon and the related work on the volcanology of Crater Lake by Howel Williams of UC Berkeley and on the vertebrate paleontology associated with Cressman's archeological finds by John Merriam of the Carnegie Institution of Washington. These studies, particularly those associated with the Paisley Caves site (e.g., see Aikens, this volume), required a study of pluvial lake histories. Thus, Allison was called in to help as part of a team of noted geologist including Ernst Antevs. In Allison's (1982) words,

> "The results of this research, as hoped, have proved to be particularly helpful in integrating the geological and archeological findings over the years. And as with mountain climbing, this investigation of pluvial Lake Chewaucan has been fascinating in its own right, because, it *was* there."

The reader is referred to articles by Licciardi and by Friedel, both in this volume, for examples of how research on the archeological and pluvial prehistories of the region complement each other.

Ernst Antevs is well known for some of the earliest attempts to form integrated global climate change models from geological observations of his own and of others such as Russell and Allison (e.g., Antevs, 1948). In this volume articles on the geology of Lake Chewaucan's bottom sediments by Negrini and by Erbes demonstrate that data from this area support Antevs' "migrating jet stream" model for Pleistocene climate change. Data from this region also played a role in the development of Antevs' phenomenological model of Holocene climate

change. In particular, he used Allison's (1945) observation of several meters of lacustrine sediments above the Mazama tephra to infer that Summer Lake had been 90-100 feet deep in the early Holocene. This was a major component of his evidence upon which his relatively moist "Anathermal" stage of the Holocene is based. Although Antevs' Holocene climate model has more or less also stood the test of time, it turns out that Allison's identification of the Mazama tephra was wrong, an error which he commendably admitted in a followup paper (Allison, 1966). The mistaken tephra has since been identified as the ~46 ka Mt St Helens Cy tephra (Davis, 1985; Berger and Busacca, 1995). Thus, the overlying lacustrine sediments are late Pleistocene in age rather than early Holocene. The reader is referred to Grayson (1993) and Negrini (in press) for more complete discussions of Antevs' work in the context of Great Basin lakes.

The modern stratigraphy of the Chewaucan sediments began with the tephrochronological study of Jonathan Davis published in 1985 (for updates on the Chewaucan area tephra and their ages, refer to papers in this volume by Kuehn and Foit; Sarna-Wojcicki; Berger; Gardner and Negrini, and Zic). Davis, an eclectic mixture of tie-died attire and Harvard-bred eloquence (he was a fourth generation Ph.D. beginning with his great-grandfather, William Morris Davis), began his work on the sediments exposed in the Ana River Canyon in the late Spring of 1980 following the eruption of Mt St Helens. At that time, he had recently published his dissertation on the tephrochronology of the Lake Lahontan area (Davis, 1978), a work that, to this day, is important toward the understanding of the Lahontan pluvial system. Under the employ of Andrei Sarna-Wojcicki of the USGS, Davis was on a mission to sample the newly deposited Mt St Helens airfall and to record thicknesses of the deposit over an assigned area. As he was passing through the Summer Lake basin on his way north, he stopped in to look at Allison's classic section of sediments and tephra near the top of the Ana River Canyon exposures. Davis was especially eager to inspect the entire >50 feet of exposed section because, in Allison's words, "volcanic material occurs throughout the section." What Davis saw did not disappoint him. In fact, he was distracted enough by the more than 50 ash layers exposed in this remarkable section that he did not arrive on the scene of the Mt St Helens 1980 eruption until after it had rained and the ash had compacted. Initially displeased with Davis, Sarna-Wojcicki quickly came to understand the importance of the Ana River section and subsequently had a very good working relationship with him until Jonathan's death in a car accident 10 years later.

Davis (1985) summed up the potential importance of the Ana River exposures with the following quote:

"The Summer lake section may represent a "Rosetta Stone" in which volcanic events, paleomagnetic stratigraphy, and paleoecology can be precisely related for much of the last 335,000 years."

Quaternary research in the Chewaucan basin is fulfilling the promise anticipated by Davis and those before him as evidenced by the contributions in this volume. As we will see this weekend, however, there is plenty yet to do.

Figure 1. Jonathan Davis *circa* 1988 contemplating thrust faulting of the ~46 ka Mt St Helens Cy tephra. Tephra layer is in sediments of Pluvial Lake Chewaucan exposed near the Ana River (behind Davis) near Stop F5b of this field trip. MSH Cy is a graded bed. Biotite crystals are responsible for the dark color at its base.

Recommended Maps

For anyone interested in starting research in the Chewaucan basin, the following maps are recommended.

Lake Abert (42120-E1-TM-100) and Christmas Valley (43120-A1-TM-100) USGS 1:100,000 topo maps.

Klamath Falls and Crescent USGS 1:250,000 (2 degree sheet) topo maps.

Fremont National Forest, US Dept. Agriculture, 1995 (Shows public vs private holdings)

Paisley Ranger District, Fremont National Forest, 1994. Topo map of rim area west of pluvial lake basins.

Walker, G.W., 1977. Geologic map of Oregon east of the 121st meridian: U.S. Geological Survey, Miscellaneous Investigations Series Map I-902, scale 1:500000.

Recommended Reading and References Cited

Allison, I.S., 1940. Study of Pleistocene lakes of south-central Oregon, Carnegie Institute Washington Yearbook., v. 39., pp. 299-300.

Allison, I.S., 1945. Pumice Beds at Summer Lake, Oregon, G.S.A. Bull., v. 56., pp. 789-808.

Allison, I.S., 1982. Geology of Pluvial Lake Chewaucan, Oregon State Univ. Press, No. 11.

Antevs, E., 1948. Climate changes and pre-white man, Univ. Utah Bull., v. 38, pp. 167-191.
Berger, G.W., 1991. The use of glass for dating volcanic ash by thermoluminescence. Jour. Geophys. Res., v. 96, pp. 19,705-19,720.
Berger, G.W. and A.J. Busacca, 1995. Thermoluminescence dating of late Pleistocene loess and tephra from eastern Washington and southern Oregon and implications for the eruptive history of Mount St. Helens, Journal of Geophysical Research, v. 100, p. 22,361-22,374.
Brown, S.G., 1957. Occurrence of Ground Water near Ana Springs, Summer Lake Basin, Lake County, Oregon, unreviewed Open-File Report prepared in cooperation with the Oregon State Engineer. 24 pages. United States Geological Survey.
Cohen et al., 2000. A paleoclimate record for the past 250,000 years from Summer Lake, Oregon, U.S.A.: II. Lithostratigraphy, ostracodes, and pollen, Jour. Paleolimn., v. 24, pp. 151-182.
Conrad, C.F., 1953. Geology of the Ana River section, Summer Lake, Oregon. 92 pages, M.S. Thesis, Department of Geology, Oregon State University, Corvallis.
Davis, J.O., 1978. Quaternary tephrochronology of the Lake Lahontan area, Nevada and California, University of Nevada Reno, Nevada Archeological Survey, Research Paper 7.
Davis, J.O., 1985. Correlation of late Quaternary tephra layers in a long pluvial sequence near Summer Lake, Oregon, Quaternary Research, v. 23, p. 38-53.
Erbes, D., 1996. Late Pleistocene lithostratigraphy of Pluvial Lake Chewaucan, Oregon: Implications for past climate variation, M.S. Thesis, Dept. Physics and Geology, CSU Bakersfield, 111 p.
Friedel, 1993. Chronology and climatic controls of late Quaternary lake-level fluctuations in Chewaucan, Fort Rock, and Alkali basins, south-central Oregon, M.S. thesis, Dept. Geography, University of Oregon, 244 p.
Grayson, D.K., 1993. The Desert's Past: A Natural PreHistory of the Great Basin, Smithsonian Press.
Langridge, R., 1998. Paleoseismic deformation in behind-arc lacustrine settings: Acambay, Mexico and Ana River, Oregon, Ph.D. Dissertation, Dept. Geology, University of Oregon, 188 p.
Licciardi, J. 2001, Chronology of Latest Pleistocene lake-level fluctuations in the Pluvial Lake Chewaucan Basin, Oregon, USA: Journal of Quaternary Science, in press.
McArthur, L. , 1973. Oregon Geographic Names: Portland, Oregon, Oregon Historical Society, 835 p.
Negrini et al., 2000. A Paleoclimate record for the past 250,000 years from Summer Lake, Oregon, U.S.A.: I. Age control and magnetic lake level proxies, Jour. of Paleolimn., v. 24, pp. 125-149.
Pezzopane, 1993. Active faults and earthquake ground motions in Oregon, Ph.D. Dissertation, Dept. Geology, University of Oregon, 208 p.
Pezzopane, S. K., R. J. Weldon, 1993. Tectonic role of active faulting in Central Oregon, Tectonics, v. 12, p. 1140-1169.
Phillips, K.N., A.S. Van Denburgh, 1971. Hydrology and Geochemistry of Abert, Summer, and Goose Lakes, and other closed-basin lakes in south-central Oregon, USGS Prof. Paper 502B, pp. B1-B86.
Russell, I.C., 1884. A geological reconnaissance in southern Oregon, USGS Ann. Rpt. 4, 431-464.
Simpson, G., 1990. Late Quaternary tectonic development of the northwestern part of the Summer Lake Basin, south-central Oregon, M.S. Thesis, Dept. Geology, Humbolt State University, 121 p.
Travis, P.L., 1977. Geology of the area near the north end of Summer Lake, Lake Co., Oregon, M.S. Thesis, Dept. Geology, University of Oregon, 79 p.
Van Denburgh , A.S. 1975. Solute balance at Abert and Summer Lakes, south-central Oregon, USGS Prof. Paper 502C, pp. C1-C29.
Zic, M., 2001. Sediment Magnetism of the B&B Core from Summer Lake, Oregon, USA: Implications for Regional and Global Millennial-Scale Climate Change from 46-23 ka, M.S. Thesis, Department of Physics and Geology, CSU Bakersfield, CA.

Acknowledgements

Many thanks to the Oregon Department of Fish and Wildlife, particularly Marty St. Louis, for their help in running the field trip and in supporting research in the Ana River area. Also, hats off to the landowners who graciously gave us access to their property for this field trip, particularly Lyle Negus and others of the Desert Springs Trout Farm and Darryl Seven, owner of the Summer Lake Inn. Alicia Parks and Terry Hansen helped with the handling of field trip fees.

Quaternary Studies near Summer Lake, Oregon

Friends of the Pleistocene
Ninth Annual Pacific NW Cell Field Trip 2001

Road Log

Rob Negrini, Silvio Pezzopane, Joe Licciardi, Gary Simpson,
Glenn Berger, and Tom Badger

Road Log – Day 1

Friday, September 28th

The first day of the field trip will focus on nearshore geomorphology, neotectonics and paleoclimate, magnetic, and chronology studies on the exposures of bottom sediments in the NW corner of the Summer Lake subbasin. All of today's stops will be in the vicinity of the corner common to the following 7.5 minute USGS topographic quadrangle maps: Egli Rim, Sheeplick Draw, Summer Lake, and Ana River. Refer to Figures R1-R7 for today's trip.

0.0 Head north on Highway 31 from parking lot of Summer Lake Wildlife Refuge and Oregon Department of Fish and Wildlife (ODFW) office.

0.5 Winter Rim lays atop the formidable fault line scarp on the west side of the Summer Lake subbasin. This fault system, one of the westernmost expressions of the Basin and Range structural province, is discussed in Langridge et al. (this volume) and Pezzopane and Weldon (1993). This particular subbasin is a semi-graben tilted toward the west. Thus, the depocenter is proximal to the west side where remnant Summer Lake is located. The total thickness of basin-fill sediments is estimated to be ~1500 m based on modeling of the basin's gravity anomaly (Travis, 1977). The east side of the basin slopes relatively gently up toward Diablo (north side) and Wildcat (south side) Mts. Abundant sand dunes are found on the east and northern end of the basin reflecting overall physiography of the basin and the prominent wind direction from the S/SW (Figures R1-R4).

1.1 Town of Summer Lake. The first major pulse of settlement in the Summer Lake Basin other than by native Americans was during the late 1870's during which ~50 homesteads were established. One of these was the Winkleman farm now occupied by the Summer Lake Store on the west side of the road (Foster, 1989).

1.2 Here the basalt at the top of Winter Rim is underlain by the "White Rock" a silicic volcanic breccia (Walker, 1973). Similar, presumably low strength rock units might be laterally continuous throughout the Winter Rim and Slide Mountain escarpments. Such weak underlying units are believed responsible for the pervasiveness of landsliding. A "series of unusual mounds" mapped by Simpson (1990) approximately 2 km basinward from the slide area have similar lithologies as the landslide deposits at White Rock, suggesting these mounds may also be landslide debris.

3.2 Intersection of Highway 31 and Carlon Road. Enter into ODFW property via small access road at NE corner of intersection.

3.6 Stop F1-Baymouth Bar of Allison (1982).

Negrini, Weldon, Pezzopane, Langridge, St. Louis. Figs. R2-5.

You're now standing on a baymouth bar described by Allison (1982). A small ephemeral lake just to the north and labeled as "bay" in Figures 2a-b, is the remnant of the pluvial backbar bay. A similar set of features probably occurs at higher elevations west of Highway 31 just below the shoreline corresponding to the pluvial maximum (see "higher bay?" in Figure 2a). The pluvial maximum shoreline as well as at least two prominent lower shorelines can be observed from this site and are also obvious on air photos (e.g., Figure 2b). See Pezzopane (this volume) for an extensive discussion of the elevations and geomorphology of shorelines exposed throughout the Lake Chewaucan subbasins.

The Ana Reservoir and Ana River Canyon are seen to the south as well as the Desert Springs Trout Farm. These

are sites of the remaining field trip stops for the day.

At the present stop we'll discuss the history of geologic research, the regional geologic setting, and the wildlife management program of the Oregon Department of Fish and Wildlife (see Preface, this volume; Langridge et al., this volume; St. Louis, this volume; Figure 5).

We'll also walk a few tens of meters to the south to view an ash layer sampled in the gravel bed by Langridge and later by Negrini. Analyses done by two different tephrochronologists (Sarna-Wojcicki and Foit, respectively) suggest that this ash may be one of the ~165 ka ashes found below the major unconformity in Ana River Canyon section C.

Some Tectonic/Geologic Background

Pluvial Lake Chewaucan lies in the Cascadia back-arc volcanic region along the northwest edge of the Basin and Range Province of Oregon, adjacent to the westward transition into the Cascade volcanic arc, northwestward transition into Newberry volcano, and northward transition into the High Lava Plains and beyond to the Blue Mountain uplift (Figure R3). These transitional margins are both geologic and tectonic. In general, the fieldtrip area is a volcanic terrain consisting of numerous widespread basaltic lava flows and locally thick sections of tuff and tuffaceous sediments of late Miocene age broken into prominent tilted blocks and cuestas by extensional normal fault networks that strike north-south, north-northwest, and north-northeast.

The bedrock geology of the pluvial Lake Chewaucan region is shown by Walker (1963), Walker and others (1967), Peterson and McIntyre (1970), and Walker and McLeod (1991). Late Tertiary stratigraphic correlations and notable geologic relations are discussed in Baldwin (1981), Walker and McLeod (1991), Orr and others, (1992). The geologic maps show deformed rocks of Oligocene and Miocene age in the base of Winter Rim, in Coglan Butte, and in the Paisley Hills. The Paisley Hills is a north trending anticline of andesitic flows and sedimentary rocks intruded by diorite, granodiorite, and quartz monzonite radiometrically dated (K-Ar) at 33.1 m.y. (Evenden and others, 1964), indicating a minimum age of early Oligocene for the host rock in the region. Early Miocene megafossils and fauna found in Coglan Butte and rare localities in the basin are thought to be equivalent to fauna in the John Day Formation (Walker and others, 1967).

The deformed Oligocene and Miocene basement in this basin formed hills which extensive late Miocene lava flows, generally equivalent to the Steens Basalt, flooded and lapped against, and in many places failed to cover, such as on Winter Rim and Abert Rim (Baldwin, 1981). Basalts at the base of Abert Rim are somewhat older than those on Winter Rim, which are probably late Miocene or early Pliocene. Basalts in the base of Abert Rim are interfingered with tuffaceous sediments and tuffs having fossil fauna of late Miocene age, thought likely equivalent to the Mascall Formation and it's correlatives, some of which are early Pliocene in age (Walker and others, 1967). The Tertiary sequence of basalt flows and tuffaceous sediments is almost 2 km in thickness and dips gently 2° to 5° in most places. Uppermost flows capping the escarpments have been radiometrically

dated (K-Ar) in the range of 6 to 7 m.y. (Diggles and others, 1990).

Winter Rim, the southern Warner Mountains, and the Steens Mountains are the only large range blocks in which the strata dip westward; most of the Tertiary strata dip eastward. Horsts like Ten Mile Butte, Coglan Butte, and Abert Rim are related to larger half-graben structures in which slip on parallel, west-dipping faults allows the range block to rotate right-handed around northward trending horizontal axes to tilt eastward forming broad cuestas separated by asymmetric valleys.

Regional fault structures have been examined by Allison (1949), Donath (1962), Walker (1973), Lawrence (1976), Reches (1983), and Crider (in press), among others. The faults show a broad range in strike, length, displacement, and connectedness. Commonly the faults strike north-south, north-northwest, and north-northeast. Donath (1962) identified two fault-strike sets (azimuths at 25° and 330°) having a conjugate angle between them (55°). Donath (1962), Reches (1983), and Pezzopane and Weldon (1993) recognized the north-northwest striking faults are more numerous, generally shorter, and have less throw than those that strike north-northeast, which have greater throw along fewer yet longer faults. Fault throw is responsible for vertical relief in the region that ranges from a couple of meters to slightly more than a kilometer. Highstand shoreline elevations indicate ancient Lake Chewaucan was 100 meters deep commonly in places near the fault escarpments. Landslides from Winter Rim into Summer Lake were perhaps more common during high lakes stands, yet the deposition was still not great enough to bury the southwestern portion of the Summer Lake basin, which has the fault having the most throw in the area.

Pluvial Lake Chewaucan occupied the composite basin that connected Summer Lake with Abert Lake via Upper and Lower Chewaucan Marsh (Figures R1, R3-R4). The four interconnected lakes are each situated in fault-controlled basins developed within a graben or half-graben bounded by horst blocks. The largest and deepest is the graben of Summer Lake basin having a floor elevation of approximately 4150 ft (1265 m). Upper and Lower Chewaucan Marsh lie within a similar, but higher, northwest-striking fault-bounded trough having a floor that slopes southward from approximately 4310 ft (1314 m) at the northwest end to 4300 ft (1311 m) at the Narrows, where the Chewaucan Marsh is split by the Tucker Hill peninsula. Lower Chewaucan Marsh is a depression sloping from approximately 4300 ft (1311 m) in the northwest, to 4280 ft (1305 m) in the middle, to 4290 ft (1308 m) near the southeast end. The southeastern end of the modern Chewaucan River channel has been ditched and the river descends to 4280 ft (1305 m) and turns abruptly northeast into Lake Abert at 4255 ft (1297 m) (Figure R4). Abert Lake basin is separated from the Chewaucan Marsh where the southeastward continuation of the Coglan Buttes fault zone merges with the southwestward continuation of the Abert Rim fault zone.

Abert Lake basin is structurally a half-graben that strikes north-northeast whereas the Summer Lake and Chewaucan Marsh grabens strike north-northwest in an apparent conjugate geometry. The principle (Miocene) fault

escarpments commonly have zigzag and sharply curved traces, and appear geometrically segmented and separated. In places, ramp and relay fault structures show a conjugate fault geometry with linked secondary splay faults. These fault characteristics have been modeled to result from the sequential evolution of displacement, that, with continued extension across stepping *echelon* normal fault segments, the faults link to form continuous composite faults having zigzag traces (Crider, in press). Chewaucan Marsh faults appear to have less throw than the other graben faults, and may represent the southward continuation of faulting that kinematically links fault slip in the Summer Lake graben with that on the Abert Rim fault.

Left-stepping *en echelon* fault pairs are common in south-central Oregon, in zones that trend from northeast to northwest. Yet, the regional horizontal extension direction is east-west to slightly southwest-northeast (Pezzopane and Weldon, 1993; Crider, in press), oblique to both northeast and northwest *en echelon* fault zones. Since horizontal principal stresses (tensor components) are not perpendicular to the faults, the tectonics is a result of extensional stresses oblique to fault strike, which creates oblique rifting. The theoretical consequence is that left-stepping faults that strike northeast have left-oblique normal displacements and left-stepping faults that strike northwest (Chewaucan Marsh to Summer Lake grabens) have right-oblique normal displacements, all within the same regional stress field. Although relatively rare in this region, right-stepping fault traces also occur along northwest and northeast trends. Clear evidence for lateral slip on all faults in the study area is rare.

4.0 Return to Hghwy 31/Carlon Rd. Intersection. Head east on Carlon Road.

6.0 Here Carlon Road drops a few meters as you cross over the escarpment of the Ana River Fault (also called the Klippel Point Fault) which dips to the east. This normal fault is responsible for the offset (east side down) of the basalt flow capping Klippel Point, prominently displayed to the north/northwest as you cross the escarpment. The age of the Klippel Point basalt may be as young as 6.3-6.6 Myr (Diggles, et al., 1990; Langridge, 1998).

In 1990, a trench and deep pits on the upthrown and downthrown sides were excavated across the Ana River fault scarp on the north side of Carlon Road just a few meters north of the fence (Pezzopane, 1993). Interbedded with offset lacustine deposits were several ashes, which were identified by Andrei Sarna-Wojcicki (USGS-Menlo Park). Latest results indicate the ashes are: the Trego Hot Springs (23.2 ka); the Wono bed (27.2 ka); Marble Bluff; a Tulelake 2080 lapilli (approx. 155-160 ka(?); and the oldest of the three Orange ash beds equivalent to Summer Lake NN (approx. >171±43 ka, > 218±10 ka). See Pezzopane et al. (1996), Langridge (1998), and Langridge et al. (this volume) for the latest results of the tephra and fault history studies.

6.0' Due northeast are well developed shorelines along the base of hills at approx. 2 to 5 miles distance. The farther and taller angular peak is marked on topos as Flatiron Point. Shoreline profiles 2 and 22 (Pezzopane, this volume) show that here at the northern end of Summer Lake are some of the best developed shorelines in the basin,

especially in the relatively sheltered coves and small embayments. Apparently, here, the water was deep and the slope steep.

6.1 Turn right onto access road to the Desert Springs Trout Farm. Follow the "path of least resistance" past a few driveways and a couple of sharp turns.

7.3 Stop F2-Ana River Canyon Section C. *Negrini, Erbes, Kuehn, Sarna-Wojcicki, Berger, Gardner, Wigand, Palacios-Fest, Quilliam, Conrey, Champion. Fig. R6-7.* Park on right side of the road before the fence and proceed on foot a couple of hundred meters westward toward Ana River Section C of Allison (1945) and Davis (1985).

Across the river is one of the most complete sections of Pluvial Chewaucan bottom sediments exposed in the Ana River Canyon. The past 200-250,000 years of depositional history is represented here, though a few tens of thousands of years is missing as evidenced by a few prominent unconformities (Davis, 1985; Berger, 1991; Cohen et al., 2000; Erbes, this volume; Negrini et al., 2000). Many lithologic features will be indicated by the labels on the outcrop and can also be seen in Figure R6 along with sediment magnetism- and ostracode-based proxies for lake-level (see articles by Negrini and by Palacios-Fest, this volume). Among the labeled features are several of the >50 tephra layers present in these sediments many of which have been correlated with other volcanic ashes and/or proximal extrusives found throughout the NW Great Basin and the Pacific Northwest (e.g., Davis, 1985; Negrini et al., 1994; Kuehn and Foit, this volume). Several older tephra have also been identified from core taken near this site (see Sarna-Wojcicki, this volume).

Many of the ash layers in this section have been dated directly with the thermoluminescence method. In 1987 Berger collected with J. Davis 4 samples of vitric ash from this section for thermoluminescence (TL) dating. These 4 samples are tephra 2 (2.1 m from top of section), tephra R (5.6 m), tephra KK (11.2 m) and tephra LL (11.9m). These are listed in Table 1 at the end of this Road Log. TL ages are provided in Berger (1991) and in this guide. These TL ages are respectively 67.3±7.5 (1σ), 165±19, 201± 27, and 162±35 ka. An outline of the dating procedures and some interpretive comments are provided in Berger (this volume), especially regarding the 162 ka result for tephra LL and independent dating of related features. Together with a 102 ka TL age from Section E (below) for tephra N, these TL results provided the first quantitative evidence of a major hiatus in sedimentation (between ~100 and ~160 ka) between tephra beds R and N. Davis (1985) recognized an unconformity between tephra beds N1 (above R) and N, marked by an ~10 cm thick ostracode layer. Berger (1991) assigned this hiatus (and ostracode bed) to the Oxygen Isotope Stage 5 interpluvial as surmised earlier by Davis (1985).

More recently, Negrini and Davis (1992) and Negrini et al. (1994,2000) have derived a supporting chrono-stratigraphy. Interestingly, the chronology produced by $^{40}Ar/^{39}Ar$ dating (Herrero-Bervera et al., 1994) of a correlated tephra bed at Pringle Falls, Oregon, appears to conflict with these TL ages. Tephra GG here has been correlated with the Pringle Falls (Oregon) tephra D, and from the TL ages here should be younger than ~200 ka,

probably ~170 ka. The $^{40}Ar/^{39}Ar$ age of 218±10 ka reported for the Pringle Falls tephra D appears to be significantly older than expected on the basis of this TL chronostratigraphy (see also Negrini, in press). This apparent difference is illustrated in Fig. 4 of the thermoluminescence text in Berger (this volume). Clearly, follow-up TL dating of additional ash beds here would help resolve this apparent disagreement.

In general, the age of sediments below the major unconformity is much less certain than it is for the sediments above the unconformity (see Figure 2 of Negrini, this volume). Tephra JJ is another good case in point. It is a bimodal tephra separated into two sublayers, one dark- and the other light-colored. It had originally been correlated geochemically to the ~260 ka Shevlin Park Tuff (Lanphere et al., 1999) from near Bend, Oregon. This tuff is also bimodal in nature and has a very similar paleomagnetic direction (Gardner and Negrini, this volume). However, the age appears to be too old. Ongoing work by Conrey and others (in press), has called into question some of the earlier correlations (e.g., Tephra JJ with the Shevlin Park tuff) which may explain some of the discrepancies between tephra ages this far down in the section. This group instead correlates the Shevlin Park Tuff (~260 ka?) with Tephra NN, a controversial result which will be debated at this field trip stop.

In addition to tephrochronology and associated age control (e.g., see Berger, this volume; Gardner and Negrini, this volume), many other studies have been done and are in progress on these sediments including, lithostratigraphy, palynology, ostracode paleontology, geochemistry, paleomagnetism and environmental magnetism (see Preface and papers by Negrini; Palacios-Fest; Wigand; all in this volume).

At this stop we'll summarize the work to date on these sediments especially in light of its paleoclimatological implications and ongoing controversies in the ages and chronologies of some of the older tephra layers. The paleoclimatological results generally support Antevs' (e.g., 1948) model in which, at Milankovitch time scales (>10^4 yr periods), pluvial lake levels increase/decrease in response to glacial advance/retreat due to the associated southward/northward migration of the northern jet stream storm track.

Note: Figure 7a-b is stratigraphic column of the composite Ana River section. It is based on Jonathan Davis' notes with additional notes provided by R. Negrini and D. Erbes. The stratigraphic positions of the lithosomes discussed in Erbes (this volume) and Cohen et al. (2000) are shown in Figure 7a-d.

7.8 Stop F3-Ana River Fault.
Langridge, Weldon, Pezzopane. Fig. R2
Park on trout farm lot as instructed. Note: you are now on private land. Please secure permission from landowners before visiting this site. Proceed on foot ~100 meters to an exposure showing the Ana River Fault cutting through the Lake Chewaucan sediment section.

At this stop, we'll review more than 100,000 years of slip history on this fault (see Langridge et al., this volume). Such a rich history of movement on this fault is made possible by the exposure and the detailed stratigraphy due to the numerous tephra layers in the Chewaucan lake sediment section.

9.5 Back to Carlon Rd. Turn left and head west.

10.4 Turn left on access road to Ana Reservoir.

11.0 Stop F4-Ana Reservoir.
Van Denburgh. Figs. R2-3

The Ana Reservoir is fed by several active springs which are responsible for most of the remaining surface water entering the Summer Lake subbasin after the late Pleistocene diversion of the Chewaucan River. At this stop we'll discuss the chemistry and source of this water.

Proceed to Stop F5 by bearing left after crossing the dam (do not cross the irrigation ditch). Keep to the main dirt road travelling on the southwest side but generally not in sight of the Ana River, until you've travelled ~1.2 miles from Stop F4. Park the car near Ana River Section E, the second time the Ana River is clearly visible from the dirt road upon which you're travelling.

12.2 Stop F5-a) Ana River Section E; b) zone of deformed lake sediments; c) Neopluvial shoreline.

This is the last stop of the day. It consists of three substops.

Stop F5a-Ana River Section E.
Negrini, Langridg, Berger

At this locality, the very top of the Chewaucan lake sediment section is exposed along the Ana River Canyon. Here we'll inspect key tephra layers, unconformities, and deformations discussed at previous stops.

Here Berger collected 3 ash-bed samples for TL dating: tephra 18 correlated to Trego Hot Springs ash, tephra 12 correlated to MSH set Cy ash, and tephra N (5.1 m). The first sample was collected to serve as an age check for the TL ash-dating method at this site. The TL age of 24.3±2.7 ka is concordant with the then-known radiocarbon age of 23.4 ka (cal. yr) (Davis, 1983), and with the more recent magneto-stratigraphic-inferred age (Negrini and Davis, 1992) of 23.8"0.8 ka (converted to cal. yr) for the Trego Hot Springs ash. This and other age-checks described by Berger (1991) and shown in Fig. 1 of Berger (this volume) lend confidence to the older TL ages from Sections C and E here. The TL age of 46.3±4.8 ka for tephra 12 provided the first direct age for the correlated MSH set Cy ash. Previous indirect radiocarbon ages (outlined in Berger and Busacca, 1995) of ~36 to >42 ka are at the limit of that method, and very probably incorrect (based on this and other TL ages discussed by Berger and Busacca, 1995). The TL age for tephra N (5.1 m) of 102±11 ka delimits the lower age for the hiatus in sedimentation mentioned at Stop Section C.

Stop F5b-Ana River Section F of Davis (1985). *Simpson*

At this site, we will evaluate thrust block deformation within late Pleistocene age lake sediments. We will discuss the extent and style of lacustrine sediment deformation in the northwestern part of the basin and speculate on the cause (see the enclosed paper by Simpson). Time permitting, we will tour several deformation sites on the way to Stop F3c.

Stop F5c-Neopluvial shoreline.
Simpson. Fig. R2

At this stop, we will visit a Holocene age "neopluvial" shoreline originally identified and described in Allison (1982) and Simpson (1990). This shoreline extends eastward from Dutchy Lake near Highway 31 in a broad arc toward the Ana River. In the field, the shoreline is preserved as a series of

crudely aligned, elongate ridges. Cross-sectional exposures of these ridges reveal a "core" of moderately indurated lacustrine sands and silts, with a cap of non-indurated wind-blown sand containing abundant Mazama pumice. A longitudinal level-line survey of the crests of the individual ridges indicates that the shoreline profile rises considerably to the east. The ridge crests at the eastern end of the shoreline are consistently 10 to 15 ft higher than those at the western end. It is unclear whether this reflects primary depositional morphology, subsequent erosion or eolian deposition, or tectonic/isostatic deformation.

Elsewhere in the basin, particularly along the eastern margin, this shoreline at 4190-4200 ft clearly washes and reworks the dunes of Mazama ash. South, near Slide Mountain, this shoreline notches a fan that has landslide debris and charcoal dated at 2130 ± 90 yr B.P. (Pezzopane, 1993).

Return to the cars and continue heading south on dirt road past Stop 5c.

12.9 Turn right on River Ranch Road

15.3 Turn left on Highway 31 back to Wildlife Refuge parking lot.

The second day of the field trip will start with a presentation of a millennial scale climate record from the B&B depocenter core which exhibits the Bond Cycle and D-O oscillations. This will follow with a focus on the nearshore geomorphology and sedimentology of several parts of the Chewaucan basin including the Summer Lake basin, the south end of the Lower Chewaucan Marsh, the Lake Abert subbasin, and the sill dividing Summer Lake from the rest of Lake Chewaucan. Location maps are based on the Coglan Buttes SE, Valley Falls, and Paisley 7.5 minute USGS quads and the Klamath Falls and Crescent USGS 2° topo maps. Refer to Figures R1, and R8-R12 for today's trip.

0.0 Head south on Highway 31 from the parking lot of the Summer Lake Wildlife Refuge and the Oregon Department of Fish and Wildlife (ODFW) office.

1.5 Highway 31 passes Jack's Lakes which are formed in small (sector?) grabens developed along the Winter Ridge range front. Highway crosses fault scarp at near parallel angle and gains elevation over scarp and onto shoreline platform at approx. 4276 ft elevation.

2.0 Well developed shorelines preserved on west side of road have several prominent wave-cuts and benches, including the bulky 4485' and 4310' beach ridges. See shoreline profile site 3 of Pezzopane (this volume) in west Summer Lake.

10.5 **Stop Sa1-Summer Lake Inn overlook of B&B coring site.** *Zic. Fig. R1*

At this locality we'll first discuss a record of relative lake-level from the B&B core taken "offshore" from the Summer Lake Inn (formerly known as the Summer Lake B&B). This record exhibits the classic features characterizing millennial scale climate change (e.g., D-O oscillations, the Bond Cycle and the associated Heinrich events) throughout the northern hemisphere. Age control provided by C-14 and TL dates and by the position of the Mono Lake Excursion between IS #6 and #7 support previous work (e.g., Benson (1999) citing an antiphase nature of Great Basin lake response to global climate change at millennial-scale periods (i.e., the lakes go up during interstadials). 40 yr averages of historic climate data (similar to the period averaged by B&B core samples) supports this model by showing that precipitation increases/decreases in the Summer Lake region as temperatures rise/fall in the north Atlantic region. (See Zic, this volume, for related discussion).

15.5 Slide Mountain. The steep-walled, bowl-shaped depression near the ridge top is the main escarpment of the Slide Mtn. mass wasting feature. This impressive cirque-like feature is ~1,300 ft tall. Extremely large mass wasting features are common from here to the north along Winter Rim. Other features include the Punchbowl/Hunter Point complex discussed at the last stop.

Landslide deposits from Slide Mtn. extend into the lake basin and include the steeply dipping (to the south) basaltic extrusives named "Monument Rock". Near the base of the slide complex, several shorelines of Lake Chewaucan are truncated, from the 4,520' highstand shoreline down to a 4,280' shoreline (Allison, 1982).

Directly at the base of Monument Rock is an arcuate scarp of the Slide Mtn fault (Pezzopane, 1993) In 1989, the fault scarp was trenched and profiled here on the Harvey Ranch, now operated by Oregon State University. The scarp curves around the southwest corner of Summer Lake and steps right along the range front behind the Withers Ranch.

The trace is approx. 9 km in length. The scarp averages approximately 6 m in height and has maximum slope angles near the angle of repose. The trench revealed well-bedded to massive sandy silty lacustrine sediments, in places reworked (or deformed?) and buried by younger slope wash, debris flows, and slope colluvium. A chunk of charcoal sampled from sediments in the footwall, 4 to 5 m beneath the "recognized" top of the lacustrine section at this site (~ 4400 ft elevation), was dated with accelerator technique at 35,920 ± 20 yr B.P., providing a maximum limit on the age of faulting. However, the faulting is much younger; the scarp is developed in pluvial and post-pluvial sediments that are likely latest Pleistocene in age.

The first drainage east of Monument Rock is Kelly Creek, which formed along the western edge of the prominent young landslide from Slide Mtn. The landslide fan from Kelly Creek buries the Slide Mtn. fault scarp, indicating the scarp is older than the fan. Yet, the landslide fan is notched by the 4190'-4200' Neopluvial shoreline. This landslide fan contains landslide debris and charcoal dated at 2130 ± 90 yr B.P. (Pezzopane, 1993). So, the most recent earthquake event on this fault is inferred to be older than this charcoal, the latest landslide event is likely near or slightly older than this charcoal, and, the shoreline that notches the fan is inferred to be near or younger.

On Sunday, the final stops of the field trip will be toward the top of the Slide Mtn. feature (see Casterline and Huff; Badger, this volume) where we will gain a good view of this complicated mass wasting feature, as well as the fault scarp and shorelines.

20.2 Summer Lake Hot Springs.

This hot spring was originally called "Woodward Spring" by Waring (1908) presumably after the Woodward couple (Jonas and Lizzie) who owned the property at the time and charged 10-15 cents for their use (Foster, 1989). According to Allison (1982) and Waring (1908) the water comes out of the spring at >120˚ F after rising along a fault from a depth of 4,500 feet or more. The fault likely projects to the ground surface at the base of the range a mile or two to the south-southwest. The southern section of the Slide Mtn. fault dips northward beneath the Hot Springs, and is marked by a scarp, on average 4 to 5 m in height, below the prominent faceted spurs at the base of the range behind the Withers Ranch. The Hot Springs is probably above the shallowest point at which the hot water and fault plane coincide at depth.

22.7 As you turn the corner and head southward toward Paisley, observe the well developed shorelines on the slope west of the highway. This is shoreline profile site 4 (Pezzopane, this volume). The highstand notch is buried by pre-pluvial-aged talus and is marked only by a subtle slope change (Allison, 1982). The uppermost well developed beach ridge is at 4465' elevation, within about sixty feet or so of the highstand. The lowermost bulky beach ridge is at an elevation from 4340' to 4365', correlating to the bay bar complex that is well developed at this elevation and mantled by Mazama ash in the northeastern corner of Summer Lake basin.

To the left one can see the broad sill dividing the Summer Lake subbasin from the three subbasins to the south, the Upper Chewaucan Marsh, the Lower Chewaucan Marsh, and the Lake Abert

subbasins, in order of decreasing proximity. Until Lake Chewaucan rises above the elevation of this sill (~4390-4,400') the lake rises as two separate lakes. One is composed of the Summer Lake subbasin; the other is composed of the remaining three subbasins. Allison (1982) named the two lakes "Winter Lake" and "ZX Lake," respectively.

The Paisley State Airport is built on the flat platform of the sill margin at 4390'. The runway was paved in July 2001 so as to allow larger LifeFlight aircraft and ZX Ranch company planes to land. The costs were about $400k, split between the State of Oregon and J.R. Simplot Company, owner of the ZX Ranch. Now, in cases of emergency, residents in the valley no longer take a 1-hr ambulance drive to Lakeview to then fly out to Portland, Bend, or Klamath Falls hospitals.

26.4 Paisley is the main town in the area formerly occupied by Lake Chewaucan. The first residents of the Paisley area were Native Americans of the Snake, Modoc and/or Paiute tribes. The first town site was about seven miles south of present day Paisley and was know as Chewaucan. (Pronounced Chee-wa-can). Chewaucan is a Klamath Indian word for small potato. Paisley was founded in 1870 as the first white settlers had arrived in the Chewaucan Precinct or Paisley as it is now known, named by an early Scot settler in memory of his hometown in Scotland. In 1873 a Post Office was established, in 1874 Lake County was legally approved and by 1875 Lake County was a separate county.

The town's claim to fame is the annual Paisley Mosquito Festival, held during the last week in July. (Let's hope that the guests of honor for this "festival" are long gone by the time we arrive!) The Pioneer Saloon has some very unique antiques; a fabulous mirror and cherywood bar that was made in Europe in the late 1800's, shipped by boat around the horn and to the Oregon coast, and then by horse and wagon to Paisley. It has been through numerous cowboy fights and shows little for it.

Paisley and this valley has supported a thriving cattle economy for more than four generations. Many original homesteads, like the Withers Ranch and Carlon Ranch, are called Century Ranches because they have been in the same family for at least 100 years, some have for four generations.

The ZX Ranch, one of the oldest and largest, was recently purchased by J.R. Simplot Company, run by J.R., or Mr. Spud, as he has been called in the press. Aside from being a famous potato farmer, Simplot is the largest supplier of cattle in the Pacific Northwest and is fourth largest in the nation. Simplot owns leases on several million acres of public land and has twelve large ranches in California, Idaho, Nevada, Utah, and Oregon that have an annual capacity of 600,000 head, which represents 750 million pounds of beef. Simplot Company runs 15,000 head of cattle on 1.3 million acres of private and public land out of the ZX Ranch in Paisley. Simplot is quoted saying about the ZX Ranch, "You couldn't buy that from me for five times what I paid for it. It is not just a ranch. It's an empire!"

28.3 Upper Chewaucan Marsh/ZX Ranch.

A USGS/US Forest Service team led by D. Adam took a series of cores in the Lake Chewaucan basins including two 55 meter cores bottoming out in sediments with reversed magnetic polarity, thus presumably >800 kyr in age. These cores exhibited tens of meters of dry valley-bottom sediments

(sheetwash deposits) as opposed to the expected lacustrine and fluvial deposits (Gardner et al., 1992; personal communication from D. Adam to D. Erbes, 1996). This result supports the hypothesis forwarded by Allison (1982) that the Chewaucan River fed the Summer Lake subbasin throughout most of the Pleistocene until diversion of this river into the higher elevation ZX subbasins by the Paisley fan/delta during the last Pleistocene highstand.

The ZX Cattle Ranch, one of the largest such holdings in the State of Oregon, has been in operation for more than 100 years.

32.6 Beachler's Trading Post 31

33.6 Moss Creek. This small creek drains a small embayment of Pluvial Lake Chewaucan extending southward on the west side of the elongate, L-shaped ridge which includes Tucker Hill. Tucker Hill is a rhyolitic dome that forms the rounded knobby peak to the S/SE of your present position. This ridge forms a prominent peninsula in part responsible for separating the Upper and Lower Chewaucan marshes. Prominent shorelines of erosional origin are exhibited on the north side of this ridge at elevations from 4370 ft to near the highstand at 4520 ft (Allison, 1982; Friedel, 1993; Profile Site 9 from Pezzopane, this volume).

36.6 Chewaucan River and "The Narrows." Here the road crosses the Chewaucan River at the Narrows which separate the Upper and Lower Chewaucan Marsh subbasins. Dolly Friedel obtained C-14 dates from shell samples taken in the gravel bed against Tucker Hill to the west of the highway. These dates are reported in Friedel (this volume). Two clean, primary tephra were also sampled and sent to Nick Foit but did not correlate to any known ashes.

41.3 More prominent shorelines are seen east of the road along the slopes descending from the elongate N/NW trending ridge containing the Coglan Buttes. Shorelines below Coglan Buttes are largely developed in alluvial and colluvial fan deposits, mostly as depositional terraces notched from these non-cohesive deposits on the slope. Shorelines around the Coglan Butte "peninsula" into the Lake Abert basin (Profile 12 as well as 17, 16, 18) compared with those on the west side of the subbasins from nearby Tucker Hill ridge (Profile 9) and west of Valley Falls (Profile 11) has revealed a discrepancy of as much as 5 to 6 meters where the east side appears to have been displaced upwards relative to the west side. This may be evidence for tectonic deformation (Pezzopane, this volume).

43.4 Chewaucan River

45.4 Abert Rim. The Abert Lake subbasin is structurally a mirror image of the Summer Lake subbasin. It is a semi-graben tilted to the east with most of the offset occurring on the east side. Thus the prominent rim is on the east side of the valley. In the low light just before sundown, the capping basalt flow takes on a remarkable electric green glow due to lichens growing on the face.

Approximately half way down the colluvial slope below the lichen covered escarpment is the youngest trace of the Abert Rim fault, cutting across talus slopes and forming a scarp on averge 8 m in height that is developed in some of the lowest (and thus youngest?) pluvial and post-pluvial colluvium and alluvium near the base of the Rim. The Abert Rim fault seems similar in length and displacement to the Slide Mtn. fault; each having slip rates in the range from

0.3 ± 0.2 m/kyr, recurrence in the range from 5 to 10 kyr, and earthquake magnitudes as large as Mw 7. See Pezzopane (1993) and Pezzopane and Weldon (1993) for more information.

47.2 Valley Falls Junction.

This is the junction of Highways 31 and 395 and County Road 2-10. This junction is ~ 24 miles north of Lakeview, Oregon, the nearest large town. A small store with hospitable proprietors is located here where gas, diesel, propane, snacks, and gifts can be purchased. According to Keith Barnhart, the proprietor of a nearby guest ranch (inquire about the guest ranch specifics at the store), "the store was originally built in the late 1800's over under Abert rim directly east of the present site by a surveyor for a railroad, which never came to being. It was moved twice, the first time across the intersection from where it now sits and again to its present location after the highway was constructed. The part of the store that you first walk into where the groceries are is the original building; the back and the BS room were added when it was last moved. Jim Mathews has owned the store since 1996 and it has had a history of many owners throughout the years."

From the store, head westward along County Road 2-10.

49.7 Intersection with Access Road to Elder Ranch.

Take the left fork at this juncture heading NW continuing along County Road 2-10.

50.6 Stop Sa2-latest Pleistocene sediments at Willow Creek. *Licciardi. Fig. R8*

Note: Do not wander away from the County Road or its shoulder. We are travelling through private land and we do not have permission to leave the road.

AMS radiocarbon ages from gastropods in shore deposits within the pluvial Lake Chewaucan basin, combined with stratigraphic and geomorphic observations, identify a rise and fall of lake level at ~12 ^{14}C ka. Exposures of fine-grained sediments along Willow Creek provide key documentation of this lake-level oscillation. The basal zone of a 5.25 m measured section is dominated by massive to weakly laminated clay and silt, and coarsens upward into thinly-bedded silt and sand. The bluffs along Willow Creek in this vicinity contain exposures of sand units with climbing-ripple cross-lamination, normally graded gravely channel fill units that truncate the laminated silts and sands, and alluvial gravels. Principal bedding planes within the units are inclined gently (>10°) to the northeast (toward the basin), and the deposits underlie a low-gradient fan surface that extends into the Lower Chewaucan Marsh.

These deposits are interpreted as an assemblage of lacustrine and alluvial deposits within a fan delta that prograded into a former lake at the mouth of Willow Creek. In this interpretation, the finer grained lacustrine strata formed in the distal prodelta, and the coarser sands and silts were deposited in the proximal prodelta and delta front regions. The channel-fill facies mark the location of distributary channels within the fan-delta complex, or may have formed during subsequent dissection of the deltaic and lacustrine units as the lake level fell and the fan delta was abandoned. The development of a prograding fan delta at the emergence of Willow Creek into the former lake is a probable consequence of

high sedimentation rates at the creek mouth during a stable lake level. Gastropods were sampled from a silt bed approximately 1.65 m from the top of the measured section at an elevation of 1325 m, and yield an age of 11,934 ± 94 ^{14}C yr B.P. The surface elevation of 1335 m near the apex of the fan delta suggests that the lake level stabilized near this elevation during much of the period of fan delta construction, hence the radiocarbon age is considered to date a lake level that is closer to 1335 m. At this level, all three eastern subbasins of Lake Chewaucan would have held a coalesced lake, and any further rise above 1335 m would have resulted in overflow of the lake across the Paisley fan into the Summer Lake subbasin. Geomorphic observations in the Paisley fan area indicate that such an overflow event probably occurred at this time. The observations are the subject of today's last stop (Sa5).

52.6 Stop Sa3-Holocene sediments at Willow Creek. *Pezzopane. Fig. R8-9*

Here Willow Creek has dissected the Chewaucan shoreline deposits, and cut and filled a terrace or fan delta that contains the Mazama tephra. Perhaps the cut-and-fill sequences occurred more than once. This fill terrace is a notable site where datable materials and excellent exposures of pluvial and post-pluvial sediments can be observed.

Willow Creek appears to have cut and filled one or more terraces, the highest of which appears to grade with the Chewaucan highstand shoreline at ~4500 ft in elevation. Walls of the terrace are, in the tallest places, ~10 to 15 m in height and expose sequences of mostly fluvial sands and gravels, although some of the layers are well-bedded and thin, perhaps consistent with shallow lacustrine deposition (Figure SP5). Near the top of the valley, the fill has a surface at approximately 4480 ft that slopes gradually down gradient to approximately 4450 ft. Another relatively flatter and lower surface appears inset into the higher one at approximately 4420 ft and slopes down and fills the mouth of Willow Creek canyon at 4400 to 4390 ft, the elevation of the sill between Summer Lake and Upper Chewaucan Marsh, the tallest sill within the basin.

Burn layers and chunks of charcoal were sampled from ~2 m below the upper terrace surface at elevations of approximately 4380 to 4390 ft, not more than ~1.5 m above a prominent yellowish ash and pumice deposit that resembles the Mazama ash. The two charcoal samples sampled by Silvio Pezzopane yielded ages of 5600 ± 110 yr B.P. (Beta #52777) and 5840 ± 70 yr B.P. (Beta #52778), one sigma standard errors. Complementary ages were also obtained by Dolly Friedel from peats sampled 0.4, 1.8, 2.1, and 2.3 m below the top of the exposed bank. These ages, in order, are 3,295±50 (AA-26747), 5,105±55 (AA-26746), 5,925±60 (AA-26746), 5,990±60 (AA-26746), all in yr B.P.

The yellow ash is inferred to be the Mazama, yet, it has not been identified with laboratory methods.

58.0 Valley Falls Junction

From here, head NE on Highway 395 toward the east side of Lake Abert.

61.9 Stop Sa4-Latest Pleistocene sediments below Abert Rim, Geochemistry of Abert Lake sediments. *Licciardi, Jones. Fig. R1, 10-11*

Park in the gravel pit area on the east side of the road.

Well-preserved segments of wave-formed terraces occur along the eastern shoreline of modern Lake Abert, and mark the former level of pluvial Lake Chewaucan in this subbasin. Gastropod-bearing shore and nearshore deposits are exposed on the outer edge of these terraces, and provide evidence for the timing of two transgressive-regressive cycles of pluvial Lake Chewaucan (see Figure R10).

The most complete measured section occurs as an 8.0 m high road-cut exposure near the south end of Lake Abert. This section contains five distinct stratigraphic units. The basal 0.9 m (unit Qps) consists of interbedded sandy and pebbly strata, representing a wave-worked nearshore or beach environment. Pebble imbrication indicates a northward longshore current, and the poorly sorted character of the sediments suggests storm-influenced episodic deposition of coarser and finer strata. This unit is overlain by 2.15 m of silt and sand (unit Qss), which is interpreted as offshore sediment that records a lake transgression. The occasional pebbles in unit Qss may be dropstones that were carried offshore by lake ice. Unit Qss is in sharp contact with an overlying 0.7 m thick unit (Qg_1) of well-rounded beach gravels. Above unit Qg_1 is a 3.3 m thick unit (Qs) dominated by sand with occasional pebbles, inferred to represent a nearshore sand facies. Unit Qs is overlain by a gravel unit (Qg_2) which forms the uppermost 0.95 m of the section, and represents another beach gravel that grades upward into colluvium-dominated material. Gastropods were sampled from a bed ~ 2.25 m below the base of the terrace-capping Qg_2 beach gravels (11,560 ± 120 ^{14}C yr B.P.), and from the sandy matrix ~0.35 m above the base of these gravels (12,030 ± 90 ^{14}C yr B.P.). Note that these ages are stratigraphically reversed.

Another terrace segment occurs about 8 km to the north along the Lake Abert shoreline, and contains a 2.9 m high exposure with two distinct stratigraphic units. These units are correlated with the uppermost two units in the previously described section, on the basis of their very similar sedimentary character and stratigraphic position. Gastropods were sampled from ~0.2 m below the base of the beach gravels at this latter section, and yield an age of 11,670 ± 90 ^{14}C yr B.P.

The three radiocarbon ages from these terrace segments have a mean of 11,750 ± 180 ^{14}C yr B.P. Stratigraphic relations suggest that the associated terrace-capping beach gravels are regressive deposits, and the ~1310 m (4300 ft) elevation of their exposure at the outer edge of the terraces probably marks the lake level near the time of terrace abandonment. The lake at this level would have formed a coalesced body of water in the Lake Abert and Lower Chewaucan Marsh subbasins.

Shoreline Profile Site 13 is here across the shorelines notched into the fan from Cold Creek. Site 13 records perhaps as many as 15 to 20 different notches and ridges, one of the best sites in the Chewaucan basin for well developed and well preserved shorelines (Pezzopane, this volume). The Abert Rim fault scarp is about 6 to 8 m in height and can be seen (not easily) above the bedrock bench at elevations above 5000 ft and above Chewaucan shorelines.

Blair Jones will summarize research on the geochemistry of the sediments of Lake Abert.

65.8 Valley Falls Junction

86.8 Chewaucan River at Paisley

Drive very slowly at this point anticipating the view of the Paisley Fan/Delta sediments.

86.9 Cliff exposure of Paisley fan/delta sediments

Look to east at the outcrops on the north side of the Chewaucan River. These are sediments of the Paisley Fan/Delta. The finer, layered sediments at the base dip gently into the basin reminiscent of foreset beds. The overlying gravels were probably spread across the top of Paisley Flat by wave motion and currents in a shallow lacustrine environment (Allison, 1982).

87.5 Paisley Caves access road

89.0 Stop Sa5-Overflow Channel. *Friedel Fig. R4, R12*

This stop overlooks a wide spot in the sinuous overflow channel cut through the sill (~4,390 ft elevation) separating the Summer Lake subbasin from the rest of the Chewaucan subbasins. The channel is usually 100 or more feet wide and 10-15 feet deep. A small delta consisting of gravel and sand removed from the overflow channel was formed at the end of the channel at an elevation of ~4,340 ft (Allison, 1982). Because of the small size of these features, Allison (1982) surmised that they were formed over a relatively short period of time.

Several lines of reasoning, many of which have been discussed separately during the first two days of this field trip and some of which will be introduced here, converge to support the following enhanced version of Allison's (1982) model forwarded by Licciardi (in press) and Friedel (manuscript in preparation). First, the Chewaucan River fed the Summer Lake basin for most of the Pleistocene until diverted into the ZX basin by its own fan/delta complex during the regression of the last pluvial highstand (~14-15 ^{14}C ka B.P.). This hypothesis is supported by a) the fact that the Summer Lake subbasin has the lowest elevation of all the subbasins, b) the abundance of lacustrine sediments at depth in the Summer Lake subbasin and c) the lack of such sediments in cores from the Chewaucan Marshes. Second, the ZX basin lake rose back to the level of the newly formed sill and spilled over into the Summer Lake basin soon thereafter at ~12 ^{14}C ka stabilizing the lake at the spillover level though for only a short interval of time. This hypothesis is supported by a) the presence of the overflow channel and its associated delta, b) the small size of these features c) nearshore lacustrine sediments and tufa of this age near the spillover elevation throughout the Chewaucan subbasins (see Friedel, this volume and field trip stops Sa2 and Sa4), and c) the fact that the Willow Creek sediments of this age (Stop Sa2) were part of a fan delta built into the basin by Willow Creek during an interval of stable lake level.

91.9 Highway 31. Turn north and head back to campground.

The last day of the field trip will start with the geomorphology and archeology of the Paisley-Five Mile Caves, continue with a visit to a fossiliferous zone in Pleistocene lake sediments, and conclude with a presentation of ongoing work on the Winter Rim mass wasting features, particularly the Slide Mountain feature. Location maps are based on the Loco Lake, Slide Mtn. and Harvey Creek 7.5 minute USGS quads. Refer to Figures R1, R13, and R14 for today's trip.

0.0 Head south on Highway 31 from parking lot of Summer Lake Wildlife Refuge.

25.8 Access Road to Paisley Caves.

29.4 Stop Su1-Paisley Caves. *Aikens. Fig. R13*

Two obvious shoreline features were cut by waves into Five-Mile Point, a linear ridge of Tertiary volcanics. The most prominent of these features (4,485 ft) is fairly close to the Chewaucan highstand elevation of 4,520 ft. It is cut directly into the bedrock volcanic breccia producing a series of caves which were occupied by humans perhaps since the Pleistocene. The Mazama tephra are present in the cave deposits. The initial work on these archeological sites and others in the region (e.g. Fort Rock Cave) by L. Cressman quickly identified a need for geologic context which, in turn, led to Allison's research on pluvial lakes (Allison, 1982). See Aikens (this volume) for details on the archeology of this and related sites.

This site is Shoreline Profile 7 which shows a subtle notch at about 4500' elevation, several notches at lower elevations that are correlative with other sites nearby, and the bulky beach bar deposit at 4390'-4400', which corresponds to the beach platform that marks the top of the sill between Summer Lake and Upper Chewaucan Marsh (Pezzopane, this volume).

34.3 Stop Su2-Parking for Pleistocene Fossiliferous site. *Hills, Foit, Gobalet,. Fig. R13*

Note: This stop requires a walk of approximately 1 mile. Bring water.

In a low relief exposure probably caused by a combination of deflation and the erosion of a small rivulet, a fossil-rich zone was found in the Pleistocene sediments of Lake Chewaucan. Fish, various gastropods and a limpet are among the represented fauna. The richest concentration of fossils are confined to a ~20 cm interval near the base of 1 m of silts and sands which, in turn lies between two tephra layers. The bottom tephra layer is ~20 cm thick and contains coarse pumice fragments. The top tephra layer, probably the ~45-50 ka Mt St Helens Cy tephra layer, is ~ 5 cm thick and is graded with coarse flakes of biotite at the bottom grading up to a fine white ash at its top.

At this stop we'll discuss in detail the tephra correlations, fish fossils, and vertebrate fossils found nearby. An open discussion will follow on possible environmental factors resulting in such restricted fossiliferous intervals. Refer to article by Gobalet (this volume).

Saxon Sharpe (Desert Research Institute) has identified two families of taxa from a sampled mailed to her by Rob Negrini. The identification and a tentative interpretation are as follows.

Taxa:
Family Planorbidae (Ramshorn Snails)
Vorticifex (Parapholyx) effusa - found today in rivers and lakes in NV and OR. This was the dominant species in the assemblage.
Menetus sp 4 individuals

Gyraulus crista 2 individuals
Gyraulus sp. 9 individuals

Family Sphaeriidae (Fingernail and Pea Clams)
Pisidium sp. only 3 individuals in the assemblage.

According to Sharpe, this assemblage contained gastropod juveniles and many ostracodes. The presence of the gastropods infers a shallow water depth (at most a couple of meters). There is little or no solute chemistry data on Vorticifex and Menetus but, using Pisidium and Gyraulus, the TDS could have ranged from 20-2500 mg/L. Using a frequency distribution for these 2 taxa, the TDS would most likely range from 200-1000 mg/L, which is relatively fresh. This would indicate 1) a flow through system, or 2) the sample was collected from a site where relatively fresh groundwater was discharging into the lake. If the TDS values were higher (say, over 1500) the waters would most likely have greater bicarbonate relative to calcium as modern Pisidium has not been found in higher TDS waters with greater calcium relative to bicarb.

41.0 Overflow channel

42.9 Highway 31. Head north.

50.9 Government Harvey Pass Road. Turn left (west).

52.9 Overlook of intact bedrock stratigraphy

From this vantage point passengers in vehicles can view outcrops revealing what is probably the intact stratigraphy of this part of Winter Rim. The most noticeable unit from this vantage point is composed of well layered white tuffaceous rocks to the west (right) of the road. Distant outcrops of the next higher unit exhibit layered grey andesitic breccias. Finally, the rim is capped with a massive basalt flow > 100 ft thick. This basalt flow(s) can be observed up close by taking Government Harvey Pass Road all the way to the top of Winter Rim (we won't do this on this trip). Just before turning south towards the top on the last switchback is an overlook which is located on top of a flow tens of feet thick. Between there and the top, more lava is exposed in the roadcuts on the right (west) side of the road.

56.4 Intersection with Road #17. Turn left.

57.5 Stop Su3-Intersection with Road #329. *Casterline, Huff, Badger. Fig. R14*

Park the cars before the intersection with Road #329 and walk a few hundred feet past the intersection (on Road #17).

Refer to articles in this volume by Casterline and Huff and by Badger.

Here, silicic vent rocks and a capping basalt (mapped by Walker, 1963) are exposed atop the dramatic headscarp of the Slide Mtn. mass wasting feature. Exposed in the road are light colored tuffaceous rocks that appear stratigraphically and lithologically similar to units within other landslides along Winter Rim, suggesting that there is considerable lateral continuity of weak underlying strata. These light colored, bedded tuffaceous rocks are suspected to be responsible for the landsliding.
It's possible that this unit is correlative with the silicic breccias exposed at the "White Rock" slide. The position of this latter unit in the north is high on the rim, where toward the south, similar units are found lower in the section. This could explain the increased size of the landslides to the south.

One hypothesis for Slide Mtn. landslide is that it is a complex feature consisting of both rotational slump and slide components. Another hypothesis

would entail retrogression of the escarpment through multiple landslide events throughout the Pleistocene. In support of this hypothesis, are the presence of Monument Rock low down on the landslide complex and a relatively young, smaller landslide in White Hill Creek within an older, much larger landslide.

Future work by Badger will involve strength testing of relevant rock units. This information will be used to perform slope stability and deformational modeling to evaluate geologic and hydrologic controls on the initiation and rheology of landslides along Slide Mtn./Winter Rim escarpments.

Proceed north on Road #329.

58.1 Intersection with Road #3360. Turn right.

59.1 Stop Su4-Slide Lakes trailhead.

Casterline, *Huff*, *Badger*. *Fig*. *R14*

Park the cars and walk up the trailhead to the first Slide Lake.

The Slide Lakes are archetypical examples of ponds filling the bottom of rotational slump blocks near the escarpment. Given the well established tephrostratigraphy of the Lake Chewaucan area, a coring program in such lakes throughout the Winter Rim area would potentially yield an excellent chronology for the extensive history of mass wasting in the region.

62.3 Government Harvey Pass Road

65.0 Highway 31. End of 2001 FOP trip.

References Cited

Allison, I.S., 1945. Pumice Beds at Summer Lake, Oregon, G.S.A. Bull., v. 56., pp. 789-808.

Allison, I.S., 1949. Fault pattern of south-central Oregon (abs.): Geological Society of America Bulletin, v. 60, p. 1935.

Allison, I.S., 1982. Geology of Pluvial Lake Chewaucan, Oregon State Univ. Press, No. 11.

Antevs, E., 1948. Climate changes and pre-white man, Univ. Utah Bull., v. 38, pp. 167-191.

Baldwin, E. M., 1981. Geology of Oregon, 170 pp., Kendall/Hunt, Dubuque, Iowa.

Benson, L., 1999. Records of millennial-scale climate change from the Great Basin of the western United States *in* Clark, P. U., Webb, R. S., Keigwin, L., eds., Mechanisms of Global Climate Change, Am. Geophys. Un., Monograph #112, Washington, D.C.) p. 203-225.

Berger, G.W., 1991. The use of glass for dating volcanic ash by thermoluminescence. Jour. Geophys. Res., v. 96, pp. 19,705-19,720.

Berger, G.W. and Busacca, A.J., 1995, Thermoluminescence dating of late-Pleistocene loess and tephra from eastern Washington and southern Oregon, and implications for the eruptive history of Mount St. Helens. Journal of Geophysical Research: v. 100, p. 22,361-22,374.

Cohen, A.S., M.R. Palacios-Fest, R.M. Negrini, P.E. Wigand, and D.B. Erbes, 2000. A paleoclimate record for the past 250,000 years from Summer Lake, Oregon, U.S.A.: II. Lithostratigraphy, ostracodes, and pollen, Jour. Paleolimn., v. 24, pp. 151-182.

Davis, J.O., 1985. Correlation of late Quaternary tephra layers in a long pluvial sequence near Summer Lake, Oregon, Quat. Res., v. 23, pp. 38-53.

Conrey, R., J. Donnely-Nolan, E. Taylor, D. Champion, T. Bullen, submitted. The Shevlin Park Tuff, Central Oregon Cascade Range: Magmatic Processes in an Arc-Related Ash-Flow Tuff, EOS Transactions of the American Geophysical Union, Fall 2001 Meeting.

Crider, J G, in press. Oblique extension and the geometry of normal fault linkage: to appear in Journal of Structural Geology.

Crider, J G, D P Schaff, D D Pollard, and G C Beroza, 2001. Considering the third dimension in stress-triggering of aftershocks: 1993 Klamath Falls, Oregon, earthquake sequence: Geophysical Research Letters, v. 28 n. 14, p. 2739-2742.

Crider, J G, and D D Pollard, 1998. Fault linkage: 3D mechanical interaction between overlapping normal faults: Journal of Geophysical Research, v. 103, p. 24,373-24,391.

Davis, J.O., 1983. Level of Lake Lahontan during deposition of the Trego Hot Springs tephra about 23,400 yrs ago. Quaternary Research: v. 19, p. 312-324.

Davis, J.O., 1985. Correlation of late Quaternary tephra layers in a long pluvial sequence near Summer Lake, Oregon. Quaternary Research: v. 23, p. 38-53.

Diggles, et al., 1990. Geologic map of the Diablo Mountain Wilderness Study Area, Lake County, Oregon, USGS Misc. Field Studies Map MF-2121.

Donath, R., 1962. Analysis of basin-range structure, south-central Oregon: Geological Society of America Bulletin, v. 73, p. 1-16.

Erbes, D., 1996. Late Pleistocene lithostratigraphy of Pluvial Lake Chewaucan, Oregon: Implications for past climate variation, M.S. Thesis, Dept. Physics and Geology, CSU Bakersfield, 111 p.

Evenden, J.F., Savage, D.E., Curtis, G.H., and G.T., James, 1964. Potassium-argon dates and the Cenozoic mammalian chronology of North America: American Journal of Science, v. 262, p. 145-198.

Foster, T., 1989. Settlers in Summer Lake Valley, Maverick Press, Bend, Ore.

Friedel, 1993. Chronology and climatic controls of late Quaternary lake-level fluctuations in Chewaucan, Fort Rock, and Alkali basins, south-central Oregon, M.S. thesis, Dept. Geography, University of Oregon, 244 p.

Gardner, J.V., J.P. Bradbury, W.E. Dean, D.P. Adam, and A.M. Sarna-Wojcicki, 1992. Report of workshop '92 on the correlation of marine and terrestrial records of climate change in the western United States, USGS Open File Rpt.

Grayson, D.K., 1993. The Desert's Past: A Natural PreHistory of the Great Basin, Smithsonian Press.

Herrero-Bervera , E., Helsley, C.E., Sarna-Wojcicki, A.M., Lajoie, K.R., Meyer, C.E., Turin, B.E., Donelly-Nolan, J.M., McWilliams, M.O., Negrini, R.M., and Liddicoat, J.C., 1994. Age and correlations of a paleomagnetic episode in the western United States by 40Ar/39Ar dating and tephrochronolgy: The Jamaica, Blake, or a new polarity episode?, J. of Geophys.l Res., 99, 24,091-24,103.

Langridge, R., 1998. Paleoseismic deformation in behind-arc lacustrine settings: Acambay, Mexico and Ana River, Oregon, Ph.D. Dissertation, Dept. Geology, University of Oregon, 188 p.

Lanphere, M.A., D.E. Champion, R.L. Christiansen, J.M. Donnelly-Nolan, R.J. Fleck, and A.M. Sarna-Wojcicki, 1999. Evolution of tephra dating in the western United States: Geol. Soc. Am. Metting and Abstr., Cord. Sect., v. 100, p. A-73.

Lawrence, R. D., 1976. Strike-slip faulting terminates the Basin and Range province in Oregon: Geological Society of America Bulletin, v. 87, p. 846-850.

Licciardi, J. 2001. Chronology of Latest Pleistocene lake-level fluctuations in the Pluvial Lake Chewaucan Basin, Oregon, USA: Journal of Quaternary Science, in press.

Negrini, R.M., D.B. Erbes, A.P. Roberts, K.L. Verosub, A.M. Sarna-Wojcicki, and C.E. Meyer, 1994. Repeating waveform initiated by a 180-190 ka geomagnetic excursion in western North America: Implications for field behavior during polarity transitions and subsequent secular variation. Jour. Geophy. Res., v. 99., p. 24,105-24,119.

Negrini, R.M., D.B. Erbes, K. Faber, A.M. Herrera, A.P. Roberts, A.S. Cohen, P.E. Wigand, and F.F. Foit, Jr., 2000. A Paleoclimate record for the past 250,000 years from Summer Lake, Oregon, U.S.A.: I. Age control and magnetic lake level proxies, Jour. of Paleolimn., v. 24, p. 125-149

Orr, E.L., and W.N. Orr, 1996. Geology of the Pacific Northwest: McGraw-Hill Co., Inc., New York, 409 p., maps

Orr, E.L., W.N. Orr, and E.M. Baldwin, 1992. Geology of Oregon: Kendall/Hunt Publishing Co., Dubuque, Iowa, 254 p., 4th Edition Rev. of: Geology of Oregon by Ewart M. Baldwin. 3rd ed., 1981.

Peterson, N. V., and J. R. McIntyre, 1970. The reconnaissance geology and mineral resources of Eastern Klamath County and Western Lake County, Oregon: Oregon Dept. of Geol. and Min. Ind. Bull. 66, 70 pp.

Pezzopane, 1993. Active faults and earthquake ground motions in Oregon, Ph.D. Dissertation, Dept. Geology, University of Oregon, 208 p.

Pezzopane, S. and R. Weldon, 1993. Tectonic role of active faulting in central Oregon, *Tectonics*, v. 12, p. 1,140-1,169.

Pezzopane S. K., A. M. Sarna-Wojcicki, R. J. Weldon, and R. L. Langridge, 1996. Slip rate and recurrence intervals for the Ana River fault, Oregon, *Geol. Soc Amer. Abstr. with Prog.*, v. 28, no. 5, p. 101.

Reches, Z., 1983. Faulting of rocks in three-dimensional strain fields, II. Theoretical analysis,: Tectonophysics, v. 95, p. 133-156.

Simpson, G., 1990. Late Quaternary tectonic development of the northwestern part of the Summer Lake Basin, south-central Oregon, M.S. Thesis, Dept. Geology, Humbolt State University, 121 p.

Travis, P.L., 1977. Geology of the area near the north end of Summer Lake, Lake Co., Oregon, M.S. Thesis, Dept. Geology, University of Oregon, 79 p.

Walker, G.W., 1963. Reconnaissance geologic map of the eastern half of the Klamath Falls (AMS) Quadrangle, Lake and Klamath Counties, Oregon, USGS Min. Invest. Field Studies Map, MF-260.

Walker, G.W., 1973. Preliminary geologic and tectonic maps of Oregon east of the 121st meridian. USGS Misc. Field Studies MF-495.

Walker, G.W., 1977. Geologic map of Oregon east of the 121st meridian: U.S. Geological Survey, Miscellaneous Investigations Series Map I-902, scale 1:500000.

Walker, G.W. and MacLeod, N.S., 1991. Geologic map of Oregon: U.S. Geological Survey, scale 1:500000.

Walker, G. W., N. V. Peterson, and R. C. Greene, 1967. Reconnaissance geologic map of the east half of the Crescent quadrangle, Lake, Deschutes, and Crook counties, Oregon: U.S. Geological Survey Map I-493, scale 1:250,000.

Waring, G.A., 1908. Geology and water resources of a portion of south-central Oregon, USGS Water-Supply Paper 220, 86 p.

Table 1. Volcanic ash samples and localities at Summer Lake associated with TL dates[a]

Name	TL Name	Locality	Reference[b]
Known Age			
tephra 18 (Trego Hot Springs)	SML-10	site E	1
Unknown Age			
tephra 12 (MSH set Cy)	SML-7	site E	1
tephra 2	SML-24ab	site C, 2.1 m	2
tephra N	SML-18	site E, 5.1 m	2
tephra R	SML-1a	site C, 5.6 m	2
tephra KK	SML-21a	site C, 11.2 m	2
tephra LL	SML-5	site C, 11.9 m	2

[a]TL results for tephra 12 (correlated to Mt. St. Helens set Cy) are in Berger and Busacca (1995), for the others, in Berger (1991).
[b]Site descriptions as follows: 1, Davis (1983, 1985); 2, Davis (1985)

Road Log Erratum

p. 14, mi 32.6: [Replace with]
Beachler's Trading Post 31

Road Log Addenda

p. 1, mi 7.3: [Add Dolly Friedel and Saxon Sharpe as coauthors]

p. 3, mi 3.6: [Add before *Tectonic/Geologic Background*].
We'll also walk a few tens of meters to the south to view an ash layer sampled in the gravel bed by Langridge and later by Negrini. Analyses done by two different tephrochronologists (Sarna-Wojcicki and Foit, respectively) suggest that this ash may be one of the ~165 ka ashes found below the major unconformity in Ana River Canyon section C.

p. 6, mi 7.3: [Add *Conrey and Champion* as field stop leaders]

p. 15, mi 36.6: [Replace with]
Chewaucan River and "The Narrows." Here the road crosses the Chewaucan River at the Narrows which separate the Upper and Lower Chewaucan Marsh subbasins. Dolly Friedel obtained C-14 dates from shell samples taken in the gravel bed against Tucker Hill to the west of the highway. These dates are reported in Friedel (this volume). Two clean, primary tephra were also sampled and sent to Nick Foit but did not correlate to any known ashes.

p. 15, mi 47.2: [Add]
According to Keith Barnhart, the proprietor of a nearby guest ranch (inquire about the guest ranch specifics at the store), "the store was originally built in the late 1800's over under Abert rim directly east of the present site by a surveyor for a railroad, which never came to being. It was moved twice, the first time across the intersection from where it now sits and again to its present location after the highway was constructed. The part of the store that you first walk into where the groceries are is the original building; the back and the BS room were added when it was last moved. Jim Mathews has owned the store since 1996 and it has had a history of many owners throughout the years."

p. 17, mi 52.6: [Add]
Complementary ages were also obtained by Dolly Friedel from peats sampled 0.4, 1.8, 2.1, and 2.3 m below the top of the exposed bank. These ages, in order, are 3,295±50 (AA-26747), 5,105±55 (AA-26746), 5,925±60 (AA-26746), 5,990±60 (AA-26746), all in yr B.P.

p. 22, mi 56.4: [Add]
Turn left.

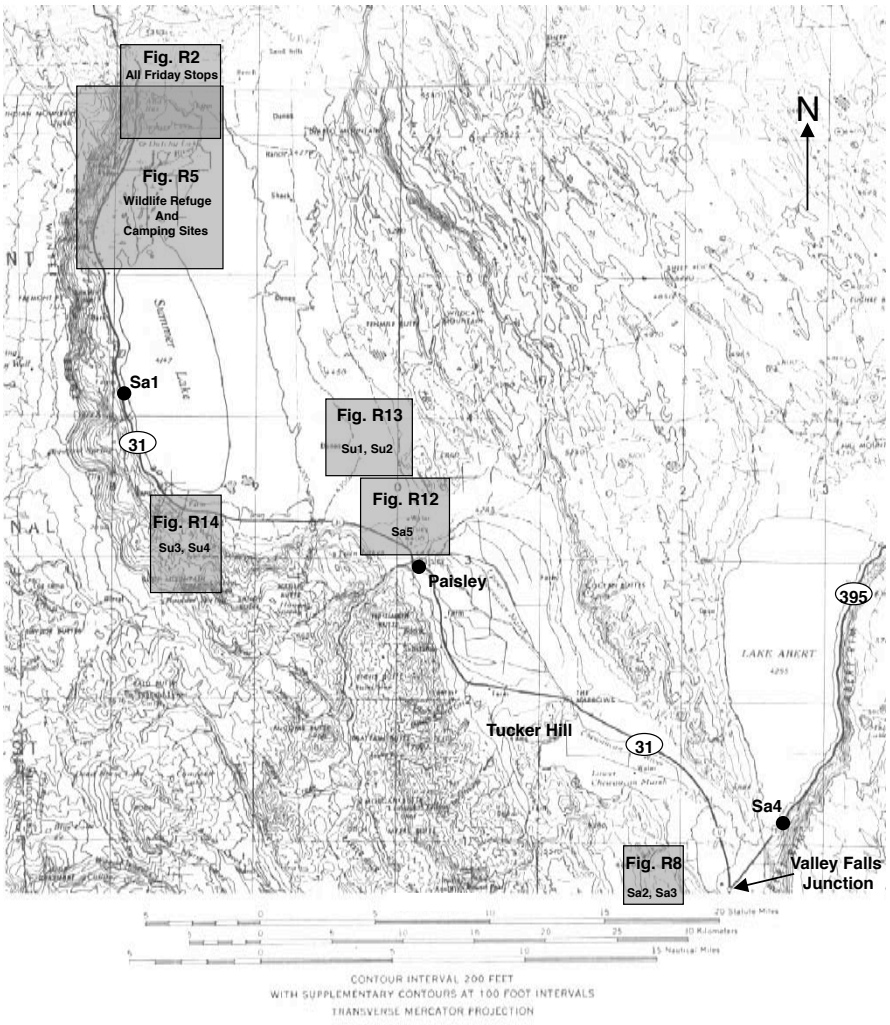

Figure R1. Locations of stops and key landmarks and Figure coverage for 2001 NWP FOP trip. Base maps are Klamath Falls and Crescent USGS 2˚ Topo sheets.

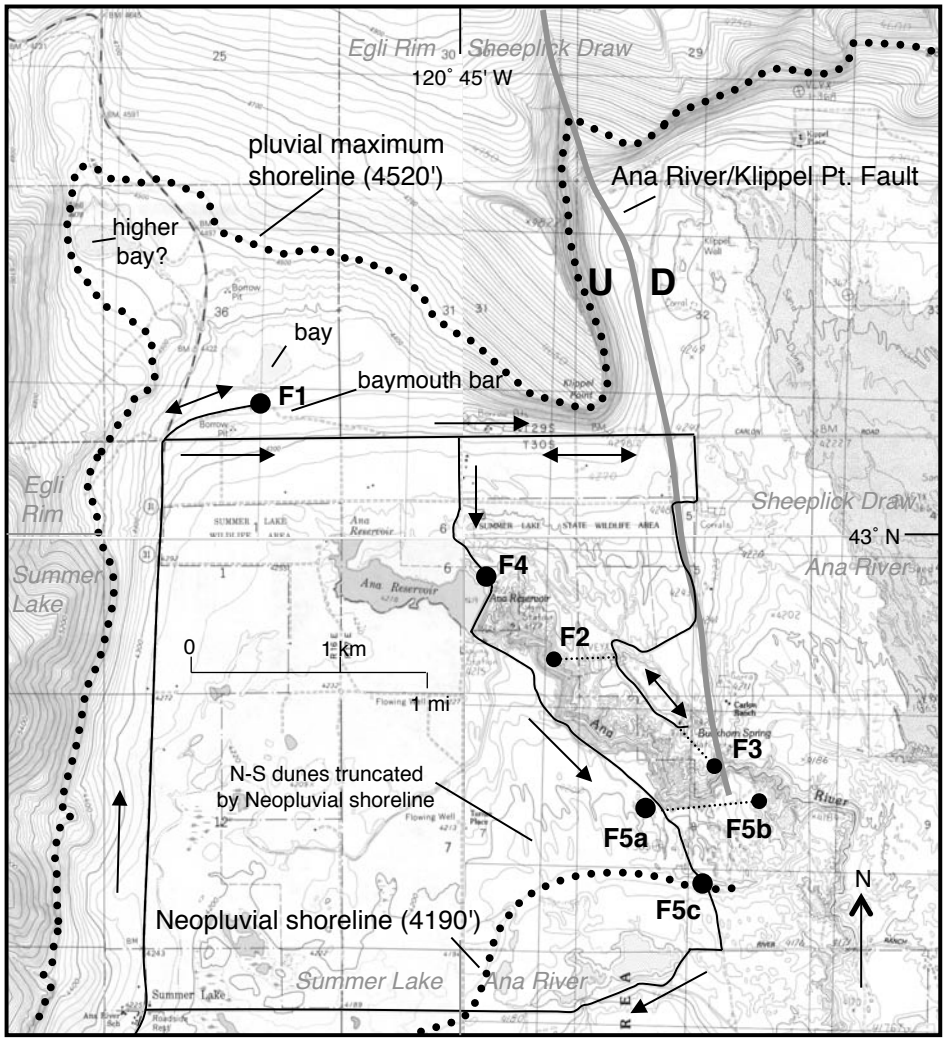

Figure R2a. Location of Day 1 route and field trip stops. The trace of the fault is plotted after Pezzopane (1993) and Simpson (1990). The position of the highest Chewaucan shoreline is after Allison (1982). The base maps are the four USGS 7.5 minute quadrangles indicated in gray italics. The black dotted lines indicate walking paths to stops F2, F3, and F5b.

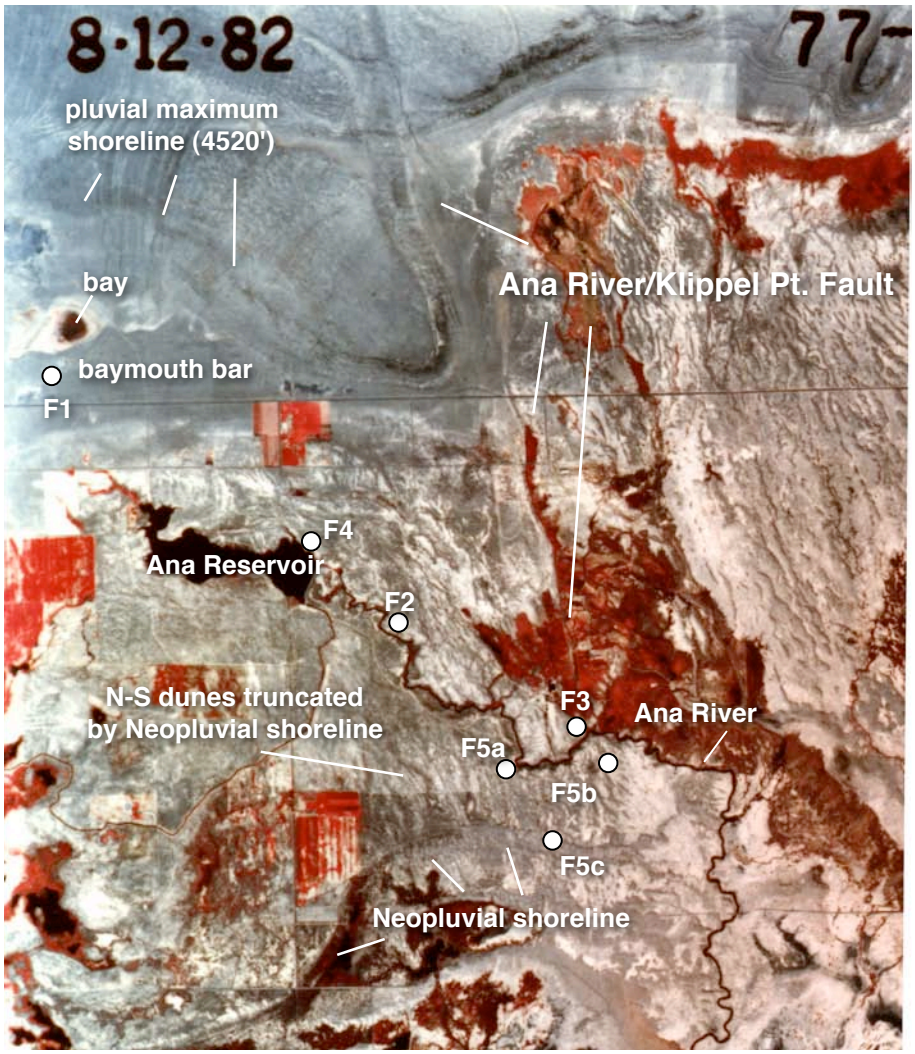

Figure R2b. Air photo at approximately the same scale as Figure 2. Note expression of pluvial maximum and neopluvial shorelines. Note also expression of fault and dune fields to the east of the fault. Field trip stops are plotted for reference.

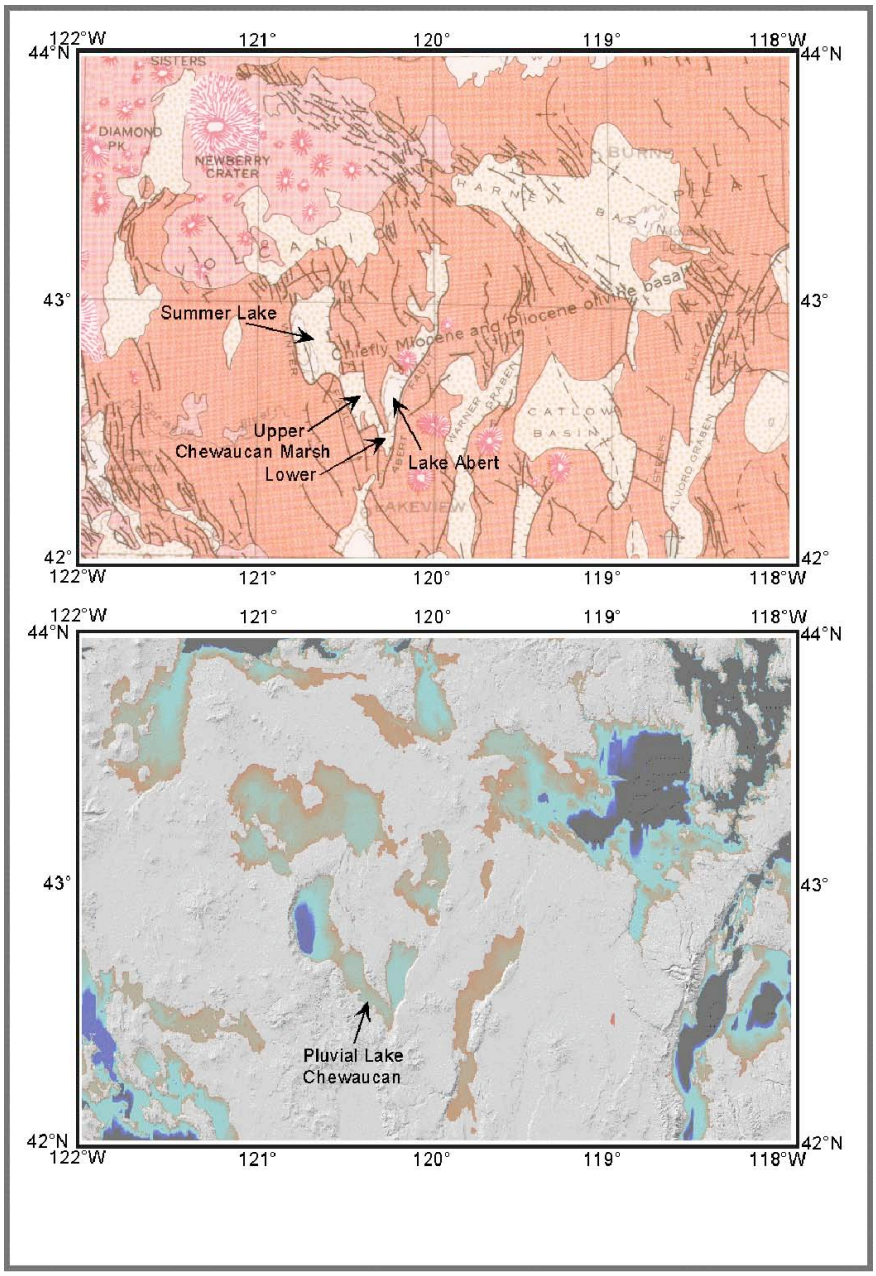

FIGURE R3. *Top:* Simplified geologic map of basement structure in the pluvial Lake Chewaucan region, south-central Oregon. *Bottom* Shaded relief elevation model of topographic features and ancient lake basins in the pluvial Lake Chewaucan region, south-central Oregon.

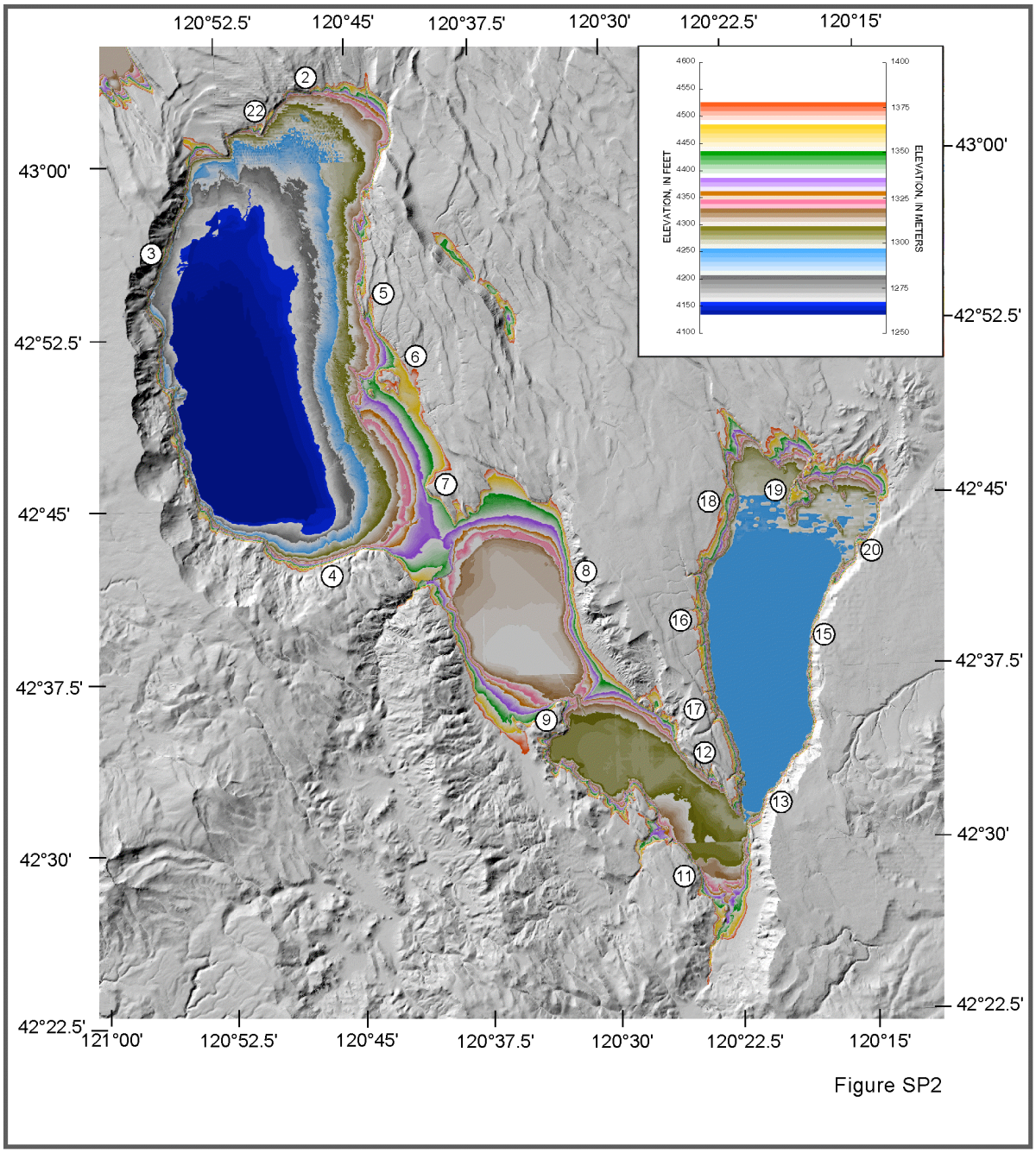

FIGURE R4. Shaded digital elevation model of the elevations of significant Lake Chewaucan shoreline features and the locations of shoreline profile sites. Color gradients are used to indicate the elevations of significant lake and shoreline features recognized by Allison (1984), Pezzopane (1993), and later unpublished work by S. Pezzopane. The digital elevation model is from U.S. Geological Survey 7.5 minute topographic maps having 10 m vertical accuracy. Some anomalous color and textural patterns are apparent at boundaries of the quadrangles where errors in the digital elevations occur.

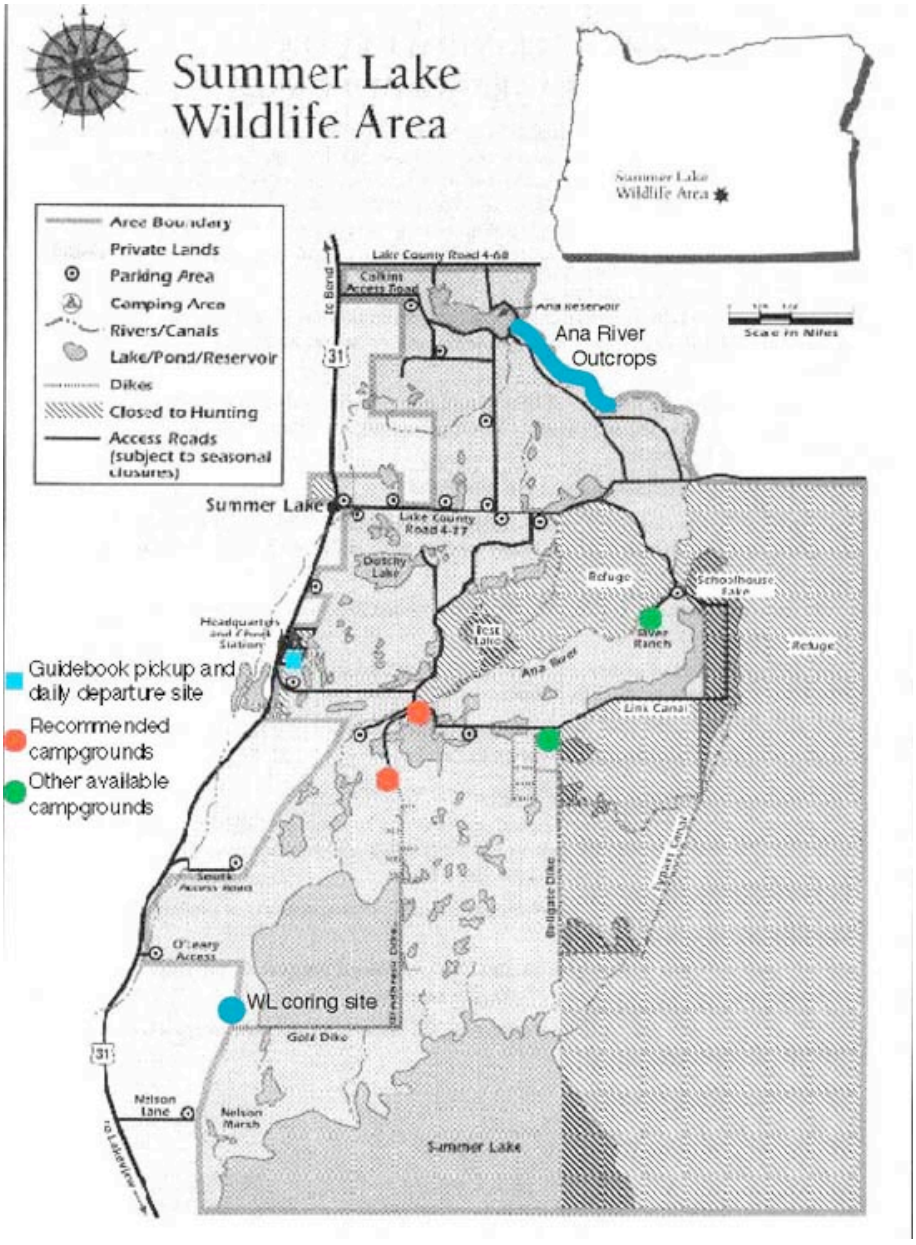

Figure R5. Map of Summer Lake Wildlife Area to accompany presentation at Stop F1 by M. St. Louis of the Oregon Department of Fish and Wildlife.

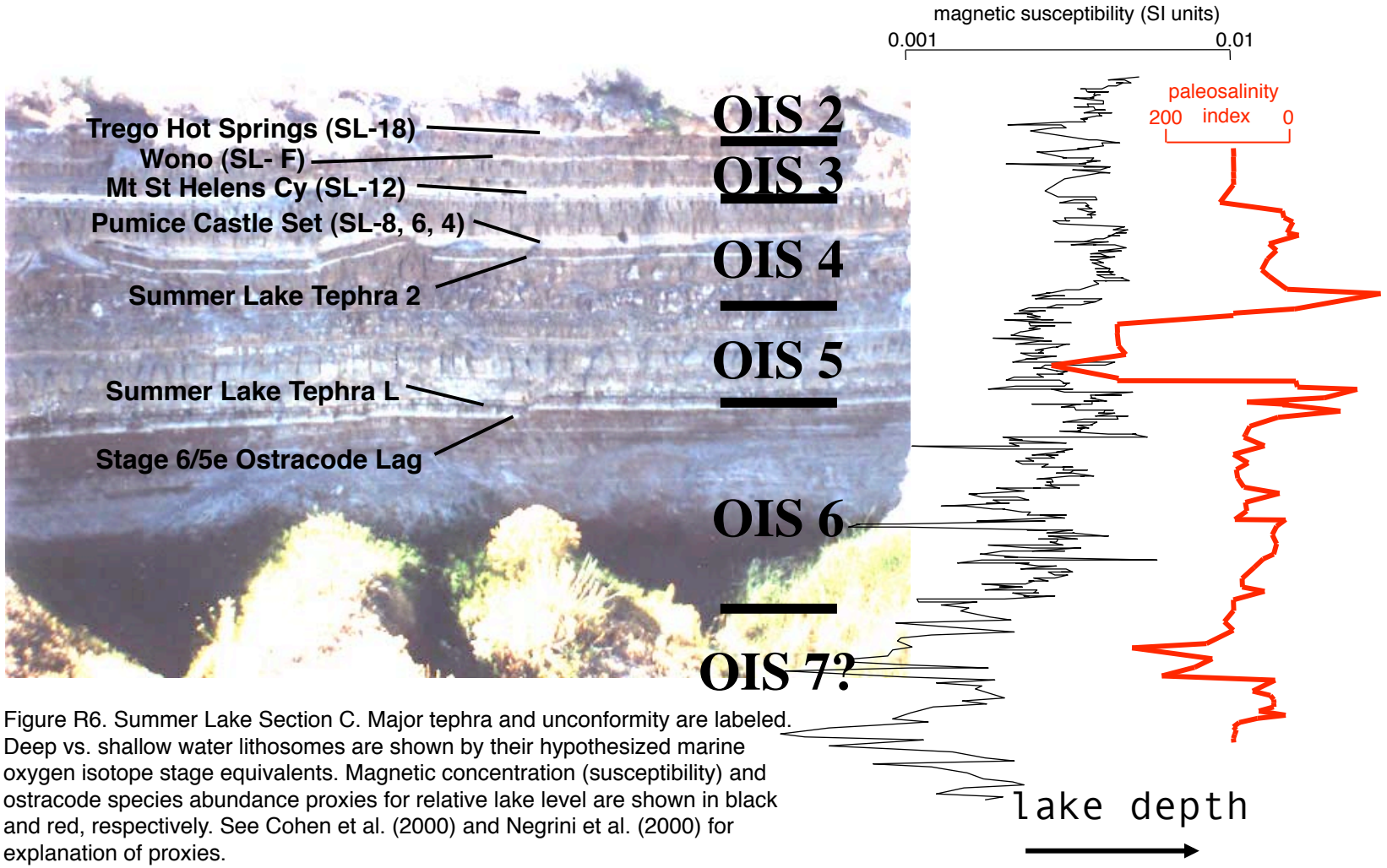

Figure R6. Summer Lake Section C. Major tephra and unconformity are labeled. Deep vs. shallow water lithosomes are shown by their hypothesized marine oxygen isotope stage equivalents. Magnetic concentration (susceptibility) and ostracode species abundance proxies for relative lake level are shown in black and red, respectively. See Cohen et al. (2000) and Negrini et al. (2000) for explanation of proxies.

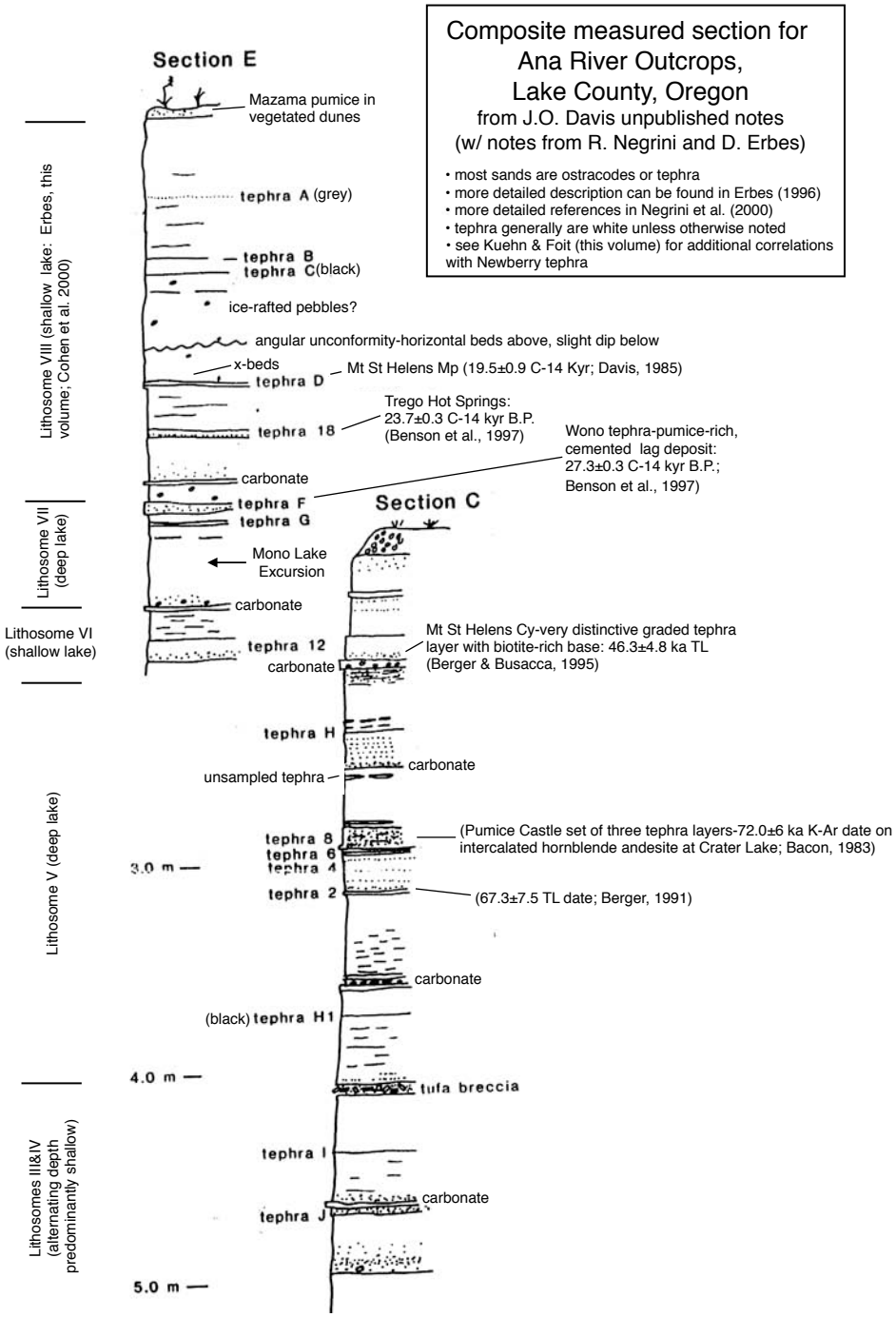
Composite measured section for
Ana River Outcrops,
Lake County, Oregon
from J.O. Davis unpublished notes
(w/ notes from R. Negrini and D. Erbes)
• most sands are ostracodes or tephra
• more detailed description can be found in Erbes (1996)
• more detailed references in Negrini et al. (2000)
• tephra generally are white unless otherwise noted
• see Kuehn & Foit (this volume) for additional correlations with Newberry tephra
Section E
Mazama pumice in vegetated dunes
tephra A (grey)
tephra B
tephra C(black)
ice-rafted pebbles?
angular unconformity-horizontal beds above, slight dip below
x-beds
tephra D
Mt St Helens Mp (19.5±0.9 C-14 Kyr; Davis, 1985)
tephra 18
Trego Hot Springs: 23.7±0.3 C-14 kyr B.P. (Benson et al., 1997)
Wono tephra-pumice-rich, cemented lag deposit: 27.3±0.3 C-14 kyr B.P.; Benson et al., 1997)
carbonate
tephra F
tephra G
Section C
Mono Lake Excursion
carbonate
tephra 12
carbonate
Mt St Helens Cy-very distinctive graded tephra layer with biotite-rich base: 46.3±4.8 ka TL (Berger & Busacca, 1995)
tephra H
carbonate
unsampled tephra
tephra 8
tephra 6
tephra 4
tephra 2
(Pumice Castle set of three tephra layers-72.0±6 ka K-Ar date on intercalated hornblende andesite at Crater Lake; Bacon, 1983)
(67.3±7.5 TL date; Berger, 1991)
3.0 m
carbonate
(black) tephra H1
4.0 m
tufa breccia
tephra I
carbonate
tephra J
5.0 m
Lithosome VIII (shallow lake: Erbes, this volume; Cohen et al. 2000)
Lithosome VII (deep lake)
Lithosome VI (shallow lake)
Lithosome V (deep lake)
Lithosomes III&IV (alternating depth predominantly shallow)

Figure R7a

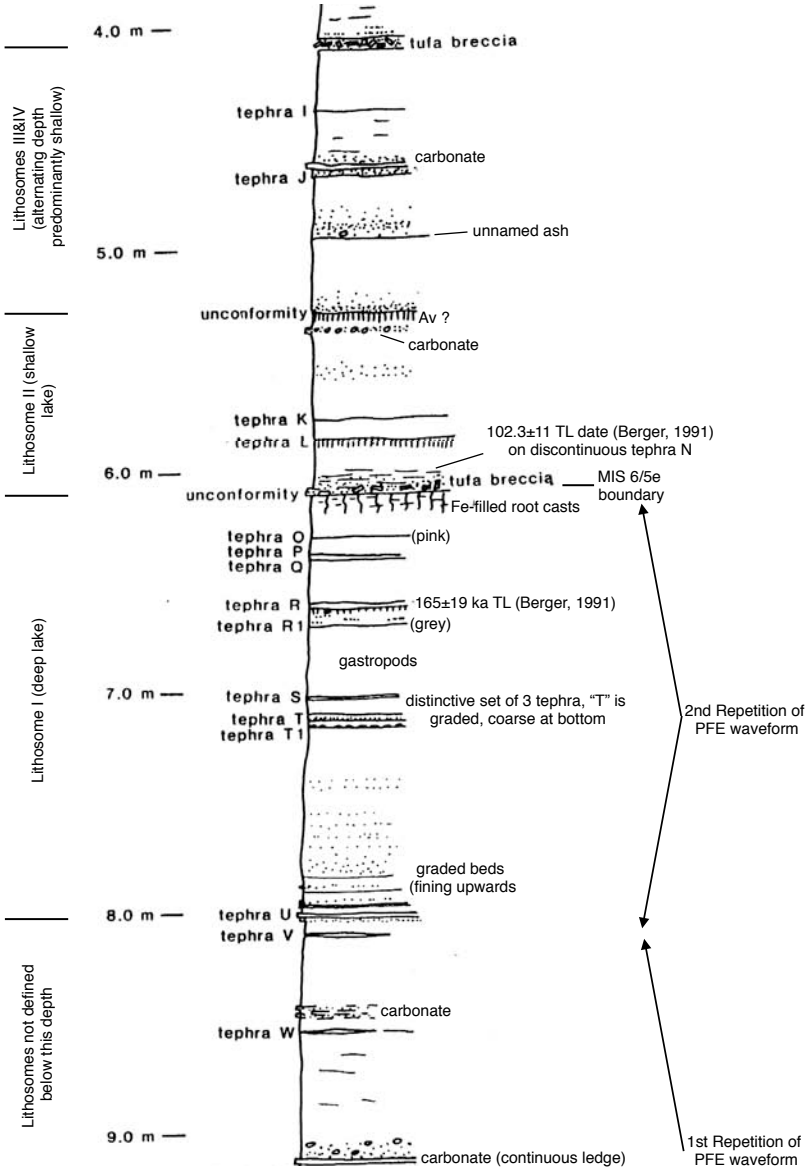
4.0 m
tufa breccia
Lithosomes III&IV (alternating depth predominantly shallow)
tephra I
carbonate
tephra J
unnamed ash
5.0 m
unconformity
Av ?
carbonate
Lithosome II (shallow lake)
tephra K
tephra L
102.3±11 TL date (Berger, 1991) on discontinuous tephra N
6.0 m
tufa breccia
MIS 6/5e boundary
unconformity
Fe-filled root casts
tephra O
(pink)
tephra P
tephra Q
tephra R
165±19 ka TL (Berger, 1991)
tephra R1
(grey)
gastropods
Lithosome I (deep lake)
7.0 m
tephra S
distinctive set of 3 tephra, "T" is graded, coarse at bottom
tephra T
tephra T1
2nd Repetition of PFE waveform
graded beds (fining upwards
8.0 m
tephra U
tephra V
Lithosomes not defined below this depth
carbonate
tephra W
9.0 m
carbonate (continuous ledge)
1st Repetition of PFE waveform

Figure R7b

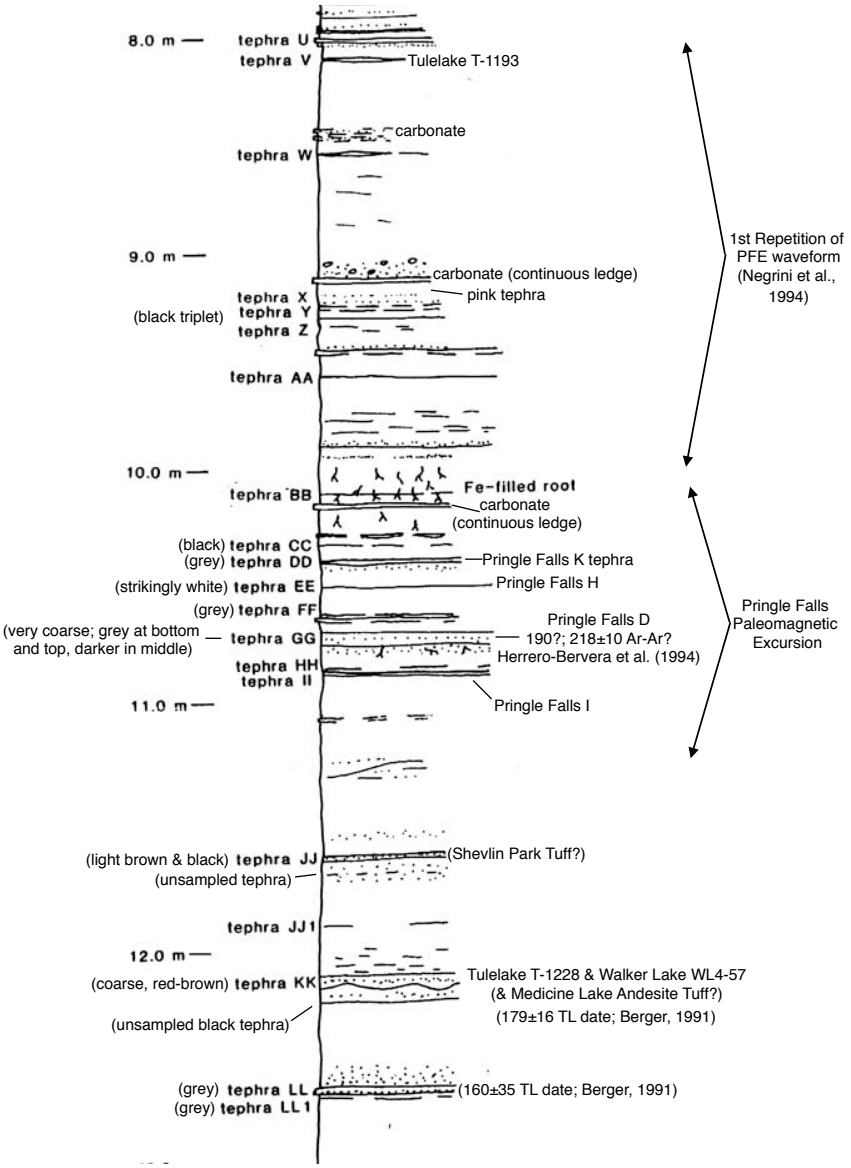
8.0 m
tephra U
tephra V
Tulelake T-1193
carbonate
tephra W
9.0 m
carbonate (continuous ledge)
pink tephra
tephra X
tephra Y
(black triplet)
tephra Z
tephra AA
1st Repetition of PFE waveform (Negrini et al., 1994)
10.0 m
tephra BB
Fe-filled root
carbonate
(continuous ledge)
(black) tephra CC
(grey) tephra DD
Pringle Falls K tephra
(strikingly white) tephra EE
Pringle Falls H
(grey) tephra FF
(very coarse; grey at bottom and top, darker in middle)
tephra GG
Pringle Falls D
190?; 218±10 Ar-Ar?
Herrero-Bervera et al. (1994)
tephra HH
tephra II
Pringle Falls I
Pringle Falls Paleomagnetic Excursion
11.0 m
(light brown & black) tephra JJ
(Shevlin Park Tuff?)
(unsampled tephra)
tephra JJ1
12.0 m
(coarse, red-brown) tephra KK
Tulelake T-1228 & Walker Lake WL4-57
(& Medicine Lake Andesite Tuff?)
(179±16 TL date; Berger, 1991)
(unsampled black tephra)
(grey) tephra LL
(160±35 TL date; Berger, 1991)
(grey) tephra LL1

Figure R7c

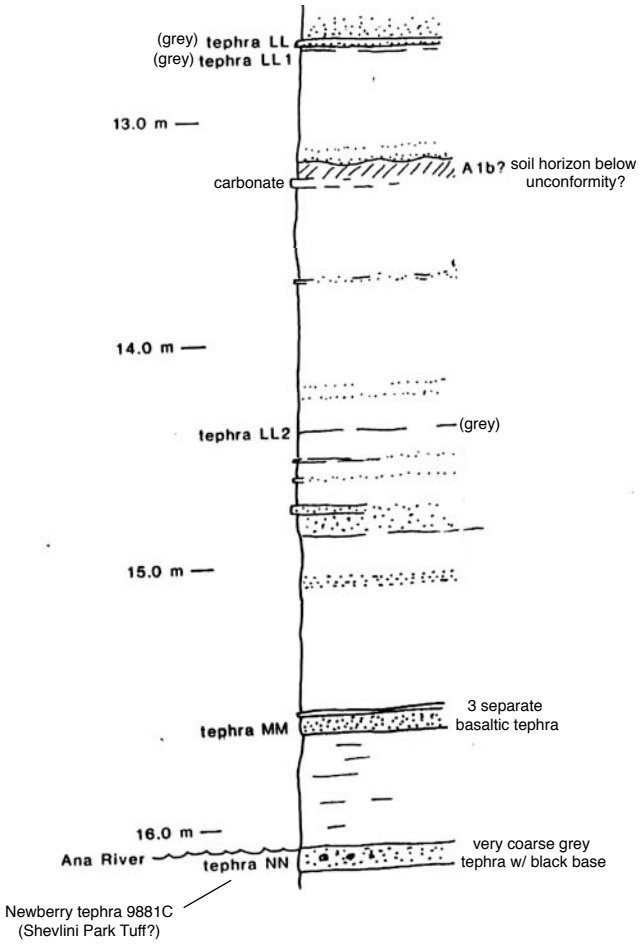
(grey) tephra LL
(grey) tephra LL1
13.0 m
A1b? soil horizon below unconformity?
carbonate
14.0 m
tephra LL2
(grey)
15.0 m
3 separate basaltic tephra
tephra MM
16.0 m
very coarse grey tephra w/ black base
Ana River
tephra NN
Newberry tephra 9881C
(Shevlini Park Tuff?)

Figure R7d

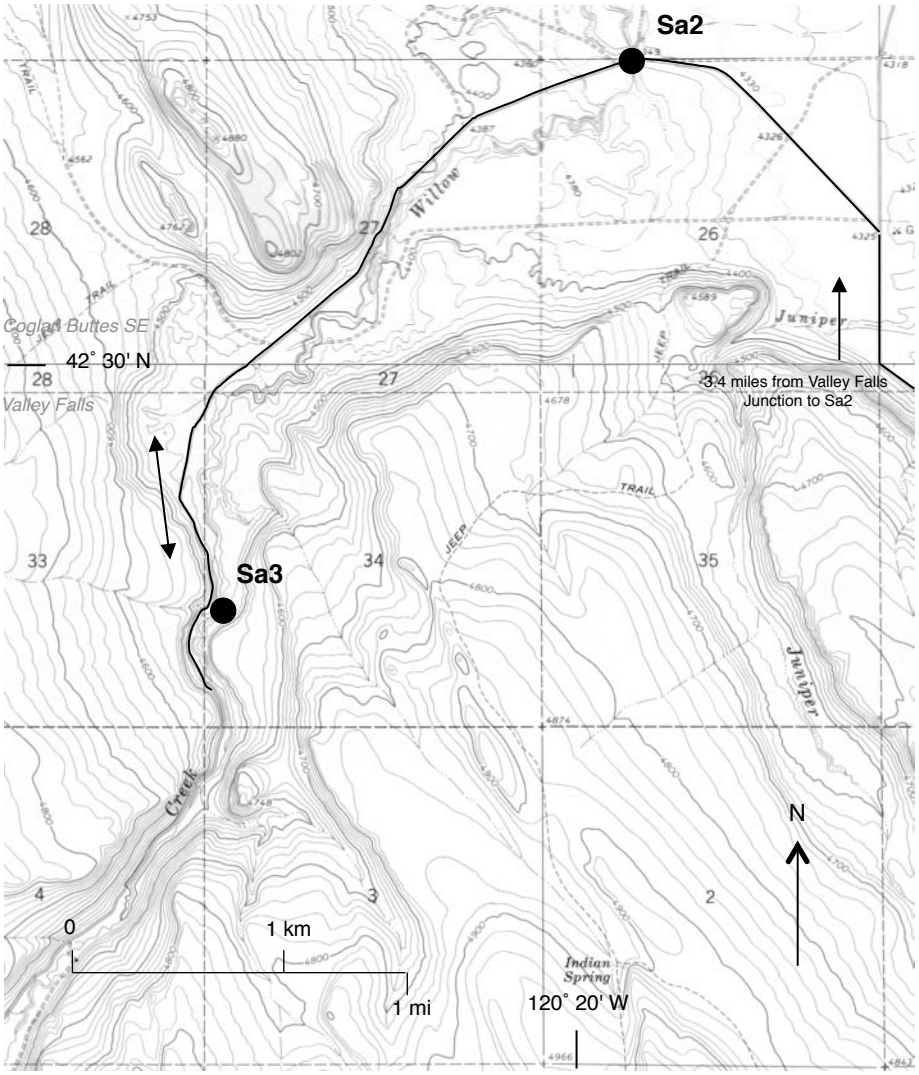

Figure R8. Location of field trip stops Sa2 and Sa3. See Roadlog for descriptions of stops.

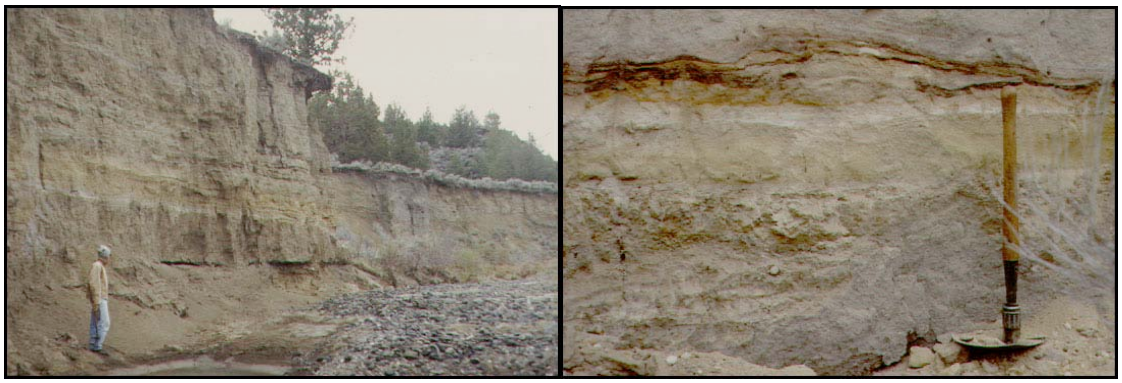

FIGURE R9. Photograph of exposures of Willow Creek fill terrace. *Left* Photograph of cut bank of Willow Creek showing exposure of fill deposits and interbedded (Mazama?) ash which is approximately 1 meter above person standing for scale. *Right:* Photograph of bedded ash with folding shovel for scale.

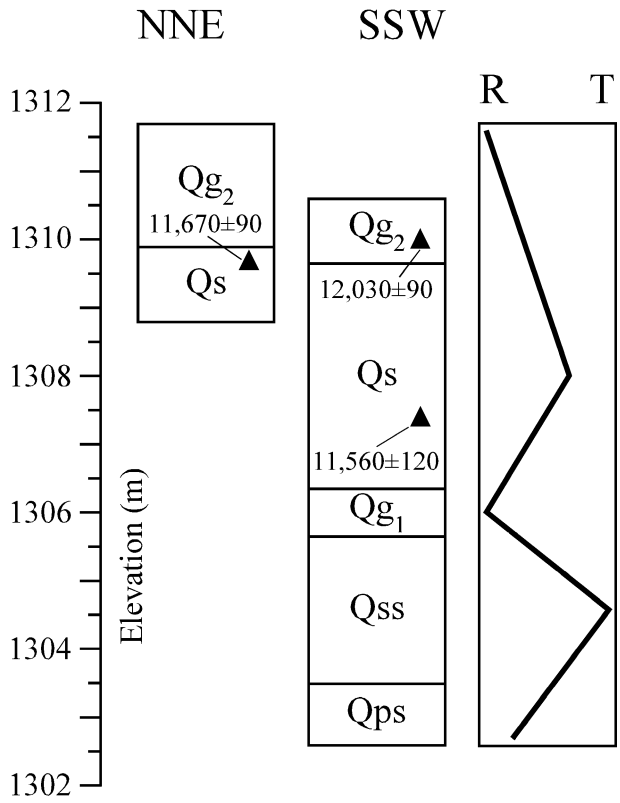

FIGURE R10. Measured stratigraphic sections along the east shore of Lake Abert, with a schematic curve of regressive (R) and transgressive (T) lake cycles. Labeled stratigraphic units are keyed to the field trip guide. Black triangles mark the location of radiocarbon-dated gastropods. Ages are in ^{14}C yr B.P. (from Licciardi, in press).

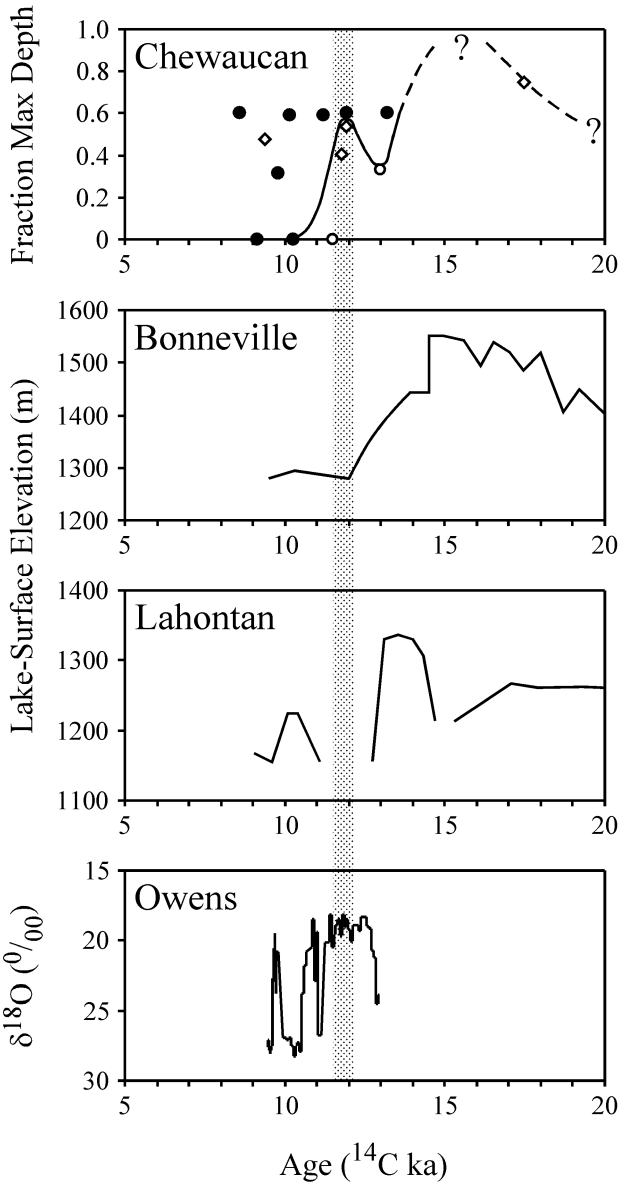

Figure R11. Lake-level curves and lake-size proxies of Great Basin pluvial lakes from 20-5 ^{14}C ka, arranged generally north (top panel) to south (bottom panel). The Lake Chewaucan curve is a composite reocrd of lake-level data, normalized to the fraction of maximum lake depth, from the Chewaucan and Fort Rock basins (after Negrini, in press, and references therein). Open diamonds denote material formed below lake level in the Fort Rock basin. Solid circles denote archeological sites and other material formed above lake level in the Fort Rock basin. The question mark obscuring the precise timing of the maximum highstand indicates the conjectural nature of its age, and dashed lines indicate poorly constrained portions of the curve. The stippled column identifies the approximate timing of the Chewaucan lake-level oscillation. The curves for lakes Bonneville and Lahontan are generalized from published data of Benson et al. (1995; 1997), Oviatt et al. (1992), Oviatt (1997), Adams and Wesnousky (1998), and references therein. The Owens Lake d18O proxy data are from core OL84B using the age model of Benson (1999); d18O minima (plotted as peaks) are proxies of wet oscillations in the basin. (from Licciardi, in press).

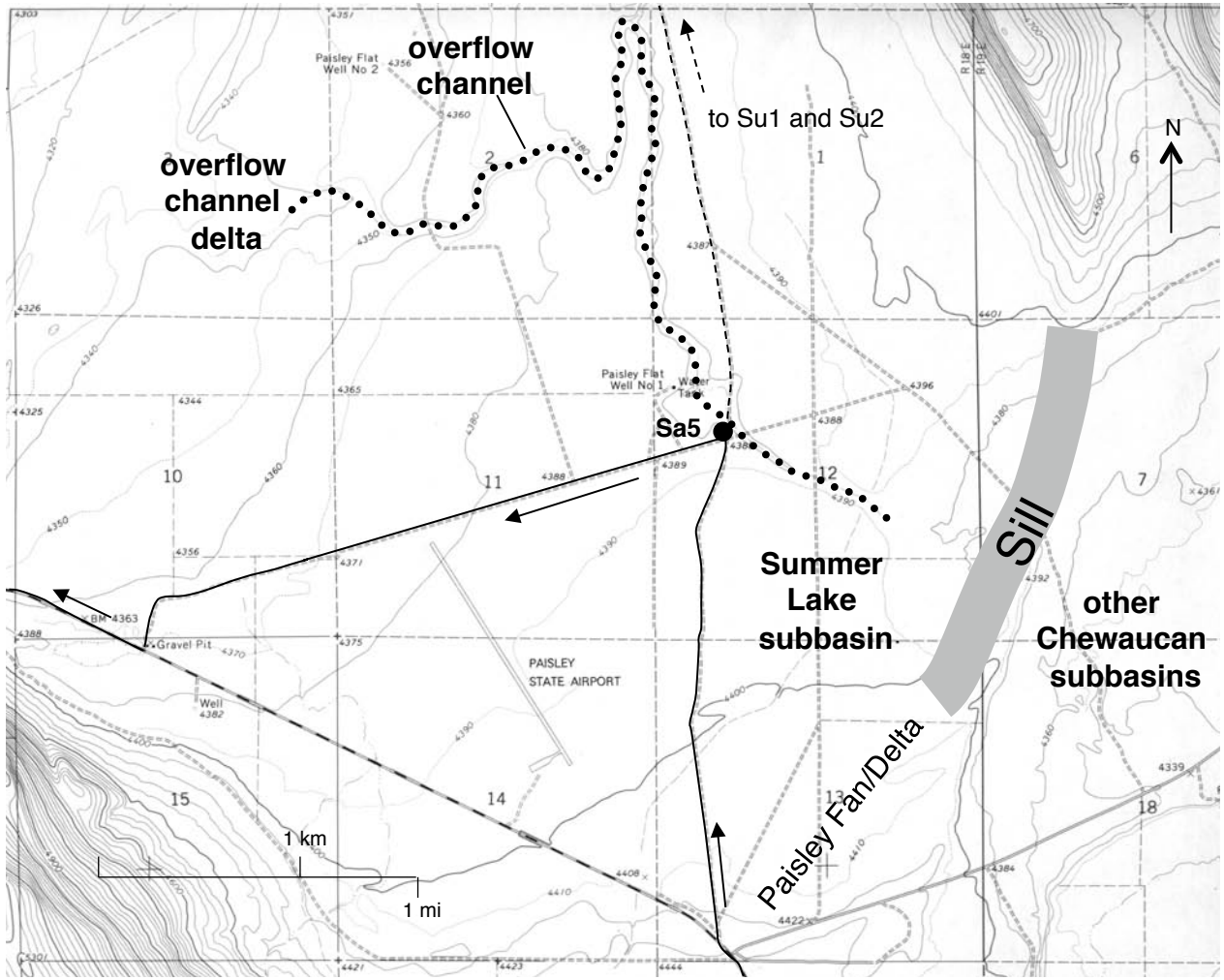

Figure R12. Location map for Stop Sa5. Note overflow channel into Summer Lake subbasin. Also note dashed line indicating route to Sunday's first stops. Base map is Paisley 7.5 USGS Topo Quadrangle Map.

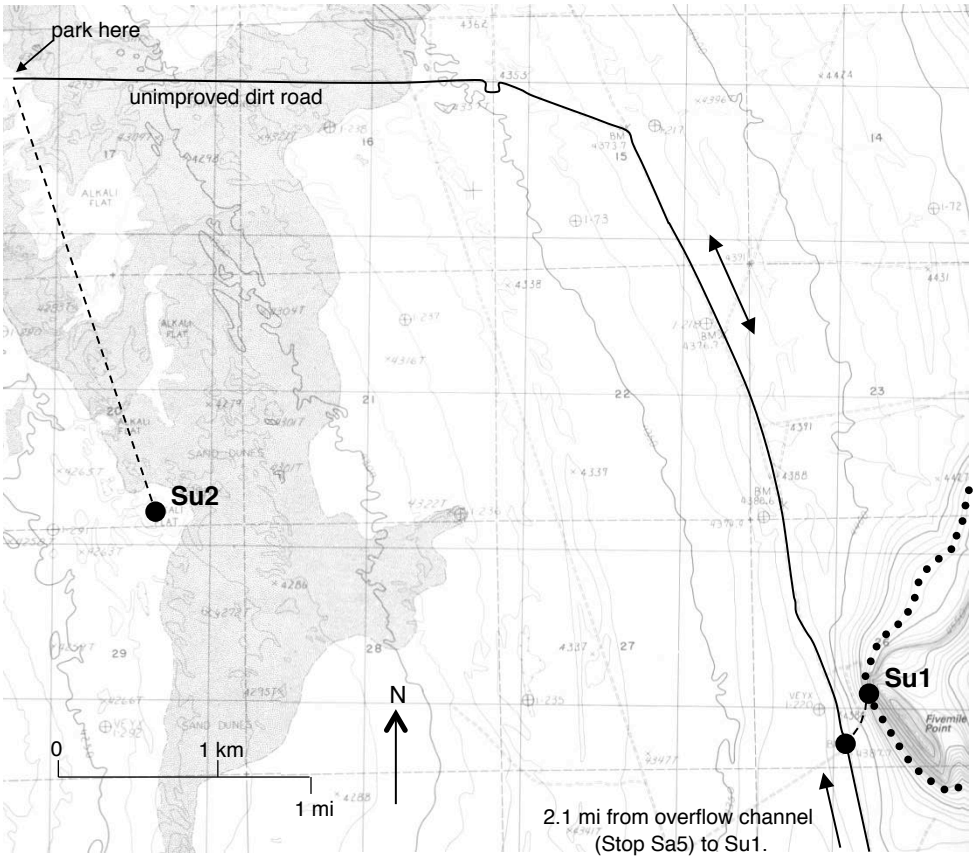

Figure R13. First two stops for Sunday (Paisley Caves and fossil site). The 4,485 ft Chewaucan shoreline is shown with heavy dotted line. The position of the highest Chewaucan shoreline is after Allison (1982). The base map is the Loco Lake 7.5 minute quad. The black dashed lines indicate walking paths to stops.

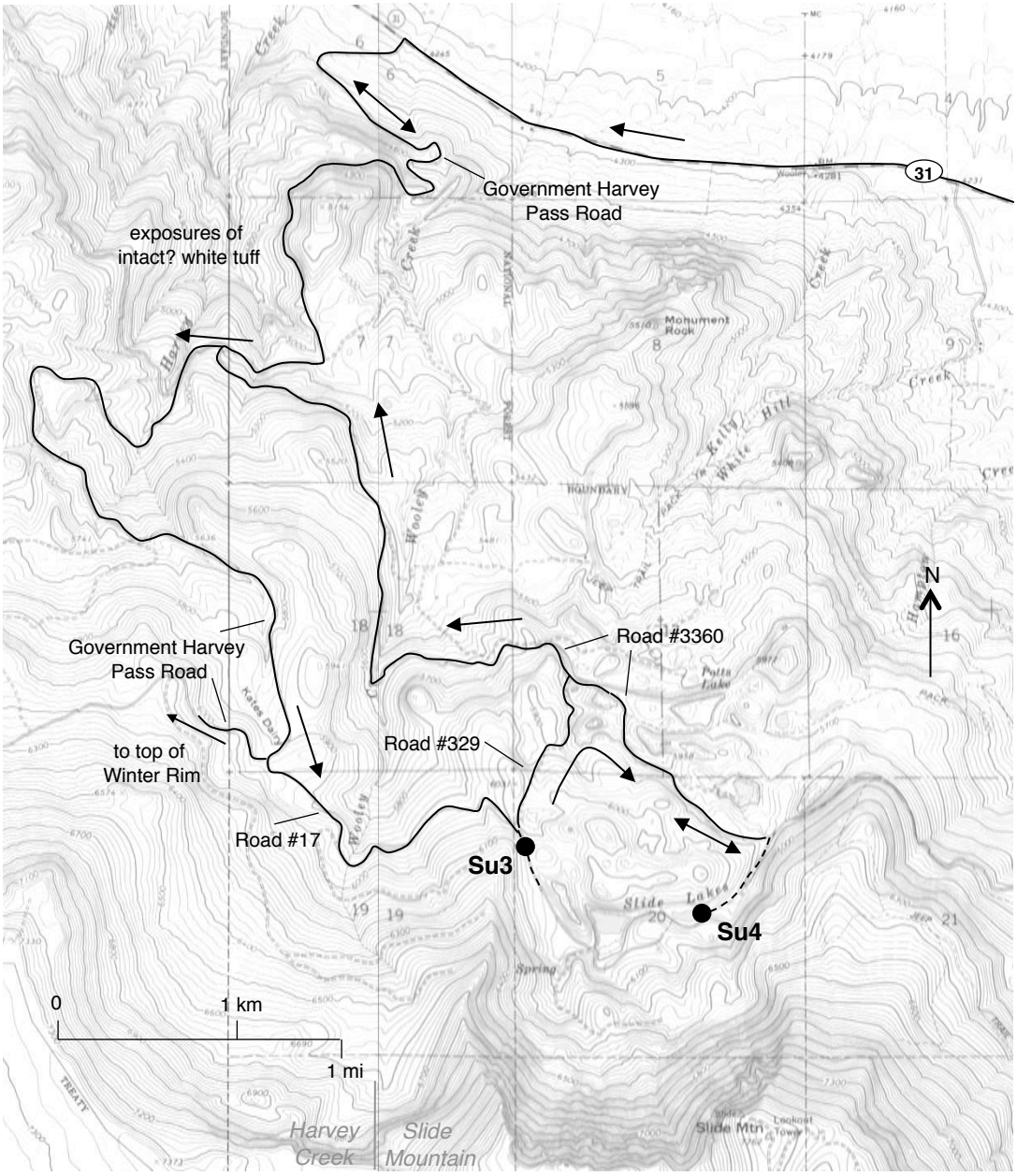

Figure R14. Final stops of 2001 PNW FOP Field Trip. Base maps are Harvey Creek and Slide Mtn. 7.5 minute quads. See articles by Casterline and Huff and by Badger (this volume) for geologic maps of Slide Mountain Mass Wasting feature.

Pluvial Lake Chewaucan Shoreline Elevations

Silvio Pezzopane, USGS, Denver, Co

Introduction

Several of the pluvial lake basins in central and eastern Oregon have three or more prominent paleoshorelines at elevations above 4350 feet, commonly 150 to 350 feet or more above the floor elevations of the modern dry lakes and playas (Figures SP1 and SP2). The upper photo in Figure SP1 shows shorelines in the Alkali Lake basin, located ~30 km N-NE of Lake Abert. The middle and lower photos in Figure SP1 show Lake Chewaucan shorelines along the northeastern edge of Lake Abert basin (Profile Site 20) and along the northern edge of Summer Lake basin (Profile Site 22) (Figures SP2 and SP3). The relative spacing between the three most prominent shorelines appears to be similar for the separate basins, however they are not.

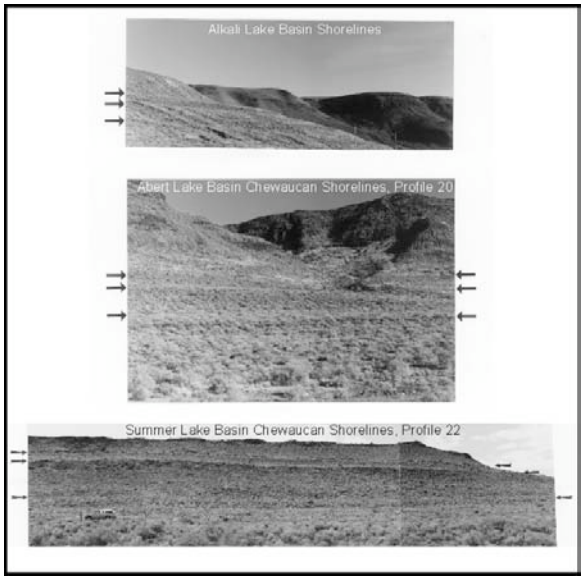

FIGURE SP1. Photographs of pluvial lake shorelines in the Alkali Lake, Abert Lake, and Summer Lake basins, south-central Oregon. Commonly three prominent shorelines occur at several sites in different basins.

Pluvial Lake Chewaucan occupied the composite basin that connected Summer Lake with Abert Lake via Upper and Lower Chewaucan Marsh (Figure SP2). The four interconnected lakes are each situated in fault-controlled basins developed within a graben or half-graben bounded by horst blocks.

Allison (1945, 1982) measured the heights of the shoreline features and studied the history of the bottom sediments in the Ana River section. Allison (1982) observed that pluvial Lake Chewaucan created erosional and depositional shorelines in various places around the Chewaucan basin. Pleistocene Lake Chewaucan shorelines along the edges of the modern basins of Summer Lake and Lake Abert indicate water reached a maximum elevation of around 4,500 to 4,520 feet, occupying an area of approximately 480 square miles. In several parts of the basin, the highest stillstand is recorded as a wave-cut notch across alluvial fans and pre-lake talus slopes.

Pezzopane (1993) measured topographic profiles of the shorelines at several selected sites throughout the Chewaucan basin (Figures SP2 and SP3) in an attempt to correlate the elevations of prominent shoreline features and evaluate whether correlative shorelines are situated at different elevations at different sites, and thus may record deformation since

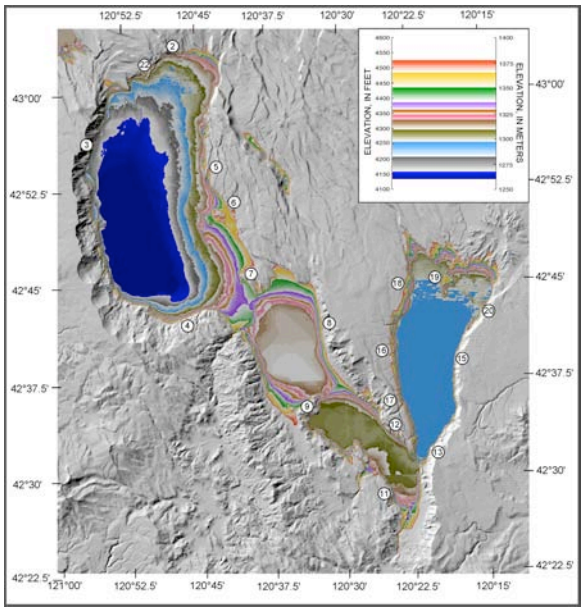

FIGURE SP2. Shaded digital elevation model of the elevations of significant Lake Chewaucan shoreline features and the locations of shoreline profile sites. Color gradients are used to indicate the elevations of significant lake and shoreline features recognized by Allison (1982), Pezzopane (1993), and later unpublished work by S. Pezzopane. The digital elevation model is from U.S. Geological Survey 7.5 minute topographic maps having 10 m vertical accuracy. Some anomalous color and textural patterns are apparent at boundaries of the quadrangles where errors in the digital elevations occur.

lake water abandoned the shorelines. Profiles across the shorelines were measured using a total-station theodolite. Backsights to nearby U.S. Geological Survey benchmarks provided elevation control. Aerial photos were used in the field to locate, survey, and correlate the prominent shoreline features.

Lake Chewaucan Shoreline Profiles

Figure SP2 shows the location of the shoreline sites and Figure SP3 shows the topographic profiles of the shorelines keyed to site by number. Shoreline profiles (Figure SP3) are shown with horizontal lines at the elevations of significant shoreline features identified by Allison (1982) and Pezzopane (1993), and later unpublished work by Pezzopane. The most obvious shoreline features that can be seen and correlated from site to site are commonly wave-cut notches and beach ridges, berms, and bars. However, a notch at one site may correlate to a beach or bar at another site, depending on the depositional settings at given elevations at given shoreline sites. Erosional features, like wave-cut notches, are generally more continuous from site to site and sites throughout the basin than are depositional features like beach ridges and bars. Yet, distinguishing between an erosional beach ridge and a depositional beach ridge is difficult without exposure. Confident correlation of the elevations of these geomorphic features is difficult because they look similar in form and profile, yet they are created at varying elevations within the nearshore zone, depending upon wave depth, fetch, and sediment supply. Bars generally form nearshore in shallow water, beach ridges form on the backshore of the beach, and wave-cut notches or beach scarps represent landward undercutting and erosion by wave action.

Pluvial Lake Chewaucan filled four interconnected basins that have three intra-basin sills (Figures SP2 and SP3). The highest in elevation, at approximately 4390', is between Summer Lake basin and Upper Chewaucan Marsh. The next lower sill is at 4350' between the Upper and Lower Marshes. The lowest sill was ditched at approximately 4280' to drain the Lower Marsh into the silled-basin of Lake Abert, having a modern water level at approximately 4255' above sea level.

The most prominent shorelines in the basins seem not to occur commonly at these sill elevations, but at various elevations above and below the sills (Figure SP3). Most of wave-cut notches and beach ridges having elevations below the intermediate sill

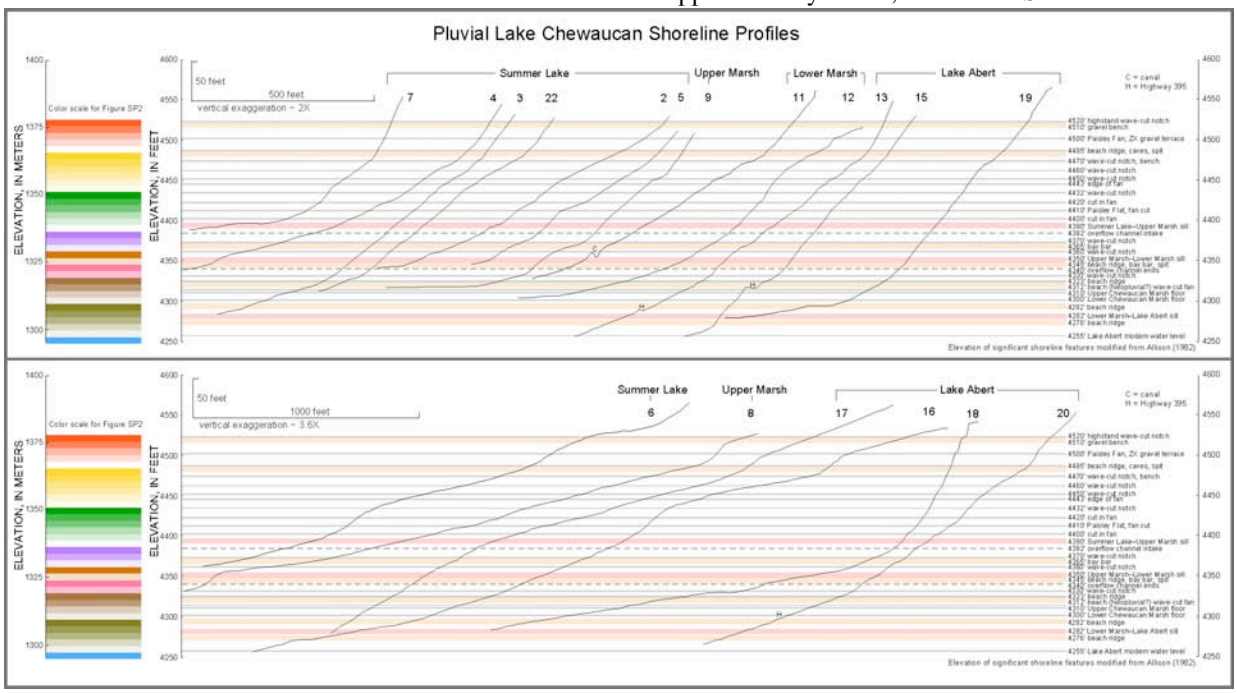

FIGURE SP3. Topographic profiles of pluvial Lake Chewaucan shorelines. Sites are numbered by location keyed to Figure SP2. Horizontal lines are shown at the elevations of significant shoreline features recognized by Allison (1982) and Pezzopane (1993). Prominent beach ridges and intra-basin sill elevations are indicated with relatively thicker shaded lines. *Top:* Vertical exaggeration ~ 2x. *Bottom:* Vertical exaggeration ~ 3.6x.

elevation (> 4350') can be correlated between Lake Abert and Summer Lake basins (Figure SP3, compare shoreline profile 3 with 17, 18, or 20), even though these pluvial lakes were separated by two sills. Perhaps all the climatic factors were appropriate to alter water levels equally within each silled basin as Lake Chewaucan dessicated. Seems more likely that surface and subsurface water flow during pluvial times maintained a potentiometric surface above the lake floor elevations. Groundwater flow in relatively permeable zones along the numerous faults in the basin may allow the water levels to equilibriate across the four sub-basins.

Shorelines in northern Summer Lake

Profiles 22 and 2 are from shorelines on the northern margin of Summer Lake, approximately 3 and 7 km, northeast of Klippel Point, respectively (Figures SP2 and SP4). Comparing these adjacent profiles illustrates the level of geomorphic variability (or lack of it) the shorelines have from site to site. Compare profiles 2 and 22 with nearby profiles 3 and 5, which are on the west and east sides of Summer Lake, respectively. The 4520' highstand notch is not obvious on any of these profiles. The 4485' beach ridge and bay bar recognized by Allison (1982) is noticable yet not prominent. Perhaps the most obvious correlative features are the numerous wave-cuts having elevations between 4470' and 4400', which are noticable in nearly all the Lake Chewaucan profiles. Profile 3, like profile 20 in Abert basin, shows the (Neopluvial?) beach and wave-cuts near 4312' as well as other cuts and ridges lower in elevation.

Shorelines in western Summer Lake

Profile 3 is across a nice shoreline sequence approximately 3.5 miles south of the town of Summer Lake, 2 miles south of the State Wildlife Headquarters, and 1.5 miles south of Jacks Lakes (Figures SP2 and SP3). In this stretch, the elevation of Highway 31 is between 4300' and 4250', below the 4312' (Neopluvial?) beach and wave-cut. As many as 7 to 9 obvious shoreline ridges or notches can be counted from the road. However, some people have noticed that one or two ridges appear to trace up and downslope slightly, like a fault scarp. The principal zone of faulting is nearby, likely beneath or slightly east of the Highway. Careful observations with a theodolite indicate that some beach ridges, commonly at erosional sites, appear to be fingerlike extensions of gravels and sands, much like small elongate spits or large longitudinal ripples. Within 10s to 100s of meters along the former shoreline, the beach ridges are not precisely parallel to the strike of the slope, and are rarely smooth and horizontally continuous.

Shorelines in southern and eastern Summer Lake

Profile 4 is approximately 4.5 miles northwest of Paisley, 1.3 miles east of Summer Lake Hot Springs, south of Highway 31 just east of Worlow Creek and west of gravel pit into shorelines at 4380'. Profiles 4, 5, 6, and 7 are from the southern and eastern margins of Summer Lake (Figure SP2). Profile 7 is near the FOP stops on Sunday. Profile 4 resembles profiles 2 and 8 as well as others.

Shorelines in Upper Chewaucan Marsh

Profiles 8 and 9 are from shorelines in the Upper Chewaucan Marsh (Figures SP2 and SP3). Profile 9 is from the northern peninsula of Tucker Hill, the prominent rhyolitic dome on the southeast side of Highway 31, approximately 3 miles east of Beachlers Trading Post and Gas, 1 mile west of the Narrows bridge across the Chewaucan River. The 4520' highstand notch is not preserved on the north face of Tucker Hill. On the southeastern and western sides, a subtle wave-cut notch is buried by talus at elevations approximately 30 to 50 feet (10-15 meters) above the relatively flat gravel terraces at 4485'. On the north face of Tucker Hill peninsula, the uppermost prominent beach ridge below the talus-covered notch is at 4450', and the bulky beach ridge near the base of the hill occurs from 4370' to 4340' (Figure SP3). The crest of the lower bulky beach is approximately 20' below the sill elevation (4390') between Summer Lake and Upper Chewaucan Marsh. The base of the bulky beach is approximately 10' to 20' lower that the sill elevation (4350') between the Upper and Lower Chewaucan Marsh.

Profile 9 resembles profile 8 from the east side of the Upper Chewaucan Marsh at the base of Coglan Buttes. The site is almost due east of the Narrows, at the base of Coglan Buttes, just east of the ZX Ranch grain camp. Profile 8 shows a prominent highstand beach scarp at 4510', a slope break coincident with the 4485' beach ridge, numerous smaller wave-cut notches into a flat alluvial fan slope down to the bulky beach ridge at 4360' to 4340', roughly coincident with the sill elevation (4350') between Upper and Lower Chewaucan Marsh.

Shorelines in Lower Chewaucan Marsh

Profiles 12 and 11 are of shorelines on the eastern and western margins of the Lower Chewaucan Marsh basin, respectively (Figures SP2 and SP3). Profile 12 shows poor correlation with profile 11 and somewhat better correlation with profile 13 nearby. The correlation seems better for shorelines below 4350' elevation. Profile 12 is sited on a peninsula where

the ancient shoreline was relatively jagged and likely overall more erosive than at profile 11, just across the Marsh, and 13 in south Lake Abert. Profile 12 also shows poor correlation with profiles 8 and 9 in Upper Chewaucan Marsh. A much better shoreline elevation correlation is obtained if approximately 10 feet is added to the elevation of profile 12. Perhaps the control elevation for profile 12 is in error, or, the shorelines have been deformed at this site. Profile 12 is sited approximately 3.3 miles (5.2 km) from profile 13 on the downthrown side of the Abert Rim fault, which has a compound scarp as much as 8 m in height, and younger inset scarps 2 to 5 m in height, all younger than latest Pleistocene pluvial and colluvial deposits.

Shorelines in Lake Abert basin

Profiles 13, 15, and 20 are along the eastern shore of Lake Abert, profiles 16, 17, and 18 are along the western shore, and profile 19 is sited near the northern shore on a peak called Sawed Horn, which was in pluvial times an small island (Figures SP2 and SP4). Most of the shoreline features in Lake Abert appear relatively well expressed and are mostly erosional, given the steep slopes. Initial examination reveals that many of the shorelines correlate well throughout the Abert basin and within other basins. Profile 20 shows a remarkable sequence of as many as 12 to 15 shoreline beaches or benches preserved in what was once a small bay. Profiles 18 and 19 show the 4520' highstand shoreline expressed as an ancient wave-cut notch or beach scarp having a shoreline angle and near vertical face at elevations above 4520'. Detailed examination reveals that certain shorelines do not correlate well in elevation, and improve with minor adjustments sometimes upwards and sometimes downwards. Comparison between profiles 16, 17, and 18 show how continuous and yet variable certain shorelines are within about 5 km from site to site along a relatively straight lakeside. Profiles 17 and 16, like profile 12, appear to have a better correlation to other sites if one adds 5 to 15 feet to the profiles.

Shoreline Elevation Correlations

Preliminary interpretations of the Chewaucan shoreline elevations indicate there may be as much as 3 to 6 m (~10 to 20 ft) of vertical difference in the elevations of Lake Abert shorelines relative to shorelines in other parts of the basin. Problems with the analysis arise from the uncertainty in what morphologic feature to choose to represent the level of the ancient lake. Most of the shorelines higher than 4400 ft in elevation are wave-cut notches and erosional benches. Initially I chose to measure the elevation of the shoreline angle, which for these shorelines I estimate occurs at or slightly above the break in slope at the top of the bench or platform. Also I concentrated on the highstand shoreline elevation as a datum and attempted to measure the sequencial elevations of lower shorelines. Aerial photos were used to confirm recognizable slope features, revealing that lacustrine erosion features on the photos sometimes appeared to be higher than the back of the platform. In some cases, correlations of the features were inconclusive.

Displacements on young fault scarps (8 m on Abert Rim and as much as 10 m near Slide Mountain) compared to the difference in shoreline elevations indicates that most of the shoreline elevation differences is probably a result of slip on faults (Pezzopane, 1993). Other processes, such as warping or folding, may be responsible for the apparent regional patterns of deformation, which for example, have tilted the modern Summer Lake basin southwestward relative to higher areas to the northeast. The floor of Summer Lake is inclined towards the southwestern corner of the basin, a region characterized by large active landslides and debris flows off of Winter Ridge which should easily fill in the lake basin here over time relative to other parts of the basin.

References

Allison, I.S., 1945, Pumice beds at Summer Lake, Oregon. Geological Society of America Bulletin: v. 56, p. 789-807.

Allison, I.S., 1982, Geology of Pluvial Lake Chewaucan, Lake County: Oregon Oregon State Monographs, Studies in Geology, v. 11.

Pezzopane, S. K., 1993, Active faults and earthquake ground motions in Oregon, Ph.D. dissertation, 208 pp., University of Oregon, Eugene.

Lithologic Evidence for the Middle and Late Pleistocene Paleo-Lake Level Fluctuation of Pluvial Lake Chewaucan, Oregon

Dan Erbes, Department of Interior, Bureau of Land Management, Carson City, Nevada

Introduction

Sediments representing lacustrine and deltaic deposition in pluvial Lake Chewaucan for the past 250,000 years are exposed north of Summer Lake, Oregon (43.0°N, 120.45°W) along the walls of the Ana River Canyon (ARC). These sediments appear to have been exposed as a result of recent block-faulting and subsequent fluvial dissection (Allison, 1982). Initial studies by Allison (1945, 1966) provided lithologic descriptions and a limited tephrochronology of the upper few meters of the ARC section. Allison (1945) named the tephra layers and the interlying clays and silts using a numerical scheme. Even numbers correspond to light colored layers (generally tephra layers) and odd numbers correspond to the interlying lacustrine clays and silts. That numbering scheme started at a clay unit below Summer Lake tephra bed 2 and increased upward to Summer Lake tephra bed 18 (Trego Hot Springs tephra bed) at the top of the section.

A more complete stratigraphic section for ARC was produced by Davis (1985) who described the lithology and identified numerous tephra beds. The laterally continuous and distinct nature of the tephra beds in the Lake Chewaucan sediments at ARC allowed Davis to construct a composite section that was more complete than the record at any single outcrop locality. The composite stratigraphic record exposed in the canyon is approximately 20-meters-thick and is composed of lacustrine clays and silts interbedded with sand layers. Most of the sands consist of ostracodes or subaqueous tephra. Davis (1985) incorporated Allison's (1945) original tephra names and added names of new tephra layers based on an alphabetical scheme starting with Summer Lake tephra bed A at the top of the section, and working down to Summer Lake tephra bed SS. Newer beds discovered in between those identified within this alphabetical scheme are denoted with an added numeral. For example, a new tephra bed found below Summer Lake tephra bed E and above Summer Lake tephra bed F was identified as Summer Lake tephra bed E1. An unpublished ARC outcrop profile by Davis showing the location of more than 54 tephra beds is presented in the Road Log of this volume as Figure R7a-d.

Lithologic Interpretation

The clay and muddy silt deposits such as those observed in the Lake Chewaucan sequence were likely deposited in water conditions which were effectively free of turbulence over extended periods of time. Sedimentary structures within the fine-grained sediment provide clues to the relative depths of deposition. Sedimentary structures exhibited in the Lake Chewaucan sequence which may be indicative of lake depth include: Thin continuous flat laminae reflecting deeper lake anoxic conditions and an absence of bioturbation; well sorted coarse silt or sand lenses reflecting wave base disturbance indicative of shallower lake conditions, and; unconformities reflecting periods of non-deposition or erosion.

Thinly laminated lacustrine muds exhibiting an absence or lesser degree of bioturbation suggest relatively deep lake conditions (Smoot, 1996). However, the absence of lamination alone does not suggest shallow lake conditions. This is because laminated sediments created in a deep lake with anoxic bottom conditions during a pluvial could become bioturbated during a subsequent recession leaving no trace of the pluvial event. Consequently, thinly laminated intervals can be interpreted as representing deep lake conditions while the absence of laminations alone is not conclusive.

The occurrence of thin, well-sorted coarse silt to sand in lenses or layers that thicken and thin rhythmically over a flat to scalloped erosional base are indicative of wave base disturbances (Smoot, 1996). These types of sand or silt laminae are common over some intervals within the Lake Chewaucan sediments. Most sand or silt laminae are less than 0.25-cm-thick and consisted primarily of ostracodes from the surrounding fine-grained sediment. A transition from sediments with no evidence of wave base erosion, to sediments with abundant evidence of wave base erosion, can be interpreted as an indication of shallowing water, or regression.

Unconformities exhibited by mud cracks (indicating short term exposure) and soil horizons (resulting from long term exposure) occur infrequently in the outcrop sequence. This suggests that lake conditions were perennial throughout the majority of the late Pleistocene. Most of the unconformities observed in the outcrop are paraconformities exhibiting relatively thick sand and pebble rich layers. These features result from the winnowing of finer grained material from the lake bottom during very low lake levels. Some

paraconformities are marked by brecciated carbonate layers which also reflect high energy, low lake conditions. The interpretation of water depth using unbrecciated carbonate layers is less conclusive because the settling out of chemical precipitates in relatively deep lake environments can also produce such layers (Smoot and Lowenstein, 1989).

Paleoclimate Model

Interpluvial and intervening pluvial episodes in the Lake Chewaucan record are proposed to be broadly consistent with respective interglacial and glacial events (Cohen et al., 2000; Negrini et al., 2000). The best records of glacial cycles are reflected in oxygen isotope ratios ($\delta^{18}O$) recorded from foraminifera in deep-sea sediment cores (e.g., see left side of Figure 3 in Negrini, this volume). Respective glacial and interglacial stages are denoted with even and odd numbers. Oxygen isotope stage 1 correlates to the Holocene interglacial or interpluvial stage, while stage 2 correlates to the last glacial or pluvial stage. Evidence for marine oxygen isotope stages 1 and 2 are mostly absent from the Lake Chewaucan record derived from the Ana River outcrops.

Based on age estimates for the top and bottom of the ARC outcrop (<18.1 ka to ~200-250 ka, respectively), evidence for most of the marine oxygen isotope stages 3 through 7 should exist in the outcrop record. This article focuses on evidence for stages 3 through 6. The marine oxygen isotope stage 5 interglacial, which is presumed to be represented in the ARC outcrop, is broken out into five interglacial fluctuations denoted by the lower case letters a through e. Stages 5a, 5c and 5e, represent interglacial minima or lower lake levels while stages 5b and 5d represent interglacial maxima or higher lake levels within a period of overall low precipitation.

Stratigraphic Relationships

Eight unconformity-bounded lithosomes can be recognized in the Ana River Canyon section. The stratigraphic positions of these lithosomes are plotted in the Road Log of this volume on Figure R7a-d. From oldest to youngest the lithosomes are as follows:

Lithosome I: (~174-162 ka) The base of this lithosome is marked by a 50-centimeter-thick sandy unconformity with a basal gravel layer which lies directly above Summer Lake tephra bed V (~174ka), at a depth of 897 cm in the outcrop section. The top of this lithosome is marked by the major unconformity at a depth of 703 cm in the outcrop section which Negrini et al. (2000) estimates to have resulted in a loss of record from 162-102 ka. That unconformity correlates with the oxygen isotope stage 5e interglacial proposed by Martinson and others (1987) at 128 ± 2 ka. Lacustrian sediments devoid of wave base indicators prevail between the upper and lower bounds of this lithosome which suggests that overall deep lake conditions persisted in the Chewaucan Basin from at least 174-162 ka. The apparent pluvial conditions observed in this lithosome likely coincide with marine oxygen isotope stage 6.

Lithosome II (~102-95 ka) comprises a thin (~60cm) sequence of sandy muds containing a weak soil horizon at the top. This soil horizon was first noted by Davis (unpublished) at a depth of 630 cm in the outcrop section and consists of a leached zone of coarse material, primarily ostracodal sands, with millimeter-scale vertical voids and a vesicular texture. The approximate age for the top of this lithosome is 95 ka. Evidence of wavebase indicators and sandy muds throughout this lithosome suggests that a shallow water environment prevailed from 102-95 ka.

Lithosome III (~95-89 ka) comprises section from the vesicular "A" soil horizon up to a carbonate replaced sandy paraconformity directly above Summer Lake tephra bed J (~89 ka), at a depth of 565 cm in the outcrop section. Massive sandy mud is evident between the soil horizon at the base of this lithosome and tephra bed J. These conditions suggest that shallow lake conditions prevailed from 95 to 89 ka.

Lithosome IV (~89-84 ka) comprises section up to a carbonate pebble conglomerate unconformity (~84 ka) which occurs below Summer Lake tephra bed H1, at a depth of 509 cm in the outcrop section. The lacustrine sequence (~50 cm) of laminated ostracodal muds within this lithosome is devoid of wave base indicators which suggests that overall deep lake conditions began approximately 89 ka followed by a lake-level decrease approximately 84 ka.

Lithosome V (~84-47 ka) comprises section up to a pebble rich sandy paraconformity with abundant carbonate which lies directly below Summer Lake tephra bed 12 (~47.0), at a depth of 274 cm in the outcrop section. The ~84 ka carbonate pebble conglomerate unconformity at the base of this lithosome is overlain by lacustrine muds exhibiting interspersed thin carbonate layers and an absence of wave base indicators. The absence of shallow lake indicators within this lithosome suggests that deep lake conditions prevailed between 84 and 47 ka.

Lithosome VI (~47-31 ka) Summer Lake tephra bed 12 at the base of this lithosome exhibits some crossbedding above its base. A very thin accumulation of lacustrine silts (15-cm-thick) is observed above that tephra and below a 2 cm thick sandy oolitic horizon (~31 ka) at the top of this lithosome. These features suggest subaerial exposure approximately 47 ka followed by shallow lake conditions up to 31 ka.

Lithosome VII (~31-27 C-14 kyr B.P.) comprises the section from the sandy oolicic horizon at a depth of 237 cm in the outcrop up to the base of Summer Lake tephra bed F (27.3 ± 0.3 C-14 kyr B.P.; Benson et al., 1998) at a depth of 188 cm. Tephra bed F in itself is an unconformity referred to as the Wono "lag deposit" by Negrini and Davis (1992). The sandy oolitic horizon (~31 ka) at the base of this lithosome is overlain by massive lacustrine silts, and clays which may be indicative of deep lake conditions.

Lithosome VIII (~27-18.1 C-14 kyr B.P.) comprises the interval from the Wono lag deposit up to the top of the outcrop section. The sedimentary sequence in this lithosome contains crossbedded sands and climbing ripples suggesting that shallow lake fluvial/deltaic conditions were apparent at the outcrop elevation from ~27 ka to at least 18.1 C-14 kyr B.P, the estimated age of the outcrop surface.

The dunefield environment observed along the ARC cliff tops and to the west of Summer Lake likely resulted after the perennial Chewaucan River changed course into the Lake Abert sub-basin following the last pluvial maximum (Davis, 1985). After the Chewaucan River switchover, the Summer Lake Basin became unusually dry. Deflation of lake sediments in the Holocene is probably responsible for eroding evidence for the last pluvial event from the outcrop.

Conclusions

The record derived from outcrop in the Summer Lake sub-basin of pluvial Lake Chewaucan reflects the major periods of lake-level fluctuation including a majority of the last two Pleistocene glacial events. Between 174 and 162 ka, deep lake pluvial conditions were existed proximal to the outcrop. This pluvial period coincides with marine oxygen isotope stage 6. Pluvial conditions terminated abruptly in the basin sometime between 162 and 102 ka with the onset of an interpluvial event representing marine oxygen isotope stage 5e. Apparent shallow perennial saline lake conditions existed in the ensuing period from ~102 to ~89 ka (perhaps associated with marine oxygen isotope stage 5d). At that time, the lake level fell below the outcrop elevation where evidence of a vesicular "A" soil horizon exists. Subsequently, lake level again rose above the elevation of the outcrop and the basin may have experienced a relatively short-lived pluvial episode (perhaps associated with marine oxygen isotope stage 5b) prior to ~84 ka when another lake level regression occurred. That regression, which is evidenced by carbonate-coated sand in the outcrop section, roughly coincides with marine oxygen isotope stage 5a.

Apparent deep lake pluvial conditions appear to have prevailed in the basin from ~84 ka to ~47 ka. The predominantly deep lake conditions observed from ~84 to ~47 ka in lithosome V likely correspond to marine oxygen isotope stage 4. At ~47 ka, lake level fell below the outcrop elevation once again followed by perennial shallow saline lake conditions which persisted in the basin until ~31 ka. This transition corresponds with the onset of marine oxygen isotope stage 3. The period from ~31 to ~27 ka appears to coincide with a gradual transgression of that perennial shallow saline lake. Lake levels fluctuated at least three times during the period from ~27 ka to the top of the lacustrine record at 18.1 ka (Negrini and Davis, 1992). Negrini and Davis (1992) noted three shallowing intervals over this time period: a lower event occurring between 27.4 and 23.2 ka; a middle event occurring between 21.7 and 20.9 ka, and; an upper event between 20.1 and 19.3 ka. These shallow episodes support the persistence of perennial saline lake conditions. Intervening time periods (from 23.2 to 21.7 ka, 20.9 to 20.1 ka and 19.3 to ~18.1 ka) were likely associated with brief pluvial episodes. The record from Lake Chewaucan representing times later than 18.1 ka have been erased by wind erosion in the Holocene.

References

Allison, I.S., 1945. Pumice beds at Summer Lake, Oregon, *Geol. Soc. Amer. Bull.,* v. 56, p. 789-808.

Allison, I.S., 1966. Pumice at Summer Lake, Oregon -- A Correction, *Geol. Soc. Amer. Bull.,* v. 77, p. 329-330.

Allison, I.S., 1982. Geology of pluvial Lake Chewaucan, Lake County, Oregon, *Oreg. State U. Stud. Geol.*, 11, 79 p.

Benson, L.V., J.P. Smoot, M. Kashgarian, A. Sarna-Wojcicki, and J.W. Burdett, 1998. Radiocarbon ages and environments of deposition of the

Wono and Trego Hot Springs tephra layers in the Pyramid Lake subbasin, Nevada, *Quaternary Research*, v. 47., p. 251-260.

Cohen, A.S., M.R. Palacios-Fest, R.M. Negrini, P.E. Wigand, and D.B. Erbes, 2000. A paleoclimate record for the past 250,000 years from Summer Lake, Oregon, USA: II. Sedimentology, paleontology, and geochemistry, *Journal of Paleolimnology,* v. 24, p. 151-181.

Davis, J.O., 1985. Correlation of late Quaternary tephra layers in a long pluvial sequence near Summer Lake, Oregon, *Quaternary Res.,* v. 23, 38-53.

Erbes, D.B., 1996. Late Pleistocene lithostratigraphy of Pluvial Lake Chewaucan, Oregon: Implications for past climate variation, M.S. Thesis, Dept. of Physics and Geology, CSU Bakersfield, 108 pp.

Martinson, D.G., N.G. Pisias, J.D. Hays, J. Imbrie, T.C. Moore and N.J.Shackleton, 1987. Age dating and the orbital theory of the ice ages: Development of a high-resolution 0 to 300,000 year chronostratigraphy, *Quaternary Res.,* v. 27, 1-29.

Negrini, R.M., and J.O. Davis, 1992. Dating late Pleistocene pluvial events and tephras by correlating paleomagnetic secular variation records from the western Great Basin, *Quaternary Res*., v. 38, p. 46-59.

Negrini, R.M., D.B. Erbes, K. Faber, A.M. Herrera, A.P. Roberts, A.S. Cohen, P.E. Wigand, and F.F. Foit, Jr., 2000. A paleoclimate record for the past 250,000 years from Summer Lake, Oregon, USA: I. Chronology and magnetic proxies for lake level, *Journal of Paleolimnology,* v. 24, p. 125-149.

Sarna-Wojcicki, A.M., et. al.., 1991. Tephro-chronologic correlation of upper Neogene sediments along the Pacific margin, conterminous United States: *in* R.B. Morrison (ed.), *The Geology of North America, vol . K-2, Quaternary Nonglacial Geology: Conterminous U.S., Geol. Soc. of Am*., p. 117-140.

Smoot J.P. , 1996. Sedimentary Record of Climatically Induced Lake-Level Fluctuations, Pyramid Lake, Nevada, *in* L.C. Benson, ed. *Proceedings of the Workshop "Ongoing Paleoclimatic Studies in the Northern Great Basin," Reno, Nevada, May 1993*. U.S. Geol. Survey Circular 1119, p. 101-102.

Smoot, J.P., and Lowenstein, T.K., 1991. Depositional Environments of Non-Marine Evaporites, *in* Melvin, J.L. (ed.), Evaporites, Petroleum, and Mineral Resources, Develop. in Sediment. 50, 189-347.

Yount, J.C., and M.F. Quimby, 1988. Grain-size data from four cores from Walker Lake, Nevada, *U.S. Geol. Survey Open-File Rpt*., #88-436.

Updated tephra stratigraphy at Summer Lake, Oregon, a sub-basin of pluvial Lake Chewaucan

Stephen C. Kuehn and Franklin F. Foit, Jr.
Department of Geology, Washington State University, Pullman, WA

INTRODUCTION

Tephra beds serve as useful chrono-stratigraphic markers in the correlation of intra- and extra-basinal sediments in the Great Basin. The reconstruction of the regional sedimentary record provides insight into the paleoclimate regimes which have influenced it. In this regard the sediments of ancient Lake Chewaucan are a fantastic repository of information on volcanism and the paleoclimate of the Pacific Northwest.

More than 50 tephra layers intercalated with Pleistocene lacustrine sediments are exposed in the Ana River canyon at the northern edge of the Summer Lake sub-basin near the town of Summer Lake, Oregon (Figure 1). This section, which represents more than 220,000 years of earth history, has been studied extensively by Allison (1945, 1966a,b), Davis (1985) and Negrini et al. 2000). Davis (1985) was the first to employ electron beam microanalysis to characterize and identify the tephra layers (at least the major layers) and establish a chronology. He demonstrated that several of the more prominent tephra layers were airfalls from major eruptions from Cascade volcanic centers, in particular Crater Lake and Mount St Helens. He correlated these and others to tephras found in sites in and around the Lake Lahontan basin in northwest Nevada.

In a recent study of the paleoclimate record of the Great Basin Negrini et al. (2000) used (among other techniques) microchemical characterization of the glass in tephra layers in two cores to establish intra-basinal correlations and age control to the Ana River outcrop at the basin's northern margin. Eleven of the tephra layers in the Wetland Levee core (transitional,

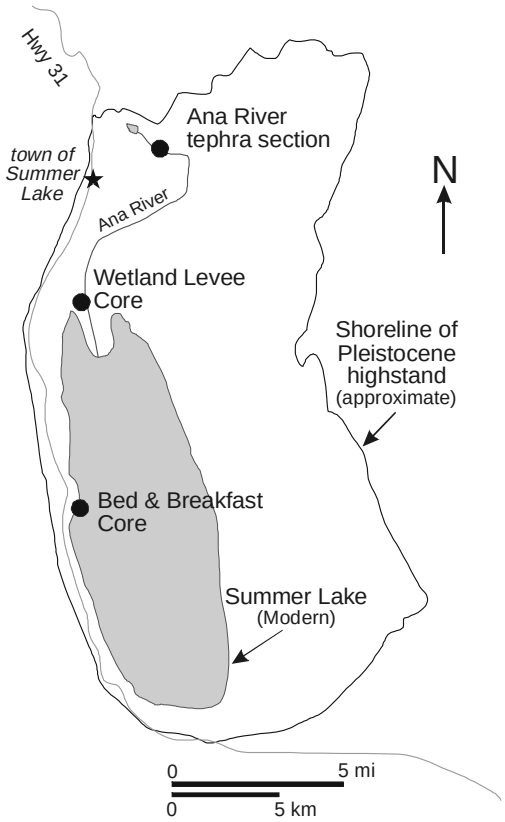

Figure 1. Map of Summer Lake sub-basin showing core and outcrop locations. Modified from Negrini and others, 2000.

current lake margin) and in the Bed and Breakfast core (current depocenter) are also found at the Ana River outcrop (basin margin) (Figures 1& 2). The correlation and sourcing of many of these tephra layers was limited by depositional conditions and lack of data on the tephra stratigraphy of regional volcanic centers. The lake has undergone at least three major changes in level and extent in the last 200,000 years and more uncertainty was encountered in correlating tephra beds deposited as part of the shallow lake lithosome than the deep lake lithosome (Figure 3). This is attributed to erosion of older tephras from the lake margin during

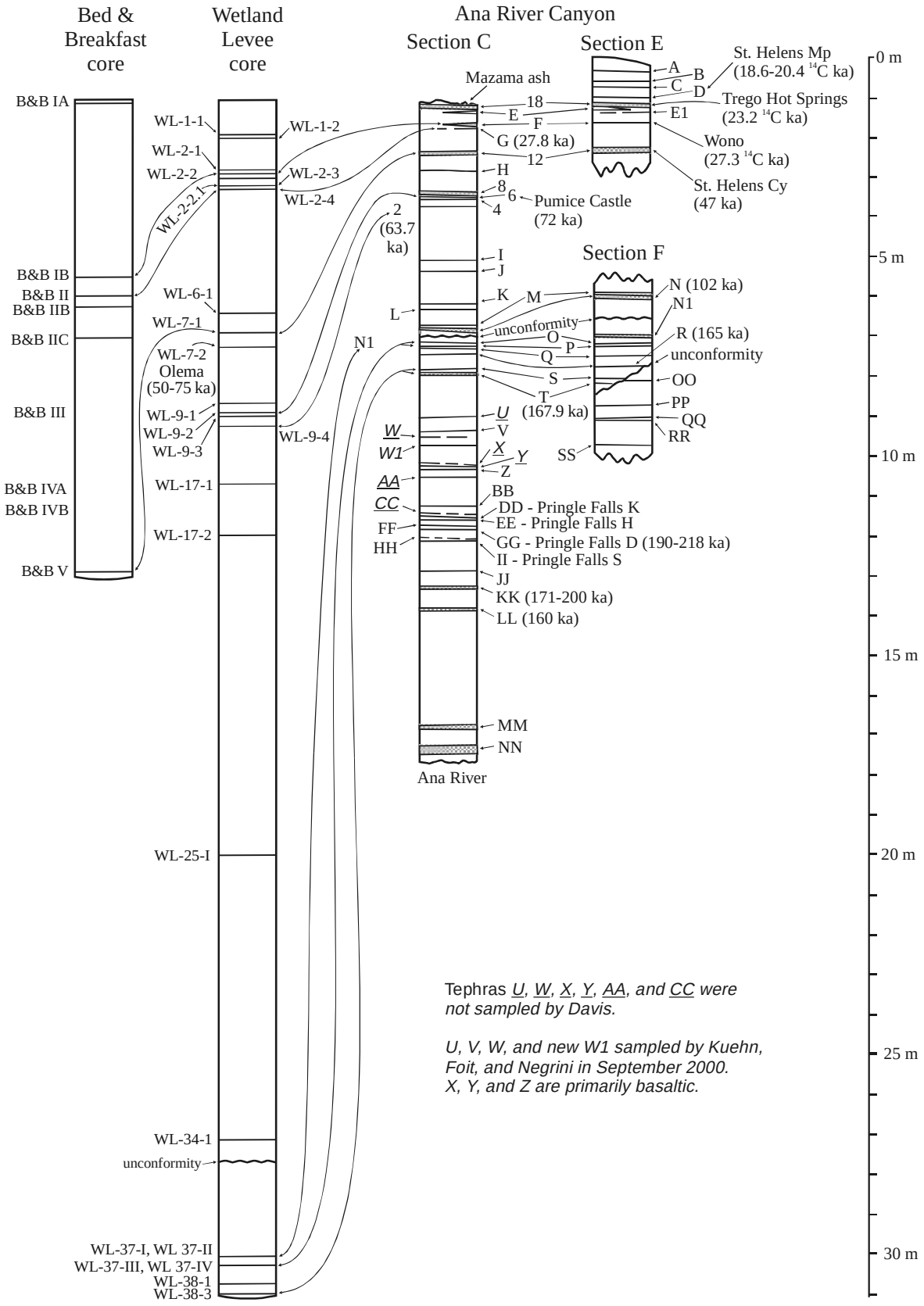

Figure 2. Tephra Stratigraphy at Summer Lake. Modified from Davis (1985) and Negrini et.al. (2000). More complete listing of WL and B&B samples from Negrini (personal communication, 2001).

low stand and mixing with younger airfall tephras towards the depocenter. Secondly, the identification of many of these tephra layers is hampered by a lack of information on the proximal stratigraphy and composition of tephras in regional volcanic centers, case in point, the Newberry volcano. Thus, the sources of many of the tephras in these sections (Figure 2), especially those below the Pumice Castle (72 $\pm$ 6 ka) remained unknown and were in need of investigation.

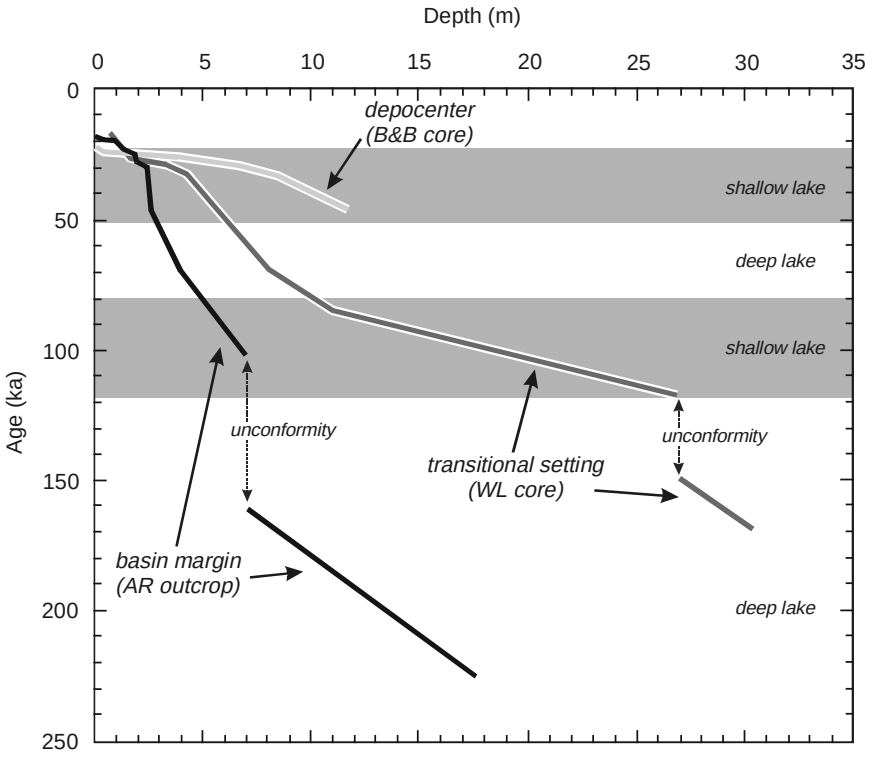

Figure 3. Age vs. depth and relative lake level for the three Summer Lake records. Modified from Negrini et. al., 2000.

TEPHRA CHARACTERIZATION AND IDENTIFICATION

Tephras from different volcanic centers and tephras of different ages from the same volcanic center often differ in their mineralogy, mineral to glass ratios, and glass composition. All of these attributes, especially glass composition, have been used to "fingerprint" a tephra as being from a particular source or from a particular eruption. The use of the electron microprobe to determine the geochemical signature of tephra glass is a well-established technique (Smith and Westgate, 1969) involving the determination of 9-12 major and minor elements. The weight percent data is normalized to a total 100 to compensate for the variable hydration of the glass and then is compared to a composition database of known tephras employing a simple discriminant, like the similarity coefficient (SC) of Borchardt et al. (1972). In situations where the composition of the glass does not vary much, such as glass from closely spaced eruptions (e.g. Mount St Helens set J tephra vs. set S tephra) the mineralogy (e.g. the presence or absence of cummingtonite) can play a key role in resolving the identity of the tephra.

NEWBERRY TEPHRAS AT SUMMER LAKE

As mentioned previously, more than 50 tephra layers found in the Ana River sections, the Bed and Breakfast (B&B) core, and the Wetland levee (WL) core are of unknown origin and are likely to be ejecta from small local eruptions or poorly characterized material from larger more distant centers. One of the more likely sources of tephra found in the Chewaucan basin is Newberry volcano which is situated approximately 90 km northwest of Summer Lake (Figure 4). The first author of this paper currently is examining the tephra geochemistry and stratigraphy at Newberry

volcano and has been able to correlate on the basis of glass chemistry (SiO_2, Al_2O_3, Na_2O, Fe_2O_3, CaO, K_2O, MgO, TiO_2, Cl) some of the tephra layers in the Chewaucan Basin to silicic volcanism at Newberry volcano (Tables 1 and 2). It appears that Newberry volcano has influencing the tephra stratigraphy in the Basin and surrounding region for at least 250,000 years.

One of the youngest tephra layers at Summer Lake (Tephra F, depth 1.9m) which is thought to have been erupted from Newberry volcano (Kuehn, 1999) is the Wono tephra (27.3 ^{14}C kyr B.P.). Although the composition of the glass (Table 1) has a Crater Lake signature, physical aspects of its thick deposit at Newberry volcano (98-79-C) suggest Newberry as the source (Kuehn, 1999) rather than Crater Lake (Davis, 1985). The main deposit of Wono tephra at Newberry is 63 cm thick and contains coarse pumice fragments, some of which exceed 3cm in length. Wono tephra also is found in soil horizons at several localities around Newberry volcano.

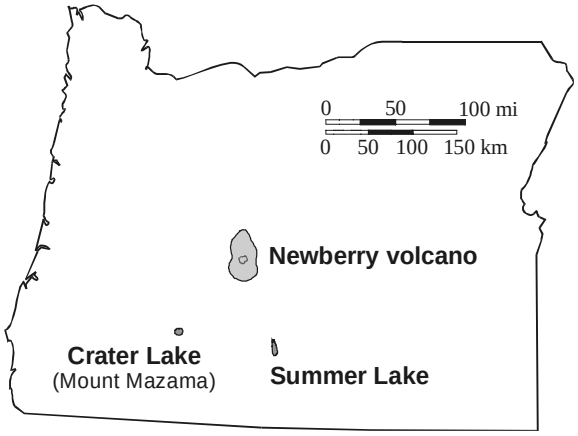

Figure 4. Locations of Newberry Volcano, Crater Lake, and Summer Lake, Oregon.

Summer Lake Tephra G (27.8 ^{14}C kyr B.P.), like the Wono immediately above it, is found in at the Ana River section C (depth 1.95m) and in both the WL and B&B cores. The compositions of the glass in these tephras is an excellent match (SC = 0.95, 0.99, and 0.97 respectively; Table 1) to tephra 9715K. 9715K is found as a 2 cm thick, white, pumiceous coarse ash in the

Table 1. Compositions of Selected Glasses in Ana River, Wetland Levee (WL) and Bed and Breakfast (B&B) Tephra Layerss and Their Sources Glass compositional data from: (1) Davis (1985), (2) Negrini et al. (2000), (3) Busacca et al. (1992), (4) Benson et al. (1997), (5) Sarna-Wojcicki et al. (1988), (6) Herrero-Bervera, et. al. (1994), (7) Kuehn and Foit (2000), (8) Kuehn and Foit (this paper, not previously published)

Location & Depth proposed source	Tephra	SiO_2	Al_20_3	Fe_20_3	MgO	CaO	TiO_2	Na_2O	K_2O	Cl	SC	*Ref.*
Ana River 1.13m	Tephra D	76.3	13.9	1.23	0.30	1.51	0.16	4.1	2.4	0.11	0.97	*(1)*
Mount St Helens	MSH M standard	76.45	13.81	1.39	0.32	1.48	0.16	3.96	2.36	0.10		*(3)*
Ana River 1.47m	Tephra 18	75.2	13.7	1.65	0.20	1.00	0.25	4.6	3.2	0.12	0.99	*(1)*
Crater Lake	Trego H.S.	75.12	13.94	1.67	0.20	1.05	0.25	4.51	3.21			*(4)*
Ana River 1.90m	Tephra F	73.7	14.1	2.23	0.28	1.30	0.31	4.7	3.1	0.10	0.96	*(1)*
WL 1.84m	WL-2-2	74.82	13.87	1.95	0.25	1.28	0.19	4.45	3.10	0.09	0.97	*(2)*
B&B 4.42m	Tephra 1B	74.86	13.87	1.95	0.25	1.29	0.20	4.38	3.11	0.09	0.97	*(2)*
	Wono standard	74.57	13.77	2.00	0.29	1.33	0.27	4.54	3.12	0.11	0.97	*(2)*
Newberry Volcano	Wono (9879C)	74.56	13.94	2.10	0.31	1.36	0.30	4.25	3.08	0.11		*(7)*
Ana River 1.95m	Tephra G	77.0	13.3	1.03	0.10	0.75	0.10	4.2	3.4	0.09	0.95	*(1)*
WL 2.2m	WL-2-4	77.39	12.91	1.16	0.12	0.81	0.09	4.07	3.35	0.10	0.99	*(2)*
B&B	Tephra II	77.51	12.86	1.12	0.12	0.80	0.09	4.00	3.42	0.08	0.97	*(2)*
Newberry Volcano	9715K	77.77	12.87	1.03	0.13	0.78	0.09	3.82	3.37	0.08		*(7)*
Ana River 2.61m	Tephra 12, glass 1	76.5	14.0	0.99	0.24	1.5	0.10	4.1	2.4	0.07	0.97	*(1)*
WL 5.7m	WL-7-1	76.54	13.71	1.15	0.29	1.60	0.12	4.04	2.48	0.07	0.96	*(2)*
B&B	Tephra V	76.58	13.77	1.12	0.26	1.63	0.10	4.03	2.41	0.10	0.97	*(2)*
Mount St Helens	MSH Cy standard	76.68	13.93	1.05	0.27	1.55	0.11	3.90	2.43	0.07		*(2)*

Table 1. Compositions of Selected Glasses - *continued*

Location & Depth proposed source	Tephra	SiO_2	Al_2O_3	Fe_2O_3	MgO	CaO	TiO_2	Na_2O	K_2O	Cl	SC	*Ref.*
WL 6.16m	WL-7-2	75.24	13.25	1.98	0.11	0.50	0.17	4.53	4.06	0.16	0.98	*(2)*
	Olema Ash Bed	75.01	13.63	1.76	0.11	0.50	0.17	4.48	4.05		0.97	*(5)*
Newberry Volcano	Paulina Creek	75.78	13.28	1.69	0.11	0.52	0.18	4.18	4.12	0.14		*(7)*
Ana River 3.62m	Tephra 6	72.2	14.7	2.47	0.49	1.77	0.49	4.7	3.0	0.14	0.96	*(1)*
WL 7.66m	WL-9-2	72.04	14.43	2.81	0.49	1.83	0.45	4.65	3.15	0.15	0.96	*(2)*
Crater Lake	Pumice Castle	72.64	14.39	2.41	0.53	1.85	0.46	4.23	3.12	0.24		*(3)*
Ana River 4.02m	Tephra 2	72.7	14.5	2.43	0.26	1.07	0.33	5.0	3.4	0.08	0.95	*(1)*
WL 8.06m	WL-9-4	72.73	14.36	2.71	0.26	1.10	0.32	4.88	3.54	0.10	0.95	*(2)*
Newberry Volcano	Ice Quarry	73.77	14.29	2.32	0.29	1.10	0.30	4.24	3.58	0.12		*(7)*
Ana River 7.05m	Tephra N1	69.7	15.0	3.59	0.51	1.65	0.49	5.5	3.0	0.12	0.98	*(1)*
WL 29.06m	WL-37-I	70.54	14.86	3.87	0.53	1.72	0.48	4.92	2.98	0.10	0.97	*(2)*
WL 29.06m	WL-37-II	70.40	14.85	3.89	0.53	1.73	0.48	5.03	2.99	0.10	0.97	*(2)*
Newberry Volcano	9912D	70.45	15.10	3.60	0.56	1.76	0.51	4.84	3.06	0.11		*(8)*
Ana River ~7.3m	Tephra P	71.6	14.4	3.12	0.33	1.15	0.34	5.3	3.5	0.11	0.97	*(1)*
Ana River ~7.3m	Tephra Q	71.8	14.3	3.10	0.32	1.15	0.33	5.2	3.5	0.11	0.97	*(1)*
Newberry Volcano	9920C	72.83	14.33	2.88	0.32	1.15	0.31	4.55	3.51	0.12		*(8)*
Ana River ~7.9m	Tephra S	74.1	13.6	2.06	0.14	0.61	0.19	5.0	4.0	0.12	0.95	*(1)*
Newberry Volcano	984F	75.30	13.73	1.91	0.14	0.63	0.18	4.09	3.90	0.12		*(7)*
Ana River 8.01m	Tephra T	74.7	13.5	1.86	0.12	0.52	0.18	4.9	4.1	0.13	0.97	*(1)*
WL 30.02m	WL-38-3	74.97	13.57	1.88	0.10	0.56	0.17	4.62	4.02	0.12	0.96	*(2)*
Newberry Volcano	984G5	75.33	13.57	1.70	0.12	0.53	0.16	4.47	3.98	0.13		*(7)*
Ana River ~9.3m	Tephra V, Davis (1985)	72.7	14.2	2.79	0.17	1.07	0.23	5.2	3.5	0.11	0.95	*(1)*
Newberry Volcano	0004F (Qaf3) overall	73.68	13.85	2.81	0.18	1.12	0.24	4.73	3.29	0.10	0.96	*(8)*
Newberry Volcano	0004F (Qaf3) ash	73.13	13.88	2.89	0.17	1.11	0.25	5.19	3.29	0.10	0.97	*(8)*
Newberry Volcano	978D	73.92	14.05	2.82	0.17	1.07	0.24	4.50	3.15	0.08	0.95	*(8)*
Ana River ~9.3m	Tephra V	74.23	14.30	2.69	0.17	1.15	0.22	3.70	3.44	0.12		*(8)*
Ana River ~9.4m	Tephra W1, glass 1	77.49	13.57	0.99	0.24	1.57	0.10	3.39	2.56	0.09	0.95	*(8)*
Mount St Helens ??	MSH Cy standard	76.68	13.93	1.05	0.27	1.55	0.11	3.90	2.43	0.07		*(2)*
Ana River ~11.3m	Tephra DD	69.2	15.5	3.54	0.62	1.88	0.6	6.1	2.3	0.11	0.96	*(1)*
Ana River ~11.5m	Tephra FF	68.70	15.40	3.85	0.65	2.00	0.64	6.10	2.30	0.12	0.97	*(1)*
Ana River ~11.6m	Tephra GG	69.00	15.30	3.82	0.59	1.85	0.59	6.10	2.40	0.12	0.97	*(1)*
Newberry Volcano	9917C	70.03	15.15	3.82	0.58	1.96	0.60	5.35	2.41	0.10		*(8)*
Ana River ~13.2m	Tephra KK	62.79	16.28	6.19	1.98	4.73	0.98	4.82	2.11		0.91	*(6)*
Medicine Lake	andesite tuff	64.56	16.09	5.37	1.60	4.08	0.89	4.88	2.45			*(6)*
Ana River ~17.3m	Tephra NN	69.4	15.0	3.93	0.67	2.15	0.68	5.1	2.7	0.09	0.95	*(1)*
Ana River ~17.3m	Tephra NN	70.03	15.07	3.85	0.69	2.30	0.64	4.52	2.80	0.09	0.99	*(8)*
Newberry Volcano	9881C	70.29	15.09	3.87	0.71	2.32	0.65	4.22	2.76	0.09		*(7)*
Ana R. Section E	Tephra OO	76.4	14.0	1.04	0.24	1.43	0.1	4.20	2.5	0.07	0.97	*(1)*
Mount St Helens ??	MSH Cy standard	76.68	13.93	1.05	0.27	1.55	0.11	3.90	2.43	0.07		*(2)*

East Draw in Newberry caldera and in a soil horizon on the northwest side of the volcano (Kuehn and Foit, 2000). The presence of traces of 9715K tephra in the main (98-79-C) deposit of Wono tephra at Newberry volcano, trends in the glass compositions of the two tephras, and the very close spacing in time of Wono and 9715K, and suggest that the two tephra units may have been erupted from the same magma chamber.

A tephra layer found only in the Wetlands Levee core at a depth of 6.16m and identified as the Olema ash (Negrini et al, 2000) also correlates to the Paulina Creek tephra (SC = 0.97). Paulina Creek tephra includes pyroclastic flows and surge and airfall deposits at numerous locations around Newberry volcano (Kuehn, 1999). If this correlation is valid, then the age of the Paulina Creek eruption is 50-75 ka. Although the core at the Bed & Breakfast locality was apparently not deep enough to penetrate the Olema/Paulina Creek bed, its absence at the Ana River canyon section remains unexplained.

Tephra 2 (depth 4.02m) at the Ana River canyon section and tephra WL-9-4 in the Wetlands Levee core both weakly correlate

Table 2. Summary of Summer Lake glasses and corelations. References: (1) Davis (1985), (2) Herrero-Bervera et. al. (1994), (3) Negrini et al. (2000), (4) Kuehn and Foit (2000), (5) Kuehn and Foit (this paper, not previously published)

Summer Lake localities and glasses			Correlations & Notes	Tephra Sources
Ana River Canyon (1)	WL Core (2)	B&B Core (2)		
Mazama			Crater Lake climactic eruption (1)	Crater Lake (1)
A			mixed glasses, not analyzed (1)	
B				
C			mixed glasses, not analyzed (1)	
D			MSH Mp (1)	Mt St Helens (1)
18			Trego Hot Springs (1)	
		Tephra IA	*exact position in overall stratigraphy uncertain*	
	WL-1-1		*exact position in overall stratigraphy uncertain*	
	WL-1-2		*exact position in overall stratigraphy uncertain*	
E			similar to THS, probably from same vent (1)	
E1				
	WL-2-1			
F	WL-2-2	Tephra IB	Wono tephra (1)	**Newberry** ? (4) or Crater Lake (1)
	WL-2-2.1			
	WL-2-3			
G	WL-2-4	Tephra II	9715K	**Newberry** ? (4)
		Tephra IIB		
		Tephra IIC		
		Tephra III		
		Tephra IV-A	*exact position in overall stratigraphy uncertain*	
		Tephra IV-B	*exact position in overall stratigraphy uncertain*	
	WL-6-1		*exact position in overall stratigraphy uncertain*	
12 - glass 1	WL-7-1	Tephra V	MSH Cy (1)	Mt St Helens (1)
12 - glass 2				
	WL-7-2		Olema ash bed (3), Paulina Creek tephra (4)	**Newberry** (4)
H				
	WL-9-1			
8			Pumice Castle-like 1 (1)	Crater Lake
6	WL-9-2		Pumice Castle (1)	Crater Lake
4			similar to Pumice Castle (1)	Crater Lake
	WL-9-3			
2	WL-9-4		Ice Quarry (4)	**Newberry (4)**
	WL-17-1			
	WL-17-2			
I			very thin, not sampled (1)	
J			mixed glasses, not analyzed (1)	
K				
L			mixed glasses, not analyzed (1)	
	WL-25-I			

Table 2. Summer Lake glasses and corelations. - continued

Summer Lake localities and glasses			Correlations & Notes	Tephra Sources
Ana River Canyon (1)	WL Core (2)	B&B Core (2)		
M				
N				
	WL-34-1			
---------- *unconformity* ----------				
N1	WL-37-I, WL-37-II		9912D (5)	**Newberry** (5)
O				
P	WL-37-III		same as Q ? (5)	**Newberry** (5)
Q	WL-37-IV		9920C (5)	**Newberry** (5)
R	WL-38-1			
S			984F(4)	**Newberry** (4)
T	WL-38-3		984G5 (4)	**Newberry** (4)
U			mixed glasses, mostly mafic glass (5)	
V			0004F (Qaf3) and/or 978D (5)	**Newberry** (5)
W				
W1			mixed glasses: one rhyolitic and one basaltic glass are dominant; rhyolitic glass is similar to MSH set C but too old (5)	Mt St Helens ?? (5)
X			very thin, not sampled (1)	
Y			very thin, not sampled (1)	
Z			mixed glasses, not analyzed (1)	
AA			very thin, not sampled (1)	
BB			mixed glasses, not analyzed (1)	
CC			very thin, not sampled (1)	
DD			Pringle Falls K (2), 9917C ? (5)	**Newberry** ? (5)
EE			Pringle Falls H (2)	
FF			9917C ? (5)	**Newberry** ? (5)
GG			Pringle Falls D (2), 9917C ? (5)	**Newberry** ? (5)
HH				
II			Pringle Falls S (2)	
JJ - clear glass				
JJ - brown glass				
KK			Medicine Lake andesite tuff (2)	Medicine Lake (2)
LL				
MM				
NN			9881C (4)	**Newberry** (4)
OO			similar to Mt St Helens set C but much older (1)	Mt St Helens ?? (1)
PP			mixed glasses, not analyzed (1)	
QQ			mixed glasses, not analyzed (1)	
RR			mixed glasses, not analyzed (1)	
SS			mixed glasses, not analyzed (1)	

(SC = 0.95) to Ice Quarry tephra at Newberry. Ice Quarry tephra is a widespread, yellow-white airfall pumice which reaches a thickness of up to 56cm on the south flank of the volcano (Kuehn and Foit, 2000). The thermoluminescence age of this tephra at Summer Lake (Berger, 1991) is 67.3 $\pm$ 7.2 ka.

Tephra N1 (depth 7.05m) just below the unconformity at Ana River section correlates (SC = 0.97) to closely spaced tephra layers WL-37-I and WL-37-II (29.06m) in the Wetland Levee core and to Newberry tephra 9912D (SC = 0.98). This Newberry tephra also is chemically very similar to 2 younger Ana River canyon tephras N (SC = 0.97) and

M (SC = 0.96) found just above the unconformity. The correlation of 9912D Newberry tephra to N1 is preferred as it would explain why one of the largest Pleistocene airfall tephra deposits (tephra 978B) at Newberry is not present in the Ana River canyon section C or Wetland Levee core --- it was lost in the unconformity

Closely spaced tephras P and Q (depth ~7.3m) correlate (SC = 0.97) to tephra 9920C, a 2.3m thick coarse white pumice exposed in the south caldera wall at Newberry volcano.

Tephra S (depth ~7.9m) and Tephra T (depth 8.01m) in the Ana River section correlate to Newberry tephras 984F (SC = 0.95) and 984G5 (SC = 0.96), respectively from locations on the eastern flank of the volcano. Tephra T also is found at the bottom of the Wetland Levee core (Figure 2, depth ~30m).

Tephra V correlates to two Newberry tephras, 0004F (SC = 0.96-0.97) and 978D (SC = 0.97). 0004F is a very coarse pumiceous pyroclastic flow deposit found on the east side of Newberry volcano. 978D is an airfall deposit found on the northeast side of the volcano. The two deposits may represent different parts of a single eruption.

Tephra OO is similar in composition to set C tephra at Mount St Helens (SC = 0.97) but is much to old to be a set C tephra. Davis (1985) suggests that tephra OO could represent an earlier eruption of Mount St Helens. Likewise, tephra W1, which also is compositionally similar to set C tephra (SC = 0.95), could represent an early eruption of Mount St Helens.

Tephra layers DD, FF, and GG all are similar to Newberry tephra 9917C (SC = 0.96, 0.97, and 0.97 respectively). Tephra 9917C is a very thick and coarse deposit found on the upper northwest side of Newberry volcano.

Tephra layer KK may correlate to an andesite tuff from Medicine Lake volcano (Herrero-Bervera et. al., 1994). The tephra is compositionally heterogeneous, and this may explain the low similarity coefficient between the average glass compositions (Table 1). Comparison of the more silicic end-member glass in both tephra deposits might provide a more solid correlation. It the correlation is correct, then the age of KK is about 170 ka.

Tephra NN the oldest tephra exposed (depth ~17.3m) in Ana River canyon section C strongly correlates strongly (SC = 0.99) to Newberry tephra 9881C. Tephra 9881C is found as a 21 cm thick deposit at a single locality on the lower southeast side of Newberry volcano. The largest pumices in this deposit reach 5 cm in length. The coarse texture of NN ash, the largest fragments of which approach 5 mm at Ana River Canyon, indicates a relatively nearby source and reinforces the correlation based on glass composition. Based on the age vs. depth plots presented in Negrini et. al. (2000) the age of this tephra is about 220 ka.

As outlined above and in Tables 1 and 2, the glass fractions in many of the older unidentified tephras observed in the Ana River canyon section and the Wetland Levee and Bed and Breakfast cores have a marked compositional similarity to those in proximal Newberry Pleistocene silicic tephras. While perhaps not proof positive it does suggest that Newberry volcano was a major supplier of volcaniclastic sediment to the Lake Chewaucan basin and likely beyond.

The presence of several even older tephras at Newberry volcano and the correlations above also suggest that additional Newberry tephras are waiting to be found in the Lake Chewaucan sediments preserved below the base of the Ana River canyon section.

References

Allison, I.S. (1945) Pumice beds at Summer Lake, Oregon. Geological Society of America Bulletin 56, 789-808.

Allison, I.S. (1966a) Pumice at Summer Lake, Oregon --- A correction. Geological Society of America Bulletin 77, 329-330.

Allison, I.S. (1966b) Fossil Lake, Oregon: Its geology and fossil faunas. Or. State Monographs Studies in Geology 9, 48.

Allison, I.S. (1982) Geology of pluvial lake Chewaucan, Lake County, Oregon. Or. State Monographs Studies in Geol., 11, 79.

Benson, L.V, Smoot, J.P., Kashgarian, M., Sarna-Wojcicki, A., and Burdett, J.W., 1997, Radiocarbon ages and environments of deposition of the Wono and Trego Hot Springs Tephra layers in the Pyramid Lake sub basin Nevada, Quat. Res., 47, 251-260.

Borchardt, G.A., Aruscavage, P.J., and Millard, Jr., H.T. (1972) Correlation of the Bishop Ash, a Pleistocene marker bed, Using instrumental neutron activation analysis, J. of Sed. Pet., 42, #2, 301-306.

Busacca, A.J., Nelstead, K.T., McDonald, E.V., Purser, M.D., Ugolini, F.C., Dahlgren, R., LaManna, J., Nuhn, W., and Zachara, J., 1992, Correlation of distal tephra layers in loess in the Channeled Scabland and Palouse of Washington State, Quat. Res., 37, 281-303.

Davis, J.O. (1985) Correlation of Late Quaternary tephra layers in long pluvial sequence near Summer Lake, Oregon. Quat. Res., 23, 38-53.

Herrero-Bervera , E., Helsley, C.E., Sarna-Wojcicki, A.M., Lajoie, K.R., Meyer, C.E., Turin, B.E., Donelly-Nolan, J.M., McWilliams, M.O., Negrini, R.M., and Liddicoat, J.C., 1994, Age and correlations of a paleomagnetic episode in the western United States by 40Ar/39Ar dating and tephrochronolgy: The Jamaica, Blake, or a new polarity episode?, J. of Geophys.l Res., 99, 24,091-24,103.

Kuehn, S.C., 1999, Could Newberry volcano be the source of Wono, Olema, and many other distal ashes?: Geological Society of America Abs. with Prog., 31, 292-293.

Kuehn, S.C. and Foit, Jr., F.F. (2000) Silicic tephras of Newberry Volcano, in Jenson, R.A. and Chitwood, L.A. eds., What's New at Newberry Volcano, Oregon: Guidebook for the Friends of the Pleistocene Annual Pacific Northwest Field Trip, pp. 135-163.

Negrini, R.M., Erbes, D.B., Faber, K., Herrera, A.M., Roberts, A.P., Cohen, A.S., Wigand, P.E., and Foit, Jr., F.F. (2000) A paleoclimate record for the past 250,000 years from Summer Lake, Oregon, USA: I. Chronology and magnetic proxies for lake level, J. of Paleolimnology, 24, 125-149.

Sarna-Wojcicki, A., Meyer, C.E, Adam, D.P., and Sims, J.D., 1988, Correlations and age estimates of ash beds in late Quaternary sediments of Clear Lake, California, Geological Society of America Special Paper 214, 141-150

Smith, D.G.W and Westgate, J.A. (1969) Electron probe technique for characterizing pyroclastic deposits. Earth and Planetary Sci. Letters 5, 313-319.

Thermoluminescence Dating of Summer Lake Tephra

Glenn W. Berger, Desert Research Institute, 2215 Raggio Parkway, Reno, NV 89512, USA [gwberger@dri.edu]

Principles of the Method

The approach under discussion is to date the fine-silt-sized glass-shard rich component of tephra. The advantage of using the fine-silt fraction is that it dominates distal ash beds. The advantage of using the glass fraction is that it is unquestionably eruptive, and usually dominates the fine-silt fraction. When it doesn't dominate, it is distinct enough to permit physical separation (with some difficulty) in quantity. This approach was first successfully applied by Berger (Berger and Huntley, 1983) to a sample of naturally purified (>99% glass) Mazama Ash from British Columbia. Since then Berger (references in Berger, 1991) developed procedures for purification of 5-10 μm diameter glass shards, and for accurate measurement of the often dim thermoluminescence (TL).

The basic concept is analogous to that exploited in the TL dating of fired pottery (Atiken, 1985). At formation, the glass shards must have zero trapped electrons in the glass matrix. The number of trapped electrons grows during burial through constant bombardment of grains and shards by ambient and cosmogenic ionizing radiations. Heating the glass shards in the laboratory releases all trapped electrons, producing TL. The TL signal is converted to an accumulated radiation dose by use of calibrated laboratory radiation sources. Dividing this TL-derived accumulated dose (paleodose or "equivalent dose" D_E) by a calculated dose rate (from measured concentrations of radio-elements in the sediments) gives a TL age.

In practice the method is more complex, and there remains much that is unknown about the luminescence micro-properties of glass-rich samples. Nevertheless, by use of independently dated samples, the accuracy of the method has been demonstrated (Figure 1) in certain volcanic regions, notably the Cascades of North America.

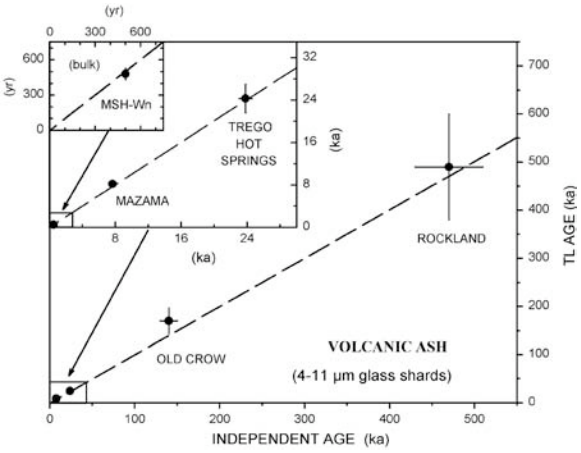

Figure 1. TL ages *vs.* independent ages (after Berger, 1995).

An example of the TL signals ("glow curves") from tephra 18 (lab sample SML-10, Trego Hot Springs ash) is shown in Figure 2.

The general principle, as for pottery dating, is to build up TL signals with added artificial doses, then extrapolate this dose response to zero TL. This is done at each of several consecutive temperature slices of the glow curves to check for the existence of a plateau in dose-axis intercept values (D_E values) This extrapolation at the 320-330°C slice of the glow curves for sample SML-10 is shown in Figure 3.

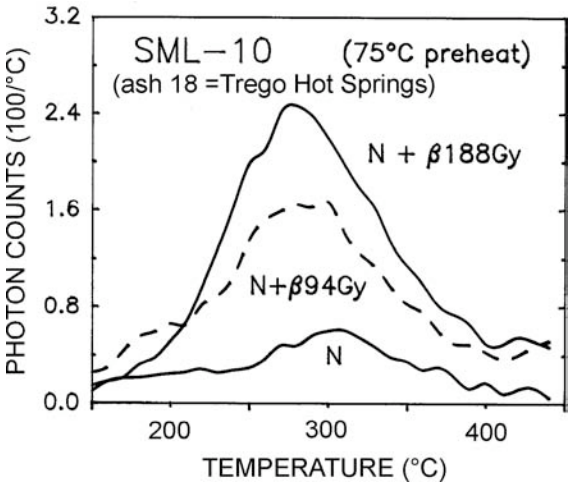

Figure 2. TL additive-dose glow curves (after Berger, 1991).

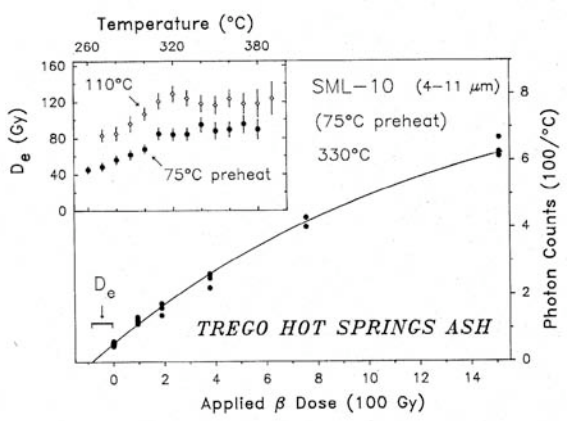

Figure 3. TL dose-response curve and D_E – T plots for ash 18 (secrtion E) (after Berger, 1991).

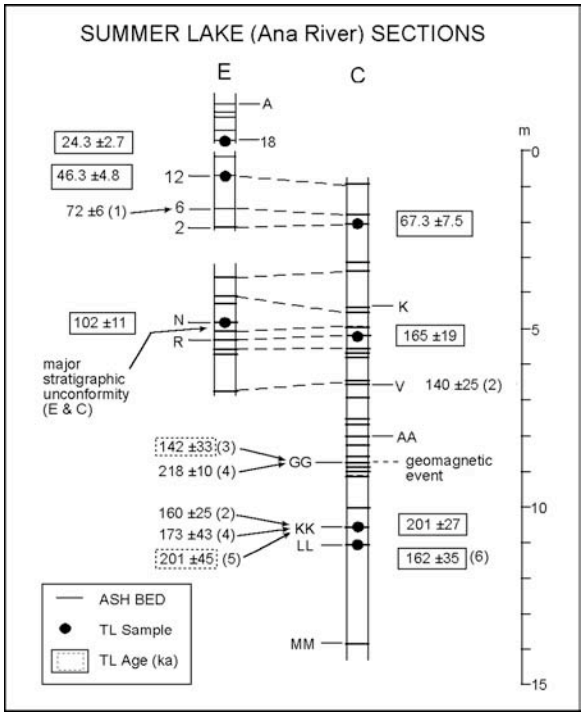

Figure 4. TL ages (solid boxes) from sections E and C, and other ages related to these (modified from Berger, 1991). Numbers in parentheses denote the following sources: (1)– Davis (1985), Negrini et al. (1994); (2)– Sarna-Wojcicki et al. (1991); (3)– Berger (unpublished data); (4)– Herrero-Bervera et al. (1994); (5)– Berger and Busacca (1995); (6)– see text.

The existence of a plateau in the intercept values suggests a temperature region of thermal stability for the TL signal. This plateau value is then used in the age calculation. Laboratory heating ("preheating") is required to empty electrons from traps filled in the laboratory irradiations, but emptied during the long burial of the sample. That is, short-lived traps must be emptied from the artificially dosed aliquots (each glow curve in Figure 2 and each filled circle on the dose-response curve in Figure 3 represents one aliquot) in order to permit comparison with the unirradiated ("as found") aliquots (zero-dose in Figure 3, "N" in Figure 2). The results in the inset show that a plateau condition, while necessary, is not a sufficient condition for age accuracy with glass-rich ash. Tests on independently dated samples (Figure 1),including the sample in Figure 3, indicate that the 110☜C result in Figure 3 is incorrect. This aspect of the method is discussed more fully by Berger (1991).

Results

The TL ages in the solid boxes of Figure. 4, excepting that for ash 12, are from Berger (1991). Analytical errors are 1☞. The 46.3±4.8 ka age (Berger and Busacca, 1995) for ash 12 is the first direct age for an ash correlated to any MSH set C ash. This age is the mean of three TL experiments, and therefore differs from the 50-ka age reported by Berger (1991). Ash 12 is correlated to MSH set Cy. Other numeric ages (dashed box and no box) are also shown, and are discussed here from top to bottom.

The 72±6 ka age is a K-Ar age for Pumice Castle from Crater Lake, that is correlated to ash 6 here (Negrini et al., 1994, 2000). The 140±25 ka age for ash V is based on correlation to the indirectly dated (interpolated from inferred sedimentation rates) ash T1193 at Tule Lake (Sarna-Wojcicki et al., 1991). The 142±33 ka age (Berger, unpublished data) is a TL date for the glass-rich fraction of an ash component of tephra bed D at Pringle Falls that is associated with the Pringle Falls geomagnetic excursion. Low TL signals created a low precision. The 218±10 ka age is from $^{40}Ar/^{39}Ar$ dating of bulk plagioclase crystals from pumice-lapilli tephra D (Herrero-Bervera et al., 1994). Single-grain Ar-Ar dating ought to be attempted. The 160±25 ka age is an inferred (interpolated, indirect) age assignment to ash T2023 from the Tule Lake core (Sarna-Wojcicki et al., 1991). The 173±43 ka age is from $^{40}Ar/^{39}Ar$ dating (Herrero-Bervera et al., 1994) of plagioclase crystals from the andesite tuff of Medicine Lake that is correlated to T2023 and ash KK here. The 201±45 ka age is a TL date (Berger, 1991) from the glass-rich fraction of Wadsworth tephra, which is correlated to ash KK here (Negrini et al., 1994).

Summary

The available direct and indirect ages for the portion of section C below ash R all suggest rapid sedimentation in the interval 160-200 ka. All but the 218-ka Ar/Ar age suggest that the Pringle Falls geomagnetic excursion occurred at ☜160-170 ka. In this context, a comment on the 162±35 ka TL age for ash LL in Figure 4 is worthwhile. That age derived

from unusual TL dose-response curves (Berger, 1991). Similar TL behavior was exhibited by the glass-rich fraction of a sample of the Alaskan Sheep Creek tephra (Berger, 1991), which yielded a TL age about half the probable age of ~200 ka (Berger et al., 1996). The implication of this comment is that the TL age of 162±35 ka for ash LL here is at best probably a minimum age. The author presently assigns more significance to the201±27 age for the overlying ash KK.

References

Aitken, M.J., 1985, Thermoluminescence Dating. Academic Press, San Diego, 351 p.

Berger, G.W. 1991. The use of glass for dating volcanic ash by thermoluminescence. Journal of Geophysical Research: v. 96, p. 19705-19720.

Berger, G.W., 1995. Progress in luminescence dating methods for Quaternary sediments. *In*, Dating methods for Quaternary deposits. (Rutter, N.W., and Catto, N., eds.). Geological Association of Canada: GEOtext no. 2, p. 81-103.

Berger, G.W. and Busacca, A.J., 1995, Thermoluminescence dating of late-Pleistocene loess and tephra from eastern Washington and southern Oregon, and implications for the eruptive history of Mount St. Helens. Journal of Geophysical Research: v. 100, p. 22,361-22,374.

Berger, G.W. and Huntley, D.J., 1983, Dating volcanic ash by thermoluminescence. Council of Europe, PACT Journal: v. 9, p. 581-592.

Berger, G.W., Péwé, T.L., Westgate, J.A. and Preece, S., 1996, Age of Sheep Creek tephra (Pleistocene) in central Alaska from thermoluminescence dating of bracketing loess. Quaternary Research: v. 45, p. 263-270.

Davis, J.O., 1983, Level of Lake Lahontan during deposition of the Trego Hot Springs tephra about 23,400 yrs ago. Quaternary Research: v. 19, p. 312-324.

Davis, J.O., 1985, Correlation of late Quaternary tephra layers in a long pluvial sequence near Summer Lake, Oregon. Quaternary Research: v. 23, p. 38-53.

Herrero-Brevera, E., Helsey, C.E., Sarna-Wojcicki, A.M., Lajoie, K.R., Meyer, C.E., McWilliams, M.O., Negrini, R.M., Turrin, B.D., Donnelly-Nolan, J.M., and Liddicoat, J.C., 1994, Age and correlation of a paleomagnetic episode in the western Unites States by $^{40}Ar/^{39}Ar$ dating and tephrochronology: A Jamaica, Blake, or a new polarity episode?. Journal of Geophysical Research: v. 99, p. 24091-24103.

Negrini, R.M., and Davis, J.O., 1992, Dating Late Pleistocene pluvial events and tephras by correlating paleomagnetic secular variation records from the western Great Basin. Quaternary Research: v. 38, p. 46-59.

Negrini, R.M., Erbes, D.B., Roberts,A.P., Verosub, K.L., Sarna-Wojcicki, A.M., and Meyer, C.E., 1994, Repeating waveform initiated by a 180-190 ka geomagnetic excursion in western North America: Implications for field behavior during polarity transitions and subsequent secular variation. Journal of Geophysical Research: v. 99, p. 24105-24119.

Negrini, R.M., Erbes, D.B., Faber, K., Herrera, A.M., Roberts, A.P., Cohen, A.S., Wigand, P.E.and Foit Jr., F.F., 2000, A paleoclimate record for the past 250,000 years from Summer Lake, Oregon, USA: I. Chronology and magnetic proxies for lake level. Journal of Paleoclimatology: v. 24, p. 125-149.

Sarna-Wojcicki, A.M., Lajoie, K.R., Meyer, C.E., Adam, D.P., and Rieck, H.J. 1991. Tephrochronological correlation of upper Neogene sediments along the Pacific margin, coterminous United States. *In*, The Geology of North America, vol. K-2, Quaternary Nonglacial Geology Coterminous United States, (R.B. Morrison, ed.) pp.117-140, Geological Society of America, Boulder, Colorado

Magnetism of Chewaucan sediments: Implications for stratigraphy, paleolake-level, and the behavior of the Earth's magnetic field

Robert M. Negrini, Department of Physics and Geology, CSU Bakersfield, CA

Introduction

This article is a summary of the published and ongoing work on the magnetism of the bottom sediments of Lake Chewaucan. These studies are divided into two subdisciplines: 1) environmental magnetism in which the concentration, mineralogy, and grain-size are determined for the magnetic mineral constituents of the lake sediments using various techniques including artificial magnetizations of sediment samples in the laboratory; and 2) paleomagnetism in which the natural remnant magnetization (NRM) of the sediments is determined with sensitive magnetometers. The NRM ideally records the vector components (declination, inclination, and intensity) of the regional magnetic field recorded at or near the time of deposition.

Environmental magnetic studies often constrain provenance and the environment of deposition. Paleomagnetic results enable us to study the behavior of the Earth's magnetic field (EMF) and also can constrain the age and post-magnetization deformation of the sediments.

Four principal localities have been sampled (Figure 1). One is a collection of outcrops along the Ana River Canyon; the other three are coring localities.

Data Quality

The bottom sediments of Lake Chewaucan carry strong and stable magnetizations which have been shown to record the EMF at the time of deposition (Negrini et al., 1988; 1992; 1994; 2000). Furthermore, these sediments are sensitive to laboratory magnetizations allowing them to be distinguished primarily due to differences in the concentration of the magnetic minerals and, to a lesser extent, to differences in the grain size of these minerals. The magnetic mineralogy is restricted to magnetite and/or titanomagnetite (Roberts et al., 1994; Negrini et al., 2000).

Age Control

Age control is critical in the interpretation of environmental and paleomagnetic records. The

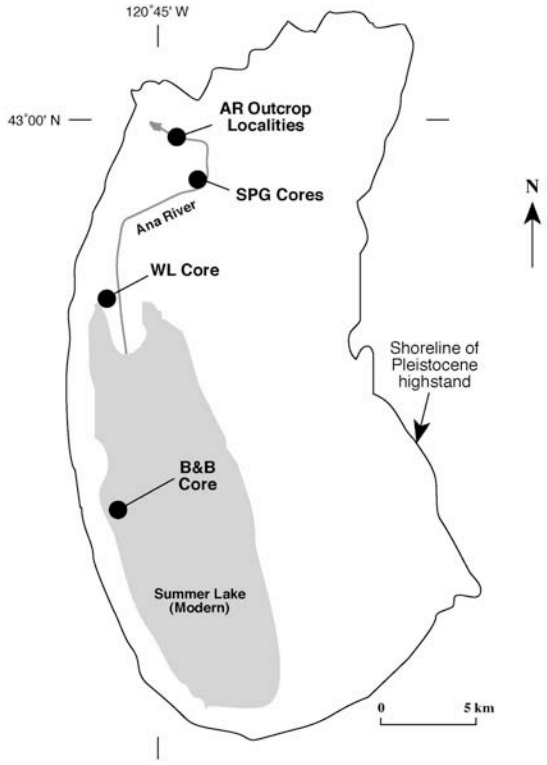

Figure 1. Locality of outcrop and coring sites discussed in this article.

chronology of the Lake Chewaucan bottom sediments (Figure 2) is summarized most recently by Negrini et al. (2000). It is generally very good for the part of the section younger than ~100 ka. Ongoing works relevant toward improving this chronology and extending it further back in time include those presented elsewhere in this volume (Kuehn and Foit; Berger; Gardner and Negrini; Conrey et al.; Zic).

Representative Results

Environmental Magnetism. The magnetite concentration of the Chewaucan sediments has been shown to be a reliable indicator of relative lake-level by its anticorrelative relationships with independent indicators of lake-shallowness such as an ostracode paleosalinity index and total organic carbon (e.g., see Figure R6, this volume; Cohen et al., 2000; Negrini et al., 2000; Zic et al., in review). The hypothesis forwarded to explain this relationship is the dissolution of magnetite during high biological productivity at low lake-level (Negrini et al., 2000 and references therein).

The parameters used to estimate magnetic mineral concentration (e.g., magnetic susceptibility "κ", isothermal remanent magnetization "IRM", etc.) can be measured rapidly relative to other

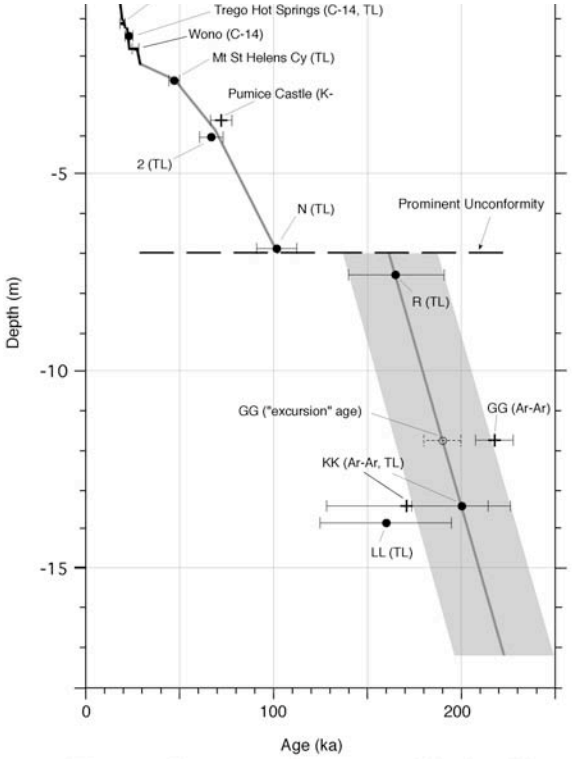

Figure 2. Summary of age control for Ana River outcrop stratigraphy (from Negrini et al. 2000).

paleoenvironmental proxies (e.g., pollen/ostracode counts, geochemical measurements, grain-size, etc.). Thus, κ and other concentration parameters were measured almost continously for the entire Ana River section and for the cores from all three coring localities thereby producing estimates of relative lake-level for at least the past 350,000 years (Negrini et al., 2000; Quilliam et al., 2000; Zic, 2001; this volume).

One of the main results of this research is shown in Figure 3. Here, relative lake level, as indicated by the κ records from both the Ana River Outcrop and the WL core, is shown to rise/fall in tune with the growth/recession of the earth's ice cap. Note that the age of the Chewaucan records is based solely on the chronology of Figure 2 and that there is no *a priori* assumption of a fit to global climate change. In particular, the age of each sample in the Ana River record is determined from the solid line in the chronology diagram and the age of the WL samples is tied into the Ana River chronology using several correlation tie points discussed in Negrini et al. (2000).

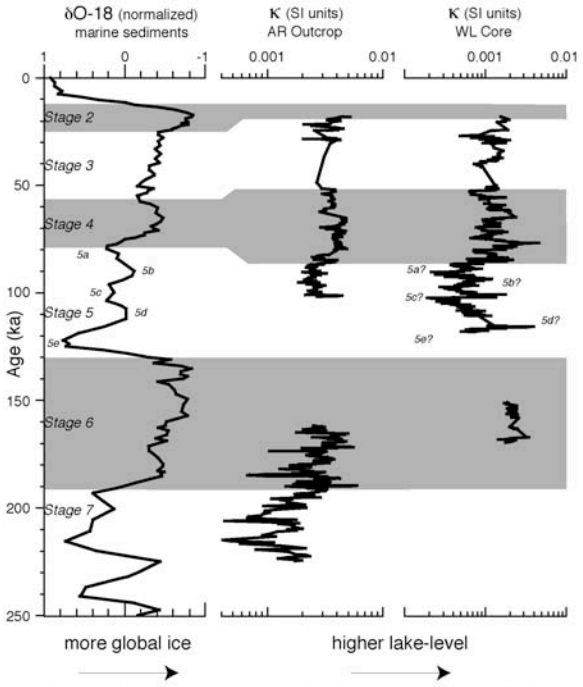

Figure 3. Magnetic concentration proxy for level of Pluvial Lake Chewaucan compared to marine O-18 proxy for global ice volume (from Negrini et al. 2000). Age of Chewaucan sediments is based on chronology shown in Figure 2. Marine data is from Martinson et al. (1987).

If we assume that the relative lake-level inferred from Figure 3 represents the precipitation / evaporation ratio for the NW Great Basin region, then these results support Antevs' model (1948) of rising/falling lake-levels in the Great Basin in response to the southward/northward migration of the northern jet stream storm tracks during the growth/recession of the ice sheets. In an article elsewhere in this volume, Zic demonstrates that the higher frequency response of this region to global climate change is exactly opposite to that shown in Figure 3. That is, at millennial (10^3) rather than Milankovitch time ($10^{4\text{-}5}$) time scales, the Summer Lake region receives more/less precipitation and Lake Chewaucan rises/falls in response to interstadial/stadial global climate conditions.

Paleomagnetism. The paleomagnetic record of the Lake Chewaucan sediments is useful for three principal reasons. First, it can be used as a chronological tool by correlating the Chewaucan record to those of other sediments and/or volcanic extrusives (e.g., Gardner and Negrini, this volume). Second, paleomagnetic directions can be used to identify post-magnetization deformation (e.g., rigid body rotations). Third, accurate, well dated

paleomagnetic records are critical to our understanding of the earth's magnetic field.

Chronological Applications. The first type of application was used to determine the ages of pluvial events and tephra layers by comparing the paleomagnetic record from the uppermost part of the Ana River Section with the relatively well dated record from the Pluvial Lake Russell sediments exposed in the Wilson Creek drainage near Mono Lake, CA (Negrini and Davis, 1992; Grayson, 1993; Bradley, 1999). One of the dated events was the ~4,000 year gap in the record associated with a recession of the lake below the outcrop after the deposition of the Wono tephra layer dated at 27.3 ^{14}C kyr B.P. by Benson et al. (1997). Subsequent work by Zic (2001; this volume) comparing a Chewaucan lake-level record from the depocenter with Greenland ice core records has shown that this low lake event is probably associated with Heinrich Event #3.

Ongoing research demonstrates that paleomagnetic records have the potential to correlate Pleistocene lake sediments with a spatial range at least continental in scale and with a temporal resolution corresponding to events as short as hundred of years (Figure 4; Negrini, in press). The first set of records (Figure 4a) demonstrates a straightforward correlation of such records across the North American continent and well into the Atlantic Ocean. All three vector components are involved in this correlation for the interval above the Pringle Falls Excursion which contains two low amplitude repetitions of the cycle initiated by that excursion (Negrini et al., 1994). This example demonstrates not only the potential of great spatial range for the method but also the ability to compare climate records from nonmarine and marine settings constrained by independently determined, paleomagnetic-based correlations.

The second set of records (Figure 4b) shows a high resolution correlation of the inclination record from the Summer Lake B&B core with the record from the Wilson Creek beds of Pluvial Lake Russell. Here 14-15 individual peaks and troughs can be correlated in the 7-8 kyr interval represented by the Lake Chewaucan record inferring the potential to correlate events as short as 500 years with this method.

Structural Control. An example of the second type of application is the use of the paleomagnetic directions to show that, except for minor fault blocks which are avoidable during sampling, Section C in the Ana River Canyon has not been rotated appreciably (Negrini et al., 1988). The principal body of evidence used in this determination is twofold. First, the paleomagnetic directions of the Pumice Castle tephra layer at Section C (D=10.1°, I=52.4°, α-95=4°) is indistinguishable from that of its correlative proximal welded tuff (D=6.6°, I=50.2°, α-95=3°). The tuff direction is unpublished data from Duane Champion of the USGS, Menlo Park. Second, the mean direction (D=3.9°, I=57.4°, α-95=5°) from the SLC set of data in Section C (~600 samples covering the past ~250,000 years) is indistinguishable from the expected Geocentric Axial Dipole field direction for the Summer Lake region (D=0.0, I=61.8°).

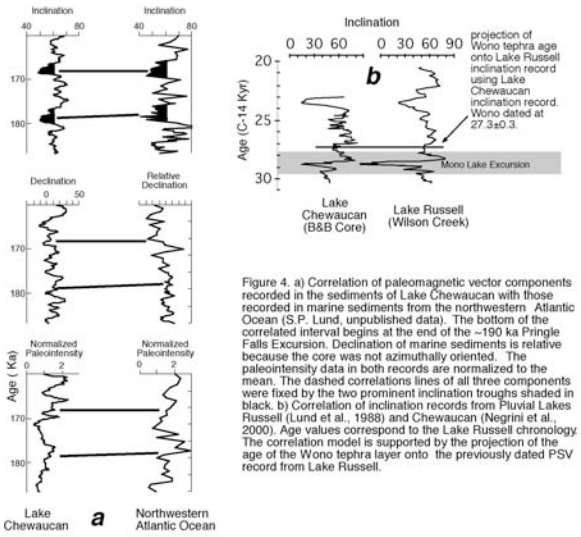

Figure 4. a) Correlation of paleomagnetic vector components recorded in the sediments of Lake Chewaucan with those recorded in marine sediments from the northwestern Atlantic Ocean (S.P. Lund, unpublished data). The bottom of the correlated interval begins at the end of the ~190 ka Pringle Falls Excursion. Declination of marine sediments is relative because the core was not azimuthally oriented. The paleointensity data in both records are normalized to the mean. The dashed correlations lines of all three components were fixed by the two prominent inclination troughs shaded in black. b) Correlation of inclination records from Pluvial Lakes Russell (Lund et al., 1988) and Chewaucan (Negrini et al., 2000). Age values correspond to the Lake Russell chronology. The correlation model is supported by the projection of the age of the Wono tephra layer onto the previously dated PSV record from Lake Russell.

Behavior of the Earth's magnetic field. The composite paleomagnetic record from the sediments of Lake Chewaucan represents much of the past ~250,000 years with each sample averaging as little as 40 years of the magnetic field. Included in this dataset are records of three geomagnetic excursions, field phenomena thought to exist somewhere in the continuum between aborted reversals and high amplitude secular variation. Accordingly, this record potentially provides constraints on the behavior of the magnetic field.

One such result is the finding that the ~200 ka Pringle Falls Excursion initiated a waveform which repeated itself twice in the low amplitude secular variation well after the excursion was over thus confirming an earlier, similar finding for the Mono Lake Excursion (Lund et al., 1988). This result is shown in Figure 5 where the vector directions are plotted as virtual geomagnetic poles (VGP). The repetitions are also plotted in field vector component form in Figure 4a. Only the very distinctive end of the waveform is plotted in Figure 5. The earlier part of the waveform (two clockwise loops) is shown in Negrini et al. (1994).

In addition to the reduced amplitude of the repetitions relative to that of the excursion (note change in scale between lowest and two uppermost plots), the reference frame for the waveform rotated 180° about the Earth's axis immediately after the excursion ended. Because this behavior is so distinctive (i.e., a repeating waveform with an unusual VGP path which underwent a dramatic mode change after the excursion) its places a restrictive constraint on the future modeling of this excursion (and perhaps others) by the magnetohydrodynamics community. Accordingly, it may reveal something specific about the behavior of the magnetic field during excursions and/or reversals such as governing boundary conditions in the core or perhaps specific mechanics governing a switch between the symmetric and asymmetric dynamo familes of Merrill and McFadden (1988).

Both the Laschamp and Mono Lake Excursion were found in the paleomagnetic record from the Summer Lake B&B core (Figure 6) marking one of the first times these elusive excursions have been found in the same high resolution record. The precise correlation of the Summer Lake B&B IRM record (a proxy for lake-level) with the GISP2 O-18 temperature proxy for the North Atlantic region supports the existence of these features as

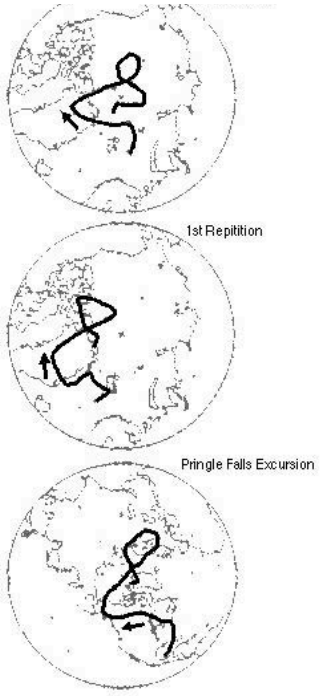

Figure 5. Virtual geomagnetic pole (VGP) paths of the last part of the Pringle Falls Excursion waveform. At the bottom is the excursion itself. The top two plots show the VGP paths corresponding to the repetitions of the waveform in the low amplitude secular variation from the sediments above the excursion zone.

geomagnetic phenomena because the Greenland ice cores also have signatures of the excursions in the same relative stratigraphic position between IS#s 6 and 7 (Wagner et al., 2000a; 2000b).

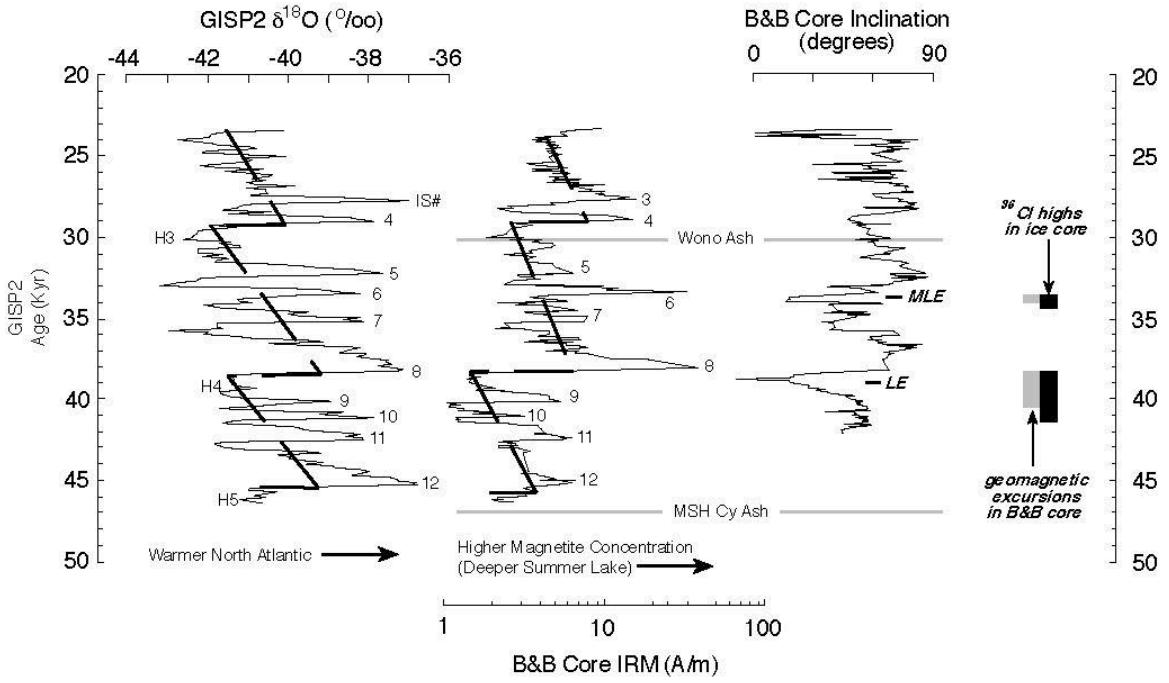

Figure 6. Laschamp and Mono Lake Excursions in paleomagnetic inclination record for Summer Lake B&B core. The stratigraphic positions of the inclination lows corresponding to the Laschamp and Mono Lake Excursions correlate well with the associated ^{36}Cl peaks found in the Greenland ice cores between IS# 6 and 7 by Wagner et al. (2000a; 2000b). For details regarding the tie to the GISP2 record, see Zic (this volume).

References

Benson, L., J. Smoot, M. Kashgarian, A. Sarna-Wojcicki, & J. Burdett, 1997. Radiocarbon ages and environments of deposition of the Wono and Trego Hot Springs Tephra layers in the Pyramid Lake sub basin, Nevada, Quaternary Research, v. 47, pp. 251-260.

Berger, G., 1991. The use of glass for dating volcanic ash by thermoluminescence, Journal of Geophysical Research, v. 96, pp. 19,705-19,720.

Bradley, R., 1999. Paleoclimatology: Reconstructing Climates of the Quaternary, Academic Press, San Diego, CA.

Cohen, A., M. Palacios-Fest, P. Wigand, R. Negrini, D.B. Erbes, 2000, A paleoclimate record for the past 250,000 years from Summer Lake, Oregon, U.S.A.: II. Lithostratigraphy, ostracodes, and pollen, Journal of Paleolimnology, v. 24., p. 151-182.

Grayson, D.K., 1993. The Desert's Past: A Natural Pre-History of the Great Basin. Smithsonian Press, Washington, D.C.

Lund, S.P., Liddicoat, J.C., Lajoie, K.L., Henyey, T.L., & Robinson, S., 1988. Paleomagnetic evidence for long-term (10^4 year) memory and periodic behavior of the Earth's core dynamo process. Geophys. Res. Lett. 15: 1101-1104.

Martinson, D.G., N.G. Pisias, J.D. Hays, J. Imbrie, T.C. Moore and N.J.Shackleton, 1987. Age dating and the orbital theory of the ice ages: Development of a high-resolution 0 to 300,000 year chronostratigraphy, Quaternary Res., v. 27, 1-29.

Merrill, R. T., and P. L. McFadden, 1988. Paleosecular variation and the origin of geomagnetic field reversals. Jour. Geophys. Res., v. 93, pp. 11,589-11,597.

Negrini, R.M., in press, Pluvial lake-sizes in the northwestern Great Basin throughout the

Quaternary Period. In Currey, D.R., R. Herschler, and D.B. Madsin (eds), Great Basin Aquatic Systems History, Smithsonian Press, Washington, D.C.

Negrini, R. M., K.L. Verosub, and J.O. Davis, 1988. The middle to late Pleistocene geomagnetic field recorded in fine-grained sediments from Summer Lake, Oregon, and Double Hot Springs, Nevada, U.S.A., Earth Plan. Sci. Lett., v. 87, pp. 173-192.

Negrini, R. M., Davis, J. O., 1992. Dating late Pleistocene pluvial events and tephras by correlating paleomagnetic secular variation records from the western Great Basin: Quaternary Research, v. 38, p. 46-59.

Negrini, R.M., D.B. Erbes, A.P. Roberts, K.L. Verosub, and A.M. Sarna-Wojcicki, C. Meyer, 1994. Repeating waveforms initiated by a 100-200 ka excursion in western North America: Implications for geomagnetic field behavior during polarity transitions and subsequent secular variation, Jour. Geophys. Res., v. 99, pp. 24,105-24,119.

Negrini, R. M., D.B. Erbes, K. Faber, A.M. Herrera, A.P. Roberts, A.S. Cohen, P.E. Wigand, and F.F. Foit, 2000. A paleoclimate record for the past 250,000 years from Summer Lake, Oregon, USA: I. Chronology and magnetic proxies for lake level: Journal of Paleolimnology, v. 24, p. 124-149.

Quilliam, M., S. Meyer, R. Negrini, 2000. Magnetic susceptibility as a proxy for climate change in greater than 250,000 year old sediments in northwestern Great Basin, U.S.A., AAPG Bull.

Roberts, A. P., K.L Verosub, and R.M. Negrini, 1994. Relative paleointensity studies of lacustrine sediments, Lake Chewaucan, western United States, Geophys. Journ. Intern., v. 23, pp. 2859-2862.

Wagner, G., Beer, J., Laj, C., Kissel, C., Masarik, J., Muscheler, R., and Synal, H. –A., 2000a, Chlorine-36 evidence for the Mono Lake event in the Summit GRIP ice core: Earth and Planetary Science Letters, v. 181, p. 1-6.

Wagner, G., Masarik, J., Beer, J., Baumgartner, S., Imboden, D., Kubik, P. W., Synal, H. –A., and Suter, M., 2000b, Reconstruction of the geomagnetic field between 20 and 60 kr BP from cosmogenic radionuclides in the GRIP ice core: Nuclear Instruments and Methods in Physics Research, v. B181, p. 597-604.

Zic, M., 2001. Sediment Magnetism of the B&B Core from Summer Lake, Oregon, USA: Implications for Regional and Global Millennial-Scale Climate Change from 46-23 ka, M.S. Thesis, Department of Physics and Geology, CSU Bakersfield, CA.

Zic, M., R.M. Negrini, and P.E. Wigand, in review. The full spectrum of late Pleistocene, millennial-scale climate change in a lake-level record from the Great Basin, Geology.

Paleomagnetic correlation of the Shevlin Park Tuff, central Oregon, with tephra layer SL-JJ at Summer Lake in south-central Oregon

Cynthia A. Gardner, USGS, 5400 MacArthur Blvd., Vancouver, WA 98661
Robert M. Negrini, UC-Bakersfield, Department of Physics and Geology, Bakersfield, CA 93311

Abstract

The Shevlin Park Tuff of central Oregon is geochemically correlated to tephra layer SL-JJ at Summer Lake in south-central Oregon, but published ages for these two units differ by about 100,000 years. We used paleomagnetic secular-variation techniques to test this correlation further. Paleomagnetic directions for two Shevlin Park Tuff sites are nearly identical and combined are D=342°, I=53°, a95=1.2°. Paleomagnetic directions for samples in lacustrine silts just above and below SL-JJ are combined to give a direction for the SL-JJ of D=343°, 53°, a95 = 4.2°. The similarity in paleomagnetic directions for the Shevlin Park Tuff and SL-JJ supports the geochemical correlation

Introduction

Five middle Pleistocene ignimbrites and two pumice-fall deposits that erupted from vents just east of the High Cascades axis are exposed near Bend, Oregon (Hill and Taylor, 1989). The youngest of these ignimbrites, the Shevlin Park Tuff, is by bulk composition an andesite (Hill and Taylor, 1989), but contains andesitic and rhyolitic glass shards in its matrix (Sarna-Wojcicki et al., 1989). Tephra layer SL-JJ at Summer Lake (Davis, 1985) also contains a bimodal population of silicic and mafic shards that have been correlated geochemically to matrix shards in the Shevlin Park Tuff (Sarna-Wojcicki et al., 1989).

If the Shevlin Park Tuff/SL-JJ correlation is correct, then there is an issue regarding the ages of these volcanic units because published ages of the tuffs differ by about 100,000 years. The Shevlin Park Tuff has a $^{40}Ar/^{39}Ar$ plateau age of 260 ± 15 ka (Lanphere et al., 1999). The SL-JJ has not been dated directly, but is inferred to be <173 ± 43 by its stratigraphic position relative to Summer Lake tephra layer SL-KK. SL-JJ lies about 40 cm above SL-KK. SL-KK is correlated to tephra layer T2023 at Tulelake (similarity coefficient = 0.98), which in turn is correlated to the andesite tuff of Medicine Lake (Rieck et al., 1992). The andesite tuff of Medicine Lake is dated at 173 ± 43 ka (Herrero-Bervera et al., 1994; also a 40 Ar/39/Ar plateau age). Therefore, if all the geochemical correlations are correct, then SL-KK is 173 ± 43 ka, and the SL-JJ is <173 ± 43 ka. Berger (1991) obtained a thermoluminescence age for the SL-KK of 200 ± 27, which supports the correlated age for the SL-KK.

Paleomagnetic data can serve as an independent test of geochemical and stratigraphic correlations provided it can be shown that the deposit sampled carries a primary remanent magnetization (see Verosub, 1981). Ignimbrites are generally emplaced at elevated temperatures making them useful deposits for paleomagnetic work (see Tarling, 1983). Paleomagnetic investigations of sediments along the banks of the Ana River Canyon near Summer Lake (Negrini et al., 1988; 1994; Roberts et al., 1994) demonstrated the presence of a stable and primary depositional remanent magnetism for lake sediments acquired at or near the time of deposition. The stability of the sediments at the Ana River Canyon suggested that we could test the Shevlin Park Tuff/SL-JJ correlation by using paleomagnetic techniques.

Field Methods

The Shevlin Park Tuff was drilled in the field using a gasoline-powered, hand-held drill and samples were oriented with both a sun and a magnetic compass (see Tarling, 1983). Two sites, several kilometers apart, were drilled to test the reliability of site paleomagnetic directions. Samples were collected from several separate blocks at each site, and each sample, or sample pair, was separated from the next by a distance of several meters and, or, by vertical fractures.

Samples were measured in the USGS paleomagnetic laboratory in Denver, CO, using a spinner magnetometer to determine natural and remanent magnetization. Each sample was subjected to progressive alternating-field demagnetization (AFD) in a tumbling demagnetizer to determine the stable component of magnetization.

Tephra layer SL-JJ is a 1-cm-thick, coarse-grained ash found along the banks of the Ana River, section C, in the Lake Chewaucan basin. The tephra is in sharp contact with lacustrine silts. Because the tephra was too coarse grained for paleomagnetic sampling, silts above and below the tephra layer were sampled using the method described in Negrini et al.

(1988). Six samples were collected below and three samples were collected above SL-JJ. Samples were analyzed at CSU- Bakersfield. Like the ignimbrite samples, a spinner magnetometer was used to determine natural and remanent magnetization, and each sample was subjected to progressive AFD.

Results

Magnetic vectors of most Shevlin Park Tuff samples decay to the origin upon AFD, showing a single component of magnetization. Some samples had a weak secondary component that was removed by AFD to 20 mT (Fig. 1-A). Most samples contain between 10 and 30 percent remanence remaining after demagnetization to 100 mT. The remaining remanence indicates the presence of a high coercivity magnetic phase. If the high coercivity phase had a component of magnetization significantly different from that removed between 20 and 100 mT, the magnetic vectors would not decay to the origin.

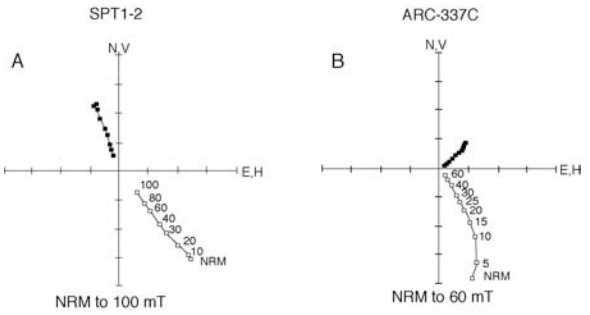

Fig. 1. Representative vector demagnetization diagrams showing sample behavior during alternating-field demagnetization. A) Shevlin Park Tuff sample from site SPT1. Demagnetization levels are 0, 10, 20, 30, 40, 60, 80, and 100 mT. Primary component of magnetization is between 20 and 100 mT. B) Lake Chewaucan silt sample stratigraphically near (within 1 meter) tephra layer SL-JJ. Demagnetization levels are 0, 5, 10, 15, 20, 25, 30, 40, 50, and 60 mT. Primary component of magnetization is between 15 and 60 mT.

Like the ignimbrite samples, the silty sediments of Lake Chewaucan showed a relatively stable primary magnetization after removal of a secondary viscous remanent magnetization by 15 mT (Fig. 1-B).

The reliability of the Chewaucan sediment directions at Section C is independently supported by previous work (Negrini et al., 1988). For example, another water-laid tephra layer in this section, the Pumice Castle tephra, was found to have a tightly constrained paleomagnetic direction which was statistically indistinguishable from the direction of its correlative tuff sampled at Crater Lake. Furthermore, the mean paleomagnetic direction from the entire 15 meters of sediment at Section C which, accounting for missing time in unconformities (Negrini et al., 2000), averages well over 100,000 years of magnetic field behavior, is statistically indistinguishable from the expected Geocentric Axial Dipole direction for the site latitude (Negrini et al., 1988).

Paleomagnetic direction for the two Shevlin Park Tuff sites are essentially indistinguishable at declination (D) =342°, inclination (I) =53° and D=342°, I=54° for sites 1 and 2 respectively (Table 1). The degree of scatter within each site is small, and the sites were combined to give a direction for the Shevlin Park Tuff of D=342°, I= 53°. The direction for six samples from the silt layer immediately below SL-JJ is D=342°, I=56°, and for the three samples in the silt above SL-JJ is D=341°, I=47°. These directions were combined to give a direction for the SL-JJ of D=342°, I= 53° (Table 1). All directions are of normal polarity.

Discussion

Paleomagnetic directions for the two Shevlin Park Tuff sites are tightly constrained and indistinguishable from each other and from the paleomagnetic direction for the SL-JJ (Fig. 2). This provides permissive evidence that the Shevlin Park Tuff and SL-JJ are coeval, which supports the geochemical correlation of Sarna-Wojcicki et al. (1989). The paleomagnetic data provide permissive evidence only, however, and not proof of correlation because the Earth's magnetic field moves in such a manner that no single direction is unique. In other words, at different times in the past, the Earth's magnetic field has been in the exactly this position. Thus one must leave open the possibility that the

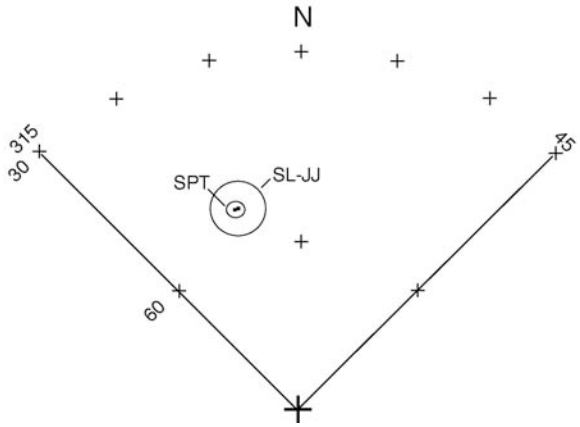

Fig. 2. Portions of equal-area stereonet projection showing paleomagnetic directions and associated cones of 95 percent confidence for the Shevlin Park Tuff (SPT) and Summer Lake tephra layer SL-JJ. Note that only a sector of the stereonet projection is shown, from 315 to 46 degrees horizontal and from 30 to 90 degrees vertical.

similarity of paleomagnetic directions is simply fortuitous.

We investigate the statistical significance of this last statement using the analysis of Bogue and Coe (1981). This analysis considers the uniqueness of the compared mean directions with the direction associated with the most probable position of the Earth's magnetic field vector at the time of the eruption. More specifically, the following two hypotheses are tested: 1) the Probability Assuming Random hypothesis and 2) the Probability Assuming Simultaneous hypothesis. The first hypothesis is tested by calculating the likelihood that data are in at least as good agreement as could arise in the two units by coincidence given the expected dispersion of the paleomagnetic field in the study region. The second hypothesis is tested by calculating the likelihood of two units having directions at least as different as the Shevlin Park and tephra layer SL-JJ assuming they acquired their magnetization simultaneously.

In our calculation we used the same conservative value for paleomagnetic dispersion (a measurement of the amplitude of variation in magnetic direction due to the Earth's magnetic field) in the Pacific Northwest as did Bogue and Coe (1981). Also, on the basis of the close fit between the two site directions for the Shevlin Park Tuff, we assumed that negligible noise was introduced into the Shevlin Park mean paleomagnetic directions from structural tilting and rotation of sampled outcrops. Negrini et al. (1988) determined that Summer Lake Section C was not rotated to an uncertainty of ± 5°. This uncertainty was included in our statistical analyses according to the method outlined in Bogue and Coe (1981).

For the proposed Shevlin Park Tuff/SL-JJ correlation, the likelihood of the simultaneous hypothesis is 995 times greater than that of the random hypothesis. This statistical measure coupled with the small uncertainties in the directions from the two volcanic units implies a very reliable correlation based on paleomagnetic directions (for a comparison of values for other correlations, see Bogue and Coe, 1981).

The paleomagnetic data require further discussion regarding the confidence of the geochemical correlations between Shevlin Park Tuff and SL-JJ as well as among SL-KK, T2023, and the andesite tuff of Medicine Lake, as well as the confidence of ages assigned to these units. For example, recently, Conrey et al. (in press) have questioned the validity of the Shevlin Park Tuff/SL-JJ correlation. Additional data are likely needed before present controversies will be resolved.

References

Berger, G.W., 1991, Dating tephra using thermoluminescence from glass: Journal of Geophysical Research, v. 96, B12, p. 19705-19720.

Bogue, S. W., and Coe, R. S., 1981, Paleomagnetic correlation of Columbia River basalt flows using secular variation: Journal of Geophysical Research, v. 86, p. 11,883-11,897.

Conrey, R.M., Donnelly-Nolan, Julie, Taylor, E.M.,Champion, Duane, and Bullen, Thomas, in press, The Shevlin Park Tuff, central Oregon Cascade Range: Magmatic processes in an arc-related ash-flow tuff: submitted to 2001 Fall AGU meeting.

Davis, J.O., 1985, Correlation of late Quaternary tephra layers in a long pluvial sequence near Summer Lake, Oregon: Quaternary Research, v. 23, p. 38-53.

Fisher, R.A., 1953, Dispersion on a sphere: Proceeding sof the Royal Society, v. A217, p. 295-305.

Herrero-Bervera, Emilio, Helsley, C.E., Sarna-Wojciciki, A.M., Lajoie, K.R., Meyer, C.E., McWilliams, M.O., Negrini, R.M., Turrin, B.D., Donnelly-Nolan, J.M., and Liddicoat, J.C., 1994, Age and correlation of a paleomagnetic episode in the western United States by $^{40}Ar/^{39}Ar$ and tephrochronology: The Jamaica, Blake, or a new polarity episode?: Journal of Geophysical Research, v. 99, no. B12, p. 24,091-24,103.

Hill, B.E., and Taylor, E.M., 1989, Oregon central High Cascade pyroclastic units in the vicinity of Bend, Oregon, *in* Scott, W.E., Gardner, C.A., and Sara-Wojcicki, A.M., eds., Guidebook for Field Trip to the Mount Bachelor-South Sister-Bend area, Central Oregon High Cascades: U.S. Geological Survey Open-File Report 89-645, p. 51-54.

Lanphere, M.A., Champion, D.E., Christiansen, R.L., Donnelly-Nolan, J.M., Fleck, R.J., and Sarna-Wojciciki, A.M., 1999, Evolution of tephra dating in the western United States: Geological Society of America Meeting and Abstracts, Cordilleran Section, v. 100, p. A-73.

Negrini, R.M., Verosub, K.L., and Davis, J.O, 1988, The middle to late Pleistocene geomagnetic field recorded in fine-grained sediments from Summer Lake, Oregon and Double Hot Spring, Nevada, U.S.A.: Earth and Planetary Science Letters, v. 87, p. 173-192.

Negrini, R. M., 1994, Repeating waveform initiated by a 180-190 ka geomagnetic excursion in western North America: Implications for field behavior during polarity transitions and subsequent secular variation: Journal of Geophysical Research, v. 99, p. 24,105-24,119.

Negrini, R. M., Erbes, D. B., Faber, K., Herrera, A. M., Roberts, A. P., Cohen, A. S., Wigand, P. E., and Foit, F. F., Jr., 2000, A paleoclimate record for the past 250,000 years from Summer Lake, Oregon, USA: I. Chronology and magnetic proxies for lake level: Journal of Paleolimnology, v. 24, p. 125-149.

Rieck, H.J., Sarna-Wojcicki, A.M., Meyer, C.E., and Adam, D.P., 1992, Magnetostratigraphy and tephrochronology of an upper Pliocene to Holocene record in lake sediments at Tulelake, northern California: Geological Society of America Bulletin, v. 104, p. 409-428.

Roberts, A. P., Verosub, K. L., and Negrini, R. M., 1994, Middle/Late Pleistocene relative paleointensity of the geomagnetic field from lacustrine sediments, Lake Chewaucan, western United States: Geophysical Journal International, v. 118, p. 101-110.

Sarna-Wojcicki, A.M., Meyer, C.E., Nakata, J.K, Scott, W.E., Hill, B.E., Slate, J.L, and Russel, P.C., 1989, Age and correlation of mid-Quaternary ash beds and tuffs in the vicinity of Bend, Oregon, *in* Scott, W.E., Gardner, C.A., and Sara-Wojcicki, A.M., eds., Guidebook for Field Trip to the Mount Bachelor-South Sister-Bend area, Central Oregon High Cascades: U.S. Geological Survey Open-File Report 89-645, p. 55-62.

Tarling, D.H., 1983, Paleomagnetism: Principles and applications in Geology, Geophysics, and Archeology: Chapman and Hall, New York, 379 p.

Verosub, K.L, 1981, The interrelationship between magnetostratigraphy and tephrochronology, in Self, S. and Sparks, R.S.J. eds, Tephra Studies: Reidel, Dordrecht, p. 62-75.

Table 1. Paleomagnetic data for the Shevlin Park Tuff sites near Bend, Oregon and SL-JJ from the Ana River area of Summer Lake. Demag level - demagnetization level at which there is the least amount of dispersion; Dec - declination in degrees; Inc - inclination in degrees down (normal polarity); N/N1 - the number of samples measured/number of samples used in the statistical analysis; alpha 95 - the cone of 95 percent confidence; k - precision parameter (Fisher, 1953); Lat - north latitude in degrees; Long - west longitude in degrees.

Site	**Unit**	**Demag level**	**Dec**	**Inc**	**N/N1**	**alpha 95**	**k**	**Lat**	**Long**
SPT-1	Shevlin	40 mT	342	53	8/8	1.5	1453	44.10	121.42
SPT-2	Shevlin	30 mT	342	54	7/6	1.9	1216	44.05	121.41
sites 1&2			342	53	15/14	1.2	1122		
ARC-380, A-F	silt below SL-JJ	15 mT	342	56	6/6	4.8	193	42.8	121.7
ARC-379, A-C	silt above SL-JJ	15 mT	341	47	3/3	6.2	399	42.8	12.7
combined 379&380	SL-JJ	15 mT	343	53	9/9	4.2	148		

Regression Models to Calculate Temperature of Calcification for the Ostracodes *Limnocythere staplini* and *Cypridopsis vidua*

Manuel R. Palacios-Fest

Terra Nostra Earth Sciences Research, 3220 West Ina Road # 8105
Tucson, Arizona 85741 USA
e-mail: terra_nostra_mx@yahoo.com.mx

Abstract: Laboratory and field experiments conducted between 1990 and 1994 show that the Mg/Ca molar ratios from ostracode valves of the species *Limnocythere staplini* and *Cypridopsis vidua* may be used to calculate water temperature at the time of calcification. The two species are eurytopic and cosmopolitan, although *L. staplini* tolerates higher salinity ranges than *C. vidua*; the two species have a short life cycle, about 30 days. These characteristics make them ideal for paleoenvironmental reconstructions.

Using ICP-MS the concentrations of Mg and Ca were measured and the Mg/Ca molar ratios determined from both the field and laboratory experiments. For *L. staplini* the molar ratios ranged between 0.010 and 0.018, while for *C. vidua* fluctuated between 0.018 and 0.032. Mg and Ca concentrations in natural and experimental waters were also measured and Mg/Ca molar ratios were calculated. For the experimental waters (*L. staplini*) the ratios varied from 6.68 to 8.66, that is, they were relatively high but virtually constant. For the natural waters (*C. vidua*) the ratios ranged from 0.306 to 0.461, again the values were fairly constant but in this case quite low.

Both experiments demonstrate that water temperature plays a major role in Mg uptake, whereas the Mg/Ca molar ratios of the host water are significantly less important. In addition, they show a great data variability suggesting that clustering 4-5 valves for ICP analysis is a good alternative. Also, these studies highlight the importance of discriminating adult from juvenile valves to avoid interpretative conflicts. Finally, these analyses conclude that ostracode biology and water temperature control shell chemistry.

Introduction

In 1922, Clarke and Wheeler were the first researchers to suggest that Mg uptake by the exoskeleton of invertebrates was influenced by water temperature. Chave (1954) and Dodd (1965) supported this view but Dodd (1967) proposed that Mg/Ca of water was also important. Hence, the problem had to be seen as one of thermodynamic equilibrium. Ever since, a number of scientists tried to find a solution to the puzzle. Although stable isotope studies made significant progress, the trace metal approach remained elusive. Over the past 20 years, several specialists suggested mechanisms to calculate water temperature from the Mg/Ca molar ratios of ostracode valves, in response to the Mg/Ca molar ratios of the host water. The signal was there but the temperature estimates remained confusing because frequently changed from site to site, suggesting that since water chemistry changes, from one lake to the other, then the only alternative to estimate temperature was through the partition coefficient (Kp) for Mg. Ostracodes have been extensively used for this purpose.

Ostracodes are microcrustaceans (0.3 to 3 mm) that form a low Mg calcite carapace (or shell) consisting of two valves (right and left) and shed their skeleton up to nine times before adulthood. In contrast to mollusks that grow by aggregation, ostracodes form a new carapace "instantaneously" within a few hours. Sr and Mg have been the main source of interest for paleoenvironmental reconstructions. In this report, I will focus on Mg uptake by *Limnocythere staplini* and *Cypridopsis vidua*. The two species share some characteristics that make them ideal for this study, both of them are eurytopic (tolerant to a wide range of environmental conditions). Although the former tolerates a higher salinity range than the latter, their life cycle is short, about 30 days and they are ubiquitous in North America (Alaska to Mexico).

Chivas et al. (1983) were the first to highlight the significance of ostracode shell chemistry. They proposed that Mg/Ca molar ratios of ostracodes may be used for estimating

water temperature at the time of calcification. Several other attempts were made in that direction (see Palacios-Fest and Dettman, 2001) with little progress and controversial results. In all cases, the Kp [Mg] was used. Some researchers demonstrated that the Kp [Mg] changes from species to species and in some cases within a species or even worse within a single population of the same species (Wansard 1996, Wansard et al., 1998, De Deckker et al., 1999).

Palacios-Fest (1994) suggested an alternative mechanism to estimate water temperature without involving the Kp [Mg], a linear regression model. The advantage of this model is that it eliminates the two unknowns imposed by the thermodynamic equilibrium model. The latter requires estimating the Mg/Ca molar ratio of the host water and in a circular exercise (since to do so it is necessary to choose a temperature value) estimate water temperature. The linear regression model is simple and addresses a single unknown equation.

This study summarizes the results of Palacios-Fest (1996) and Palacios-Fest and Dettman (2001) with a few examples of applications of the standard coefficients generated by two experiments, a laboratory experiment and a field experiment. In addition, this paper discusses the significance of selecting the appropriate species, and the advantage of grouping valves for ICP analysis.

Materials and Methods

For the laboratory experiments specimens of *L. staplini* (a small cytheracean: 0.6-0.8 mm) were collected from Antero Pond, South Park, Colorado in the summer of 1991 (Fig. 1a). This species reproduces at around 13°C, but its survival range is wide (<2 to >30°C). *L. staplini* lives either in ephemeral or permanent water bodies, hence its tolerance to salinity variations is high (500 to 75,000 mg L^{-1}). It preferably grows in Ca^{2+}-rich and HCO_3^--depleted waters, dominated by Na^+, Mg^{2+}, and Cl^- or SO_4^{2-}. Experimental temperatures ranged from 5 to 25°C (at 5°C intervals). The lower temperature experiments (5 and 10°C) failed. The remaining three experimental settings allowed to understand the control mechanisms of Mg uptake for *L. staplini*. Palacios-Fest (1996) described the methodology followed for the experiments.

The field experiment consisted of a year-round (monthly) sampling in a small pond in the outskirts of Magadlena, Sonora, Mexico from January to December 1990 (Fig. 1b). *Cypridopsis vidua* (a small cypridacean, 0.7 1 mm) was collected from Presa El Yeso (a small dammed lake). As *L. staplini*, this species is eurytopic and reproduces best at about 13°C but also tolerates a wide range of temperature (<2 to >32°C). In contrast with *L. staplini*, *C. vidua* develops better in spring systems, therefore it prefers long-term to permanent, but may survive in ephemeral water bodies (Taylor, 1992). Its salinity tolerance range is lower than that of *L. staplini* (10 to 10,000 mg L^{-1}) (Delorme, 1989). During the field experiment living specimens were collected as well as water and sediments. Palacios-Fest and Dettman (2001) describe the field methods and the region's characteristics.

Analytical Procedures

Specimens of the two species were immersed in a diluted (5%) solution of H_2O_2 to remove the soft bodies and to separate the valves. Then, the split valves were rinsed three times in 18MΩ water, for consistency the right valves were used. Individual valves were weighed using a Cahn 29 electronic balance capable or reading micrograms (detection limit ±0.002 μg). The valves were dissolved in 3 ml of distilled 2% HCl. Up to ten specimens were used for the analyses. Ca^{2+} and Mg^{2+} were measured using a Turner TS Sola inductively coupled plasma argon mass spectrometer (ICP-MS). Detection limits for Mg^{2+} is 0.001 μg L^{-1} and 10 μg L^{-1} for Ca^{2+} (see Palacios-Fest and Dettman, 2001 for details).

Results

For the experimental study 45 adult specimens of *L. staplini* were used and 102 of *C. vidua* for the field experiment. The Mg/Ca molar ratios for *L. staplini* ranged from 0.0089 to 0.0254, while for *C. vidua* they ranged from

0.010 to 0.048. The evident difference in molar ratios between the two species demonstrates the biological effect on Mg uptake during ecdysis. Significantly, both the experimental and natural experiments show the increasing values of the Mg/Ca ratios with increasing temperature, highlighting the strong metabolic effect of ostracodes. However, variability also increases with increasing temperature in the two cases (Fig. 2).

Constants and coefficients generated for the laboratory and field experiments were obtained from the empirical and independent relations between host water temperature and the Mg/Ca molar ratios for *L. staplini* and *C. vidua*. The linear relation using the experimental and monthly points provide the correlation between temperature and the Mg/Ca molar ratios for each species (Fig. 2) (see Palacios-Fest and Dettman, 2001 for details). The results obtained for these two species are similar to those of Wansard (1996) and Wansard and Mezquita (2001) for other species of marine and continental water ostracodes from Europe (e.g., *Cyprideis torosa*, *Heterocypris intermedia*).

The life cycle of *L. staplini* and *C. vidua* are very short, about 30 days (Kesling, 1951, Forester, personal communication, 1988; Anderson et al., 1998) what means that, particularly for the field experiments, they are congruent with the temperatures measured in the field. With respect to the natural experiment this explains the monthly differences of the Mg/Ca ratios in *C. vidua* suggesting their response to seasonal environmental conditions. Figure 3 shows the monthly variation of the Mg/Ca ratios of the valves, indicating the rapid change due temperature effects, as shown by the anomaly of July. With the beginning of the monsoon a sudden decrease in water temperature was recorded by ostracode shell chemistry in *C. vidua*. Other anomalies, like high Mg/Ca ratios in specimens lighter than 3 μg suggested incomplete calcification, therefore, they were not included in the linear regression for *C. vidua*. The laboratory experiment did not show these anomalies, but variability was greater than in the field experiments with increasing temperature (see Palacios-Fest, 1996).

Discussion

Systematically, the relationship between the Mg/Ca ratios of ostracode valves and temperature has been modeled as a simple relation of the partition coefficient (Kp). Temperature and the Mg/Ca ratios of the host water, have been considered the controlling factors, as suggested by the thermodynamic equilibrium model (e.g., De Deckker et al., 1999, Engstrom and Nelson, 1991, Xia et al., 1997). The experiments summarized in this paper suggest that this is not necessarily true. Determining the Kp for Mg in calcite has proven conflicting enough in natural carbonates (Given and Wilkinson, 1985). Thorough laboratory studies (under strictly controlled conditions) on calcite precipitation have also been problematic and have demonstrated the complexity of the system, strongly influenced by other ions in solution (Morse and Bender, 1990). Therefore, it is recommended to be cautious when trying to use partition coefficient models for biologically generated carbonates, like ostracode valves.

The strong biological influence is clear in the Mg/Ca ratios of the early calcite ostracode shells forming from the chitinous exoskeleton at the beginning of ecdysis. Initially, magnesite is nearly precipitated but as the process continues the carapace calcifies calcite with less than 4 mol % of Mg. Chivas et al. (1986) reported values as high as 400,000 and 152,000 mg $L^{\infty 1}$ of Mg in poorly calcified valves with Mg/Ca ratios between 1.64 and 1.32. Cadot et al. (1975) showed wide gradients across the valves of marine ostracodes, with increasing concentrations of [Mg] towards the inner layer. The experimental results obtained in this study show the strong significance of calcification (expressed as μg valve mass) on the Mg/Ca ratio (Fig. 4). All the valves analyzed for these experiments were the adult stage and full sized for this population. However, light valves with low total Ca were present, generating significantly higher Mg/Ca ratios from the expected for the species (*L. staplini*: 0.0089-0.0259; *C. vidua*: 0.018-0.032). Valves lighter than 3 μg showed Mg/Ca ratios higher than

0.040, a value that is well over the values obtained at the highest experimental temperatures. Therefore, these valves were discarded on the reasonable assumption that the valves were not fully calcified.

The high [Mg] concentrations at the initial stages of calcification suggest the significance of metabolic fluids on mineral uptake. Turpen and Angell (1971), questioned the effect of metabolism suggesting that for *Heterocypris* sp. water was the only source for Ca. However, that study only proves that part of Ca comes from water, but does not demonstrate that it is the only source to form the valves; metabolic sources, especially food, may play a significant role in calcification. These authors cited the work of Fassbinder (1912) who demonstrated that *C. vidua* (part of this study) may produce a fully-calcified carapace in absence of Ca in water, suggesting that metabolism was the source of calcium to produce the calcite carapace. Other crustaceans have the ability to decalcify their exoskeletons and store Ca in gastroliths and in (Ca-rich) hemolymph immediately prior to ecdysis (Mann and Pieplow, 1938). In at least one crustacean species, *Procambarus clarkii*, temperature strongly affects the Mg concentration in body fluids of this crayfish (De Legarra et al., 1985). It is proposed here that similar processes may occur in ostracodes leading to carapaces enriched in Mg at higher temperatures.

Last, but not least, Mg/Ca ratios higher than 0.05 are extremely uncommon in fully calcified ostracode valves of any species. Nonetheless, these organisms survive in most aquatic systems with Mg/Ca ratios in water are three orders of magnitude greater than those recorded by ostracodes. The natural and laboratory experiments showed Mg/Ca ratios of the host water fluctuating between 0.30-0.46 (natural experiments) for *C. vidua*, and 6.68-8.66 (laboratory experiments) for *L. staplini*. In contrast, the Mg/Ca ratios of the fully calcified valves of *C. vidua* ranged from 0.010 to 0.038, while for *L. staplini* from 0.0089 to 0.0259. These results are in good agreement with other results obtained for ostracode populations analyzed from aquatic systems with much higher Mg/Ca ratios. In fact, the ratio of 0.01 to 0.04 is the typical range reported for ostracodes whether they grew in dilute waters with low Mg/Ca (<1 like in the field experiment and Wansard and Mezquita, 2001) or in saline waters with Mg/Ca as high as 305 (Chivas et al., 1986; De Deckker et al., 1999). Hence Mg/Ca ratios of the host water cannot be significant in determining the Mg/Ca ratio of ostracode valves. None of our experiments showed that a variation of 50% in the Mg/Ca ratio of the water had an effect on shell chemistry.

The regression model proposed by Palacios-Fest (1996) suggests that the organisms metabolically control Mg uptake as a function of temperature with no effect of the Mg/Ca ratios of the host water. Therefore, the thermodynamic equilibrium model is not an essential step to calculate temperature. Xia et al. (1997) and De Deckker et al. (1999) questioned the possibility of estimating temperature in a way different from the thermodynamic equilibrium model but their efforts have not generated satisfactory results. The regression model proposed by Palacios-Fest (1996) and Palacios-Fest and Dettman (2001) is based on the equation (1):

$$Mg/Ca_v = \beta_0 + \beta_1 (T°C) \quad (1)$$

where the suffix 'v' is for valve, β_0 is the constant for the species, β_1 is the coefficient for temperature and T is temperature in °C. Re-arranging the equation to solve for temperature, the regression becomes equation (2):

$$T (°C) = (Mg/Ca_v - \beta_0)/\beta_1 \quad (2)$$

for *L. staplini* $\beta_0 = -0.0035$ and $\beta_1 = 0.00089$ that is significantly different from zero ($p<0.001$) and for *C. vidua* $\beta_0 = 0.0103$ and $\beta_1 = 0.00066$ ($p<0.001$).

Palacios-Fest (1996) and Palacios-Fest and Dettman (2001) explain the details of the multiple regression models for *L. staplini* and *C. vidua*. In this paper, the interest is to highlight the viability of the alternative proposed regression model not involving the

partition coefficient that in addition creates a two unknowns equation and a circular exercise to 'estimate' temperature. In other words, in the geologic record the water chemistry, and more importantly the Mg/Ca ratio of the water is unknown and has to be calculated assuming a temperature range for the Kp, in doing this, calculating temperature is an unnecessary step; the Kp coefficients are inappropriate.

Some laboratory experiments suggest the strong influence of Mg/Ca of the water in ostracode valves (Chivas et al., 1983; Engstrom and Nelson, 1991; De Deckker et al., 1999). But the extreme culturing conditions in which the organisms were deprived of food and other sources of nutrients may have contributed to the bias. To date, it is unknown how ostracodes would respond to the calibrated supply of Mg either by food or water. De Deckker et al. (1999) suggest that ostracodes may respond in different ways to water chemistry given the wide range of the Mg/Ca spectrum in water. They suggest that if the Mg/Ca ratios in host water are low the ostracode valves enrich in Mg beyond a predictable Kp [Mg]. In contrast, if the Mg/Ca ratios are high, Mg is excluded, but in the intermediate range (possibly between 1 and 20) Mg/Ca_v follows a simple Kp.

Palacios-Fest and Dettman (2001) differ from this view for the following reasons: 1) there are still many questions about the response of ostracodes to natural settings and it is quite possible that this suggested pattern does not pertain to all taxa of ostracodes; 2) ostracode biology may also play a significant role in how different species respond to water chemistry. Rosenthal and Katz (1989) demonstrated that the two species of freshwater gastropods of the species Melanopsis control the Mg/Ca ratio of their body fluids independent of water chemistry. In contrast, Sr and Ba concentrations were not metabolically controlled and followed simple Kp. Many taxa of mollusks seem to be able to control [Ca] and [Mg] in their body fluids (Wilbur and Saleuddin, 1983).

Therefore, it is suggested that the regression models originally proposed by Palacios-Fest (1996) and replicated by Palacios-Fest and Dettman (2001) are a good alternative to reconstruct paleoclimate using the Mg/Ca ratios of L. staplini and C. vidua, respectively. It is recommended to use this paleothermometer in similar systems to the experimental ones described in Palacios-Fest (1996) and Palacios-Fest and Dettman (2001). For example, Figure 5 shows the estimated temperatures obtained from three sites in Summer Lake, Oregon (Pleistocene pluvial Lake Chewaucan) (for details see Cohen et al., 2000).

Conclusions

1. Temperature is the major factor controlling the Mg/Ca ratios in ostracode valves, at least for *L. staplini* and *C. vidua*. These ratios may be used as proxy for temperature in water bodies with a broad spectrum of Mg/Ca as shown by the experiments.
2. One must be cautious in using partition coefficients (Kp) for Mg in biogenic calcite. This is particularly important for Kp values that are greater than two orders of magnitude of those observed in the natural and laboratory experiments summarized in this paper.
3. An exhaustive laboratory and field research program is needed to understanding the role of the Mg/Ca ratios in ostracode populations in their natural settings. Ideally, both natural and laboratory experiments for the same species are encouraged. In the latter case it is suggested not to stress the organisms to conditions that will affect their response to Mg uptake.

Acknowledgments

I am grateful to Rob Negrini for inviting me to contribute this brief summary of ostracode shell chemistry and its application to the geologic record to the Friends of the Pleistocene Field Guidebook to Summer Lake (September, 2001).

References

Anderson, D.H., S. Darring and A.C. Benke. 1998. Growth of crustacean meiofauna in a forested floodplain swamp: implications for biomass turnover. *Journal of North American Benthological Society* 17: 21-36.

Cadot, H.M., R.L. Kaesler and W.R Schmus. 1975. Applications of the electron microprobe analyzer to the study of the ostracode carapace. *In* Swain, F. (Ed.). *Biology and Paleobiology of Ostracoda*. Bulletin of American Paleontology 65 (282): 577-585.

Clarke, A.N. and W.C.Wheeler. 1922. The inorganic constituents of marine invertebrates. *U.S. Geological Survey Professional Paper* 124: 1-62.

Chave, K.E. 1954. Aspects of the biogeochemistry of magnesium. Part I. Calcareous marine organisms. *Journal of Geology* 62: 266-283.

Chivas, A.R., P. De Deckker, and J.M.G. Shelley. 1983. Magnesium, strontium and barium partitioning in nonmarine ostracode shells and their use in paleoenvironmental reconstructions: A preliminary study. *In* Maddocks, R.F. (Ed.). *Applications of Ostracoda*. Houston, University of Houston, Geosciences 238-249.

Chivas, A.R., P. De Deckker and J.M.G. Shelley. 1986. Magnesium content of non-marine ostracod valves: a new paleosalinometer and paleothermometer. *Palaeogeography, Palaeoclimatology, Palaeoecology* 54: 43-61.

Cohen, A.S., M.R. Palacios-Fest, R.M. Negrini, P.R. Wigand and D.B. Erbes. 2000. A paleoclimate record for the past 250,000 years from Summer Lake, Oregon, USA: II. Sedimentology, paleontology and geochemistry. *Journal of Paleolimnology* 24: 151-182.

De Deckker, P., A.R. Chivas and J.M.G. Shelley. 1999. Uptake of Mg and Sr in the euryhaline ostracod Cyprideis determined from in vitro experiments. *Palaeogeography, Palaeoclimatology, Palaeoecology* 148: 105-116.

De Legarra, I., E.S. Andreu-Moliner, R. Montoro and A. Núñez-Cachaza. 1985. Influence of ambient temperature on the concentrations of calcium, magnesium, sodium and potassium in the hemolynph and urine of *Procambarus clarkii*. *Revista Española de Fisiología* 41 (3): 325-330.

Delorme. L.D. 1989. Methods in Quaternary ecology #7: Freshwater ostracodes. *Geoscience Canada* 16: 85-90.

Dodd, J.R. 1965. Environmental control of strontium and magnesium in *Mytilus*. *Geochimica et Cosmochimica Acta* 29: 385-398.

Dodd, J.R. 1967. Magnesium and strontium in calcareous skeletons: A review. *Journal of Paleontology* 41: 1313-1329.

Emiliani, C. 1955. Pleistocene temperatures. *Journal of Geology* 63: 538-578.

Engstrom, D.R. and S. Nelson. Paleosalinity from trace metals in fossil ostracodes compared with observational records at Devils Lake, North Dakota, USA. *Palaeogeography, Palaeoclimatology, Palaeoecology* 83: 295-312.

Fassbinder, K. 1912. Beitrage zur Kenntnis der Susswaasserostracoden. *Zool. Jahrb. Abt. Anat. Ont. Tiere*. 32: 533-576.

Fritz, P., T.W.Anderson and C.F.M. Lewis. 1975. Late-Quaternary climatic trends and history of Lake Erie from stable isotope studies. *Science* 190: 267-269.

Given, R.K. and B.H. Wilkinson. 1985. Kinetic control of morphology, composition and mineralogy of abiotic sedimentary carbonates. *Journal of Sedimentary Petrology* 55 (1): 109-119.

Kesling, R.V. 1951. The morphology of ostracode moult stages. *Illinois Biological Monographs* 21: 1-324.

Mann, H. and U. Pieplow. 1938. Der Kalkhaushalt bei der Hautung der Krebse. *Sizungsberichte der Gesellschaft Naturforschender Freunde der Berlin, Jahrgang* 1: 1-17.

Morse, J.W. and M.L. Bender. 1990. Partition coefficients in calcite: examination of factors influencing the validity of experimental results and their application to natural systems. *Chemical Geology* 82: 265-277.

Palacios-Fest, M.R. 1996. Geoquímica de la concha de ostrácodos (*Limnocythere staplini*): Un método de regresión múltiple como indicador paleoclimático. *GEOS* 16 (3): 130-136.

Palacios-Fest, M.R. 1994. Trace element shell chemistry of continental ostracodes and the applicability of experimentally-derived multiple regression models to paleoenvironmental reconstructions in Southwestern North America. *Dissertation*, Department of Geosciences, University of Arizona, Tucson, 279 pp.

Palacios-Fest, M.R. 1997. Paleoenvironmental reconstruction of human activity in Central Arizona using valve chemistry of Hohokam canal ostracodes. *Geoarchaeology* 9: 1-29.

Palacios-Fest, M.R. and D.L.. Dettman. (En prensa.) Temperature controls monthly variation in ostracode valve Mg/Ca: Cypridopsis vidua from a small lake in Sonora, Mexico. *Geochimica et Cosmochimica Acta*. (Accepted February 2, 2001.)

Palacios-Fest, M.R., A.L. Carreño, J.R. Ortega-Ramírez y G. Alvarado-Valdéz. (En prensa.) A paleoenvironmental reconstruction of Laguna Babícora, Chihuahua, Mexico based on ostracode paleoecology and trace element valve chemistry. *Journal of Paleolimnology*. (Accepted March 15, 2001.)

Rosenthal, Y. and A. Katz. 1989. The applicability of trace elements in freshwater valves for paleochemical studies. *Chemical Geology* 78: 65-76.

Taylor, L.C. 1992. The response of spring-dwelling ostracodes to intra-regional differences in groundwater chemistry associated with road salting in southern Ontario: A test using an urban-rural transect. *M. Sci. Thesis*, University of Toronto, Toronto, 222 pp.

Turpen, J.B. and R.W. Angell. 1971. Aspects of molting and calcification in the ostracod *Heterocypris*. *Biological Bulletin* 140: 331-338.

Urey, H.C. 1947. The thermodynamic properties of isotopic substances. *Journal of the Chemical Society* 152: 190-219.

Wansard, G. 1996. Quantification of paleotemperature changes during isotopic Stage 2 in the La Draga continental sequence (NE Spain) based on the Mg/Ca ratio of freshwater ostracods. *Quaternary Science Review* 15: 237-245.

Wansard, G., P. De Deckker and R. Juliá. 1998. Variability in ostracod partition coefficients D(Sr) and D(Mg): Implications for lacustrine paleoenvironmental reconstructions. *Chemical Geology* 146: 39-54.

Wansard, G. and F. Mezquita. 2001. The response of ostracod shell chemistry to seasonal change in a Mediterranean freshwater spring environment. *Journal of Paleolimnology* 25: 9-16.

Wilbur, K.M. and A.S.M. Saleuddin. 1983. Valve formation. *In* Saleuddin, A.S.M. and Wilbur, K.M. (Eds.). *The Mollusca- Physiology, Part 1*. Academic Press, New York, pp. 235-287.

Xia, J., E. Ito and D.R. Engstrom. 1997. Geochemistry of ostracode calcite. Part 2. The effects of water chemistry and seasonal temperature variation on *Candona rawsoni*. *Geochmica et Cosmochimica Acta* 61: 383-391.

a) Antero Pond, South Park, Colorado

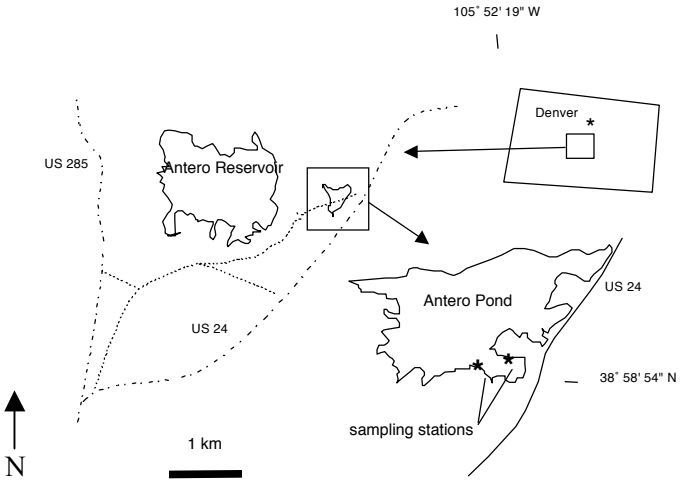

b) El Yeso Dam Magdalena de Kino, Sonora

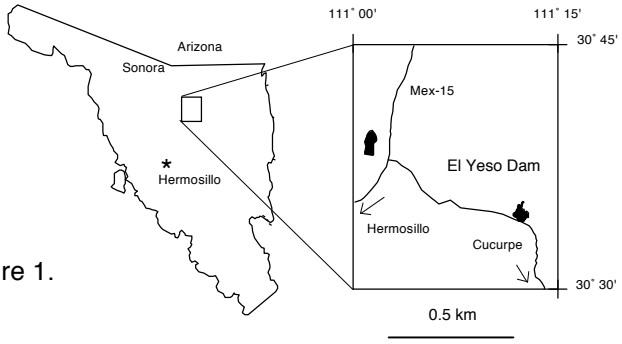

Figure 1.

Figure 1. Location maps of provenance of ostracode species discussed in this paper: a) Antero Pond, South Park, Colorado, USA, the specimens of *Limnocythere staplini* were collected during the summer of 1991; b) El Yeso Dam, Magdalena, Sonora, Mexico, the specimens of *Cypridopsis vidua* were collected from January to December 1990.

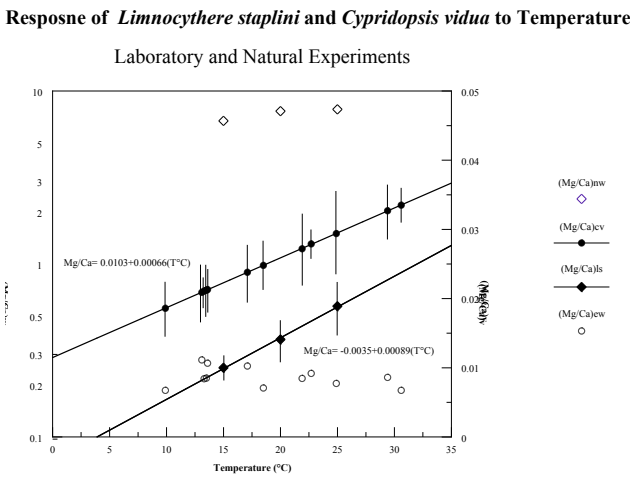

Figure 2. Linear regressions for *Limnocythere staplini* and *Cypridopsis vidua*. (Mg/Ca)nw = the Mg/Ca ratios of field waters, (Mg/Ca)ew = the Mg/Ca ratios of the experimental waters, (Mg/Ca)cv = the Mg/Ca ratios for *C. vidua*, and (Mg/Ca)ls = the Mg/Ca ratios for *L. staplini*. Error bars indicate the variability within a given set of valves. Notice how, usually, variability increases with temperature.

Mg/Ca ratios Monthly Variations in *Cypridopsis vidua*

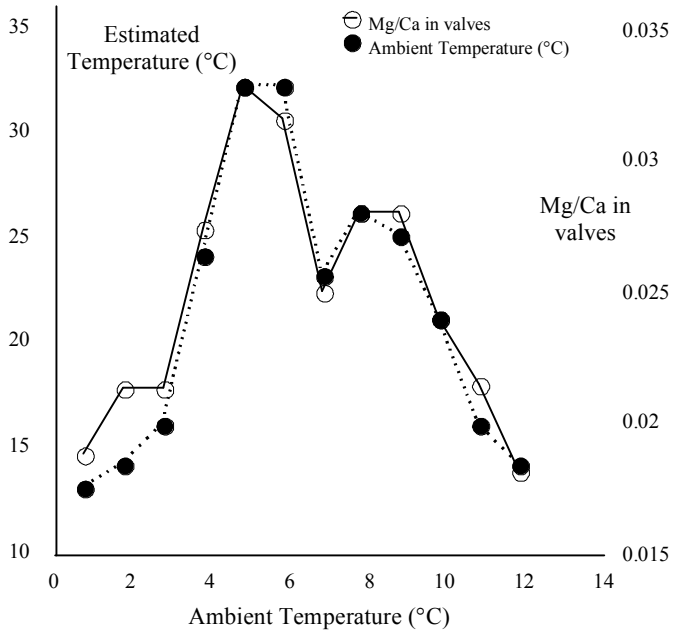

Figure 3. Monthly variation of the Mg/Ca ratios in the *C. vidua* valves and their correlation with measured temperatures from January to December 1990. Open circles indicate Mg/Ca ratios in valves, solid circles show measured monthly temperatures.

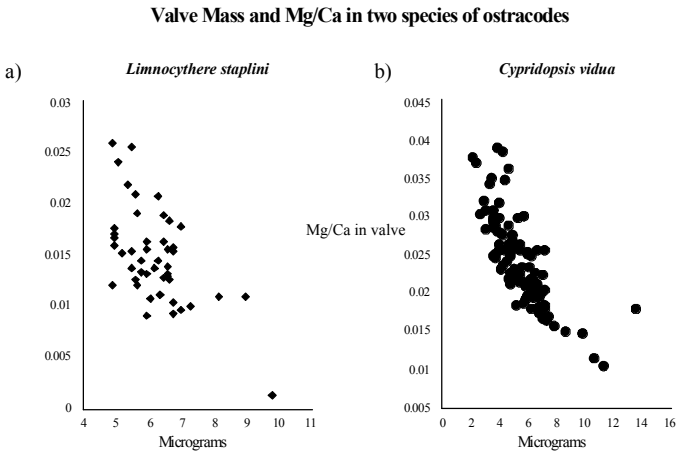

Figure 4. Valve mass correlation with the Mg/Ca ratios for a) *L. staplini* and b) *C. vidua*.

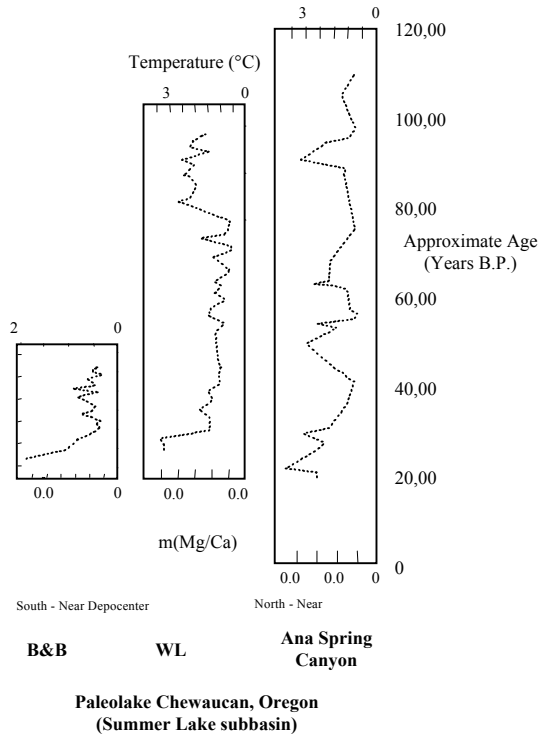

Figure 5. An example of application of the linear regression model for the genus *Limnocythere* in Summer Lake, Oregon (Pleistocene pluvial Lake Chewaucan). In this case the standard coefficients for *L. staplini* were applied to its close relative species *L. ceriotuberosa*. Temperature estimates are in good agreement with expected temperatures for the Pleistocene in the Great Basin area (see Cohen et al., 2000 for details).

Slip rate, recurrence intervals and paleoearthquakes for the Ana River Fault, central Oregon

R. M. Langridge[1], S. K. Pezzopane[2], and R. J. Weldon[3]

[1]Inst. of Geological and Nuclear Sciences Ltd., 69 Gracefield Rd., Lower Hutt, New Zealand; r.langridge@gns.cri.nz
[2]U.S. Geological Survey, Box 25046, Denver Federal Center, Denver, CO 80225-0046; spezzo@usgs.gov
[3]Dept. of Geological Sciences, University of Oregon, Eugene, OR 97403-1272;

Abstract

The Ana River fault (ARF) represents one of the best opportunities to study active back-arc and Basin and Range normal faulting in Oregon, due to the combination of exposure, lacustrine stratigraphy, tephras, and chronological control at the northern end of the Summer Lake basin. Data collected from three trenches across the fault trace and numerous exposures nearby show that the ARF has meter-scale (0.5-2 m) vertical displacements demonstrated across a 2-4 m high "post-lake" scarp near the margin of pluvial Lake Chewaucan. We recognize two earthquake events since the lake receded from its pluvial maximum to lowstand level, and four other events that occurred during highstand times since Oxygen Isotope Stage 5 ended. The average recurrence interval (RI) over this period is ~15,000 years, though we believe it is possible there were more events, reducing the average RI. The slip rate of the ARF, based on displaced units and their calibrated ages, differential sedimentation rates, and recurrence generally falls in the range 0.1-0.3 mm/yr. Our results imply that large earthquakes (M ~6.9) ruptured not only the ARF but also other faults totaling 30-40 km in the Summer Lake region. Other outcomes of this study have been the recognition and characterization of sub-lacustrine deformation, erosion, and event horizons, and the
advancement of knowledge concerning the latest Quaternary history of pluvial Lake Chewaucan.

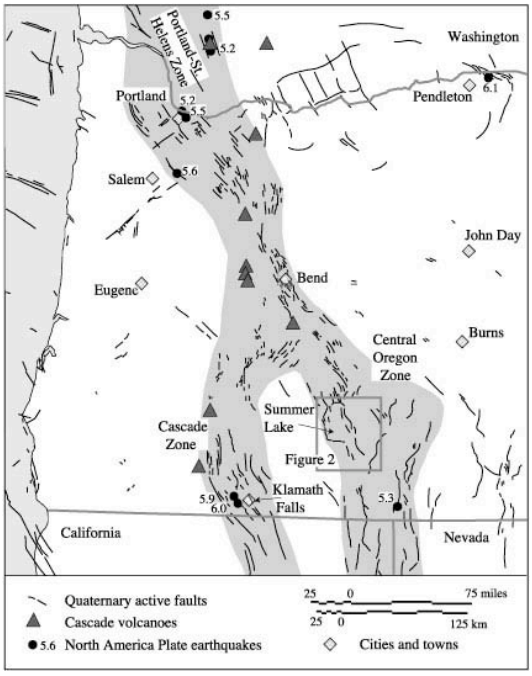

Figure 1. Quaternary fault map of the western half of Oregon, and surrounding areas, with historic macro-seismicity (M >5) of the North American Plate (Goter, 1994). The back-arc Cascade and Central Oregon Zones, and Portland-St. Helens Zone of Pezzopane (1993) are highlighted.

Introduction

The Ana River fault (ARF) is one of several late Pleistocene to Holocene active normal to normal-oblique faults in the Central Oregon Zone, a N to NW trending back-arc fault zone east of the Cascades volcanic arc on the NW margin of the Basin and Range province (Figure 1) (Pezzopane, 1993; Pezzopane and Weldon, 1993). Due to the incredible exposure and age control provided by tephra-rich lacustrine sediments (Allison, 1982; Davis, 1985) of pluvial Lake Chewaucan (Figure 2) traversed by

the ARF, this structure has come under more intense study than other faults in this region (Langridge, 1998). This is because the ARF has potential to yield well-constrained neotectonic data with broad application to other similar active faults in Oregon, and to analyses of earthquake recurrence and fault behavior. Dated, age-calibrated tephras allow the calculation of vertical slip rates for the ARF. Additionally, the long well-dated record of the ARF allows for an extended paleoseismic record with the recognition of multiple earthquake events and recurrence intervals, which rivals long records on other faults (e.g., Sieh et al., 1989).

In this summary paper we present results from three trenches across the ARF fault trace and the collective data from many exposures along the Ana River canyon, Ana Reservoir, and Desert Springs Trout Farm (Figure 3). This work has required an integrated knowledge and re-evaluation of the tephrochronology (Davis, 1985; Negrini et al; 2000), the Pleistocene lacustrine history of pluvial Lake Chewaucan (Negrini and Davis, 1992; Freidel, 1993), calibration of age data toward a unique chronology, integration of data from previous neotectonic studies (Simpson, 1985; Pezzopane, 1993) and the recognition of co-seismic deformation and event horizons related to "sub-lacustrine" surface rupture (Langridge, 1998).

Ana River fault

The Ana River fault is a short active normal fault at the northern end of the Summer Lake Graben (Figure 2) (Allison, 1945; Pezzopane and Weldon, 1993), a region of low historic seismicity with significant evidence of active

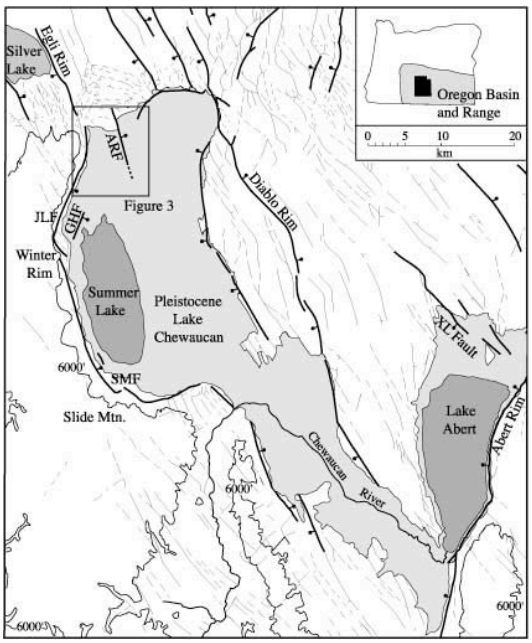

Figure 2. Late Pleistocene and Holocene active faults (bold lines) in the region of pluvial Lake Chewaucan. Lake highstand (light shading) of 4480 ± 20 ft and active faults from Pezzopane (1993). Regional faults from Walker and McLeod (1991). ARF, Ana River fault. Other abbreviated fault names are discussed in text.

faulting. It is recognized by a scarp of up to 4 meters height striking N10°W, over a distance of 3-5 km across young surfaces (Figure 4) at the northern margin of pluvial Lake Chewaucan. Topographic profiling reveals that this scarp has a low-angle bevel on the footwall (west) side of the fault with approximately 2 meters of separation across it in the near-field. A prominent tilt block in Miocene (6.3-6.6 Myr.) volcanic rocks (Diggles et al., 1990; Walker and MacLeod, 1991) at Klippel Point highlights the escarpment that demonstrates the longer history of the ARF. Adjacent to this escarpment the ARF cuts several late Pleistocene shorelines, before climbing out of the basin to the north, forming a scarp in bedrock. The ARF then terminates at a series of arcuate E-W trending perpendicular faults.

Southward, the well-defined scarp progresses across Ana River (Figure 3), but is truncated at ~4190 ft. by a Neopluvial (2000-

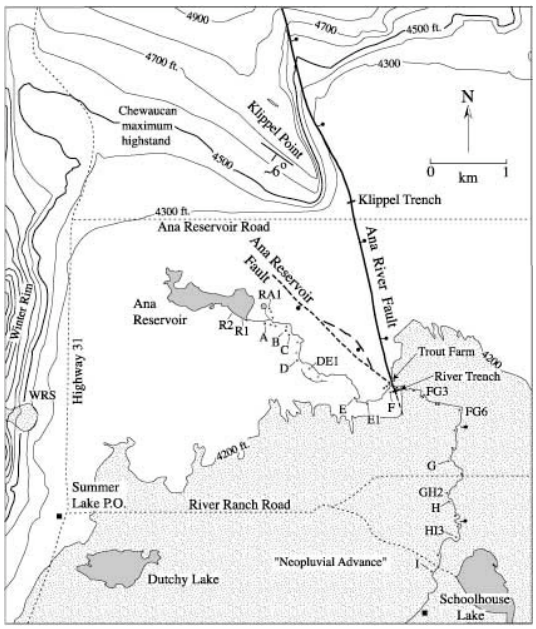

Figure 3. Location map of the Ana River fault and study sites. Elevation contours are in feet. The late Holocene advance of Winter Lake is approximated by the 4190 ft. contour (Neopluvial advance). Sections lettered along the Ana River are those of Davis (1985) and Langridge (1998). Other sections are at the Desert Springs Trout Farm and Ana Reservoir. WRS is White Rock landslide of Simpson (1985).

4000 yr. B.P.) shoreline advancement of Winter Lake (Allison, 1982; Pezzopane, 1993). Further southward continuation of the ARF is not known due to washing and burial of the fault trace. Differing models suggest either a long, straight ARF that links into the Slide Mountain fault system downbasin (Pezzopane, 1993), or a complicated set of short fault segments and secondary structures that step across to Winter Rim at the Jacks Lake segment (Simpson, 1985; Langridge, 1998).

Stratigraphy and Chronology

The lacustrine sequence and tephras of Lake Chewaucan are well documented (e.g., Allison, 1982; Davis, 1985; Erbes, 1996; Negrini, in press; Cohen et al., 2000) and need not be thoroughly discussed here. However, in Figure 5 we present the stratigraphy and chronology of deposits observed in the River trenches (Figure 6) which represents a near complete section from the end of Oxygen Isotope Stage 5 through to the Holocene.

The key units, which include tephra, ostracod sands, and post-lake subaerial deposits, are interbedded in brown lacustrine silts, implying generally deepwater conditions at this site. Tephras are named according to the terminology of Davis (1985) or given names based on accepted correlations to other sites (Negrini et al., 1988). We establish a chronosection here by combining all age data from tephrastratigraphy (e.g., Sarna-Wojcicki and Davis, 1991), radiocarbon (C-14), thermoluminescence (TL), and Potassium-Argon (K-Ar) dating (Bacon, 1983; Berger, 1991). Stratigraphic position (SP) and sedimentation rate (SR) are the means by which intervening undated layers are assigned ages.

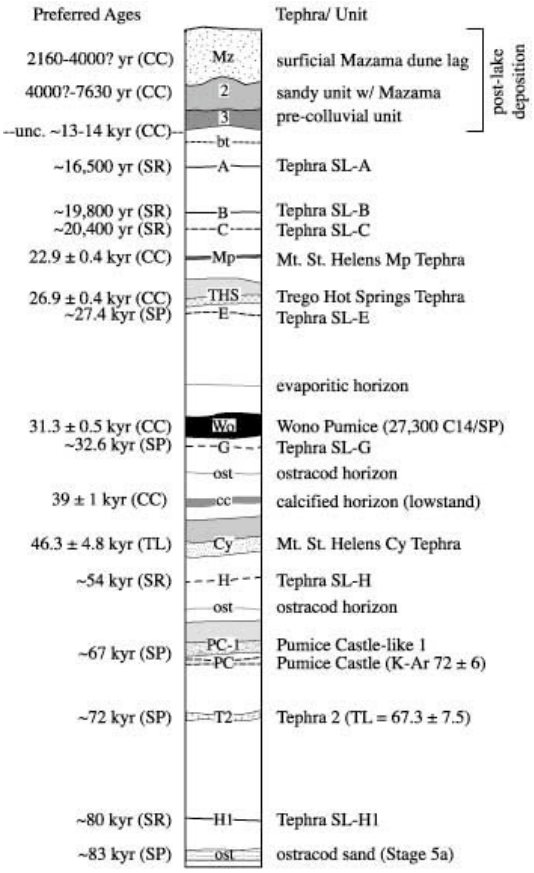

Figure 5. Detailed stratigraphic log of the Ana River section exposed in River Trench 1 and nearby sections along the Ana River. Ages of units are their preferred calibrated ages used for neotectonic calculations. Abbreviations are discussed in text. Unit patterns and shading are used in Figures 6 and 7.

All ages are brought together into a single chrono-framework (Figure 5) by calendar-calibrating (CC) all C-14 dates (Bard et al., 1990; Stuiver and Reimer, 1983; Taylor et al., 1996) including ages based on SP/SR, and by

placing a higher reliability on TL over K-Ar dates. This means that some of the published ages become older (C-14) or younger (K-Ar). However, the real benefit of these procedures comes from being able to calculate event ages and slip rates from offset units. The age and history of pluvial lake development (e.g., Benson et al., 1990), specifically Lake Chewaucan (Freidel, 1993; 1994) is also crucial to understanding and quantifying the activity of the ARF.

Key markers in connecting the River Trenches to the Klippel Trench of Pezzopane (1993) are the Trego Hot Springs (THS), Wono Pumice, and Mt. St. Helens Cy (MSH Cy) Tephras (Davis, 1985; Pezzopane et al., 1996). Two other tephra were recognised in the Klippel Trench and have been chemically matched to the SL-NN and SL-KK Tephras. At the Trout Farm the deposits are older than observed in trenches, but appear to fit into the master stratigraphy of Section C at Ana River (Davis, 1985). Other important dates and timelines are provided by unconformities that occur during Chewaucan lowstands. Age control on the Holocene section is limited to deposits containing Mazama Tephra (~7,630 cal. yr B.P.) and the Neopluvial advance dated at Slide Mountain by Pezzopane (1993) at ~2130 C-14 yr B.P.

River Trench 1

The River Trenches, RT1 and RT2, were excavated on an elevated block across the Ana River fault, south of Ana River to further investigate faulting and event relations of the ARF (Langridge, 1998; Langridge et al, 1999). RT1 trends N70W, is 40 m long, and ~3 m deep (Figure 6). Despite the lack of a big scarp (~30 cm high) this site was considered to offer a continuous late Quaternary section not present at Klippel Trench (Pezzopane, 1993; Pezzopane et al., 1996). Deformation in RT1 occurs over a broad zone and can be subdivided into two styles. The first is subaerial surface faulting, characterized by high-angle faults, vertical offsets, and focused deformation. Subaerial deformation is accompanied by scarp development and colluvial wedge stratigraphy. The second is subaqueous deformation, characterized by warping and folding of units, as seen by Simpson (1985), low-angle faulting or sliding, boudinage of section containing thick tephra units, and re-stacking of section (Langridge, 1998).

RT1 was divided into four domains to separate styles and timing of deformation. Domain I begins near Section F (Davis, 1985) and spans meters 1-12 (m1-12) in RT1. This is the true footwall of the ARF, c.f. Klippel Trench, and is characterized by the oldest section, generally flat stratigraphy, unconformities, and missing section, e.g., Section F. There is little deformation observed post-Tephra H times. Below this we observe boudined and isoclinally folded Tephra 2 and Pumice Castle (PC) set tephras, displaced PC set, and misplaced Tephra 2 (Figure 6). These observations imply at least one event affecting these units between Tephra 2 and MSH Cy times.

Domain II spans the middle part of RT1 and the main zone of deformation from m12-24. Domain II shows a focused zone of high-angle faults that offset all units below the surficial dune lag deposit. There is a clear step down-to-the-east of stratigraphy, consistent with the Holocene fault scarp elsewhere, and thickened Holocene fill buttressed against the scarp. MSH Cy Tephra is clearly thickened and offset through this zone of faults, so is used as a marker in stepwise retro-deformation of Domain II events (Figure 7). In Figure 7b we first remove vertical displacement totaling >1 meter on MSH Cy from m13-21. In addition, we remove all Holocene post-lake deposits from the top of the section. While this may involve more than one post-lake event it offers us the potential to see new mismatches created by this restoration. For example, the most recent event (MRE) is probably demonstrated by the upward-termination of several faults at the level of the dune lag deposit, Mazama-filled fissures, and buttressing of units against a scarp of ~0.5 m height. However, units between the THS Tephra and post-lake unconformity are then mismatched. A package containing Tephras A-C is faulted or slumped into the fault zone – essentially protecting it from basinwide stripping once Lake Chewaucan had receded. Additionally, the THS Tephra appears to step down (to the west) across the restored section. Thus, it appears there are probably two "post-lake" events, the older of these events perhaps occurring at or about the time that lake water left this site.

Further events are required to take out the broad warp in MSH Cy tephra seen in Figure 7b, and to create a trough across the fault zone, which allowed for sedimentation of a thickened

package of reworked MSH Cy Tephra. This evidence shows that earlier deformation was also localized around the zone of Holocene faulting and involved more ductile deformation. The broad warp in MSH Cy also involves the Wono Tephra as it mantles the warp, but probably does not involve the THS Tephra or Tephra E, as they do not appear to be folded. Figure 7c shows the reconstruction of MSH Cy to its original position upon deposition. This step shows a dish-shaped depression on the back of a flattened isoclinal fold in PC set tephras, that have included Tephra H and an ostracod layer. The unfolding reconstruction process has an amplitude of ~1 meter.

Domain III (m24-35) is characterized by relatively flat beds and less evidence of deformation. None of the high-angle faults or fissures has significant vertical separation, though they often break up high and contain Mazama Pumice. The THS Tephra is gently folded, rotated, and boudined. Wono and MSH Cy are warped up beyond m31 and truncated by a high-angle fault. PC set is folded and overturned at the bottom of the trench. Domain IV consists of a tilted section of lake sediments from THS Tephra to above Tephra A. This tiltblock may lie on a low-angle fault or slide plane. Beneath this plane the section, which contains Tephra H and ostracods, is highly folded and appears to have a cleavage. At the top of the slide block a package that appears to contain Tephras B and C is repeated. This process we call section re-stacking. A summary of the event history will be presented in the discussion section.

River Trench 2

RT2 was excavated about 2 meters north of RT1 and has about 5 m of overlap with RT1 at its east end (Figure 6). RT2 is 16 m long and has the same stratigraphic section as RT1, and also displays the two main styles of deformation. High-angle faults break up to the base of the post-lake sequence and flower open into fissures near the surface. The oldest deformation in RT2 is seen as a series of discontinuities in Tephra 2 that create small offsets and rotation, but have no effect on the PC set tephras. Above this level, we see low-angle faults with both west- and east-vergence. One set of low-angle faults breaks up to the level between the Wono and THS Tephras, while another set breaks up higher, toward the top of the lake section above Tephra A. Thus, the event information in RT2 is consistent with, though less spectacular than, the record in RT1. From these two trenches we recognize that the main zone of the ARF (m14-18 in RT1) is consistent with the location of the fault from geomorphology, and relatively narrow. However, there is a broader zone of deformation of 40-50 meters width in this area, particularly evident when earthquakes occurred during pluvial times.

The Trout Farm

Four cleared exposures were investigated above the north bank of the Ana River (Figure 4) at the Desert Springs Trout Farm (Langridge, 1998). Three of these exposures TF1-TF3 occur on the footwall (western) side of the ARF trace and had stratigraphy that could be matched into Section C of Davis (1985). Here we present Outcrop TF1 as an example of the section and deformation (Figure 8).

A package of flat-bedded lake sediments (TF1a) containing Tephras N1 through U occurs on the east side of the outcrop juxtaposed against deformed (TF1b) and tilted (TF1c) packages on the west. TF1b is a highly extended and deformed mass of sediments separated from TF1a by a low-angle listric structure that shallows beneath the outcrop. TF1b contains units from Tephra T through Tephra N1 and deposits above this representing lowstand facies missing from Section C. TF1c is a coherent package of lake sediments from Tephra N through Tephra K, dipping 13°SW. The contact between packages TF1b and TF1c may be an unconformity, as shown by Davis (1985), or it may represent the top of a zone of chaotic basal sliding.

Outcrop TF1 displays a shallow low-angle slide from the footwall block with vergence downslope away from the ARF. Package TF1b probably represents a chaotic basal breccia related to this slumping or low-angle faulting. TF1c may have ridden coherently on top of this mobilized package. A slot dug perpendicular into the face of TF1 (Langridge, 1998) confirms the 3-D geometry of the slide block and plane, with dip direction S47W, ~44°. This is 33° from the dip direction of the ARF, but roughly parallel to that for a secondary structure, referred to as the Ana Reservoir fault (p. 25 in Weldon et al., 1992). The age of the main event affecting this outcrop is unclear and depends on the preferred mode of deformation

and the youngest deposits involved, which may have been removed. Additionally, the relevance of the small-separation, high-angle faults is not clear. However, this outcrop is shown mainly as an indicator of the styles of deformation and ages of units present in the Ana River area.

Klippel Trench

The Klippel Trench was excavated across the post-lake fault scarp of the ARF near Klippel Point (Pezzopane, 1993). Scarp profiles across the fault near the basin floor 1 km south of the trench show a broad, 4 m high, far-field bevel above a steep, 2-m-high scarp. In the Klippel Trench a sequence of marginal to deep lacustrine facies and interbedded tephras occurs on the footwall block and in a deep pit to the west (Figure 9). The tephra occur in unconformity-bounded packages and have been chemically correlated to the MSH Cy Tephra (possibly older Carp Lake Tephra, 80-90 kyr), a Tule Lake (SL-KK?) tephra (200 ± 27 kyr) (Berger, 1991), and Tephra SL-NN (~257 kyr) (Langridge, 1998). In addition to evidence for bevel unconformities and missing section we also see evidence for the waxing and waning of the pluvial lake over this long period, through the preservation of granule gravel and medium to coarse sand facies.

In contrast, the stratigraphy of the hangingwall block and pit (25 m east of trench) contain deposits that reflect a higher sedimentation rate and younger section. Two tephras were identified in the east pit and chemically matched to the THS and Wono Tephras (Pezzopane et al., 1996). MSH Cy tephra is not exposed in the hanging wall. Using sedimentation rates calculated from the depths to and age ranges of the Trego and Wono tephras we estimate depths to the MSH Cy tephra in the hanging wall. This reveals that the difference in elevation across the fault for MSH Cy corresponds to between 8 and 8.7 m of fault displacement.

In the trench the fault zone is expressed as a narrow ~1 m wide zone of high-angle anastomosing faults of different ages representing multiple events. The two most-recent events are marked by colluvial wedges that overlie a section of well-bedded lacustrine sands that are eroded from and beveled on the footwall side. The most-recent event (MRE) displaces an older fault-related colluvium and soil that appear to have been reworked and eroded by the waning pluvial lake. The MRE predates erosion and burial of the scarp by the late Holocene shoreline advance, and the penultimate event probably occurred during or slightly after the latest Pleistocene dessication of the lake. Thus, the 2-m-high scarp was formed during two post-lake earthquakes. The older beveled scarp was formed during one or more earlier events that occurred since deposition of the MSH Cy tephra when this site was underwater. This history of events is also consistent with that of the River Trenches. Deeper in the trench, more events are recorded by units displaced increasing amounts and unconformities where units are entirely missing or change thickness across the fault. The geomorphic and stratigraphic relations indicate that, in sub-lacustrine settings, earthquake event horizons can be marked by subtle angular unconformities and missing units in the footwall that may correlate with layers or wedges of reworked sediments in the hanging wall.

DISCUSSION

Slip Rate

The ARF has some of the best controls on slip and slip rate of any active fault in the back-arc zones of Oregon. In Table 1 we present near- and far-field vertical displacements on important stratigraphic contacts from the Klippel and RT1 trenches, and geomorphic profiles. Slip rates are calculated from selected dated horizons and from scarp heights. We consider that the best slip and slip rate data comes from the Klippel Trench where the last few earthquakes have resulted in brittle faulting events. Due to bevel erosion we use the far-field separations from Pit 1 to Pit 3 (Figure 9) to represent the true slip and slip rate for the ARF. Ages used for slip rate calculations come from Figure 5. There are several salient observations we can make about slip. First, there is increasing vertical separation of units with increasing age, to as much as 8.7 m on the MSH Cy Tephra.

Table 1. Summary of Slip Data from the Klippel and RT1 trenches

Location Offset Unit	near-field separtn. (m)	far-field separtn. (m)	slip rate (mm/yr)
Klippel Trench			
ground surface	0.8	2.3	-
wedge/ top of LS1	1.2	2.4	0.17-0.18
base of LS1	0.9	3.3	-
base of BS	3.6	4.0	0.29-0.31
THS Tephra	4.1	4.6	0.17
Wono Tephra	4.8	5.3	0.17
MSH Cy Tephra	7.2-8.2	7.7-8.7	0.15-0.21
Sedimentation rate	-	-	*0.1-0.19*
Profiles			
#75	2.5	3.9	0.28-0.32
#73	1.8	2.8	0.20-0.23
#74	2.4	3.3	0.23-0.27
River Trench 1			
ground surface	0-0.3	0.9-1.1	-
top of lake section	0.9-1.0	0.9-1.0	0.06-0.08
THS Tephra	0.6	1.0	-
Wono Tephra	1.2	0.9	-
MSH Cy Tephra	0-1.1	0.8	0.02

Second, there is ~2.4 m separation on the top of the lake section, of which about half (0.8-1.2 m) can be accounted for by the most recent earthquake. These results are consistent with two post-lake events. Third, the THS and Wono Tephras are removed from the footwall block. Therefore, we use the separation on the base of BS on the footwall to calculate minimum values for slip and slip rate on the THS and Wono Tephras. Four, the maximum slip rates come from geomorphic profiles where the far-field scarp is up to 4 m in height.

The calculated slip rates from Klippel Trench and the profiles occur over a narrow range of 0.16-0.32 mm/yr, most of the data falling between 0.17-0.23 mm/yr. An independent measure of slip rate is found by differencing the sedimentation rates from one side of the ARF to the other, from pit to pit. This yields differences in the range 0.1-0.19 mm/yr. Given the inherent errors in ages, sedimentation rate, and contacts we conservatively express the slip rate for the ARF as 0.2 ± 0.1 mm/yr.

At the River Trench (RT1) there is evidence for 0.8-1 meter of vertical displacement on all major units up to the eroded top of the lake section. Little net vertical slip is accrued by events below this unconformity. We believe that this lack of vertical separation is related to non-brittle flow of unconsolidated section across the scarp during sub-lacustrine events. However, Holocene slip and slip rate are less than half as great as those at Klippel Trench, implying there may also be a structural reason for their lack.

Chronology of Paleoseismic Events

In Figure 11 we present the events in time with respect to previously outlined stratigraphy. Most of the event horizon data for each trench has been discussed, so this section focuses on the timing of each event. There are considerable errors inherent in dating landforms, bracketing ages, using radiometric techniques, and relying on sedimentation rate to pinpoint event ages. These errors get larger with increasing age and approach the value of earthquake recurrence, e.g. PC set tephra is K-Ar dated at 72 ± 6 kyr. While we recognise this error, we typically have a preferred time for events (an event horizon position), particularly for those events registered in the lake section, that has a reasonably constrained median time.

Event I, the MRE, is bracketed by the washing of the scarp by the Neopluvial lake advance (>1920 cal. yr B.P.) (Pezzopane, 1993), but probably >4000 cal yr B.P. (Allison, 1982), and by the age of Mazama Pumice (<7790 cal yr B.P.). Event II appears to have occurred shortly after Lake Chewaucan left the River Trenches, given enough time to develop a weak soil at the already abandoned Klippel Trench site, and with conditions likely to still enhance slumping of section, e.g., Tephras A-C, that was elsewhere deflated away throughout the basin. Given the recent dating of latest Pleistocene shoreline features (Freidel et al., this volume) of 13.5-15.5 cal kyr. B.P., we suggest an event age of 12-14 cal. kyr B.P. for Event II. This is likely coincident with deformation observed at an exposed area of isoclinal folding of young section (up to MSH Mp) about 1 km southwest of the River trenches (Simpson, 1985). The folding event was placed between 12-19 kyr (Simpson, 1985, p. 24 in Weldon et al., 1992) and attributed to landsliding originated from Winter Rim. We believe the consequence of Event II faulting on the ARF, rather than landsliding.

Event III is latest sub-lacustrine event. Its timing comes from Domain 2 in RT1 trench where there are angular differences in the relations between THS and Wono Tephras (Figure 6) related to the folding of section containing MSH Cy through Wono. Event II is also highlighted by the slide block floored by THS Tephra in Domain 4 of trench RT1. Its age is therefore bracketed between the THS and Wono Tephras (29 ± 1 cal. kyr). Event IV in

RT1 is shown by the isoclinal folding of PC set and Tephra H across the scarp, with the creation of a small piggy-back fill basin, constraining the event to some time before deposition of MSH Cy Tephra. We assign an age of 49 ± 5 kyr to Event IV based on its stratigraphic position, age, and uncertainty. Event V separates additional deformation seen on Tephra 2 in both River trenches and at Section C (Allison, 1945), from deformation on PC set tephras. This event, placed between the two, yields and age of 70 ± 6 kyr. Evidence for one additional older event (Event VI) since Oxygen Isotope Stage 5 times comes from Section E and F (Davis, 1985) and affects units up to and above Tephra SL-I (Langridge, 1998). We assign an age of 81 ± 6 kyr to Event VI.

While the evidence for these events is compelling and consistent between sites, it must be compatible with other neotectonic data. That is, there must be enough events to account for the accumulated vertical slip observed at the Klippel Trench and from the scarp profiles (1-2 m per event). Also, there must be enough agreement between slip per event, slip rate, and recurrence to create mutually consistent results. For example, four meters of displacement separates the base of BS at the Klippel trench. This may have been accomplished by 2-3 events there, though only two events have been identified in the stratigraphy present. In other words, our event history may be incomplete and may require a section with better latest Quaternary definition and chronology to assure the correct result.

Recurrence intervals and their implications

Six paleoseismic events produce five complete recurrence intervals for the ARF over the last ~83 kyr. More specifically, within the limits of our chronology, these five intervals occur over a period of ~75,000 years. This produces an average recurrence interval of ~15,000 years for the Ana River fault. The five intervals range between about 7-21,000 years. While it would be easy to speculate about the variability between different recurrence intervals, or the differing effects of lake size on fault stress, we do not feel that we have the resolution in event definition or chronology yet to make these kinds of arguments.

Knowing the average recurrence also allows an opportunity to produce another independent measure of slip rate for the fault, by dividing the recurrence time by the average displacement observed at the Klippel trench (~1.2 m), or the maximum from scarp profiles (~2 m). Thus, the slip rate appears to be ~0.08 mm/yr, or 0.13 mm/yr, respectively. As mentioned earlier, the slip rate is directly dependent on the recurrence time (recognition of event horizons) and measurement of single event displacement. If we were to confirm the presence of more paleoseismic events then the slip rate would increase and be more consistent with the overall observations at Klippel Trench.

Neotectonic fault structure

As discussed earlier, the slip per event for the Ana River fault ranges from 0.5-2 m. Using the relations of Maximum (MD) and Average (AD, from profiles and trenches) displacement from Wells and Coppersmith (1994) for normal faults we calculate a Moment Magnitude for surface-rupturing earthquakes on the ARF of M 6.8-6.9. Inversion of M, MD, and AD for surface rupture length (Wells and Coppersmith, 1994) yields mean values of 30-37, 32, and 50 km, respectively. Therefore, we should expect that the earthquakes that formed the ARF scarp and offsets, produce surface rupture on perhaps 30-40 km of fault length in the Summer Lake region, while we currently see evidence for ~5 km of preserved fault scarp on the ARF. This can be explained by two main hypotheses. First, surface rupture of an ARF lengthwise through the Summer Lake basin on the east side of the modern lake for 30-40 km with MD of ~2 m and AD closer to 0.8 m, the scarp having been washed away below 4200 ft. Second, structural linkage of faults and surface ruptures from the ARF to segments of the Winter Rim-Slide Mountain fault system including the Grange Hall (GHF) fault (Langridge, 1998), Jacks Lake segment (JLF) etc. (Simpson, 1985), to the Slide Mountain (SMF) fault (Pezzopane, 1993) over a distance of >40 km (Figure 2), with higher M, MD, and AD. Either of these hypotheses is consistent with the styles, complexity, and magnitude of observed historical surface rupture within the Basin and Range province (dePolo et al., 1990).

Summary

We have used an integrated approach combining tephrastratigraphy with age calibration and lacustrine history from basin

floor to marginal settings to develop a late Quaternary picture of faulting on the Ana River fault. The Ana River fault offers us the opportunity to investigate the parameters of fault slip (0.5-2 m), slip per event, recurrence time (~15,000 years), and slip rate (0.1-0.3 mm/yr) for a typical Oregon Basin and Range active normal fault. These results all point to the occurrence of surface-rupturing (M ~6.9) earthquakes occurring over broad time periods in this geologic province. The Ana River fault offers one of the longest extended paleoseismic records for any fault and can also teach us about fault behaviour. Other outcomes of this study have been the recognition and characterization of sub-lacustrine deformation, erosion, and event horizons, and the advancement of knowledge concerning the late Quaternary history of pluvial Lake Chewaucan.

References

Allison, I.S., 1982, Geology of pluvial Lake Chewaucan, Lake County, Oregon: Oregon State Monographs, Studies in Geology Number 11, 79 p.

Allison, I.S., 1945, Pumice beds at Summer Lake, Oregon: Geological Society of America Bulletin, v. 56, p. 789-807.

Bacon, C. R., 1983, Eruptive history of Mount Mazama and Crater Lake caldera, Cascade Range, U.S.A.: Journal of Volcanology and Geothermal Research, v. 18, p. 57-115.

Bard, E., B. Hamelin, R. G. Fairbanks, A. Zindler, G. Mathieu, and M. Arnold, 1990, Calibration of ^{14}C timescale over the past 30,000 years using mass spectrometric U/Th ages from Barbados coral: Nature, v. 345, p. 405-410.

Benson, L., D. R. Currey, R. I. Dorn, K. R. Lajoie, C. G. Oviatt, S. W. Robinson, G. I. Smith, and S. Stine, Chronology of expansion and contraction of four Great Basin lake systems during the past 35,000 years: Paleogeography, Paleoclimatology, Paleoecology, v. 78, p. 241-286, 1990.

Berger, G., 1991, The use of glass for dating of volcanic ash by thermoluminescence: Journal of Geophysical Research, v. 96, p. 19,705-19,720.

Berger, G. W., and Busacca, A. J., 1995, thermoluminescence dating of late Pleistocene loess and tephra from eastern Washington and southern Oregon ands implications for the eruptive history of Mount St. Helens: Journal of Geophysical Research, v. 100, p. 22,361-22,374.

Cohen, A. S., Palacios, M., Negrini, R. M., Wigand, P. E., and Erbes, D. B., 2000, A paleoclimate record for the last 250,000 years from Summer Lake, Oregon, U.S.A.: II. Sedimentology, Paleontology, and Geochemistry: Paleolimnology, v. 24, p. 151-182.

Davis, J. O., 1985, Correlation of late Quaternary tephra layers in a long pluvial sequence near Summer Lake, Oregon: Quaternary Research, v. 23, p. 38-53.

dePolo, C. M., D. G. Clark, D. B. Slemmons, and A. R. Ramelli, 1991, Historical surface faulting in the Basin and Range Province, western North America: Implications for fault segmentation: Journal of Structural Geology, v. 13, p. 123-136.

Erbes, D. B., 1996, Late Pleistocene lithostratigraphy of pluvial Lake Chewaucan, Oregon: Implications for past climate variation [M.S. thesis]: California State University, 73 p.

Freidel, D. E., 1994, Paleolake shorelines and lake-level chronology of the Fort Rock basin, Oregon, in Aikens, C. M., and Jenkins, D. L., eds., Archaeological Researches in the Northern Great Basin: Fort Rock Archaeology since Cressman, Anthropological Papers 50: Eugene, University of Oregon Department of Anthropology and State Museum of Anthropology, p. 21-40.

Freidel, D. E., 1993, Chronology and climatic controls of late Quaternary lake-level fluctuations in Chewaucan, Fort Rock, and Alkali basins, south-central Oregon [Ph.D. dissertation]: University of Oregon, 244 p.

Goter, S., 1994, Earthquakes in Washington and Oregon, 1872-1993: U.S.G.S. Open File Report 94-226A, 1994.

Langridge, R. M., 1998, Paleoseismic deformation in behind-arc lacustrine settings: Acambay, Mexico and Ana River, Oregon, [Ph.D. dissertation]: 188 pp., University of Oregon, Eugene.

Langridge, R. M., R. J. Weldon, and S. K. Pezzopane, 1999, Paleoseismology of the Ana River Fault, Central Oregon: Implications for Recurrence Behavior: Geological Society of America Abstracts with Programs, v. 31, p. A-72.

Negrini, R. M., Verosub, K. L., and Davis, J. O., 1988, The middle to late Pleistocene geomagnetic field recorded in fine-grained

sediments from Summer Lake, Oregon, and Double Hot Springs, Nevada, U.S.A.: Earth and Planetary Science Letters, v. 87, p. 173-192.
Negrini, R. M., in press, Pluvial lake sizes in the northwestern Great Basin throughout the Quaternary period, in Hershler, R., Currey, D. R., and Madsen, D. B., eds., Great Basin Aquatic Systems History.
Negrini, R. M., and Davis, J. O., 1992, Dating late Pleistocene pluvial events and tephras by correlating paleomagnetic secular variation records from the western Great Basin: Quaternary Research, v. 38, p. 46-59.
Negrini, R.M., D.B. Erbes, K. Faber, A. M. Herrera, A. P. Roberts, A. Cohen, M. Palacios-Fest, P. Wigand, F. Foit, 2000, A Paleoclimate record for the past 250,000 years from Summer Lake, Oregon, U.S.A.: I. Age control and magnetic lake level proxies: Journal of Paleolimnology, v. 24, p. 125-149.
Pezzopane, S. K., 1993, Active faults and earthquake ground motions in Oregon [Ph.D Dissertation]: University of Oregon, 208 p.
Pezzopane, S. K., and Weldon, R. J., 1993, Tectonic role of active faulting in central Oregon: Tectonics, v. 12, p. 1140-1169.
Pezzopane, S. K., R. J. Weldon II, A. M. Sarna-Wojcicki, and R. M. Langridge, 1996, Slip rate and recurrence intervals for the Ana River Fault, central Oregon, Geol. Soc. Am. Abstr. Programs, v. 28, p. 101.
Sarna-Wojcicki, A. M., and J. O. Davis, 1991, Quaternary tephrochronology: In, Quaternary Nonglacial Geology: Conterminous U.S., v. K-2, p. 93-116.
Sieh, K., Stuiver, M., and Brillinger, D., 1989, A more precise chronology of earthquakes produced by the San Andreas Fault in southern California, Journal of Geophysical Research, v. 94, p. 603-623.
Simpson, G. D., 1990, Late Quaternary tectonic development of the northwestern part of Summer Lake basin, south-central Oregon, [M.S. thesis]: Humboldt State University, 121 p.
Stuiver, M., and P. J. Reimer, Extended C-14 database and revised Calib 3.0 C-14 age calibration program: Radiocarbon, v. 35, p. 215-230, 1993.
Taylor, R. E., M. Stuiver, and Reimer, P. J., 1996, Development and extension of the calibration of the radiocarbon time scale: archeological applications: Quaternary Science Reviews, v. 15, p. 655-668.
Walker, G. W., and N. S. MacLeod, 1991, Geological Map of Oregon, 2 sheets, scale 1: 500 000: U.S. Geological Survey, Washington D.C.
Weldon, R. J., Pezzopane, S. K., Stimac, J. P., McDowell, P.F., and Freidel, D. E., 1992, Guidebook to Active Faulting in South-Central Oregon: Geological Society of America, Field Guide to Cordilleran Section Fieldtrip #5.
Wells, D. L., and K. J. Coppersmith, 1994, New empirical relationships among magnitude, rupture length, rupture width, rupture area, and surface displacement: Bull. Seismol. Soc. Am., v. 84, p. 974-1002.

Acknowledgements

We would like to acknowledge the work and legacy of Jonathan Davis, without whom the rapid definition of Ana River stratigraphy would be most difficult. We would also like to acknowledge considerable field help from U of Oregon students and partners. Thanks also to Rob Negrini and Andrei Sarna-Wojcicki for numerous discussions and advice. RML wishes to acknowledge FRST Post-Doctoral Fellowship CO5903 for time to write this manuscript and funds to attend the FOP Meeting

Latest Pleistocene Soft-sediment Deformation of Lacustrine Sediments in the Northwestern Part of the Summer Lake Basin, Oregon

By
Gary D. Simpson
SHN Consulting Geologists
Eureka, CA

Introduction

The lacustrine sediments in the Summer Lake basin are unique for both the duration of the stratigraphic record, which spans a significant portion of the late Pleistocene (Davis, 1985), and the abundance of volcanic tephra (Allison, 1945, 1966, 1982). Due to the loss of surface water flow that supplied the basin (i.e., the Chewaucan River), pluvial Lake Chewaucan largely dried up at the end of the last pluvial period about 12,000 years ago, and is now a small alkaline remnant (Summer Lake) fed primarily by the Ana River. The Ana River, a spring-fed stream originating in the northwestern corner of the basin, has down-cut through the Pleistocene lacustrine sediments and creates spectacular exposures.

Virtually all of the exposed lake beds in the northwestern part of the Summer Lake basin are in the banks of the Ana River, and in a few tributary gullies. Early studies of the pluvial Lake Chewaucan stratigraphy exposed along the Ana River focused on several outcrops described by Allison (Sections A, B, and C; 1945; 1982) and Davis (Sections D through F; 1985). These stratigraphic sections expose planar, tabular beds (silt/tephra interbeds) that are largely undeformed. Mapping of late Quaternary tectonic features in the northwestern part of the basin for my Masters thesis was less site-specific, however, and several areas where the sediments have been intensely deformed were discovered (Simpson, 1990; Simpson and Davis, 1989).

Deformed lacustrine sediments were observed at Davis' F Section, and in a concentrated zone along the Ana River directly to the east. Several features are exposed in a series of gullies around a small closed depression in this area ("Mud Lake" on Figure 1). A large fold is present along the southeastern shore of the Ana Reservoir, and folding has been reported northeast of the reservoir (J.O. Davis, pers. comm., 1988). Definition of the areal extent of the deformation is impossible since exposures are only present along the Ana River. Enough stratigraphy is exposed along the Ana River to determine that the deformation occurs as knots of fold and thrust complexes occurring sporadically within broad undeformed zones.

Deformation of lacustrine sediments in the southern Summer Lake basin is described in Allison (1982). Photographs in that paper show a thick section of tilted strata, and a liquefaction vent (i.e., "ball and pillar structure"). These features are located in the toe of one of the large Winter Rim landslides in the southern part of the basin.

The abundance of tephra layers in the Chewaucan deposits provides numerous marker horizons with which to interpret the deformational history. In the northwestern part of the basin, silt layers

within the stratigraphy deformed in a fluid manner, and are virtually indistinguishable. Tephra layers on the other hand behaved in a more rigid or brittle fashion, are traceable over large areas, and provide a spectacular record of soft sediment deformation in saturated latest Pleistocene age lacustrine deposits.

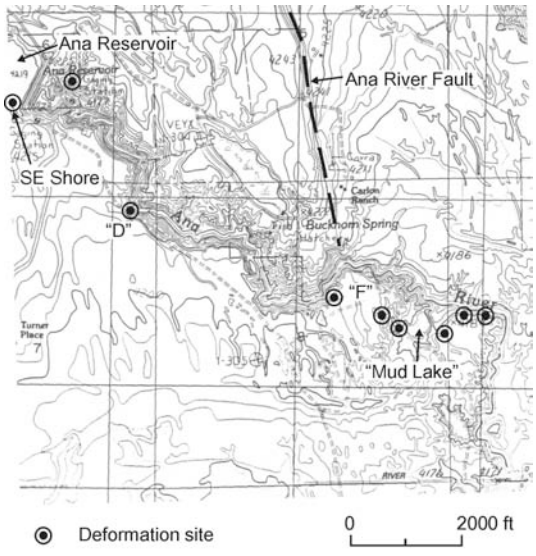

Figure 1. Location map showing exposures of deformed lake sediments ("D" and "F" per Davis, 1985).

Style of Deformation

Deformation of the lacustrine sediments in the northwestern Summer Lake basin consists of small- to large-scale isoclinal folds and thrust faults. These features typically overlie, or are sandwiched between, undeformed layers. Individual outcrops often display evidence for horizontal shortening on the order of 2 to 5 meters, although a much greater amount of shortening is present at Davis' F section, where a large thrust block is exposed. The deformation is notable for its fluid character; individual folds give the impression of saturated sediment "waves" moving across the floor of the lake bed in response to some intense dynamic trigger. The presence of thrust blocks is significant in that it indicates movement of large pieces of the lake floor. Much of the stratigraphy in the area is undeformed, suggesting the deformation is concentrated in zones (fold and thrust belts?).

Deformation is most prevalent in the upper sediments. The Mt. St. Helens Mp, Trego Hot Springs, Wono, and Marble Bluff tephra layers are repeatedly exposed in folds. Whether this is a function of more frequent surface exposure is unclear, but it should be noted that deformed areas are not accompanied by significant topographic relief. Therefore, folding are faulting appear confined to discrete layers, and does not encompass the entire stack of sediments.

Field identification of tephra layers is based on the location of the 30-35 ka Marble Bluff/St. Helens "C" ash (Davis, 1985; Allison's tephra 12, 1945), which contains abundant macroscopic biotite. This layer is very distinct, and provides an excellent marker bed. Other ash layers within the upper stratigraphy have characteristic traits that aid in their field identification (e.g., grain size, degree of mixing, thickness, etc.), but correlation of a section is ultimately based on the identification of the Marble Bluff ash. Interpretation of deformation is aided by the ability to determine the top and bottom of most ash beds, since all were laid down in the lake and demonstrate some form of grading.

The exposure showing the largest magnitude of displacement is the F section of Davis (1985). The stratigraphic relationship at this site was initially interpreted by Davis as an unconformity based on exposures on the south side of this gully. Detailed analysis of the structure on the north

side, however, revealed drag-folding of beds in the foot wall beneath a large thrust block. The hanging wall is characterized by a sharp hinge separating undeformed, essentially horizontal layers to the west from the tilted beds that have ramped over, and partially dragged up, the foot wall sediments. Sediment transport was essentially from west to east during this thrust event. The Marble Bluffs/St. Helens "C" tephra layer lies near the top of the exposed thrust block sediments, meaning the deformation has affected a lower portion of the stratigraphy at this location than is apparent at other exposures. The overall horizontal shortening at this site is not known because it is larger than the exposure, a minimum of about 10 meters.

Other examples of soft sediment deformation in the area include tight recumbent "S" folds, thrust faults, and detached, "floating" slabs of rigid tephra, sometimes juxtaposed above overturned pieces of younger ash beds. The fold along the southeastern shore of Ana Reservoir is notable in that it is a recumbent isoclinal antiform (the lower limb is overturned). The direction of movement in this fold appears to be from the southwest to the northeast, which is an oblique uphill trend, and indicates a minimum of several meters of shortening. In general, the fluid nature of the deformation in these exposures indicates saturated conditions at the time of the event.

Timing of Deformation

The lacustrine sediments of the northwestern Summer Lake basin were deformed between about 12,000 and 19.000 years ago. The age of this event is constrained by the following:

1. the 19 ka St. Helens Mp tephra layer is deformed;

2. the sediments were saturated at the time of deformation;

3. deformation was followed by lacustrine erosion and deposition (Davis, pers. comm., 1989), and;

4. pluvial Lake Chewaucan probably dried up about 12,000 years ago (see discussions elsewhere in this volume).

Cause of Deformation

The driving cause of the deformation of lacustrine sediments in the northwestern Summer Lake basin is not known. During the course of my Master's work, and in subsequent years (when I can't sleep), I have considered a number of scenarios to explain the episode, but there are no "smoking guns" and no easy explanations. The deformation is primarily compressive in nature, in an extensional tectonic setting.

To evaluate the deformation of sediments in the northwestern part of the basin, we conducted a structural analysis. 117 total attitudes were measured on bedding planes, fracture planes, fold axes, and fold hinges. These attitudes were plotted on steroenets, and the directions of principal shortening were plotted onto topographic maps. Deformation in the vicinity of Mud Lake and Davis' F section has a strong east-west compressive orientation. Exposures farther north (i.e., southeast shore of Ana Reservoir) tend to have a northeast-southwest principal compressive direction, thus forming a

radial pattern focused on the northern Winter Rim.

The most obvious explanation for the deformed lake sediments, and the one most assume at first glance, is that a large landslide from Winter Rim crashed down into Lake Chewaucan and the deformation is a result of this impact. There are a number of problems with this interpretation, however. Seismogenically induced deformation associated with a faulting event along the Winter Rim range front is the favored alternative explanation.

In his discussion of deformed lake beds in the southern part of the basin, Allison (1982) cites landsliding as the cause. The deformed deposits are located "in the toe of a landslide west of Summer Lake", which probably refers to one of the mega-slides in that area. One slide in the southern basin is 3.5 km wide. The style of deformation shown by Allison (1982) appears different than that observed in the Ana River area. Allison shows a thick tilted stack of sediments and a liquefaction vent, both of which are consistent with being bulldozed or over-run by a large slide deposit. Deformation in the Ana River area is far more fluid in nature, and is not in the toe of a slide.

Landslide deposits are, in fact, present west of the deformed sediments near the Ana River. These are associated with a moderate size slide from Winter Rim. This slide initiated in the "White Rock" (local name) volcanic breccia, along the rim just north of the community of Summer Lake. The head scarp for this slide is less than 1 km across, relatively small compared to other slides farther south along Winter Rim. The slide is associated with a large debris fan that extends out approximately .7 km from the range front (to about Highway 31). A slope break on the fan defines the geomorphic transition from an upper hummocky surface (subaerial deposition) to a smooth surface (sub-lacustrine deposition or modification by a subsequent highstand). Several low, streamlined mounds on the basin floor east of the debris fan, a maximum of 2 km from the range front, may be slide-related. Several of the higher mounds are capped by accumulations of large boulders with flanks consisting of gravelly silty sands containing angular pebbles and cobbles. Lithologies of the boulders are consistent those in the main landslide deposit, including dark gray microcrystalline volcanics and light colored volcanic breccias. The mounds either represent the distal extent of the sublacustrine debris deposition, or are ice-rafted blocks freed from the head scarp of the slide.

In any case, the nearest exposure of deformed lake sediment is over 1 km away from the mounds, and 2.3 km from the toe of the fan. Interpretation of the deformation of lake sediments as a result of Winter Rim landsliding requires the impact of the slide deposit to have sent a considerable "shock wave" through the saturated sediments to the east. It does not appear plausible to interpret that the deformation observed near the Ana River resulted from bulldozing or end-loading associated with direct debris impact because of the distance from the fan and/or the possibly slide-related mounds.

The sediments in the Ana River area may have been deformed seismogenically during a range front

faulting event. Near-source seismic energy, even if generated during a normal faulting event, could produce extensive soft-sediment deformation in an adjacent lake. A range front event would explain the magnitude of deformation and the radial "wave pattern" of observed folds. In this scenario, the folds we observed on the basin floor are analogous to seismic waves frozen in the lake bed sediments. Winter Rim is a basin-and-range style fault scarp, and several active faults have been identified along the length of its base (Pezzopane and Weldon, 1993; Simpson, 1990). In the northern basin, recent fault scarps have been identified crossing the White Rock slide deposit and near Jacks Lakes south of the Summer Lake community. The scarp crossing the White Rock deposit offsets a late Pleistocene/Holocene age alluvial fan that is forming on the side of the slide deposit; the "Jacks Lakes" fault offsets lacustrine deposits at its southern end. Without specific paleoseismic data on the timing of range front faulting events, however, interpretation of seismogenic deformation of lake sediments remains speculative.

References

Allison, I.S., 1982, Geology of Pluvial Lake Chewaucan, Lake County, Oregon. Oregon State Monographs, Studies in Geology #11. Oregon State University Press, Corvallis, Oregon, 79 p.

Allison, I.S., 1966, Pumice at Summer Lake, OR – a correction. Geological Society of America Bulletin, v. 77, p. 329-330.

Allison, I.S., 1945, Pumice beds at Summer Lake, Oregon. Geological Society of America Bulletin, v. 56, p. 789-807.

Davis, J.O., 1985, Correlation of Late Quaternary Tephra Layers in a Long Pluvial Sequence near Summer Lake, Oregon. Quaternary Research, v. 23, p. 38-53.

Pezzopane, S. K. and Weldon, R.J., 1993, Tectonic Role of active Faulting in Central Oregon. Tectonics, v. 12, no. 5, p. 1140-1169.

Simpson, G. D., 1990, Late Quaternary Tectonic Development of the Northwestern Part of the Summer Lake Basin, South-central Oregon. Unpublished Masters Thesis, Humboldt State University, 121 p.

Simpson, G.D., and Davis, J.O., 1989, Compressional Deformation of Late Pleistocene Pluvial Sediments in the Northwestern Summer Lake Basin, South-Central Oregon (abs). GSA Programs with Abstracts, v. 21, no. 5, p. 144, Cordilleran meeting.

Millennial-Scale Global Climate Change Recorded in Summer Lake Depocenter Sediments

Mladen Zic
Department of Physics and Geology, CSU Bakersfield

Overview

Historical records and paleoclimate proxies of effective precipitation suggest that the sediments of Summer Lake area may hold a reliable record of both regional and large-scale climate change documented over multi-decadal to multi-millennial time scales. Summer Lake historical precipitation is well represented in a more regional multi-decadal record of precipitation which appears to increase synchronously with both winter intensification of North Pacific basin air circulation and with an increase in Greenland Ice Sheet Project 2 (GISP2) $\delta^{18}O$ (a proxy for warmer North Atlantic temperature). In the paleoclimate record, the Summer Lake paleoprecipitation proxies are based on palynological, geochemical, lithologic and sediment magnetism data from the B&B core sediments retrieved from the basin depocenter (Cohen et al., 2000; Negrini et al., 2000; Zic, 2001). For example, Negrini et al. (2000) have shown that over the last 250 kyrs high/low concentration of magnetite in Summer Lake sediments correlates with high/low lake-levels. A follow-up high resolution magnetism study revealed that isothermal remanent magnetization (IRM) provides a lake-level proxy during the interpluvial period from ~50-20 ka that can be well correlated to the same GISP2 $\delta^{18}O$ record as the one used for the comparison of historical precipitation (Zic, 2001). In particular, three repetitions of the low-frequency Bond cycle, the associated Heinrich events, and the high-frequency Dansgaard-Oeschger cycles are all observed in the B&B core magnetic-concentration record. These correlations are supported by previous independent age control and B&B core palynological, geochemical, and lithologic data of lower sampling resolution which indicate lake levels (Cohen et al., 2000; Negrini et al., 2000; Zic, 2001). The results are consistent with previous studies that show increases in late Pleistocene precipitation and lake-levels in the Great Basin during the interstadial halves of D-O cycles (Hakala et al., 1997; Benson, 1999).

Historical Precipitation and Large-Scale Correlations

Summer Lake is located near the border of Oregon Climate Zones 5 and 7 as determined by the National Climatic Data Center (Oregon Climate service, 2001). Thus, it is not surprising that Summer Lake precipitation record (Western Regional Climate Center, 2001) closely follows an average of both Climate Zones 5 and 7 precipitation records (Figure 1). This observation demonstrates that the precipitation in the immediate area surrounding Summer Lake can be represented by the more regional precipitation record which dates back to 1895 when both Climate zone 5 and 7 precipitation records begin. In order to better compare historical and paleoclimate records of precipitation in the Summer Lake area a series of 40-year averages (similar to ~41 yr average from the paleorecord sample spacings) of total monthly precipitation was calculated from 1895 through 1984. These calculations were repeated for the Pacific Circulation Index (PCI; King et al., 1998) and GISP2 $\delta^{18}O$ record (Stuiver and Grootes, 2000). When the results of these calculations are compared with south-central Oregon precipitation, it appears that all records increase/decrease synchronously (Figure 2). This observation implies that higher precipitation occurs during extended periods of warmer global climate concomitant with winter intensification of North Pacific basin air circulation associated with westerly and southwesterly wind flow which directs storms along the west coast of North America (Cayan and Roads, 1984; Cayan and Peterson, 1989; King et al., 1998), and into eastern Oregon generally from the southwest from October to June (Sneva and Calvin, 1978).

Correlation of Summer Lake Paleolake-levels with Global Millennial-Scale Climate Variations

Summer Lake effective paleoprecipitaton can be deduced from proxies of lake level determined in previous studies, such as from palynological,

geochemical, lithologic and sediment magnetism data (Cohen et al., 2000; Negrini et al., 2000; Zic, 2001). For example, Negrini et al. (2000) show that the

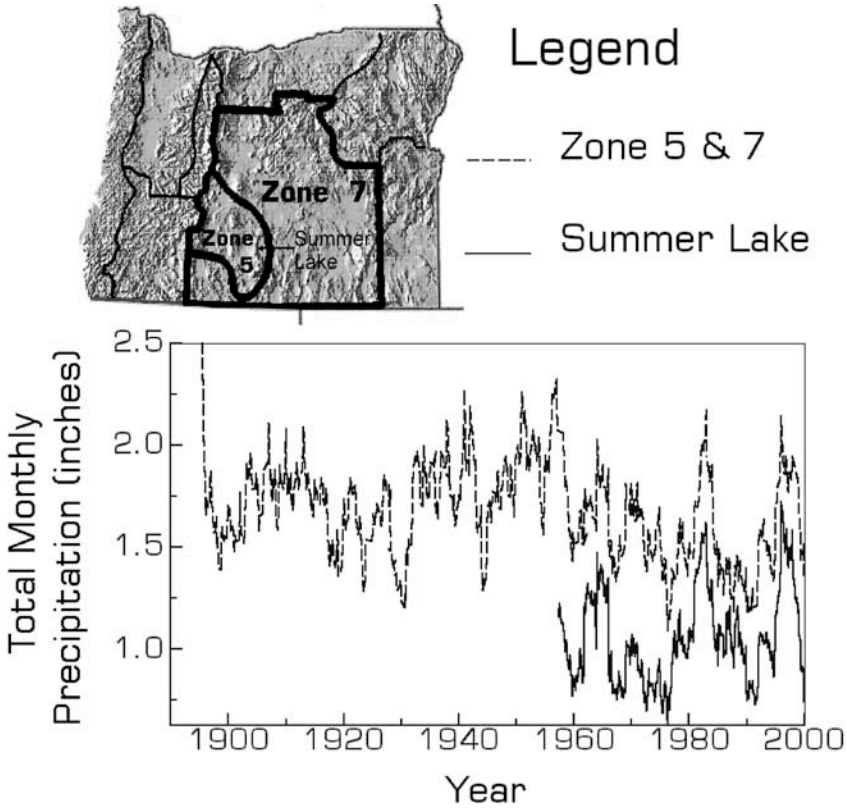

Figure 1. Correlation of Summer Lake total monthly precipitation with an average of combined Oregon Climate Zone 5 and 7 total monthly precipitation for the period from January 1895 through December 1999 (12-month moving average calculated from data available from Western Regional Climate Center and Oregon Climate Service). Oregon climate divisions have been established by the National Climatic Data Center. Topography is based on USGS data.

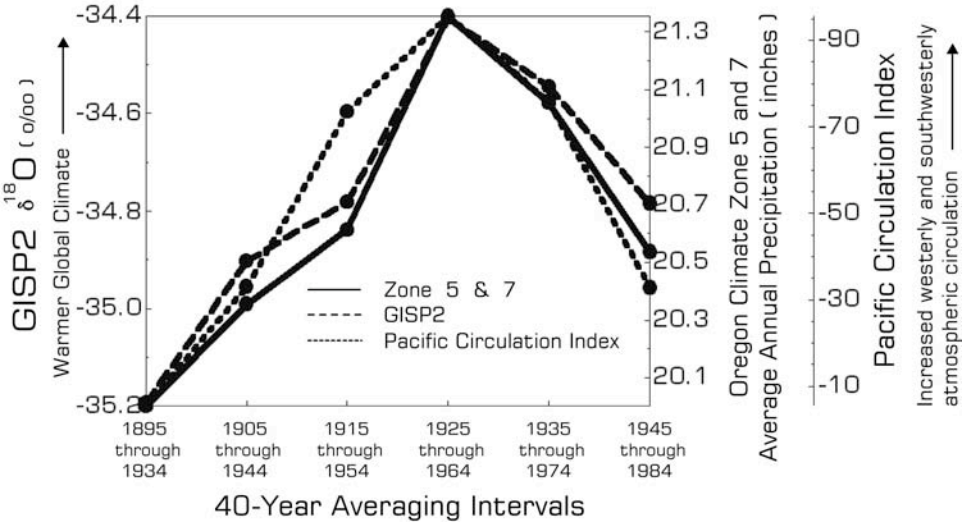

Figure 2. Correlation of a south-central Oregon precipitation record with GISP2 ice core $\delta^{18}O$ record and Pacific Circulation Index. Raw data are compared via 40-year averaging intervals among Oregon Climate Zone 5 and 7

precipitation (Oregon Climate Service, 2001), GISP2 ice core $\delta^{18}O$ (Stuiver and Grootes, 2000), and Pacific Circulation Index for December through March (King et al., 1998).

250 kyr magnetic concentration record from Summer Lake basin correlates with lake-levels. In the present paper I expand on these initial results with a higher-resolution record from the ~50-20 ka B&B core based on the use of isothermal remanent magnetization (IRM) as an estimate of magnetic concentration.

If paleoclimate controls were the same throughout the late Pleistocene and Holocene periods, it is expected that the B&B core IRM record can be correlated to the same GISP2 $\delta^{18}O$ record as the one used for the comparison of historical precipitation. Indeed, this seems to be true based on the correlations shown in Figure 3.

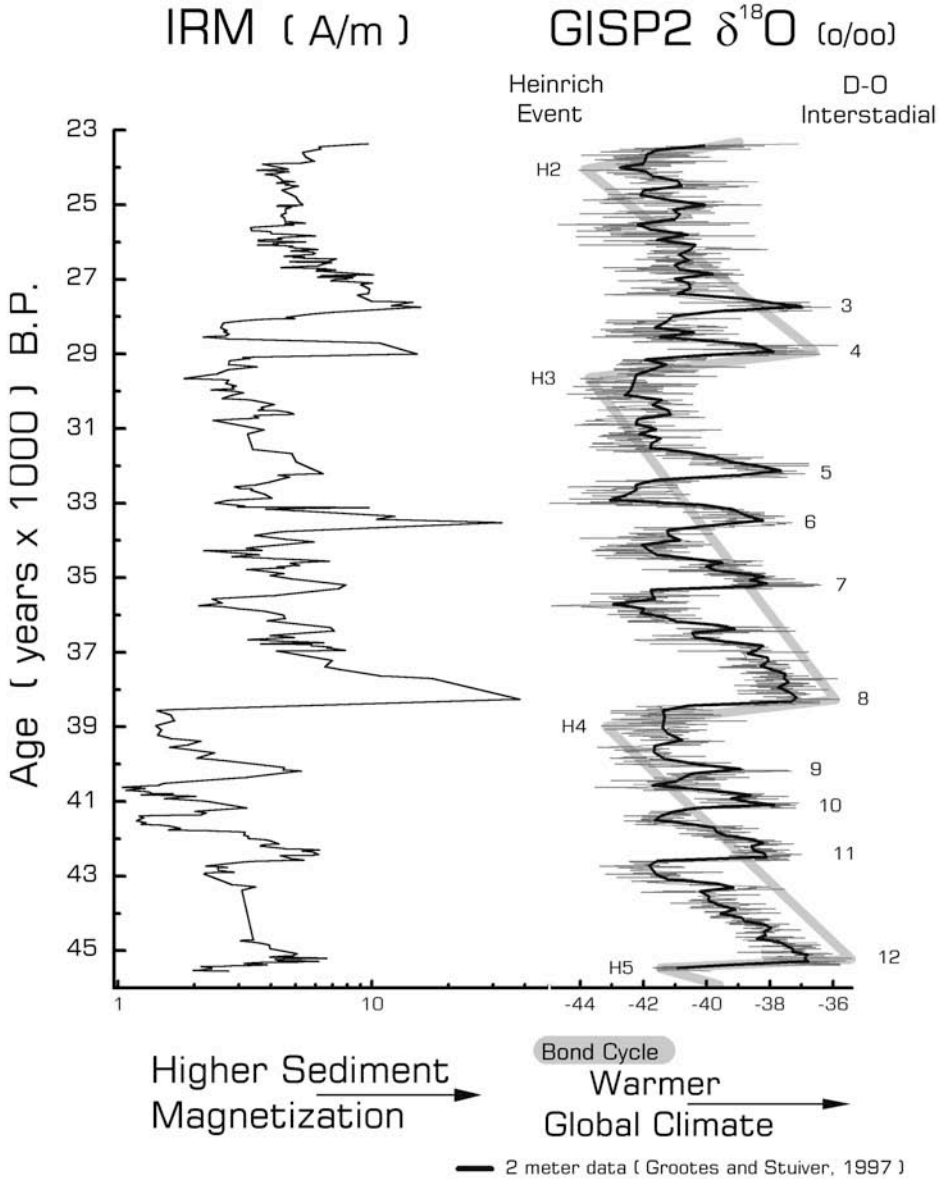

Figure 3. Correlation of B&B-core IRM with isotopic records from GISP2 ice core (Grootes and Stuiver, 1997; Stuiver and Grootes, 2000) versus GISP2 age. Correlations between records are largely based on the similar features and

the same number of interstadial cycles (numbered) which mark the end to Heinrich events (Heinrich, 1988), and the beginning of Bond cycles (Bond et al., 1993) and Dansgaard-Oeschger cycles (Dansgaard et al., 1993).

The IRM record reflects three low-frequency (~6 to 10 kyr) Bond cycles (Broecker, 1994), Heinrich events (H2 to H5; Heinrich, 1988), and high-frequency (~2 kyr) Dansgaard-Oeschger cycles (D-O cycles; IS3 to IS12; Dansgaard, et al., 1993; Bond et al., 1993). These correlations are supported by previous independent age control (Negrini et al., 2000; Zic, 2001) which is summarized in Figure 4.

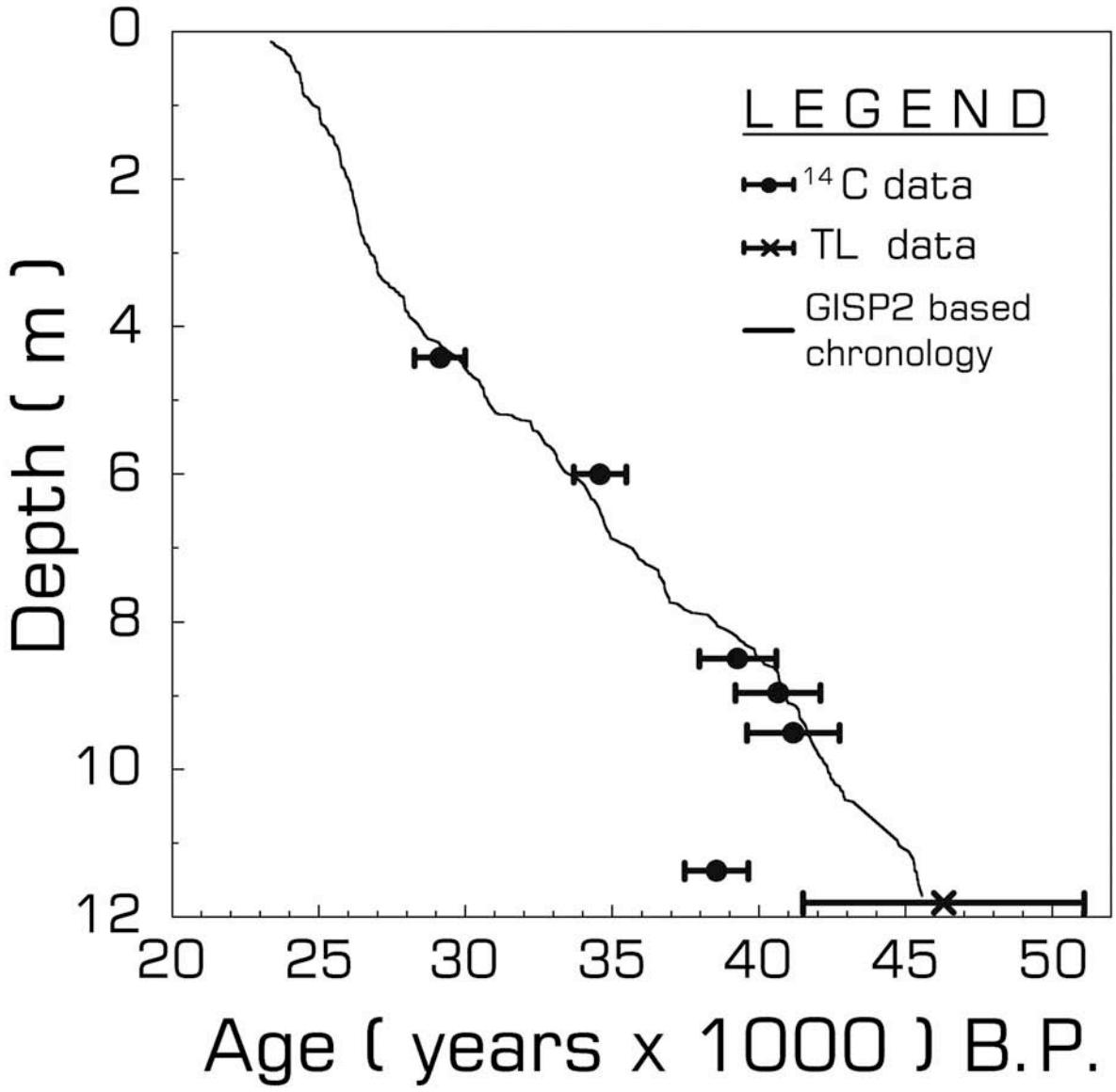

Figure 4. Depth vs. age for B&B-core sediments. Chronology for B&B core is based on correlation features between B&B-core IRM and stable isotopes in GISP2 ice core (Figure 3). Independent age-control points and associated error are plotted for the radiometric dates, and thermoluminescence data.

This Figure shows that for the most part the chronology predicted by the correlation model is within the limits of independent age control. To facilitate these comparisons the B&B core ^{14}C ages were first converted to an absolute age (GISP2 time scale; see Zic, 2001 for details). Additionally, this correlation model is also supported by the same relative positions of the Mono Lake and Laschamp paleomagnetic excursions in both the B&B core and GISP2 records (Zic et al., in review). In particular, in

both the GISP2 and B&B core records the Mono Lake Excursion occupies the same position within the stadial interval between IS 5 and 6.

To further test whether the IRM record represents lake-levels, it was compared to B&B core palynological, geochemical, and lithologic data indicating lake-level change. As shown in Figure 5, all lake-level proxies correlate reasonably well with IRM considering the difference in sampling frequencies and an incomplete stratigraphic overlap among different types of samples.

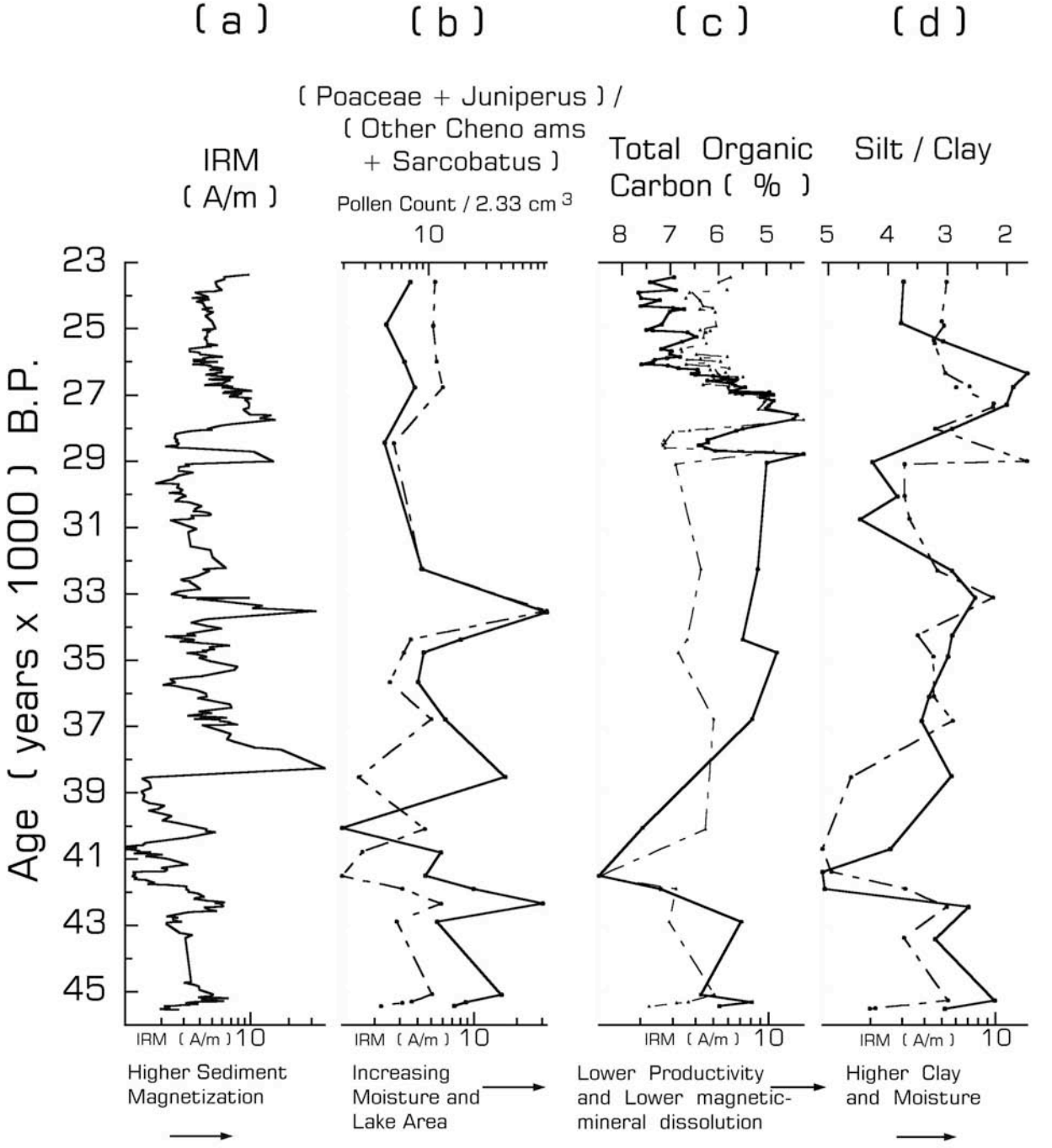

Figure 5. B&B-core IRM (Zic, 2001), and B&B-core palynological, geochemical, and lithological data (Cohen et al., 2000) versus age. (a) IRM, (b) (Poaceae + *Juniperus*)/(Other Cheno ams + *Sarcobatus*), (c) Total Organic Carbon

(%), and (d) Silt/Clay ratio. Figures 5b-5d include IRM (dashed) of samples overlapping samples of other data shown in these figures. Symbol size is not indicative of sample thickness.

IRM generally correlates well with the palynological moisture index (Poaceae+*Juniperus*)/(Other Cheno ams+*Sarcobatus*) (e.g., Wigand, 1987; Mehringer and Wigand, 1990; Wigand, 1997; Mensing, 2001; P.E. Wigand, pers. comm.). The geochemical record of total organic carbon (TOC%) correlates inversely with lake-levels (Negrini et al., 2000) and IRM probably due to magnetite dissolution during high biological productivity at low lake levels (e.g., Karlin, 1990; Leslie et al., 1990; Hawthorne and Mc Kenzie, 1993; Bloemendal et al., 1992; Snowball, 1993, Negrini et al., 2000; Lanci et al., 2001). Silt/clay ratio, previously shown to be an indicator of lake-level in this basin (Erbes, 1996; Negrini et al., 2000) also supports IRM as a lake-level proxy.

In conclusion, the above comparisons show that the magnetic concentration of the B&B-core sediments may serve as a climate proxy for regional precipitation and relatively extreme millennial-scale climate events preceding the late Pleistocene glaciation. Furthermore, correlations between modern south-central Oregon precipitation and Greenland $\delta^{18}O$ record suggest that this family of late Pleistocene climatic controls may still be active. However, more data are needed at higher resolution than relatively sparsely sampled palynological, lithological, and geochemical data currently available to gain higher confidence in these results, and to better characterize the dynamic response of climate in the northern Great Basin to global, millennial-scale climate change.

Selected References

Benson, L., 1999, Records of millennial-scale climate change from the Great Basin of the western United States, *in* Clark, P.U., et al., eds., Mechanisms of Global Climate Change at Millennial Time Scales: American Geophysical Union, Monograph 112, p. 203-225.

Bloemendal, J., King, J.W., Hall, F.R., and Doh, S.J., 1992, Rock magnetism of late Neogene and Pleistocene deep-sea sediments: Relationship to sediment source, diagenetic processes, and sediment lithology: Journal of Geophysical Research, v. 97, p. 4361-4375.

Bond, G., Broecker, W., Johnsen, S., Mc Manus, J., Labeyrle, L., Jouzel, J., and Bonani, G., 1993, Correlations between climate records from North Atlantic sediments and Greenland ice: Nature, v. 365, p. 143-147.

Broecker, W.S., 1994, Massive iceberg discharges as triggers for global climate change: Nature, v. 372, p. 421-424.

Cayan, D.R., and Roads, J.O., 1984, Local relationships between United States west coast precipitation and monthly mean circulation parameters: Monthly Weather Review, v. 112, p. 1276-1282.

Cayan, D. R., and Peterson, D. H., 1989, The influence of North Pacific atmospheric circulation on streamflow in the west, *in* Peterson, D.H. (ed.), Aspects of climate variability in the Pacific and the western Americas: Geophysical Monograph 55, American Geophysical Union, p. 375-397.

Cohen, A.S., Palacios-Fest, M. R., Negrini, R.M., Wigand, P.E., and Erbes, D.B., 2000, A paleoclimate record for the past 250,000 years from Summer Lake, Oregon, USA: II. Sedimentology, paleontology and geochemistry: Journal of Paleolimnology, v. 24, p. 151-182.

Dansgaard, W., Johnsen, S.J., Clausen, H.B., Dahl-Jensen, D., Gundestrup, N.S., Hammer, C.U., Hvidberg, C.S., Steffensen, J.P., Sveinbjörnsdottir, A.E., Jouzel, J., and Bond, G., 1993, Evidence for general instability of past climate from a 250-kyr ice core record: Nature, v. 364, p. 218-220.

Erbes, D.B., 1996, Late Pleistocene Lithostratigraphy of Pluvial Lake Chewaucan, Oregon: Implications for Past Climate Variation [M.S. thesis]: Bakersfield, California State University, 108 p.

Hakala, K.J., Adam, D.P., and Best, P.J., 1997, Late Quaternary submillenial climate variations based on pollen and lithological changes at Grass Lake, southern Cascade Range, California: Abstracts with Programs - Geological Society of America, v. 29, p. 375.

Hawthorne, T.B., and McKenzie, J.A., 1993, Biogenic magnetite; authigenesis and diagenesis with changing redox conditions in Lake Greifen, Switzerland, *in* Aissaoui, D.M, et al., eds., Applications of Paleomagnetism to Sedimentary Geology: Special Publication - Society of Economic Paleontologists and Mineralogists, v. 49, p. 3-15.

Heinrich, H., 1988, Origin and consequences of cyclic ice rafting in the northeast Atlantic Ocean during the past 130,000 years: Quaternary Research, v. 29, p. 142-152.

Karlin, R., 1990, Magnetic mineral diagenesis in suboxic sediments at Bettis Site W-N, NE Pacific Ocean: Journal of Geophysical Research, v. 95, p. 4421-4436.

King, J.R., Ivanov, V.V., Kurashov, V., Beamish, R. J., and McFarlane, G. A., 1998, General Circulation of the Atmosphere over the North Pacific and its Relationship to the Aleutian Low: North Pacific Anadromous Fish Commission, Doc. No. 318, 18 p. (document is available via http://www.pac.dfo-mpo.gc.ca/sci/sa-mfpd/english/downloads/npafc318.pdf).

Lanci, L., Hirt, A.M., Lotter, A.F., and Sturm, M., 2001, A record of Holocene climate in the mineral magnetic record of Alpine lakes: Sägistalsee and Hinterburgsee: Earth and Planetary Science Letters, v. 188, p. 29-44.

Mehringer P.J., and Wigand, P.E., 1990, Comparison of late Holocene Environments from Woodrat Middens and Pollen: Diamond Craters, Oregon, *in* Betancourt, J.L., et al., eds., Packrat Middens: The Last 40,000 Years of Biotic Change: University of Arizona Press, p. 294-325.

Mensing, S.A., 2001, Late-Glacial and early-Holocene vegetation and climate change near Owens Lake, eastern California: Quaternary Research, v. 55, p. 57-65.

Negrini, R.M., Erbes, D.B., Faber, K., Herrera, A.M., Roberts, A.P., Cohen, A.S., Wigand, P.E., and Foit, Jr., F.F., 2000, A paleoclimate record or the past 250,000 years from Summer Lake, Oregon, USA: I. Chronology and magnetic proxies for lake level: Journal of Paleolimnology, v. 24, p. 125-149.

Oregon Climate Service, 2001, Oregon climate divisions precipitation data, available at http://www.ocs.orst.edu/pub_ftp/climate_data/divisions/orprcp.html.

Sneva, F.A., and Calvin, L.D., 1978, An improved thiessen grid for eastern Oregon: An interstation correlation study determining the effect of distance, bearing, and elevation between stations upon the precipitation correlation coefficient: Agricultural Meteorology, v. 19, p. 471-483.

Snowball, I.F., 1993, Geochemical control of magnetite dissolution in subarctic lake sediments and the implications for environmental magnetism: Journal of Quaternary Science, v. 8, p. 339-346.

Stuiver, M., and Grootes, P.M., 2000, GISP2 oxygen isotope ratios: Quaternary Research, 53, p. 277-284. (Data file gisp2_measured.txt is available at http://depts.washington.edu/qil/datasets/gisp2_main.html).

Wigand, P.E., 1987, Diamond Pond, Harney County, Oregon: Vegetation history and water table in the eastern Oregon desert: Great Basin Naturalist, v. 47, p. 427-458.

Wigand, P.E., 1997, A late-Holocene pollen record from Lower-Pahranagat Lake, southern Nevada, USA: High resolution paleoclimatic records and analysis of environmental responses to climate change, *in* Isaacs, C.M., and Tharp, V.L., eds., Proceedings of the Thirteenth Annual Pacific Climate (PACLIM) Workshop, April 15-18, 1996: Interagency Ecological Program, California Department of Water Resources, Technical Report, v. 53, p. 63-77.

Western Regional Climate Center, 2001, Oregon Climate Summaries - Summer Lake 1S, Oregon, Desert Research Institute, Reno, Nevada (http://www.wrcc.dri.edu/cgi-bin/cliMAIN.pl?orsumn).

Zic, M., 2001, Sediment Magnetism of the B&B core from Summer Lake, Oregon, USA: Implications for Regional and Global

Millennial-Scale Climate Change from 46 to 23 ka [M.S. thesis]: Bakersfield, California State University, 93 p.

Zic, M., Negrini, R.M., and Wigand, P.E., *in review*. The full spectrum of late Pleistocene, millennial-scale climate change in a lake-level record from the Great Basin: Geology.

Pleistocene Lake Chewaucan: Two Short Pieces on Hydrological Connections and Lake-level Oscillations

Dolly Friedel, Department of Geography, Sonoma State University, Rohnert Park, CA

Hydrological Connections Between Pleistocene Lake Chewaucan and Fort Rock and Alkali Basins

There is evidence that during the periods of highstands in Chewaucan, Fort Rock, and Alkali basins, the three basins were hydrologically connected (Freidel, 1993). Geomorphic evidence indicates that when Lake Alkali filled to its highest level, it spilled into Lake Fort Rock through an overflow channel (Allison, 1979; Freidel, 1993). Lake Alkali's high stand beaches lie 19 m higher than those of Lake Fort Rock, and alluvial fan/delta sediments are deposited at the Fort Rock end of the overflow channel but are not seen at the Alkali end. The drainage divide is within the channel near the Alkali end, at 1381 m, and is marked only by scattered water-worn cobbles with little incision.

The hydrologic connection between Chewaucan and Fort Rock basins is not so obvious. However, study of the hydrology of Fort Rock and Summer Lake basins (McFarland and Ryals, 1991) and lake-level modeling of the three basins (Freidel, 1993) support the hypothesis that the subsurface flow between Fort Rock and Chewaucan basins was reversed at the time of high stand.

The two basins are separated by a brecciated fault zone associated with an anticline that includes highly permeable layers many meters thick interspersed with basalt and andesite flows (Allison, 1982, McFarland and Ryals, 1991). At present numerous springs located along the northern basin floor of Summer Lake basin, including Ana Springs, discharge water thought to originate primarily from Fort Rock aquifer to the north (McFarland and Ryals, 1991, F.D. Trauger, 1950). The water flows through the fault zone between the two basins. A 12.5 m difference in elevation presently exists between the ground water levels in the Fort Rock basin, at Silver Lake, and at Ana Springs in Summer Lake basin. Since the highest shoreline of Lake Chewaucan (1372 m) is 6 m higher than the most recent high shoreline of Lake Fort Rock (1366 m), flow has been postulated in either direction between the two basins, depending on which basin had the higher water level. Thus during their high stands ground water may have flowed from Lake Chewaucan into Lake Fort Rock. Lake level modeling of the high stands of the three basins supports this hypothesis (Freidel 1993).

Preliminary reconnaissance of the distribution of lake-deposited carbonates in north Summer Lake basin indicates discontinuous deposition. On shorelines just north of Ana Springs in Summer Lake basin, coatings of carbonate are seen commonly on beach cobbles and boulders at and below the 1342 m level between Klippel Point and Flatiron Point to the east, yet appear to be absent at higher levels. Sparse carbonate coatings are also found in Fandango Canyon along the southern shores of Fort Rock basin only at or above the 1355 m level. If this carbonate was precipitated in association with ground water discharge, the absence at higher levels in Chewaucan basin and presence only at higher levels in Fort Rock basin may have a bearing on direction of flow between the basins. On the other hand, this distribution may be associated with alternating permeable and impermeable rock layers, and have no relation to direction of ground water flow.

The levels of the three paleolakes were not, therefore, perfectly simple reflections of changes in effective moisture. Lake Chewaucan had no outlet except the postulated subsurface seepage into Lake Fort Rock. The highest level of Lake Alkali was topographically controlled by the spillway into Lake Fort Rock. Finally, lake-level modeling has supported Allison's (1979) hypothesis that Lake Fort Rock may have spilled or seeped into the Deschutes drainage to the north (Freidel, 1993).

A latest-Pleistocene oscillation

Prior research in south-central Oregon suggests that Lake Chewaucan and two neighboring paleolakes reached their most recent high stands before 16,400 C14 yrs B.P. (radiocarbon years before present) and then dropped to moderate levels before 12,500 C14 yrs B.P. (Allison, 1979, 1982; Freidel, 1993). After this time, a warming trend caused all of the Great Basin lakes to shrink rapidly, and sometime after 9000 C14 yrs B.P. the semi-arid conditions of today were established (Thompson et al. 1993).

GCM simulations indicate that the position of the jet stream responded to changes in the height and volume of the continental ice sheets, so that during the last glacial maximum, about 18,000 C14 yrs B.P., the jet stream was split into two branches around the continental ice sheet. The southern branch lay far south of its present position and its winds were stronger than present. The simulations further suggest that by about 12,000 yrs B.P. the jet stream had begun to move north over the Great Basin toward its present configuration (Kutzbach and Guetter,

1986). These simulations have been corroborated by paleoenvironmental data (Thompson et al., 1993).

Shifts in the mean position of the polar jet stream could have been responsible for fluctuations in levels of the Great Basin paleolakes during the transition period from the late Pleistocene to the Holocene. The Oregon lake high stands were probably controlled by the increased cloudiness and some increased moisture from the westerly cyclonic storms in summer, and by the very cold, dry glacial anticyclone circulation to the north in the winter (Freidel, 1993). By 13,500 C14 yrs B.P., when the mean polar jet position began to migrate north, the Oregon lakes had already dropped to moderate levels (Allison, 1979, 1982).

In the present study (Freidel 1996, 1998), field investigation of the shoreline record of Lake Chewaucan was undertaken in order to learn more about the response of this lake to rapid climatic changes during the late Pleistocene-Holocene transition period. Objectives of the study were to establish the timing and significance of a lake level oscillation in Lake Chewaucan that occurred sometime after 16,400 yrs B.P. but before about 10,000 yrs B.P.

Geomorphic and stratigraphic evidence in backhoe trenches and gravel pits indicate that sometime after its high stand, Lake Chewaucan dropped below the level of the delta of the Chewaucan River (Paisley fan/delta). At this point the lake was divided into two sub-basins, Winter Lake to the north, and ZX Lake to the south, with the Chewaucan River flowing south through the Chewaucan marshes to Abert basin. Prior to the recession of Lake Chewaucan below the Paisley fan/delta, it seems likely that the Chewaucan River flowed north into Summer Lake basin. This hypothesis is supported by the contrasting deep lake sediments exposed at Ana Springs (Negrini and Davis, 1992) representing many lake cycles, and very shallow lake sediments and marsh peat deposited in Chewaucan Marshes south of the fan/delta that may represent only one mid-level lake stand (Allison 1982).

A subsequent increase in effective moisture caused ZX Lake to fill and overflow into Winter Lake, carving an overflow channel across the delta and depositing sediment in a small fan draped on the shore of Winter Lake. To investigate this episode, two transects of backhoe trenches were excavated across this small fan and underlying shoreline deposits in search of stratigraphic evidence and datable materials to establish the timing of the overflow and the concurrent level of Winter Lake. The trenches provided stratigraphic evidence of the lake level oscillation, but produced no materials for dating. Datable materials were obtained from lake deposited calcium carbonate on wave worn boulders at the north end of Summer Lake basin and along the shores of Lake Abert at the south end of ZX basin. Two shell layers from Tucker Hill were also dated (Table 1). The sequence of dates show Winter Lake rising from the1310 m level around 12,500 C14 yr BP to a peak of 1337 m by ca. 12,000 C14 yr BP and then falling to 1321 m by 11,900 C14 yr BP (Fig. 1). This sequence fits well with Licciardi's (in press) dates on the Chewaucan Marshes and Lake Abert (Fig. 2).

Two hypotheses regarding the climatic cause of this oscillation were (1) that colder temperatures associated with the Younger Dryas reduced evaporation, increasing effective moisture, and (2) precipitation increased as the mean path of the polar jet stream migrated northward during deglaciation.

Table 1
RADIOCARBON DATES ASSOCIATED WITH LOW LEVEL SHORELINES IN WINTER AND ZX LAKE BASINS

Elev	Age	Sample No.	Location	Ref
Winter Lake				
1310	12,340±90	AA25320	Klippel Pt	Freidel
1310	12,495±90	AA25321	Klippel Pt	Freidel
1321	11,910±100	AA25322	Klippel Pt	Freidel
1329	11,880+/-80	Beta82260	Flatiron Pt.	Freidel
1337	12,050±130	AA25323	Klippel Pt	Freidel
	All Winter Lake dated materials are tufa			
ZX Lake				
1310	11,670±95	AA13589	East L.Abert shell	Licciardi (2001)
1310	12030+/-90	AA13591	East L. Abert shell	Licciardi (2001)
1311	11,550±15	Negrini	SE L Abert shell	Licciardi (2001)
1321	12,170±115*	AA20142	Tucker Hill shell	Freidel
1321	12,340±80*	AA20143	Tucker Hill shell	Freidel
1325	11,930±95	AA13588	Willow Cr shell	Licciardi (2001)

*adjusted for $\delta^{13}C$

The lake level oscillation and spilling from ZX Lake into Winter Lake apparently peaked around 12,000 ^{14}C yrs B.P., well before the Younger Dryas event (Freidel, 1998).

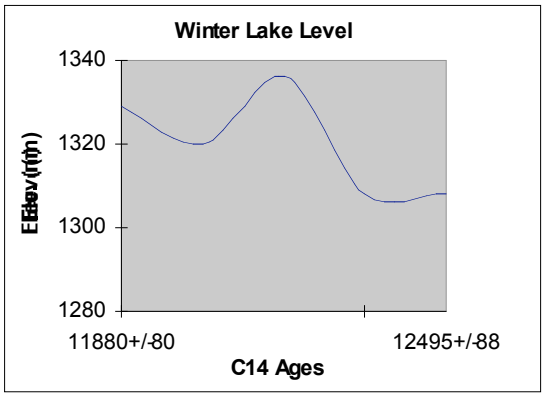

Figure 1

Lake level modeling suggests that the rise in lake level was associated with increases in precipitation (+60% relative to present) and runoff (+240% relative to present), as well as a small decrease in evapotranspiration (-20%) resulting from cooler than present temperatures, rather than colder, drier conditions (Freidel, 1998). These are conditions consistent with passage of the mean path of the jet stream over the region during deglaciation. They are also consistent with paleoclimatic data for 12 ka from the western U.S. summarized in Thompson et al. (1993).

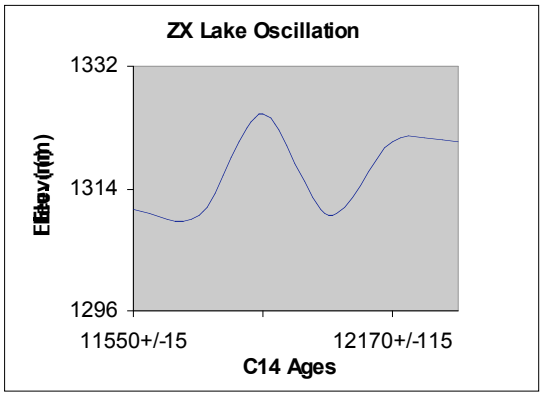

Figure 2

References Cited

Allison, I.S., 1979. Pluvial Fort Rock Lake, Lake County, Oregon. Oregon Dept. of Geology and Mineral Industries Special Paper No. 7.

Allison, I.S. 1982. Geology of Pluvial Lake Chewaucan, Lake County, Oregon. Studies in Geology No. 11. Oregon State University Press, Corvallis.

Freidel, Dorothy E., 1993. Chronology and Climatic Controls of Late Quaternary Lake-Level Fluctuations in Chewaucan, Fort Rock, and Alkali Basins, South-Central Oregon. Unpublished Ph.D. Dissertation, University of Oregon.

Freidel, Dorothy E. 1996. Modeling of a low-amplitude lake-level oscillation during the Pleistocene-Holocene transition in Chewaucan basin, Oregon. American Quaternary Assn. Program and Abstracts of the 14th Biennial Meeting, Flagstaff.

Freidel, Dorothy E. 1998. Lake-level oscillation at Paleolake Chewaucan, Oregon, during the Pleistocene-Holocene Transition. American Quaternary Assn. Program and Abstracts of the 15th Biennial Meeting, Puerto Vallarta.

Kutzbach, J.E. and Guetter, P.J., 1986. The influence of changing orbital parameters and surface boundary conditions on climate simulations for the past 18,000 years. Journal of the Atmospheric Sciences, 43:1726-1759.

Licciardi, J.M., in press. Chronology of latest Pleistocene lake-level fluctuations in the pluvial Lake Chewaucan Basin, Oregon, USA. Journal of Quaternary Science.

McFarland, William D. and Gary N. Ryals, 1991. Adequacy of available hydrological data for evaluation of declining groundwater levels in the Fort Rock basin, south-central Oregon. U.S. Geological Survey Water Resources Investigation Report No. 89-4057.

Negrini, Robert M. and Davis, Jonathan O., 1992. Dating late Pleistocene pluvial events and tephras by correlating paleomagnetic secular variation records from the western Great Basin. Quaternary Research, 37:46-59.

Thompson, R.S., Whitlock, C., Bartlein, P.J., Harrison, S.P., and Spaulding, W.G., 1993. Climatic changes in the Western United States since 18,000 years B.P. *In* "Global Climates Since the Last Glacial Maximum" (H.E. Wright, Jr., J.E. Kutzbach, T. Webb II, W.F. Ruddiman, F.A. Street-Perrott, and P.J. Bartlein, Eds.) pp. 468-513. University of Minnesota Press, Minneapolis.

Trauger, F.D., 1950, Basic ground-water data in Lake County, Oregon: U.S. Geological Survey open-file report, 287 p.

Artifacts and Faunal Remains of Pre-and Post-Mazama Age from the Paisley Five-Mile Point Caves at Summer Lake

Mel Aikens, Department of Anthropology, University of Oregon

Introduction

The Paisley Caves, 5 miles north of Paisley, Oregon were excavated in 1938 and 1939 by L.S. Cressman of the University of Oregon. They represent the first documented archaeological excavations in the Summer Lake Basin, and remain even today one of the few archaeological localities reported there. Cressman spent the summers of 1935-38 looking for evidence of early human occupation in the northern Great Basin by excavating caves found on pluvial lake shorelines in Catlow Valley, the Summer Lake Basin, and Fort Rock Valley. Cressman's early work, distinguished by its interdisciplinary nature, included collaborations with such pioneers of Pleistocene and Holocene research as Ira Allison, Ernst Antevs, Henry P. Hansen, W.D. Smith, and Howel Williams, among other luminaries (Cressman and Williams 1940, Cressman et al., 1942).

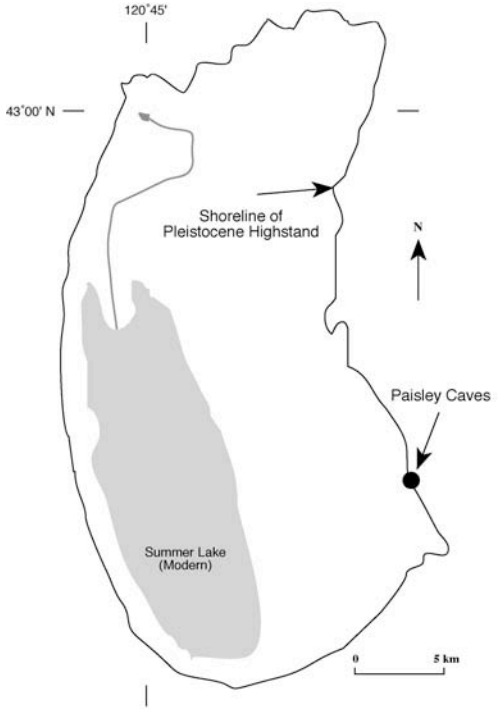

Figure 1. Location of Paisley Caves

.

Stratigraphy, Artifacts, Fauna

Paisley Cave 1 exhibited an upper layer that contained a fairly complete sandal and two large sandal fragments, all of tule; three small fragments of twined basketry and a fragment of twined matting; obsidian artifacts including 6 flake scrapers, 7 arrowheads, and a possible dart point; and 1 mano and 1 metate, both stained with red pigment. Beneath was a sterile layer of Mazama tephra, and below that a layer of dust and organic material that contained ash lenses, the butt of a dart point, and 12 flaked artifacts or fragments.

Paisley Cave 2 was disturbed by collector's

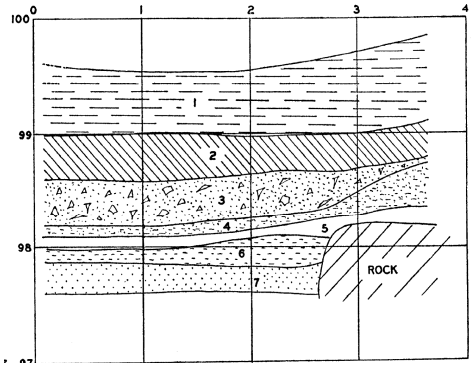

Figure 2. Profile of Paisley Cave 3. Distances are in meters. 1: Surface; 2: Pumice; 3: Broken rock, dust, and roof debris; 4: Dust, bat guano (very compact, reddish); 5: Dust (very compact, reddish); 6: Dust (soft), rodent remains, ash, artifacts, extinct faunal remains; 7: Dust, beach sand, gravel, ash, artifacts, extinct faunal remains. From Cressman et al. 1942, Fig. 53.

excavations but nevertheless showed the same three layers as Cave 1. It yielded some stone pieces, tule sandals, a bone awl, and the butt of an atlatl shaft.

Paisley Cave 3 produced no artifacts in the loose fill above an unbroken layer of Mazama tephra about .4 m. thick. Below was spall rock, dust and guano, and about 2 m below surface a sand and gravel layer from which are reported four worked obsidian flakes, ash/charcoal lenses, and the bones of hawk, sagehen, pintail, teal, bison, mountain sheep, camel, horse, large dog (wolf?), fox, and probably bear.

Age Control

Age control in the Paisley caves is most surely provided by the presence in all three of

Mazama tephra, identified at the sites by Howel Williams (later confirmed by the geochemical and petrographic analyses of Randle, Goles, and Kittleman (1971). Mazama tephra has been dated to about 6850 RCYBP or roughly 7600 calendar years ago. One radiocarbon date from Paisley Cave 3, on material found beneath the Mazama tephra, is 7610+/-120 RCYBP (Y-109), Preston *et al*. 1955:958). The horse and camel bone identifications from Paisley Cave 3 suggest an age within the Pleistocene, while the remaining fauna could represent any part of the Holocene. Large and small projectile points indicate presence of the atlatl and dart early, and the bow and arrow later.

Two radiocarbon dates obtained on fragments of Catlow Twine basketry from Paisley Cave 1 are: Sample # 1-5345, 145+/50 RCYBP; Sample # 1-5344, 6560+/- 70 RCYBP (Connolly, Fowler, and Cannon 1998). Cressman reports that these specimens had been excavated by a local man named Perry, who believed that both came from beneath the Mazama tephra. The older date falls among other determinations for pre-Mazama archaeological contexts, but the date of the younger specimen suggests stratigraphic ambiguities within Paisley Cave 1.

Future Research

For Cressman, the significance of the Paisley Caves research lay in the fact that it demonstrated human presence there in pre-Mazama times. Thus it established the textile-rich Basketmaker-like assemblages of the Oregon caves (and by extension Lovelock and other Great Basin caves) as much older than the classical Basketmaker culture of the Southwest, to which they were often compared. Cressman also believed that the horse and camel bones from the bottom of his Cave 3 excavation established human presence there in late Pleistocene times. The former belief has now been confirmed many times over, but the latter remains highly suspect because of the poor documentation of both the bone identifications and the reported association between lake sands and gravels, artifacts, and bones of extinct horse and camel. Though the Paisley caves have been heavily looted over the years, there may yet be undisturbed deposits left on some of the cave aprons, giving opportunity for future research to improve on the minimal documentation provided in Cressman's brief reports.

References

Connolly, Thomas J., Catherine S. Fowler, and William S. Cannon, 1998. Radiocarbon Evidence Relating to Northern Great Basin Basketry Chronology. Journal of California and Great Basin Anthropology 20(1): 88-100.

Cressman, L.S., and Howel Williams 1940. Early Man in Southcentral Oregon: Evidence from Stratified Sites, pp. 53-78 in Early Man in Oregon: Archaeological Studies in the Northern Great Basin, by L.S. Cressman, Howel Williams, and Alex D. Krieger. University of Oregon Monographs, Studies in Archaeology 3.

Cressman, L.S., Frank C. Baker, Paul S. Conger, Henry P. Hansen, and Robert F. Heizer, 1942. Archaeological Studies in the Northern Great Basin. Carnegie Institution of Washington Publication 538.

Preston, R.S., E. Person, and E.S. Deevey, 1955 Yale Natural Radiocarbon Measurements, II. Science 122:954-960.

Randle, Keith, Gordon G. Goles, and Laurence R. Kittleman, 1971. Geochemical and Petrological Characterization of Ash Samples from Cascade Range Volcanoes. Quaternary Research 1: 261-282.

Fossil Fish of the Northern Great Basin

Kenneth W. Gobalet, Department of Biology
California State University, Bakersfield, CA 93311

An intriguing problem dealing with the freshwater fishes of the western United States is the geographic and temporal origin of the native freshwater fishes of the Central Valley of California where seven unique living genera are found (*Archoplites, Hesperoleucas, Hysterocarpus, Lavinia, Mylopharodon, Orthodon, Pogonichthys*, Table 1) (Moyle 1976). These taxa generally inhabit all but the upper reaches of the Sacramento and San Joaquin Rivers. The community of fishes that most closely parallels this assemblage is found in the Late Miocene (Chalk Hills) and Pleiocene (Glenns Ferry) formations of "Lake Idaho" (Table 2) (Smith et al. 1982). In fact the abundance of fish species in the Pliocene of Idaho suggests that the native fishes of the Central Valley of California are a depauparate assemblage. Of the genera unique to the Central Valley that require a freshwater connection, only *Hesperoleucas* and *Pogonichthys* lack representation in the "Lake Idaho" formations. Clearly the presence of *Ptychocheilus, Gila,* and *Catostomus* in California and "Lake Idaho" further suggest a freshwater aquatic connection across space and time (Minckley et al. 1986). Fossil fishes of southern Oregon contribute to our understanding of these relationships.

The distribution of fishes thus can provide evidence for ancient hydrology. Wheeler and Cook (1954) suggested a former course of the Snake River south and west toward the present Klamath River drainage or across Nevada to the Great Valley of California. Minckley et al. (1986) reviewed the geological evidence for the shifting watercourses. One possible connection might even have been to the headwaters of the San Joaquin River by way of what is now the Mono Lake Basin. The San Joaquin River previously had its headwaters well into Nevada (Huber 1981). Evidence is most supportive of a connection that crossed northern Nevada and enters the Sacramento River system in northeastern California with tributaries toward the Klamath River and paralleling the eastern boundary of Northern California (Wagner et al. 1997). Wagner et al. (1997) reported Early Pliocene *Ptychocheilus*, *Lavinia*, and *Gila coerulea* from northeastern California. *G. coerulea* is currently in the Klamath River system and is related to the fossil *G. milleri* of the Glenns Ferry Formation (Smith 1975).

It is clear that numerous details of the aquatic connections and the fishes carried by them are in need of attention. I have identified the following fishes from Late Pliocene sediments of the Carson Valley, Nevada: *Lavinia, Ptychocheilus, Siphateles bicolor, Catostomus, Chasmistes*, and *Oncorhynchus*. See Kelly (1994) for a discussion of the formation. Pliocene fishes of the Mono Lake Basin of California are: *Siphateles bicolor, Ptychocheilus Catostomus* and *Chasmistes*. Miller and Smith (1981) have identified *Idadon* (=*Lavinia*) from the same locality, but I have been unable to confirm its presence. Considering the lack of consistency among faunal identification specialists, getting secondary confirmation of the taxonomic designations is essential (Gobalet 2001). Middle Pleistocene (770,000-610,000 ybp) fishes of the Humboldt Canyon in pre-Lake Lahontan sediments are probably identical to the current fauna of Pyramid Lake, the largest remnant of terminal Pleistocene Lake Lahontan. Fossil species identified are *Siphateles bicolor, Oncorhynchus clarki, Catostomus* cf. *tahoensis*, *Chasmistes* cf. *cujus*, and *Cottus beldingi*. These findings demonstrate that some of these fishes were widely distributed in the Pliocene and we have a lot to learn about the ancient watercourses.

The fossil fishes of southern Oregon have been reviewed by Orr and Orr (1981) and by Minckley et al. (1986). The fishes of Miocene Deer Butte formation of eastern Oregon were essentially the "Lake Idaho" fauna and possibly had species that were ancestral to those of the Glenns Ferry fauna (Kimmel 1975). Much of southern and southeastern Oregon is known for the inland basins or "Oregon Lakes" (Minckley et al. 1986). Because most of the basins lack drainage, they are included in the hydrographic Great Basin by Grayson (1993). Because of the lack of connections between basins, the fishes able to survive demonstrate considerable endemism (Hubbs and Miller 1948, Hubbs et al. 1974) and extinction. Smith (1978) has identified 150 distinct drainages, many of which are inhabited by the extinction resistant *Siphateles bicolor* and *Rhinichthys osculus*. In the basin of glacial Lake Chewaucan, Gobalet and Negrini (1992) have demonstrated characters of the fossils suggestive of endemism in the local tui chub, *Gila* (*Siphateles*) *bicolor*. *S. bicolor, Rhinichthys osculus*, and *Oncorhynchus* (redband) (Minckley et al. 1986) today inhabit the basin.

About the "Oregon Lakes" in general Minckley et al. (1986) state the following:

" Fossil fishes of this region were dealt with by Cope (1883b, 1884, 1889), and little information has since appeared that aids in interpretation of older drainage relations. *Oncorhynchus* sp. from Pliocene beds indicates connections with the Columbia River (Cavender and Miller 1972). Late Pleistocene (Allison 1941, 1966) species now recognized (G.R. Smith 1981a) include *Gila (Siphateles) altarcus,* a relative of *G. bicolor* (Uyeno 1960; Uyeno and Miller 1963) and *Chasmistes bratrachops* (also known as referred material from Inyo County) California, and Washoe County, Nevada; Miller and Smith 1981). *Salmo* sp. (similar to S. *clarki*), *Gila (Siphateles*)sp. and *Catostomus (Catostomus* or *Deltistes*) sp. are associated with Oregon *C. batrochops* in the Fossil Lake area (Fort Rock Basin). The *Salmo* has recently been identified as *Salmo* sp. (redband) by Allison and Bond (1983)."

The trout genus *Salmo* (*S. gairdneri, S. clarki,* and redband) are included within the genus *Oncorhynchus*, with all species of Pacific salmon and *S. gairdneri* is now *O. mykiss* (Robins et al. 1991). *Salmo* is reserved for Atlantic salmon and trout. Salmon and trout both were evidently represented in the Pliocene waters of the "Oregon Lakes."

Fossil fishes of the "Oregon Lakes" tend to be a depauparate mix of Pliocene and Pleistocene lacustrine fishes. In particular, members of the lake sucker genus *Chasmistes*, a salmonid *Oncorhynchus* and tui chub *Siphateles bicolor* are represented (Orr and Orr 1981). A species of the sucker genus *Catostomus* is present as well. This suggests that Pyramid Lake in Nevada is a good model for studying the ecology of the "Oregon Lakes" and that additional species like a sculpin *(Cottus)* and speckled dace (*Rhinichthys osculus)* will be identified.

Literature Cited

Gobalet, K. W. 2001. A critique of faunal analysis; inconsistency among experts in blind tests. Journal of Archaeological Science 28: 377-386.

Gobalet, K.W. and R.M. Negrini. 1992. Evidence for endemism in fossil tui chub, *Gila bicolor,* from Pleistocene Lake Chewaucan, Oregon. *Copeia* 1992(2): 539-544.

Grayson, D. K. 1993. The Desert's Past. Washington D.C.: Smithsonian Institution Press.

Hubbs, C. L. and R. R. Miller. 1948. The zoological evidence: correlation between fish distribution and hydrologic history in the desert basins of western United States. *in* Great Basin with Emphasis on Glacial and Postglacial Times. Bulletin of the University of Utah 38 (20): 17-166.

Hubbs, C.L., R. R. Miller, and L. C. Hubbs. 1974. Hydrographic history and relict fishes of the north-central Great Basin. Memoirs of the California Academy of Sciences. Volume VII.

Huber, N. K. 1981. Amout and timing of Late Cenozoic uplift and tilt of the central Sierra Nevada, California-Evidence from the upper San Joaquin River basin. Geological Survey Professional Paper 1197.

Kelly, T. S. 1994. Two Pliocene (Blancan) vertabrate faunas from Douglas County, Nevada. Paleobios 16 (1): 1-23.

Kimmel, P. G. 1975. Fishes of the Miocene-Pliocene Deer Butte Formation, southeastern Oregon. University of Michigan, Museum of Paleontology, Papers on Paleontology No. 14.

Miller, R. R. and G.R. Smith. 1981. Distribution and evolution of *Chasmistes* (Pisces: Catostomidae) in western North America. Occasional Papers of the Museum of Zoology University of Michigan No. 696.

Minckley, W. L., D. A. Hendrickson, and C. E. Bond. 1986. Geography of Western North America freshwater fishes: description and relationships to intracontinental tectonism. pgs. 519-613 *in* The Zoogeography of North American freshwater Fishes. C. H. Hocutt and E. O. Wiley, editors. New York: John Wiley and Sons.

Moyle, P.B. 1976. Inland Fishes of California. Berkeley, University of California Press.

Orr, W. N. and E. L. Orr. 1981. Handbook of Oregon Plant and Animal Fossils.

Robins, C. R., R.M. Bailey, C.E. Bond, J.R. Brooker, E.A. Lachner, R.N. Lea, and W.B. Scott. 1991. Common and Scientific Names of Fishes from the United States and Canada. 5th edition. American Fisheries Society Special Publication 20.

Smith, G. R. 1975. Fishes of the Pliocene Glenns Ferry Formation, southwest Idaho. University of Michigan Museum of Paleontology Papers on Paleontology No. 14.

Smith, G. R. 1978. Biogeography of intermountain fishes. Great Basin Naturalist Memoirs 2:17-42.

Smith, G.R., K. Swirydczuk, P.G. Kimmel, and B.H. Wilkinson. 1982. Fish Biostratigraphy of Late Miocene to Pleistocene sediments of the western Snake River Plain, Idaho. Pgs 519-541

in B. Bonnichsen and R. M. Breckenridge, editors. Cenozoic Geology of Idaho: Idaho Bureau of Mines and Geology Bulletin 26.

Wagner, H.M., C.B. Hanson, E.P. Gustafson, K.W. Gobalet, and D.P. Whistler. 1997. Biogeography of Pliocene and Pleistocene vertebrate faunas of northeastern California and their temporal significance to the development of the Modoc Plateau and the Klamath Mountains orogeny. San Bernardino County Museum Association Quarterly *44*(1): 13-21.

Wheeler, H.E. and E. F. Cook. 1954. Structural and stratigraphic significance of the Snake River capture, Idaho-Oregon. Journal of Geology 62: 525-536.

Table 1. Native Freshwater Fishes of the Central Valley of California (Moyle 1976)

Genera unique to the Central Valley	
Archoplites interruptus	Sacramento perch
Hesperoleucas symmetricus	California roach
Lavinia exilicauda	hitch
Mylopharodon conocephalus	hardhead
Orthodon microlepidotus	Sacramento blackfish
Pogonichthys macrolepidotus	splittail
Genera with representatives outside the Central Valley	
Gila crassicauda	thicktail chub (extinct)
Ptychocheilus grandis	Sacramento squawfish
Rhinichthys osculus	speckled dace
Catostomys occidentalis	Sacramento sucker
Cottus spp.	sculpins
Taxa likely derived from marine species	
Hysterocarpus traski	tule perch
Oncorhynchus spp.	trouts and salmons
Acipenser sp.	sturgeons
Lampetra sp.	lampreys
Hypomenesus transpacificus	delta smelt
Spirinchus thaleichthys	longfin smelt
Gasterosteus aculeatus	threespine stickleback

Table 2. Fishes from "Lake Idaho" (Smith et al. 1982)

Chalk Hills Formation (Late Miocene 8.5-5.5 mya)	Glenns Ferry Formation (Pliocene)
Archoplites	*Archoplites*
Idadon (=Lavinia)	*Idadon*
Mylopharodon	*Mylopharodon*
Orthodon	*Orthodon*
Ptychocheilus	**Ptychocheilus**
	Gila (Gila) milleri
	Catostomus
Chasmistes	*Chasmistes*
Oncorhynchus(=Rhabdophario)	*Oncorhynchus*
Acrocheilus	*Acrocheilus*
Mylocheilus	*Mylocheilus*
	Richardsonius
	Prosopium
Ictalurus	*Ictalurus*
Hucho	*Cottus*
Smilodonichthys	*Kerocottus*
	Myoxocephalus

Landslides along Winter Rim, Southwest Summer Lake Basin, Oregon

Tom Badger
University of Nevada, Reno

Winter Rim, the western escarpment of Summer Lake basin, extends more than twenty miles from the northern part of the basin to the southern terminus of Summer Lake. An east-trending escarpment, that includes Slide Mountain, bounds the basin on the south. Most striking about the Winter Rim and Slide Mountain escarpments is the pervasiveness of gigantic landslides. Each of the major landslide complexes exceeds several square miles in area. Named features on this escarpment, such as "Slide Mountain", "The Punchbowl", and "Big Flat", tell of the landsliding and its characteristic topography. Along much of its length, the rim is scalloped by broad, cirque-like bowls, which are the headscarps of major landslides/complexes of landslides. The slopes below are commonly hummocky with closed depressions and deranged drainages. Landslide deposits generally extend to the present shoreline.

Landslide deposits mostly obscure bedrock along the lower half of the escarpments. From limited exposures, Walker (1963) identified the lower bedrock assemblage to consist of Oligocene- (?) to Miocene-age silicic and mafic pyroclastics, volcanic flows, and sedimentary rocks. Above the landslide debris, and exposed roughly between elevations 6000 and 7000 feet, is a continuous band of mostly tuff and tuffaceous sedimentary rocks with minor dacite and andesite flows (Walker, 1963 and Travis, 1977). Miocene- to Pliocene-age basalt flows of the Picture Rock Basalt cap much of the escarpment.

This masters thesis researches the stratigraphic and tectonic controls of these gigantic landslides. It also will investigate the engineering mechanics associated with the formation of these large landforms. At this time, I have only performed reconnaissance-level mapping and airphoto interpretation, so the following observations and interpretations are very preliminary.

- Landslide deposits in the toe area are typically light-colored and appear clay-rich. Lowermost outcrops along Winter Rim are comprised of light tan, clay-rich, bedded tuffaceous rocks. There appears to be some lateral continuity of this unit along the southern Winter Rim and Slide Mountain escarpments. Slope failure may be controlled by this unit.

- Morphology of the landslide deposits becomes more subdued and less hummocky southward from The Punchbowl landslide complex (very hummocky topography) to the Bennett Flat landslide (smooth upper bowl). Closed depressions and deranged drainages dominate to the north. Both Foster Creek and Bennett Flat landslides possess relatively flat, hanging bowls. Bennett Flat is about 400 feet higher than Big Flat in Foster Creek. Between Foster Creek and The Punchbowl landslides, a relatively fresh fault ruptures the surface. The hanging bowls in Foster Creek and Bennett Flat landslides are likely due to faulting (propagating through the

landslide deposits), and the fault is highly segmented. Based upon these observations and interpretations, I am considering a model that relates basin subsidence with landsliding, which is illustrated in the following figure. The essence of this tectonic/landslide model involves more rapid/older basin subsidence in the south along a highly segmented fault. This subsidence exposes a weak underlying strata. Landslides initiate first in the south and are followed by progressively younger slides to the north. This model may be further supported by the fact that the lowest part of the basin and the highest part of Winter Rim is in the southwest.

- At least the lower portions of these landslides have been active during the late Pleistocene. Much, if not all, of The Punchbowl landslide complex may have failed during the late Pleistocene. These interpretations are based in part upon the absence of preserved, higher-stand, pluvial shorelines.

- The landslides typically have relatively long runouts. This rheologic character may be due to clay-rich deposits, a saturated landslide mass at the time of failure, liquefaction of the lake deposits due to rapid, undrained loading of the landslide deposits, or ???

I expect that both limit equilibrium and deformational modeling of the landslides will provide additional geologic and hydrologic information about the underlying stratigraphy and the conditions under which these landslides could have been triggered.

REFERENCES

Travis, P. L., Jr., 1977, Geology of the area near the north end of Summer Lake, Lake County, Oregon, M.S. thesis, University of Oregon, 95 p.

Walker, G. W., 1963, Reconnaissance Geologic Map of the Eastern Half of the Klamath Falls (AMS) Quadrangle, Lake and Klamath Counties, Oregon, USGS Map MF-260.

Model relating basin subsidence and landsliding
SW Summer Lake basin, Oregon

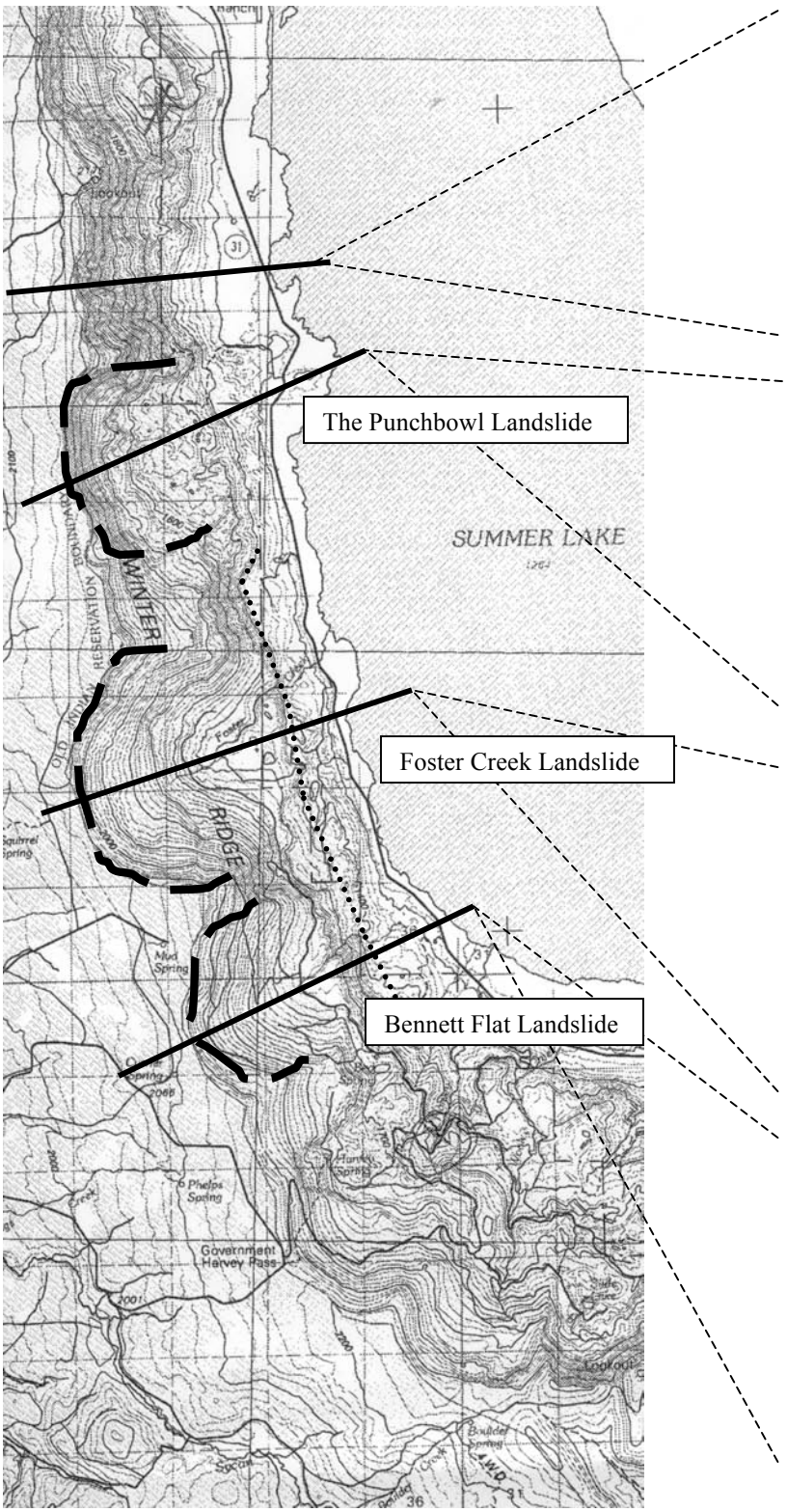

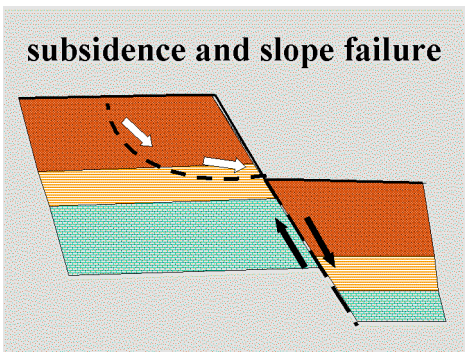

(a)

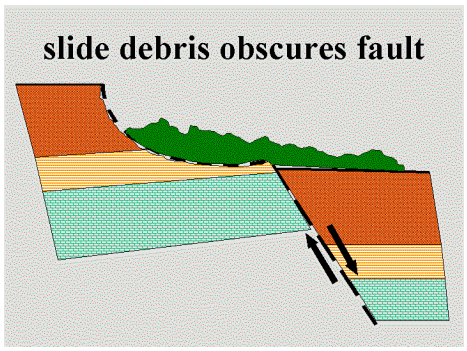

(b)

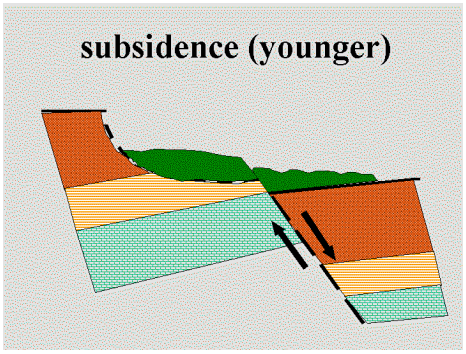

(c)

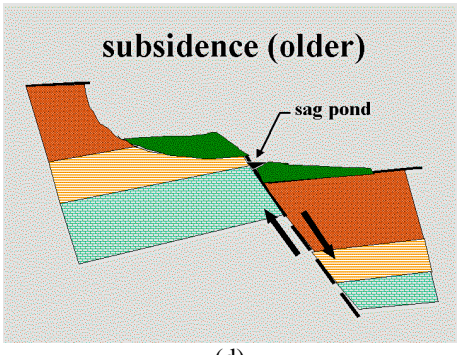

(d)

The figure illustrates the theorized relationship of (a) basin subsidence and exposure of a weak underlying strata (intermediate unit), (b) subsequent landsliding (headscarps denoted by heavy dashed line on topo map), and (c) and (d) fault propagation through the landslide (dotted line on topo map) and "smoothening" of landslide deposits. Slope morphology, drainage pattern, and development of fault rupture suggest landslides to the south are older than those to the north.